UNIVERSITY OF CALIFORNIA

Los Angeles

Tuning the Local Immune Environment via Engineered Microneedle Patches

A dissertation submitted in partial satisfaction of the

requirements for the degree Doctor of Philosophy

in Bioengineering

by

Xuexiang Zhang

2023

© Copyright by

Xuexiang Zhang

2023

ABSTRACT OF THE DISSERTATION

Tuning the Local Immune Environment via Engineered Microneedle Patches

by

Xuexiang Zhang

Doctor of Philosophy in Bioengineering

University of California, Los Angeles, 2023

Professor Song Li, Chair

The immune system serves as a vital defense mechanism, protecting the body against exogenous pathogens and endogenous aberrations through a complex network of cells and signaling pathways. Many diseases arise as a consequence of imbalanced or ineffective immune responses. However, altering the immune system systematically can lead to a range of complications and negative outcomes. Thus, targeted and controlled modulation of the local immune cells and their responses is highly desirable, which minimizes side effects throughout the body and provide precision medicine with the lowest effective dose at local tissues. My thesis harnesses principles of immunoengineering, drug delivery and regenerative medicine to achieve local immune modulation via engineered microneedle patches (MNP) that enables minimally invasive tissue penetration and local retention. To address the critical role of destructive immune cells in tissue loss and achieve periodontal tissue regeneration, I engineered a modular MNP that allows a multistage and controlled release of antibiotics and cytokines. My work demonstrated that the dual delivery of antibiotics and cytokines modulated immune cells, promoted pro-regenerative signals locally, and reversed the degeneration of soft tissue and bone. I further

simplified the formulation by identifying a bifunctional antibiotic that not only suppresses bacterial growth but also modulates the macrophages to suppress inflammation, and utilized a fast-degrading MNP loaded with biodegradable PLGA microparticles. Significant therapeutic effects, including suppression of pro-inflammatory cytokine secretion, induction of pro-regenerative cytokines and promotion of tissue/bone regeneration markers were observed in rat periodontitis model. In another application, to suppress the immunogenicity of viral vectors during *in vivo* gene delivery and boost gene transduction efficiency, I optimized a dissolvable MNP that maintains the virus integrity and releases immunomodulatory agents slowly via microparticles that can be integrated into MNP, and showed that local and slow release of immunosuppressants (i.e. dexamethasone) enhances gene transfer efficiency. Our results in mouse ischemia-reperfusion model demonstrated a significant increase of gene transduction efficiency in the heart. Overall, this work uses MNP as a drug delivery strategy for its minimal invasiveness, local penetration, sustained release and controlled delivery. It reveals the feasibility and efficacy to locally modulate immune responses for more efficient tissue regeneration and gene therapy.

The dissertation of Xuexiang Zhang is approved.

Alireza Moshaverinia

Amy Catherine Rowat

Cun Yu Wang

Song Li, Committee Chair

University of California, Los Angeles

2023

TABLE OF CONTENTS

ABSTRACT ..... ***II***

LIST OF FIGURES ..... ***VIII***

ACKNOWLEDGEMENTS ..... ***XI***

VITA/BIOGRAPHICAL SKETCH ..... ***XVI***

1. BACKGROUND ***1***

1.1 Overview **1**

1.2 Microneedle Patch (MNP) **3**

1.3 Biomaterial-enabled Local Immune Modulation **6**

1.4 Tissue Regeneration and Chronic Inflammation **9**

1.4.1 Tissue Regeneration 9

1.4.2 Case Study: Periodontal Diseases and Immune Networks Involved 10

1.5 Cell Reprogramming and Gene Delivery **15**

1.5.1 Direct Cardiac Reprogramming 15

1.5.2 Gene Delivery Systems 16

2. BASE-DISSOLVABLE HYDROGEL MICRONEEDLES FOR GINGIVAL DELIVERY OF IMMUNOMODULATORY FACTORS ***20***

2.1 Abstract **20**

2.2 Introduction **21**

2.3 Results **23**

2.3.1 Design and fabrication of periodontal MN patch 23

2.3.2 Physical characterization and mechanical property of MN patch 24

2.3.3 Delivery of antibiotics by periodontal MN patch and antibacterial effects in vitro. 26

2.3.4 Anti-inflammatory properties of periodontal MN patch in vitro. 29

2.3.5 In vivo studies of MN patches for periodontitis treatment 31

2.4 Discussion **35**

2.5 Materials and Methods **37**

3. DISSOLVABLE MICRONEEDLES FOR LOCALIZED DELIVERY OF BI-FUNCTIONAL MICROPARTICLES ***45***

3.1 Abstract **45**

3.2 Introduction **45**

3.3 Results **48**
3.3.1 Screening of bi-functional small molecules 48
3.3.2 Design and characterization of AZM-MN patch 50
3.3.3 In vitro evaluation of MN patch 52
3.3.4 In vivo evaluation of MN patch for periodontal treatment 54
3.4 Discussion **58**
3.5 Materials and Methods **60**
4. VIRUS-LOADED MICRONEEDLES FOR IN SITU CELL REPROGRAMMING ***65***
4.1 Abstract **65**
4.2 Introduction **65**
4.3 Results **68**
4.3.1 Local immune suppression enhanced gene transfer efficiency 68
4.3.2 Design and fabrication of virus-loaded microneedle patch 71
4.3.3 In vivo enhancement of gene transfer efficiency for cardiac reprogramming 73
4.4 Discussion **78**
4.5 Materials and Methods **79**
5. CONCLUSIONS AND FUTURE WORK ***83***
5.1 Conclusions **83**
5.1.1 Periodontal local immunomodulation 83
5.1.2 Gene delivery with local immunosuppression 84
5.2 Future Work **85**
5.2.1 Microneedle patch design 85
5.2.2 Periodontal local immunomodulation 87
5.2.3 Gene delivery with local immunosuppression 88
6. APPENDIX A. SUPPLEMENTARY FIGURES ***90***
6.1 Base-dissolvable Hydrogel Microneedles for Gingival Delivery of Immunomodulatory Factors **90**
6.2 Dissolvable Microneedles for Localized Delivery of Bi-functional Microparticles **98**
6.3 Virus-loaded Microneedles for In situ Cell Reprogramming **105**
7. APPENDIX B. HORMONE DELIVERY ***108***
7.1 Abstract **108**

7.2 Introduction **108**

7.3 Results **109**

7.3.1 Optimization of MNP 109

7.3.2 Characterization of MNP 111

7.3.3 In vitro drug release profile 112

7.3.4 In vivo drug release profile 113

7.4 Discussion **114**

8. APPENDIX C. MECHANOBIOLOGY OF IMMUNE CELLS ***117***

9. APPENDIX D. BIOMATERIAL-BASED IMMUNOENGINEERING TO FIGHT COVID-19 AND INFECTIOUS DISEASES ***128***

10. REFERENCES ***156***

LIST OF FIGURES

Figure 2-1. Physical and chemical characterization of MN patches. 25
Figure 2-2. Sustained release of IL-4 and TGF-β from silica-heparin microparticles 28
Figure 2-3. Immunomodulatory properties of MN patches in vitro. 30
Figure 2-4. In vivo evaluation of the immunomodulatory effects in a rat model of periodontitis. 34
Figure 2-5. Effects of therapeutic MN patches on the regeneration of periodontal tissue in vivo. 35
Figure 3-1. Screening of small molecules for macrophage polarization. 49
Figure 3-2. Physical Characterization of PVP microneedle. 51
Figure 3-3. Sustained release of azithromycin from microneedles shows antibiotic effects for prolonged period and immunomodulatory effects in vitro. 53
Figure 3-4. In vivo evaluation of bacterial growth and inflammation in a rat model of periodontitis. 56
Figure 3-5. In vivo evaluation of anti-inflammatory markers and macrophage polarization status. 57
Figure 3-6. In vivo evaluation of tissue healing and bone regeneration. 58
Figure 4-1. The effects of local immune suppression on in vivo gene transfer. 70
Figure 4-2. Design and optimization of DsRed-retrovirus loaded MNP. 73
Figure 4-3. In vivo efficacy of gene transfer in murine heart. 74
Figure 4-4. DsRed fluorescence and particle distribution. 75
Figure 4-5. Immunostaining of macrophage marker CD68 (pan macrophage) and CD206 (M2 macrophage) 76
Figure 4-6. Immunostaining of macrophage marker CD206 (M2 macrophage) and CCR7 (M1 macrophage). 77
Figure 7-1. Schematics of MNP design. 111
Figure 7-2. Mechanical test of MNPs. 112
Figure 7-3. Release of testosterone from MNP in vitro. 113
Figure 7-4. Release profiles of testosterone. 114

Supplementary Figure S2-1. Proposed working mechanism of designed immunotherapeutic periodontal patch. 90
Supplementary Figure S2-2. Fabrication of particles loaded microneedle patch. 91
Supplementary Figure S2-3. Co-culture of primary bone marrow derived murine macrophages with IL-4-containing MNs with and without UV curing. 92

Supplementary Figure S2-4. Swelling of microneedle. 93
Supplementary Figure S2-5. Sterilization with x-ray irradiation. 94
Supplementary Figure S2-6. Dynamic light scattering (DLS) was used to measure hydrodynamic diameter of PLGA-tetracycline NPs. 94
Supplementary Figure S2-7.Antibacterial test. 95
Supplementary Figure S2-8. Secreted IL-1β level after treatment of IL-4-loaded MNP. 95
Supplementary Figure S2- 9. Effects of MN in contact with cells in vitro. 96
Supplementary Figure S2-10. In vivo evaluation of the immunomodulatory effects in a rat model of periodontitis. 97

Supplementary Figure 3-1. Cytotoxicity of immunomodulators. 98
Supplementary Figure 3-2. Antibacterial effects of azithromycin on P.g. and A.a. plate culture. 99
Supplementary Figure 3-3. Flow cytometry analysis gating strategy 100
Supplementary Figure 3-4. Release profile from PLGA of various densities. 101
Supplementary Figure 3-5. Antibacterial effects of azithromycin on P.g. and A.a. plate culture. 102
Supplementary Figure 3- 6. In vitro effects of azithromycin on human PBMC. 103
Supplementary Figure 3-7. Dissolvable microneedle fabrication strategy. 104

Supplementary Figure 4-1. The effects of local immune suppression on in vivo gene transfer. 105
Supplementary Figure 4-2. Optimization of trehalose amount. 106
Supplementary Figure 4-3. Virus-loaded CMC-based microneedle fabrication strategy. 107

LIST OF TABLES

Table 7-1. Microneedle material design 110
Table 7-2. Properties of each organic solvent..... 110

ACKNOWLEDGEMENTS

Ph.D. journey is like a glass of wine with a symphony of flavors. Whether bitter or sweet with each twist and turn, this journey is filled with blessings and kindness. I am sincerely grateful for the ones who made everything possible and left memorable marks in my life. I would like to extend my heartfelt appreciation to the following people.

First and foremost, I would like to give my sincere thanks to my graduate advisor – Prof. Song Li for his invaluable mentorship, guidance, support, and encouragement. He is super supportive on new ideas and innovations, providing a handful of resources and establishing appropriate connections. He taught me no matter the barriers, always make things happen! He pushed me to solve problems and climb over many obstacles in research by thinking out-of-the-box, analyzing critically, asking unceasingly and working collaboratively. With his encouragement and reassurance, I become a more proactive person who can provide solutions to problems, communicate timely with collaborators and manage research projects. The training on thought process and change of attitude when tackling a problem will be valuable for me life-long. Thank you Prof.Li for your sincere trust, constant encouragement and significant investment in me over the past five years.

I would also like to thank Dr. Mahdi Hasani, who enlightened, inspired and empowered me academically and personally since Day 1 of my graduate school. He oriented me with loads of knowledge related to immunoengineering; he introduced me to all the available resources on campus and collaborator labs; he helped me whenever I needed guidance and support. His immense knowledge and bold brainstorms have encouraged me in all the time of my research and career. Our discussions are always densely loaded with useful information, great inspirations and action items. He is not only a knowledgeable mentor to support me intellectually but also a very dear friend, who cares about my struggles and growth. He cheered me up when I was at the border line of giving up. He pushed me to get out of my comfort zone and speak up. I won't be

who I am without his inspiration. Thank you, Mahdi, for your support, patience, genuineness, and kindness as always.

My gratitude extends to my thesis committee members. Prof. Amy C. Rowat supported my exploration on mechanobiology and biomaterials. I am grateful for her kindness and brilliant criticism that guided my research, as well as the full pages of red marks and comments after editing my draft review paper. Prof. Alireza Moshaverinia and Prof. Cun Yu Wang as collaborators and experts in dentistry provided professional and clinical insights on treatments for periodontal diseases and mechanisms of chronic inflammation. Prof. Zhen Gu, who was on my committee during his time at UCLA, gave lots of technical insights and suggestions on microneedle patches and instills the spirit of zero-to-one innovation. Prof. Manish Butte, who was on my committee for some period of time, gave insights on the mechanobiology of T cell and biomaterials.

Working on interdisciplinary projects, I am incredibly grateful for all the collaborators. Dr. Reihaneh Haghniaz trained me with microneedle fabrication which laid the foundation for the PhD thesis. Dr. Erfan Dashtimighadam from Troy University helped with most of the animal experiments of microneedle patch on ligature-induced periodontitis model in rat. Dr. Tara Aghaloo and Dr. Olga Bezouglaia also helped with some dental surgeries with the same periodontitis model. Dr. Bhumika Shokeen from Dr. Renate Lux lab taught me anerobic bacterial culture and developed antibacterial assay with me. Dr. Peng Zhao from Dr.Reza Ardehali lab supported open-heart surgeries for cardiac infarction model in mouse. Dr. Ke (Kevin) Huang from North Carolina State University Ke Cheng lab conducted further cardiac infarction model with microneedle patch and helped to examine the heart functionalities.

Furthermore, I am deeply thankful for all former and current lab members in Li lab and Butte lab. Thank you for a supportive and collaborative environment to conduct research; for your smile and greetings every day; for every conversation casual or technical; for sincere suggestion that facilitated my growth. Many thanks to our lab “Wikipedia” - Dr. Jennifer Soto for managing the lab nicely and always having an answer to most of my questions and asks; Dr. Fatemeh

(Negin) Majedi for her patience and gentleness on showing me many experimental procedures and for encouraging me on the startup journey with her own stories; Dr. Yang Song for teaching me animal handling and primary cell culture techniques in the early days of research; Dr. Jana Zarubova for collaborating on some immunoengineering and dental-related projects and lightening my day every time with her warm smile in beautiful dresses; Matthew Miller for all the miscellaneous help I needed in Butte lab and the warm greetings every time; Dr. Tim Thauland for providing technical help with various experiments and editing my review on mechanobiology; Crystal Xiao for assisting with rat handling and blood collection and more importantly going through many challenges together to explore commercialization of a prototype; Dr. Zeyang Liu for generously introducing me to potential collaborator and sharing his experience with microneedle fabrication and commercialization; Tyler Hoffman for coordinating mouse heart surgeries and helping me to be brave at grabbing a mice and injecting substances; Joyce Huang for heart fixation, cryosection and immunostaining; my undergraduate student Isabelle Hong for assisting with experiments and graphic illustrations, and for bringing sweetness into my routine laboratory life. Also, all other lab members from Li lab: Dr. LeeAnn Li, Dr. Xili Ding, Dr. Pingping Wang, Dr. Weikang Zhao, Buwei Hu. Dr. Jun Fang, Binru Chen, Shiyi Li, Yifan Wu, Ramzi Massad, Jing Tian, Yu Zhu, and Xiao Han and all other lab members from Butte lab: Eta Atolia, Jennifer Aron, Humza Ali Khan, Michael Trump, and Rina Nagarajan.

My additional appreciation to those who generously shared science with me: Zejun Wang and Hongjun Li from Zhen Gu lab, Tae-Hyung Kim and Chau Ly from Amy Rowat lab, Ruxing Fu from Yang lab, Hossein Montazerian from Ali Khademhosseini lab, Joshua Karam from Stephanie Seidlits lab, Wei-Chia (Elizabeth) Luo from Gerald Wong lab, Dr. Fan Bai, Dr. Zhichao Liu, Dr. Yi Zhang from Neuroiz Co., Ltd., Zheng Cao from Yunfeng Lu lab, Xiyao Li from Cun-Yu Wang lab, Dr. Bo Yu.

Many thanks to the technical assistance and training at core facilities: the CNSI Crump Preclinical Imaging Technology Center and especially its staff Shili Xu, the Electron Imaging

Center for NanoMachines (EICN), the Division of Laboratory Animal Medicine (DLAM). Also, great thanks to the former and current administrative staffs at bioengineering department, Stacy Fong, Andrew Lao, Apryll Chin, Daphne-Jane Dizon, Lili Bulhoes, Sarah Matautia, and Emilia Rodriguez-Vera.

I am also incredibly grateful for the mentors and professors who shaped my life path and academic career step by step: Zhilin Zhao (literature teacher), Dr. Harold Craighead (Cornell undergraduate research), Dr. David Putnam (Cornell master research), Dr. Jinhong Chang and Dr. Ju-Tao Guo (Blumberg Institute).

The past five years won't be so transforming and life changing without my friends, sisters and brothers. Pastor Wang's and Pastor Xiao's sermons and the fellowship every week supplied nutrients and courage to continue my PhD journey and felt like home. My deep gratitude to every person who I won't be naming everyone here. Moreover, for friends not in LA but supporting with a distance: Yiyi Zhang has been gone through valleys and mountains by my side and enlighten me with true wisdom; Pinyuan Xian inspired me on scientific graphic illustrations from her professional designer perspective and refreshed me with adorable kids' videos.

My boundless gratitude to my husband Junjun Cheng. Thank you for going through the storms with me, holding hands and waiting in hope. Your love frees me from feeling insufficient and insecure. Your presence reminds me how truly blessed I am.

Last but most important, to my dear family members for their unwavering love and attentive care: my parents for loving me with all their hearts and encouraging me to pursue my dream; my Aunt Amy and Uncle Peter for generously providing me with the greatest opportunities and deeply inspiring me with their entrepreneurship and innovative souls; my in-laws for giving Junjun and I total freedom to live out our own life and supporting us with no conditions but love; Mr. and Mrs. Ichihashi for their gracious care and all the Japanese delicacy filled with love and tenderness.

This work is supported in part by grants from the National Institute of Dental & Craniofacial Research (R56DE029157), Center for Dental, Oral and Craniofacial Tissue Organ Regeneration

(U24 DE026914), Eli and Edythe Broad Center of Regenerative Medicine and Stem Cell Research Award Program, National Heart, Lung, and Blood Institute (R01HL149940), and National Institute of Diabetes and Digestive and Kidney Diseases (R01DK112939).

Chapter 2 is a version of **Zhang, X.**, Hasani-Sadrabadi, M. M., Zarubova, J., Dashtimighadam, E., Haghniaz, R., Khademhosseini, A., Butte, M. J., Moshaverinia, A., Aghaloo, T., & Li, S. (2022). Immunomodulatory microneedle patch for periodontal tissue regeneration. *Matter*, *5*(2), 666–682. https://doi.org/https://doi.org/10.1016/j.matt.2021.11.017

Chapter 3 and Chapter 4 includes data and text from unpublished manuscripts in preparation.

Appendix C is a version of **Zhang, X**., Kim, T.-H., Thauland, T. J., Li, H., Majedi, F. S., Ly, C., Gu, Z., Butte, M. J., Rowat, A. C., & Li, S. (2020). Unraveling the mechanobiology of immune cells. *Current Opinion in Biotechnology*, *66*, 236–245. https://doi.org/https://doi.org/10.1016/j.copbio.2020.09.004

Appendix D is a version of Zarubova, J., **Zhang, X.,** Hoffman, T., Hasani-Sadrabadi, M. M., & Li, S. (2021). Biomaterial-based immunoengineering to fight COVID-19 and infectious diseases. *Matter*, *4*(5), 1528–1554. https://doi.org/https://doi.org/10.1016/j.matt.2021.02.025

VITA/BIOGRAPHICAL SKETCH

EDUCATION

2014	B.S. in Chemical and Biomolecular Engineering Cornell University, Ithaca, NY
2015	M.Eng. in Chemical and Biomolecular Engineering Cornell University, Ithaca, NY
2016-18	Research Fellow Baruch S. Blumberg Institute, Doylestown, PA

PUBLICATIONS

- Gao, Z., **Zhang, X.,** Zhang, L., Wu, S., Ma, J., Wang, F., Zhou, Y., Dai, X., Bullitt, E., Du, Y., Guo, J.-T., & Chang, J. (2022). A yellow fever virus NS4B inhibitor not only suppresses viral replication, but also enhances the virus activation of RIG-I-like receptor-mediated innate immune response. *PLOS Pathogens*, *18*(1), e1010271. https://doi.org/10.1371/journal.ppat.1010271

- Zarubova, J., Hasani-Sadrabadi, M. M., Dashtimoghadam, E., **Zhang, X.,** Ansari, S., Li, S., & Moshaverinia, A. (2022). Engineered Delivery of Dental Stem-Cell-Derived Extracellular Vesicles for Periodontal Tissue Regeneration. *Advanced Healthcare Materials*, *11*(12), 2102593. https://doi.org/https://doi.org/10.1002/adhm.202102593

- **Zhang, X.,** Hasani-Sadrabadi, M. M., Zarubova, J., Dashtimighadam, E., Haghniaz, R., Khademhosseini, A., Butte, M. J., Moshaverinia, A., Aghaloo, T., & Li, S. (2022). Immunomodulatory microneedle patch for periodontal tissue regeneration. *Matter*, *5*(2), 666–682. https://doi.org/https://doi.org/10.1016/j.matt.2021.11.017

- Zarubova, J., **Zhang, X.,** Hoffman, T., Hasani-Sadrabadi, M. M., & Li, S. (2021). Biomaterial-based immunoengineering to fight COVID-19 and infectious diseases. *Matter*, *4*(5), 1528–1554. https://doi.org/https://doi.org/10.1016/j.matt.2021.02.025

- **Zhang, X.,** Kim, T.-H., Thauland, T. J., Li, H., Majedi, F. S., Ly, C., Gu, Z., Butte, M. J., Rowat, A. C., & Li, S. (2020). Unraveling the mechanobiology of immune cells. *Current Opinion in Biotechnology*, *66*, 236–245. https://doi.org/https://doi.org/10.1016/j.copbio.2020.09.004

- **Zhang, X.,** Cheng, J., Ma, J., Hu, Z., Wu, S., Hwang, N., Kulp, J., Du, Y., Guo, J.-T., & Chang, J. (2019). Discovery of Novel Hepatitis B Virus Nucleocapsid Assembly Inhibitors. *ACS Infectious Diseases*, *5*(5). https://doi.org/10.1021/acsinfecdis.8b00269

- Ma, J., **Zhang, X.,** Soloveva, V., Warren, T., Guo, F., Wu, S., Lu, H., Guo, J., Su, Q., Shen, H., Solon, E., Comunale, M. A., Mehta, A., Guo, J.-T., Bavari, S., Du, Y., Block, T. M., & Chang, J. (2018). Enhancing the antiviral potency of ER α-glucosidase inhibitor IHVR-19029 against hemorrhagic fever viruses in vitro and in vivo. *Antiviral Research*, *150*. https://doi.org/10.1016/j.antiviral.2017.12.008

- Ma, J., Wu, S., **Zhang, X.,** Guo, F., Yang, K., Guo, J., Su, Q., Lu, H., Lam, P., Li, Y., Yan, Z., Kinney, W., Guo, J.-T., Block, T. M., Chang, J., & Du, Y. (2017). Ester Prodrugs of IHVR-19029 with Enhanced Oral Exposure and Prevention of Gastrointestinal Glucosidase Interaction. *ACS Medicinal Chemistry Letters*, *8*(2). https://doi.org/10.1021/acsmedchemlett.6b00332

RESEARCH & ACADEMIC EXPERIENCE

2018 – present	**Song Li lab** (Ph.D. Advisor), UCLA Bioengineering
2019 – 2020	Teaching Assistant, Cell Engineering; Stem Cell Engineering; System Integration in Biology, Engineering, and Medicine
2015 – 2018	**Jinhong Chang Lab**, Baruch S. Blumberg Institute
2014 – 2015	**David A. Putnam lab**, Cornell University Biomedical Engineering
2012 – 2014	**Harold G. Craighead** lab, Cornell University Applied Engineering and Physic

1. BACKGROUND

1.1 Overview

The immune system is responsible for defensing the body against pathogens and maintaining health. It recognizes antigens, eliminates pathogens or infected cells, produces antibodies, generates memories and checks for damaged or mutated cells. However, when the delicate balance of the immune system is disrupted, the immune cells can no longer make the most appropriate reaction, or they are not in a favorable environment to respond with an advantageous behavior. It may attack healthy cells and tissues, leading to autoimmune diseases; or mis-react to a harmless substance, leading to allergies. Also, overreaction to an infection may cause tissue damages or even organ failures, whereas underreaction increases the susceptibility of infections and cancers. A balanced immune response is critical to prevent hyperactive or hypoactive immunity.

The scenarios for hyperactive immunity are complicated and differ case by case. For inflammatory diseases, immune systems can be misled by pathogens and trigger ineffective responses. As pathogens are not killed, persistent inflammatory responses lead to chronic inflammation and tissue damages. Moreover, during medical treatments such as organ transplantation, cell therapy and gene therapy, immune systems can hinder a good cure for the body by rejecting all foreign materials (*i.e.,* tissues, cells, viruses, genetic materials) regardless of their therapeutic impacts. In both natural pathogen and medical intervention cases, they can trigger a severe immune response known as the cytokine storm. The excessive and uncontrolled release of signaling molecules - cytokines circulates all over the body and lead to widespread tissue damage, which can be life-threatening. Immune suppressants are typically used to calm down cytokine storm. However, if local tissue environment is controlled and local immune cell behavior is guided, we can prevent the inflammation evolves into a whole-body immune defense mechanism and circumvent systemic immunosuppression[1].

The increasing understanding of the immune system leads to a new generation of immunomodulatory strategies - local immunomodulation. Immunomodulatory agents including small molecules, cytokines, growth factors and cells are placed locally at the target site for a localized and controlled release. To be noted, local delivery is different from targeted delivery although they are both intended for a specific targeted site. Targeted delivery is usually still administered systematically, but the therapeutic agents – either molecules or nanoparticulate systems – can end up at the desirable site from the blood circulation. However, local immunomodulation utilizes local drug delivery methods to restrain the modulation to a specific site. Immunomodulation via localized treatment techniques will be the scope this dissertation. Nevertheless, local immunomodulation is not limited to local consequences. Trafficking of the immune cells throughout the lymphatic system allows systematic effects and immune memories throughout the body. As the microenvironment plays a key role to drive the immune cells trafficking and guide their behaviors, local immune modulation aims to turn the wheel towards a desirable direction when immune cell reactions trapped in a vicious circle, thus restoring the immune balance and homeostasis. Comparing to traditional administration via an intravenous bolus injection, local immunomodulation regulates the immune cell responses at the target site without causing systematic hyperactivation or hypoactivation[2].

The development of biomaterials and innovative drug delivery methods enables numerous possibilities for local immunomodulation. Implants, injections, adhesive patches, and other engineered systems are investigated and optimized for local immunomodulation. To construct novel delivery systems, a variety of biomaterials, including scaffolds, hydrogels, nanoparticles and microparticles, nanoscale fibers and porous foams are being developed to enable new immunomodulatory interventions[3]. Macroscale biomaterial scaffolds are used as a local niches for immune cell recruiting and manipulating[2,4]; hydrogels are used as protective shields to encapsulate allogeneic cells for transplantation[5–7] and in other cases are modified to be adhesive hydrogels for transdermal applications[8]; biodegradable particles to provide sustained and

controlled release or mimic antigen presenting cells[3,9,10]. Many applications are developed for vaccines in the area of infectious diseases and cancer immunotherapies. But it also worth the attention to engineer novel local immunomodulation system for correcting the hyperactive local immunity to (1) mitigate inflammation and regenerate tissues as well as (2) promote effective gene delivery and *in situ* reprogram cell types.

To address these challenges, my research utilizes an innovative delivery platform - microneedle patches (MNP) as a minimal invasive and easy-to-use local delivery strategy, which opens up new avenues to modulate local immunity and promotes the clinical development of therapeutics. My research is focused on two topics at the interface of immunoengineering, drug delivery and tissue regeneration: (1) developing local immunomodulatory MNP to reverse periodontal degeneration in periodontitis, and (2) boosting gene transfer efficiency of live therapeutic viral vector via MNP to regenerate cardiomyocytes after myocadiac infarction.

1.2 Microneedle Patch (MNP)

Microneedle or microarray patches (MNPs or MAPs) are micron-scaled sharp protrusions arrange in arrays. Due to its improved penetration, even spread, fast healing and painless administration, MNP can be a good candidate for local immunomodulation. The release profile can be tuned for prolonged and controlled drug release to minimize the peak of drug concentration and reduce systematic toxicity[11]. Their unique administrative flexibility of applying and removing MNP further improves patient compliance and makes self-administration possible for hospital-to-home treatment solutions. Some concerns of MNP includes its loading capacity due to limited volume, varied drug amount due to application variation and potential irritation due to surface contact[11]. Thus, designing appropriate materials and therapeutics of MNP delivery is crucial to cope the challenge.

From a broad perspective, drug delivery microneedles are generally classified into five types by their design and drug delivery mechanisms: hollow, solid, coated, dissolvable, and biodegradable microneedles[11–13]. Hollow microneedles are micro-scale version of conventional needles, which create channels to infuse liquid medication to be injected from a drug reservoir. Solid microneedles (also known as microneedling techniques) are commonly used for tissue pretreatment techniques to puncture the surface and promote permeation and diffusion of drugs through the holes. Therapeutic patches, gels or creams are needed afterwards for actual drug delivery. Coated microneedles eliminate the two-step process of tissue pretreatment and drug application by having water-soluble therapeutics directly coated on the surface of solid microneedles. With a quick delivery and dissolution of the coat, the body of microneedle is removed and discarded. Unlike the hollow, solid and coated microneedles which need sharp disposal and has potential safety concerns, dissolvable and biodegradable microneedles can be made into drug-encapsulated patch formulations which are easy to administrate and safe to dispose. Dissolvable MNPs are made of water-soluble materials and the needles melt immediately after being pushed into the tissue, whereas biodegradable microneedles are made of biodegradable polymers or cross-linked hydrogels and the needles degrades slowly over time for a sustained release.

MNPs refer to the polymeric microneedles in patch formulation which are typically made of dissolvable/degradable polymers or cross-linked hydrogels. Fabrication techniques include (1) micromold solvent casting using centrifugation, vacuum, atomized spraying or droplet dispensing[14], and (2) liquid drawing methods[15]. Conventionally, a master micromold is made by photolithography, photochemical etching, laser cutting and 3D printing to customize the desirable size, shape and spacing. Followed by having a master MNP with durable materials, negative molds are casted using PDMS-based materials. Casting by centrifugation fills the microneedle to its tips and if any particles enclosed are accumulated at the tips for delivery. Vacuum can be used in two ways: unidirectionally at the other side of gas-permeable molds; ubiquitously to expel the

air at the tips. On the contrary of the casting methods, no molds are needed for drawing methods. The core technology and barrier are dispensing droplets in arrays and modulating the thickness of matrix materials to dry quickly. Hyungil Jung's group is the pioneer in drawing methods and they developed two droplet-based drying methods - droplet-born air blowing (DAB) methods and centrifugal lithography[15–17].

After knowing the potential fabrication techniques to make MNP, the goal is to optimize the MNP design for maximal dose administered and minimal side effects. Mark Prausnitz's group systematically examine the efficiency of dose administered to human subjects. By assessing dose delivery efficiency, total dose delivered, dose delivered per MN, depth of MN penetration and whole-MN delivery efficiency after MNP application to human subjects, Li, W. *et al.* discovered that all these parameters generally increased with decreased MN length (800-1500μm), increase number of MNs (225-900 MNs per patch) and increased MN-MN spacing (600-1100μm)[18]. To further improve the efficacy and precision of therapeutic dose delivery, various shapes have been explored. The most common ones are pyramid, cone with casting method and pointed with DAB method. Researcher manipulated pyramid to elevated it on a stem or pillar to get obelisk or bevel obelisk shapes[19–21]. Bubble and pedestal designs were designed for easy peel-off the base layer after application[22,23]. More creative shapes were evolved such as arrowhead, shark-tooth inspired shape, Christmas tree shape, and many other shaped microneedle patches[24–26].

In addition to the MN size, shape and spacing, another critical parameter to characterize MNP is its mechanical strength, which also contribute to the success of penetration[27]. Thus, suitable materials are selected to provide sufficient mechanical strength, for burst or controlled drug release and to protect the integrity of active pharmaceutical ingredients (APIs). Carbohydrates such as hyaluronic acid (HA), chitin, chitosan, chondroitin sulfate, cellulose, sucrose, dextran and galactose and dissolvable/degradable polymers such as carboxymethyl cellulose (CMC), poly (glycolic acid) (PGA), polylactic-co-glycolic acid (PLGA), poly (vinyl alcohol) (PVA), poly (vinylpyrrolidone) (PVP) are employed for MNP production[14,28,29]. Crosslinked

polymers such as poly(methylvinylether co. maleic acid) (PMVE/MA) with poly(ethylene glycol) (PEG), methacrylated HA (MeHA) and gelatin (GelMA) and multiple other polymers such as PVA, poly(2-hydroxyethyl methacrylate) (pHEMA), and poly(styrene)-*block*-poly(acrylic acid) (PS-*b*-PAA) are used for hydrogel-based MNP fabrication[30].

MNP has been introduced first as a device for transdermal drug delivery[31] and later evolved into various application to eyes, scalp, nail and vagina[32]. It is used both as a local delivery platform for skin diseases and wound healing as well as a systematic delivery strategy for vaccines, insulin and hormones. One of the most researched applications is transdermal vaccination due to the abundant presence of antigen-presenting cells in the dermis rather than muscles[12,13]. Clinical trials have been established for influenza, SARS-COV2, hepatitis B, varicella, poliomyelitis and many other infectious diseases[33–45]. Upon pandemics or epidemics, MNP can be easily distributed and applied without the disposal of sharp syringes. Recent advance of MNP extends to mucosal layers and internal organs[46]. Inside the oral cavity, there are buccal MN delivery for macromolecules such as insulin[47]; intratumoral delivery for oral squamous cell carcinoma[48]; and oral mucosal delivery of lidocaine for topical anesthesia[49]. For cardiac delivery, MNs are used as tissue penetrator for diffusing of the regenerative factors from stromal cells [50]. It is very beneficial to be tissue adhesive when applying MNPs to these wet physiological environments. Thus, many bio-inspired adhesive MN “bandage” were engineered[51–53].

1.3 Biomaterial-enabled Local Immune Modulation

Drug delivery approaches based on engineered biomaterials open the avenues for localized immunotherapies, which augment or suppress intrinsic host immunity locally and mitigate side effects[2,54–56]. The immune cell behaviors in their microenvironment are modulated by physical and chemical properties of the biomaterials. Thus, various biomaterial-based systems have been explored for local immune modulation.

First, on a macroscale, biomaterial scaffolds offer a niche environment for modulating the local immune cell behaviors. Design and synthesis of scaffolds are intended to be biocompatible, biodegradable and minimal invasive if possible. Injectable systems are developed for in situ gelation or as preformed scaffolds with shape memory or shear thinning properties, whereas implantable systems are designed to pair with surgeries[2]. The injectability of a scaffold depends on its physical and chemical properties as well as the polymerization mechanism. The rheological properties of a scaffold play a significant role in determining its flow behavior and viscosity. It must have low viscosity and flow easily through a needle or catheter. To improve the flow properties, adjustments can be made to the concentration of the scaffold components, addition of plasticizers or surfactants, or by using shear-thinning materials. The particle size and distribution can also affect injectability, with smaller particles and narrower size distribution being preferred. In situ polymerization is enabled by enzyme-mediated crosslinking, Schiff base crosslinking, photocrosslinking, and thermosensitive polymers.

Three-dimensional polymeric networks are purposefully designed for different mechanism of action and release kinetics. They have been widely used for cell encapsulation and controlled release of therapeutic cargos[57]. Macroporous networks allow trafficking of cells into and out of the scaffolds while nanoporous scaffolds typically deliver therapeutics cargo to local and surround tissues without cellular infiltration[22]. Choice of base materials range from synthetic polymers such as PEG to natural polymers such as gelatin, hyaluronic acid and alginate[57,58]. Surface chemistries can affect cargo affinity to the material (i.e. most ubiquitous adhesion ligand is the tripeptide sequence arginine-glycine-aspartic acid (RGD)), enable cargo immobilization onto the materials (i.e. stimulatory antibodies anti-CD3 and anti-CD28 for T cell activation) and influence the rate of degradation. Following the overarching design principles, David Mooney's group employs implantable PLG macroporous scaffold and injectable alginate-based gels as cancer vaccines to elicit immune responses[59,60]. Pore-forming gels are formed in situ when mixed with a porogen and a calcium source; and cryogels are premade porous scaffolds by freeze-drying which can create

a porous structure that is easily rehydrated and injected[2]. Majedi, FS. *et al.* utilizes peritumorally implanted macroporous scaffolds made from alginate to deplete regulatory T cells locally and attract effector T cell to promote their activation towards tumor antigens globally[4]. Inflammatory-modulating hydrogels loaded with inflammation inhibitors and anti-inflammatory cytokines are also used to mitigate osteoarthritis and promote cartilage regeneration[61]. Jennifer Elisseeff's groups develops a tissue ECM-derived scaffolds to drives T helper 2 cells differentiation and guides interleukin-4-dependent macrophage polarization[62].

Second, on a microscale, particulate systems are used to deliver therapeutics locally and/or mimic antigen presenting cells (APCs). The activation of immune cells depends on particle size, shape, surface charge, molecular weight and hydrophobicity[63,64]. In general, because of their size, nanoparticles are more commonly used for targeted modulation of immune cells and tissues[65,66]. However, when the particles are on a micro-size or they are hitchhiking onto a micro-sized cell, they can used for local onsite delivery to a specific tissue. PLGA microparticles are used as depots for controlled and sustained release of APIs for immunotherapies[67,68]. A single shot of mesoporous silica rods containing synthetic molecules and peptides induces humoral responses again small antigen[69]. Moreover, erythrocytes, macrophages, neutrophils and myeloid cells have been explored as biological carriers to drugs to tissue targeted delivery[70–73]. Specifically for local immune modulation, IFN-γ backpacks are robustly adhered onto macrophages and adoptive transfer into immunosuppressive environment of tumors to trigger immune responses intratumorally and reducing metastasis[70]. Another strategy for inducing immune responses is artificial APC, which displays immunomodulatory ligands and releases antigens or soluble immunomodulators. With a better understanding of the immunological synapses, many engineered approaches have been attempted such as carbon nanotube display of T cell agonists and multivalent polymeric presentation of immune stimulants[64,74–77].

Finally, depending on the accessibility of the local tissues, multiple strategies have been evolved for local immune modulation. For inflammatory skin diseases such as atopic dermititis,

topical application of corticosteroids as immunosuppressants has been used since long time ago. Creams, gels, patches and nowadays MNPs are applicable for transdermal local delivery. Also, for dental inflammations like periodontitis and periimplantitis, films, composites, and injectable particles are explored in dental research. Local immunomodulation plays a key role for training immunity, reestablishing the immune homeostasis and regenerating tissues. It is important to understand how to talk to the immune cell effectively with the help of biomaterials. Novel biomaterial frameworks and delivery strategies enable better treatment with more control and precision.

1.4 Tissue Regeneration and Chronic Inflammation

1.4.1 Tissue Regeneration

Immune homeostasis is critical to tissue development, regeneration and repair[78]. Although stem cells are responsible for regenerating, their regenerative capacity is influenced by regulatory networks and orchestrated by local immune responses. Cellular and molecular signals of the local stromal microenvironments contribute to successful tissue regeneration. The mobilization and specialization of endogenous stem cells towards regions of tissue damage is heavily dependent on an inductive "niche" consisting of supportive cells such as macrophages, myofibroblasts, and other immune cells, and typically, a well-defined extracellular matrix (ECM) that stimulates the process of tissue restoration[79]. Therefore, recreating the local “niche” with appropriate immune environment is critical to guide stem cell regenerative behaviors.

Both innate and adaptive immune cells play a pivotal role in the intricate process of tissue regeneration, exerting their effects through complex signaling pathways. Biomaterial-based tissue engineering approaches have been developed for immunomodulation of innate and adaptive[80]. Generally, inflammation causes imbalanced immune microenvironment and chronic inflammation leads to tissue damages. Neutrophils and mast cells are short lived first responders after injury to recruit monocytes to the damaged cite. They rapidly react to restore barrier integrity

and maintain tissue homeostasis. Macrophages are abundant at all stages of fighting pathogens from acute inflammation to tissue repair[81]. They play a central role for the injury response and coordinator of tissue restoration. Classically, they are categorized into proinflammatory M1 and tissue-repairing M2 phenotypes; but the reality is the more complicated with a full spectrum of states that depend on their functions in the microenvironment[79,82]. There are tissue-resident macrophages as well as monocyte-derived macrophages. The tissue-resident macrophages have been shown to have tissue-specific and niche-specific functions; and involved in immune surveillance, resolution of inflammation, epithelialization, diminished scarring and providing additional support for tissue stem cells and progenitor cells[79,83]. Regulatory T cells are the policemen in adaptive immunity to regulate and maintain a dynamic balance of various T cell populations. Studies have shown distinct populations of Treg cells after myocardial infarction and skeletal muscle injury protects against adverse ventricular remodeling and contribute to muscle regeneration respectively[79]. Further investigation is necessary to elucidate the heterogeneity of macrophages and Tregs in various tissues and possess a comprehensive understanding of the immune cell's role in each case of tissue regeneration.

As periodontitis is a model inflammatory disease in my research to illustrate local immunomodulation for tissue repair, current knowledge on the disease progression and detailed immune networks involved is discussed in the following section.

1.4.2 Case Study: Periodontal Diseases and Immune Networks Involved

Periodontal disease is a dysbiotic and inflammatory disease[84,85]. The homeostatic balance between microbiome and host is disrupted: a keystone pathogen outgrows in the periodontal microbiota and ineffective immune defense causes chronic inflammation, tissue damages, ligament detachment and eventually bone loss. Deciphering the immune networks behind periodontitis provides in-depth understanding of the local niche involving immune cells, fibroblasts and stem cells. To harness the power of immune system, immunotherapies have been evolved

to target immune cells, regulate local immune environment, and remodel the local tissue towards regeneration. Here, we will discuss in depth the biochemical and immunological cues for the progression of periodontal diseases.

Oral microbiome consists of 200-300 bacterial[86], but only limited bacteria are pathogenic. *Streptococci* is often the initial colonizer unto the teeth surface. With nutrients, it proliferates and set a bedding for other bacteria colonizer in the saliva such as *Actinomyces* species and *Veillonella*. As the plaque builds up and the dental pocket grows deeper, subgingival plaque flora gradually shifts to anaerobic and Gram-negative bacteria such as *Porphyromonas gingivalis* and *Prevotella intermedia.* These pathogenic bacteria outgrow and break the balance of microbiome. They release virulence factors and toxins which can antagonize and/or trigger host inflammatory responses in the subgingival tissue. For instance, *P.gingivalis* produces a group of cysteine proteinase called gingipains and *Aggregatibacter actinomycetemcomitans* secretes a protein toxin known as leukotoxin[87,88]. Gingipains cleave and degrade host proteins including plasma proteins, extracellular proteins, cytokines and antibodies. In this way, it can dysregulate both the innate immunity first-line of defense involving neutrophils, tissue-resident macrophages, complement system and antibacterial peptides, and the adaptive immunity involving antibodies, dendritic cells and cytotoxic T cells. Similarly, leukotoxin shows a direct killing and inhibiting effect on neutrophils *in vitro* and thus prevents a protective host reaction. To decipher the pathogenesis trigged by the bacteria, we will delve into the host immune system next. (Figure of pathogenesis adapted[89])

In contact with the bacteria, tissue-resident immune cells and non-professional mucosal epithelial cells sense the pathogen-associated molecule patterns (PAMPs) on bacteria through pattern recognition receptors (PRR)[90]. For instance, the detection of lipopolysaccharides (LPS) can swiftly activate toll-like receptor 4 (TLR-4) and initiate a series of reaction to release PRR-mediated inflammatory factors. Tissue-resident immune cells are like initial sentinels, but not enough to fight back the bacteria. Thus, to recruit immune cells, a chemokine gradient is

established along the epithelium surround the teeth and the vascular endothelial cells at the inflamed site are activated to upregulate the expression of adhesion molecules such as E-selectin and P-selectin[91].

Neutrophils are the early responder to a foreign pathogen and are the initiator of innate immunity. P-selectin glycoprotein ligand 1 (PSGL 1) mediates the tethering and rolling of neutrophils on P-selectin[92]. During rolling, neutrophils come to close contact with chemokines deposited on the endothelium. Interkeukin-8 (IL-8) activates neutrophils via receptor CXCR2 and activated neutrophiles transmigrate from the blood vessels towards pathogens[93]. Their defense strategy against pathogens includes phagocytosis to engulf bacteria, reactive oxygen species (ROS) production to cause oxidative damage to microbes, granule release to undergo exocytosis and neutrophil extracellular trap (NET) formation with antimicrobial ability to control biofilm buildup[93]. Periodontal pathogens can interfere with any steps in the normal signaling pathways to inhibit recruitment such as inhibiting IL-8 or E-selectin production, blocking the detection of chemokines, and suppressing the actin cytoskeleton rearrangement[93]. Functionally, P. gingivilis also prevents phagocytosis and evade various killing mechanisms. However, inflammation is not the more the better. Periodontitis have been associated with elevated production of ROS and NETs compared with those of healthy control.

Besides neutrophils, macrophages are another type of phagocytic cell. They can be either resident in tissue or differentiated from monocytes. Their functions include antigen uptake, antigen presenting, phagocytosis, nitric oxide release, and wound healing. Without a terminally differentiated lineage, they can be polarized and switched between M1 pro-inflammatory and M2 pro-healing phenotypes. This is possible because of two competing arginine metabolism pathways in macrophages, via nitric oxide synthase (NOS) or arginase[94,95]. Nitric oxides produced by NOS are effective in bacteria killing, while ornithine generated by arginase is an essential amino acid that assists in the proliferation of cells and promotes healing[94]. Studies have been shown that M1/M2 ratio was significantly higher in periodontitis patients compared to healthy

controls and positively correlated with clinical probing depth (PD) and expression of inflammatory cytokines such as IFN-γ and IL-6[96,97]. Induction of M2 macrophages prevents bone loss in *P. gingivalis*–induced mouse model[98].

Moreover, macrophages at the bone can further specialize and differentiate into osteoclasts, which degrade bone[99]. Osteoclasts play an important role in normal bone remodeling together with osteoblasts and mediate alveolar bone loss in the case of periodontitis[100]. Unresolving inflammation in the gingival tissue creates a high concentration of inflammatory mediators and in proximity with the alveolar bone, thus stimulates bone resorption[101]. Major regulator of osteoclasts is RANKL; osteoprotegerin (OPG) is a "decoy receptor" for RANKL and thus act as a suppressor. Elevated RANKL/OPG ratio has been used as a potential biomarker for periodontitis progression[102].

Complement system is another important player in the innate immunity to fight infection and adaptive immunity can also produce factors that feed to the loop. It consists of an interactive cascade of soluble, membrane-associated, and intracellular molecules (C1-9)[103]. C3 is a representative of the entire complement system as it is involved in classical, lectin and alternative pathways. In clinic, elevated C3 level in gingival crevicular fluid (GCF) in periodontitis patients have been observed and complement-dependent hemolytic activity was detected[104,105].

On the adaptive immunity side, there is mucosa-associated lymphoid tissue, structurally similar to lymph node in the oral cavity and gingival lining. Theses lymphoid tissue are the bed for dendritic cells (DC), B cells and T cells. Dendritic cells (DCs) are professional antigen presenting cells and there are various subsets in oral mucosa. They are the first line of immune surveillance to process internalized antigens via a fine control of lysosomal degradation to preserve antigenic epitopes[106]. Then, they trigger various T cell responses, thus becoming the bridge between innate immunity and adaptive immunity. Certain strains of keystone bacteria like *P. gingivalis* weaken the abilities of DCs. Elsayed, R. *et al.* have reported the induction of premature autocrine

senescence in DCs by *P. gingivalis* through direct cellular invasion and amplification of paracrine senescence of bystander DCs through inflammatory exosomes[107].

T cells are activated by recognizing specific antigens presented by antigen-presenting cells, such as dendritic cells, in the periodontal tissue. Once activated, T cells differentiate into different subsets, including effector T cells, such as Th1, Th2, and Th17 cells, and regulatory T cells (Tregs). Each subset has distinct functions and contributes differently to the inflammatory response in periodontitis. T helper 17 (Th17) cells have been identified as major contributors to the pathogenesis of periodontitis. Persistent activation of Th17 cells leads to the production of high levels of pro-inflammatory cytokines, which further exacerbates the inflammatory response in periodontal tissues. Additionally, Th17 cells promote the differentiation of osteoclasts, cells responsible for bone resorption, and induce the production of matrix metalloproteinases (MMPs), enzymes that degrade the extracellular matrix crucial for tissue regeneration[108,109]. The dysregulated activity of Th17 cells contributes to the destruction of periodontal tissues observed in the disease. On the other hand, T regulatory (Treg) cells play a critical role in immune regulation and prevention of excessive inflammation. However, in chronic periodontitis, the functions of Treg cells are impaired, and their numbers are reduced. This imbalance in Treg cell activity compromises their ability to effectively suppress the activity of other immune cells and control the inflammatory response. Understanding the intricate interplay between Th17 cells, Treg cells, and their associated cytokines is crucial for restoring immune homeostasis and promote tissue healing in periodontal diseases.

With profound understanding of the local niche involving immune cells for periodontitis, immunotherapies start to emerge but local immunomodulation using innovative biomaterials is still lack the attention in dental fields. It is critical to regulate local immune environment to modulate immune cells functions and remodel the local tissue towards regeneration.

1.5 Cell Reprogramming and Gene Delivery

1.5.1 Direct Cardiac Reprogramming

Expansion and differentiation from endogenous stem cells are not the only way for tissue regeneration, restoration can also be accomplished by cell engineering. The discovery of induced pluripotent stem cells (iPSCs) by Shinya Yamanaka and Kazutoshi Takahashi in 2006 laid the foundation for a new branch of regenerative medicine. They discovered the fundamental factors later known as Yamanaka factors (Oct3/4, Sox2, c-Myc, and Klf4) to reprogram somatic cells into pluripotent stem cells[110]. Later, direct cell reprogramming or transdifferentiation is inspired to alter the fate of a cell through the introduction of lineage-specific factors, ranging from transcription factor-based methods to small molecule-driven approaches. By directing the expression of key regulatory genes that govern cell fate, cell identity is converted into a new cell type for therapeutic applications, including the regeneration of damaged or diseased tissues[111]. It has been explored to yield a diverse range of cell types from fibroblasts, including neurons, cardiomyocytes, endothelial cells, hematopoietic stem/progenitor cells, and hepatocytes.

Cardiac reprogramming is a promising strategy for heart regeneration, which aims to convert non-cardiac cells into functional cardiomyocyte-like cells in situ. One of the key approaches for cardiac reprogramming sets of defined transcription factors, such as Gata4, Mef2c, and Tbx5 (GMT) - the minimum required to reprogram endogenous cardiac fibroblasts (CF) into induced cardiomyocyte-like cells (iCMs)[112]. GMT-mediated cardiac reprogramming involves the direct activation of cardiac gene expression and the suppression of fibroblast-specific genes, resulting in the conversion of fibroblasts into cardiomyocyte-like cells. In 2012, two labs reported independently that GMT-mediated cardiac reprogramming from fibroblasts improve the cardiac functions of infarcted mouse hearts with and without Hand2[112]. In additional to gene delivery of GMT, administration of a specific combination of microRNA also showed to be effective in reprogramming noncardiac myocytes directly into mature functional cardiac

myocytes in situ, improving cardiac function and repair damaged myocardium[113]. Last but not least, small molecules-based reprogramming modulates signaling pathways and epigenetic modifications in non-cardiac cells to promote their conversion to a cardiac fate. Wang, H. *et al.* reported a small molecule cocktail (SB431542, CHIR99021, parnate and forskolin) which are TGFβ signaling inhibitor, Wnt/β-catenin signaling pathway activator, LSD1/KDM1 inhibitor and adenylyl cyclase activator respectively still enable the cardiac conversion from fibroblast in conjugation with a single transcription factor Oct-4[114]. Cao, N. *et al.* fully chemically induced cardiomyocyte-like cells via a combination of nine compounds and reduced to six compounds under xeno-free conditions in their recent advances[115,116].

To translate this approach into clinical application, it is essential to ensure that the reprogramming process is safe, efficient, and scalable. Challenges remain in optimizing the efficiency and safety of reprogramming methods, as well as ensuring the functional stability and long-term safety of reprogrammed cells. Improving the gene transfer efficiency and localizing the gene transfer region are in urgent need for better clinical tissue regeneration.

1.5.2 Gene Delivery Systems

Gene delivery is a critical step in cell reprogramming when new genetic materials need to be introduced into the cell to alter its gene expression profile and change cell fate. Gene transfer techniques are also widely used in gene therapy, where therapeutic gene is delivered into the cells to replace, alter, or edit a defective gene. Gene transfer can be carried out by direct administration of the gene-transfer vector to the host (aka an in vivo or in situ approach) or by refusion of cells extracted from the recipient that have been genetically modified outside the body (aka an ex vivo approach)[117]. While ex vivo approach suits for engineered cell therapies such as chimeric antigen receptor T-cell (CAR-T) therapy for blood cancers, in situ approach is ideal for local therapy to a specific site because of the low dose, reduced immunogenicity and no systemic side effects[118]. Despite the obstacles and failures faced by clinical gene therapy, gene therapy

is at an inflection point. The blossom of in situ gene transfer is evident in the rapid growth in the number of clinical protocols for different diseases ranging from monogenetic to multifactorial diseases and the approval of genetic medicine since 2017. The approved gene therapy drugs which directly injected into their target tissue or organ are like Neovasculgen, Glybera, Defitelio, Rexin-G, Onpattro, Eteplirsen, Spinraza, Kynamro, Imlygic, Oncorine, Luxturna, Macugen, Gendicine, Vitravene as well as Zolgensma[119].

Viral and nonviral gene delivery systems have been developed in the past a few decades and biomaterial-based vectors aid the delivery of genetic materials at each length scale – nano, micro and macro[120]. Viral gene delivery utilizes the infectious nature of virus to target cells efficiently and selectively while engineers the virus to minimize harmful effects and immunogenicity. Some common viral vectors are retrovirus, lentivirus, adenovirus, adeno-associated virus (AAV), herpes virus and pox virus[121]. The pathogenic and toxic components of the virus are deleted from their genome to ensure the safety and in some cases, the receptors are redesigned to transfer genes into other cell types which are not their original target cells. Nonviral gene delivery involve physical (electroporation, hydrodynamic, ultrasound, magnetofection) and chemical (cationic lipids, cationic polymers, lipid polymers) methods[121]. COVID-19 pandemic accelerates the rapid development of mRNA vaccines and nanoparticle delivery of genetic materials. Polymeric nanoparticles accumulate at a desired site by passive, active and endogenous targeting and self-assembled nanoparticles based on lipid and polymer materials are the state-of-the-art delivery for genetic medicine[122]. Microscale delivery vectors made of PLGA, poly(orthoesters) and poly(β-amino ester) (PBAEs) are primarily focused on DNA vaccination by delivery to antigen-presenting cells for controlled release[120]. At the macroscale originated from tissue engineering, polymer/cell hybrid architectures are utilized for localized gene delivery. Moving forwards, continued innovation of biomaterial-based scaffolds via exquisite control of the chemical composition and mechanical properties of the scaffold materials will expand the field of gene and cell therapy[120].

Among the viral vectors, each of them has its own unique characteristics, advantages, and limitations, making them suitable for different applications and target tissues. Retroviruses are RNA viruses that can integrate their genetic material into the host cell's genome, providing long-term gene expression. Retroviral vectors are one of the most frequently used forms of gene delivery due to their ability to transduce dividing cells and large packaging capacity to deliver larger genes or gene regulatory elements. However, they has the potential of immunogenicity and carry a risk of insertional mutagenesis to possibly cause oncogene activation or tumor-suppressor gene inactivation. With all the pros and cons of retroviruse, lentiviruses are a subclass of retrovirus that can infect both dividing and non-dividing cells. Adenoviruses are DNA viruses that efficiently transduce a wide range of dividing and non-dividing cells. Adenoviral vectors have high transduction efficiency and can achieve robust gene expression in target tissues. They do not integrate into the host genome, which eliminates the risk of insertional mutagenesis. However, they induce significant immune responses, limiting their long-term gene expression and requiring careful consideration of immunogenicity issues. Adeno-Associated Viral vectors are derived from a non-pathogenic virus Adeno-Associated Virus (AAV) which can infect both dividing and non-dividing cells. AAV vectors provide long-term and stable gene expression without inducing strong immune responses. Thus, they are one of the leading platforms for gene delivery in clinic[123]. AAV vectors have a relatively large packaging capacity and can target specific cell types using engineered capsids. However, their packaging capacity is limited compared to retroviruses, and pre-existing immunity to AAV in the population can reduce their effectiveness. Herpes Simplex Virus (HSV) vectors are derived from the herpes simplex virus, which can establish latent infections in neurons. HSV vectors are primarily used for gene delivery to the nervous system. They have a large packaging capacity and can infect both dividing and non-dividing cells. However, their application is limited to specific cell types and can elicit immune responses.

Gene therapy has made great success in a wide range of genetic and acquired diseases, including genetic disorders, cancer, and infectious diseases[124–126]. However, there are still challenges that need to be overcome to make gene therapy a safe and effective treatment option, including issues related to the safety and efficacy of gene delivery, the immune response to the delivered gene therapy, and the potential for unintended off-target effects.

Engineered biomaterials have been designed and developed not only for local immunomodulation but also for *in situ* tissue regeneration. Modulating the immunity and remodeling local tissue are two closely related topics: the prior is the methodology while the latter is the ultimate objective, in this research. Two biomaterials approaches *for in situ* tissue regeneration was described by Gaharwar A., *et al.* in their review[127]. The first approach involves bioresponsive materials that direct endogenous cells for tissue healing and regeneration. The second approach focuses on *in situ* cellular reprogramming using transcription factors, RNA-based therapeutics, gene editing, and epigenetic transformation. This thesis explores both approaches: modulating extracellular signaling in chapter 2, 3 and enhancing intracellular reprogramming in chapter 4.

2. BASE-DISSOLVABLE HYDROGEL MICRONEEDLES FOR GINGIVAL DELIVERY OF IMMUNOMODULATORY FACTORS

2.1 Abstract

Periodontal diseases are caused by microbial infection and the recruitment of destructive immune cells. Current therapies mainly deal with bacteria elimination, but the regeneration of periodontal tissues remains a challenge. Here we developed a modular microneedle (MN) patch that delivered both antibiotic and cytokines into the local gingival tissue to achieve immunomodulation and tissue regeneration. This MN patch included a quickly dissolvable gelatin membrane for an immediate release of tetracycline and biodegradable GelMA MNs that contained tetracycline-loaded poly(lactic-co-glycolic acid) nanoparticles and cytokine-loaded silica microparticles for a sustained release. Antibiotic release completely inhibited bacteria growth, and the release of IL-4 and TGF-β induced the repolarization of anti-inflammatory macrophages and the formation of regulatory T cells *in vitro*. *In vivo* delivery of MN patch into periodontal tissues suppressed pro-inflammatory factors and promoted pro-regenerative signals and tissue healing, which demonstrated the therapeutic potential of local immunomodulation for tissue regeneration.

Graphic Abstract

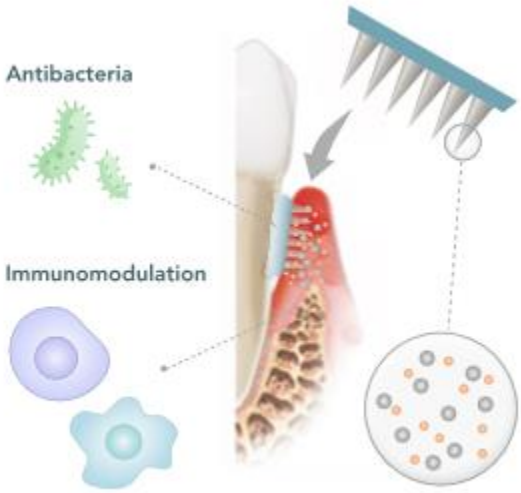

2.2 Introduction

Periodontitis is one of the most common diseases of mankind, and approximately 50% of the American population has some degree of periodontal diseases[128]. It is a prevalent chronic destructive inflammatory disease affecting tooth-supporting tissues in humans[129]. The bacterial colonization of the periodontal pocket and the inflammatory responses of the host collaboratively cause periodontitis. As the disease progresses, tissue inflammation leads to progressive periodontal detachment and the degeneration of the periodontium, including periodontal ligament, and root cementum, alveolar bone, which may eventually lead to early tooth loss[128–130].

Antibiotics have been administered in many forms and formulations as a conventional strategy to combat bacterial infection. Oral administration of antibiotics requires large dosages to reach the effective level at the diseased site. Local administration using biodegradable materials such as poly(lactic-co-glycolic acid) (PLGA) nanoparticles (NPs) can achieve a prolonged release[131,132], but has little effect on periodontal tissue regeneration. Furthermore, none of the existing regenerative treatments directly addresses the problem of inflammatory immune cells in the periodontal microenvironment.

Although microbial infection is the fundamental cause of the periodontitis, the accumulation of destructive immune cells such as macrophages plays a critical role in the periodontitis progression[133,134]. Secretion of inflammatory cytokines and proteases accelerates gingival tissue degeneration, alveolar bone resorption, and periodontal connective tissue damage[133–136]. In addition to macrophages, helper T cells also respond to the micro-immune environment and contribute adversely to the accumulation of inflammatory cytokines and chemokines[137]. We hypothesized that a conversion of inflammatory M1 macrophages and T cells into anti-inflammatory M2 macrophages and T regulatory cells (Tregs) could create a pro-healing microenvironment for periodontal tissue regeneration. It has been shown that cytokines such as interleukin 4 (IL-4) can induce the conversion of macrophages from M1 to M2 type to enhance tissue regeneration[138–140]. In addition, IL-4 can control inflammation by differentiating naïve T cell

into induced regulatory T cells (Treg) in the presence of transforming growth factor b (TGF-β), which also helps repolarize macrophages toward anti-inflammatory (M2) lineages (**Figure S1**)[141]. It is worth noting that IL-4, as determined by meta-analysis, is the only cytokine that decreases in chronic periodontitis patients and increases after periodontal treatment[142,143]. Furthermore, IL-4 can downregulate pro-inflammatory cytokines[144] and restrain osteoclastogenesis[145,146].Therefore, we investigated whether a sustained delivery of IL-4 and TGF-β was sufficient to modulate macrophages and T cells for periodontal tissue regeneration.

Drug delivery in the oral cavity is challenging due to bacterial infection, saliva secretion and poor local retention. To address this challenge and achieve local and sustained drug delivery, we have developed a biodegradable microneedle (MN) patch that can be inserted into the pocket between the tooth and gingival tissue for a painless and suture-free placement into the gingival tissue (**Figure 1a**). For a human patient with severe periodontitis, MN patch can be inserted immediately after scaling and root planning procedure by dentists or hygienists. For less severe periodontitis or gingivitis, MN patch may be placed on the outer surface of the gingiva by patients themselves. This MN patch offers penetration through the gingival tissue and leaves bullets of MNs inside for a sustained delivery of antibiotics and immunomodulatory cytokines. Although MN patches have been employed for transdermal, ocular, vascular and mucosal drug deliveries[147,148], MNs are generally used to deliver a single therapeutic, and there is a lack of a flexible modular design for a controlled delivery of multiple therapeutics at different rates. Here we design a modular MN patch for a multiplex delivery: (1) the base membrane of the MN patch is dissolvable for a burst release of antibiotics, (2) biodegradable NPs in MNs offers a sustained delivery of antibiotics, and (3) heparin-coated mesoporous silica microparticles (SiMPs) are used as carriers to maintain protein stability[149] and ensure a prolonged delivery of IL-4 and TGF-β. This modular MN patch can be easily adopted for various multiplex drug delivery applications. In this study, we explored its application for a multiplex delivery of antibiotic and immunomodulatory cytokines to promote periodontal tissue regeneration.

2.3 Results

2.3.1 Design and fabrication of periodontal MN patch

We designed and fabricated the MN patch with two parts: a dissolvable base membrane and MNs loaded with NPs and SiMPs **(Figure 2-1b**). The supporting base membrane is made of 10% gelatin, which solidifies at room temperature and is dissolvable at body temperature. Antibiotics can be loaded directly into the gelatin membrane and released quickly regardless of the crosslinking state of gelatin. To achieve a burst release with a simple patch design, we did not crosslink the gelatin membrane, which allowed the membrane to be dissolved within minutes. The MNs are made of gelatin methacryloyl (GelMA) crosslinked by UV light. This crosslinked GelMA network does not dissolve immediately but forms a hydrogel structure that degrades over time. The hydrogel holds drug carriers (NPs and SiMPs) in place and allows released therapeutic agents passing through its porous structure. Detailed synthesis and properties of GelMA can be found in our previous publication[150]. After applying MN patch to gingival tissue, the base membrane dissolves quickly for a burst release of antibiotics to immediately reduce bacterial content in the microenvironment, while the biocompatible and bioresorbable MNs penetrate and stay in gingival tissue for a sustained release of antibiotics and cytokines.

For the selection of active ingredients in the formulation, a commonly used antibiotic tetracycline was selected as a model drug, which was loaded into the gelatin base for a burst release and NPs in MNs for a sustained release. IL-4 and TGF-β were loaded into heparin-SiMPs and encapsulated in GelMA MNs. IL-4 and TGF- b have isoelectric points of 9.17 and 8.83, respectively at physiological pH. Enhanced affinity of IL-4 and TGF- b toward PEG-heparin[151] and alginate-heparin [152] based hydrogels has been reported before. Here, negatively charged heparin modified SiMPs can also interact strongly with these cytokines not only to prolong their release but also to protect them from denaturation during the MN fabrication.

The fabrication process is illustrated in **Figure 2-S2**. To fabricate MNs, 20% (w/v) GelMA containing photoinitiator, tetracycline-loaded NPs and IL-4/TGF-β loaded SiMPs were cast on

negative MN molds and centrifuged to fill the molds. The extra mixture was removed, and 10% gelatin containing 5mg/ml of tetracycline-HCl was laid evenly on the top of the mold to create a patch. The MN patches were peeled off from the mold following UV irradiation followed by drying at room temperature. UV light exposure did not cause significant changes of protein stability as the release of IL-4 from MNs with and without UV exposure had similar effects on the gene expression of phenotypic markers in macrophages (**Figure 2-S3**).

2.3.2 Physical characterization and mechanical property of MN patch

As shown in electron microscopy images, the resulting MNs were conical, with a base diameter of 300 μm, a height of 600 μm and a tip diameter of ~15 μm (**Figure 2-1 c,d**). SiMPs accumulated more at the tips of the needle after centrifugation, and roughly occupied 15% of the needle volume due to their high density. Using green fluorescence-labeled NPs and red fluorescence-labeled SiMPs, the distribution of particles in MNs can be seen from the fluorescent images in **Figure 2-1e**.

The mechanical property of MNs is critical for gingival tissue penetration. We performed compression test of MNs with and without NPs or SiMPs. Adding NPs did not significantly affect the mechanical property of MNs, but the addition of SiMPs to MNs strengthened the mechanical strength by two folds (**Figure 2-1f**). These composite MNs had sufficient mechanical strength to penetrate the freshly extracted pig or rat gingival tissues (**Figure 2-1g,h,i**). Slight swelling was observed when MNs were in contact with phosphate-buffered saline (PBS) (**Figure 2-S4**). The degradation rate of the GelMA MNs were characterized in physiologically relevant solutions (**Figure 2-1j**). UV-crosslinked GelMA MNs were degraded by half in PBS with collagenase after 5 days. MN degradation was slightly slower in human saliva (**Figure 2-1j**), which might be accelerated in the acidic environment at the disease sites of periodontitis. In addition, a standard sterilization of MN patches with x-ray irradiation did not change the physical properties of patches (**Figure 2-S5**).

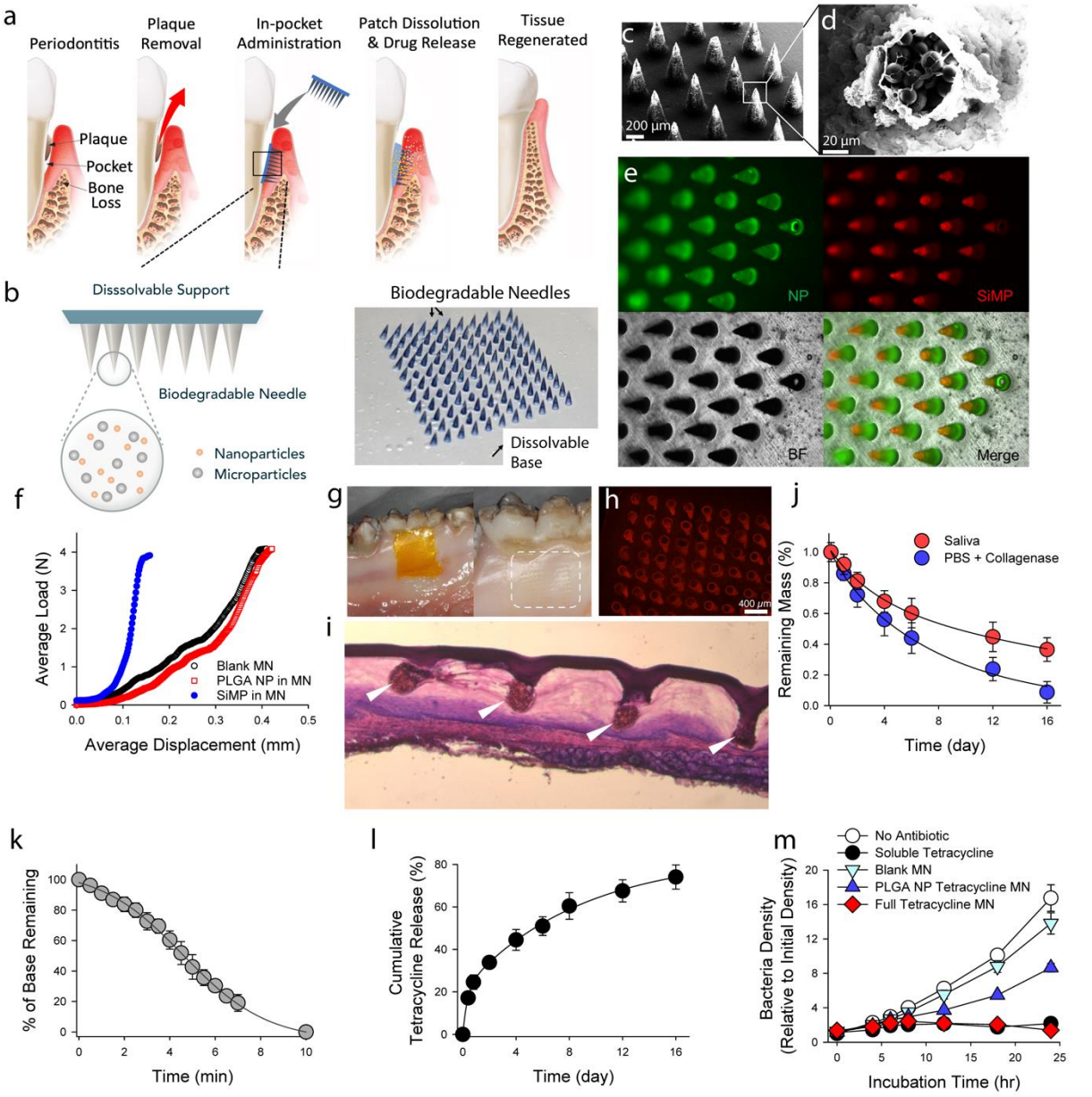

Figure 2-1. Physical and chemical characterization of MN patches.

a, Proposed working mechanism of the designed immunotherapeutic periodontal MN patch. MN patches are designed to provide transgingival administration of antibiotics and anti-inflammatory cytokines. Following administration, MNs will detach from the supporting membrane upon gelatin dissolution and stay in gingival tissue, release their cargos, and degrade. **b**, Illustration of the multifunctional MN patch design. The image on the right shows an example of fabricated MN patch. MNs were visualized by encapsulating Trypan Blue dye. **c**, Scanning electron microscopy (SEM) image of fabricated MNs. **d**, Encapsulated SiMPs can be seen inside truncated needles. See also Figure S2. **e**, Fluorescent imaging demonstrates the distribution of fluorophore-conjugated PLGA NPs (in Green) and SiMPs (in Red) inside GelMA-based MNs. **f**, Mechanical strength of MNs measured by Instron compression test. **g**, MN patch penetrated on freshly harvested porcine gingiva. Following the administration, the tissue was kept in 37°C incubator

for 30 minutes to monitor gelatin dissolution. Pig's gingival surface is showing insertion of MNs. **h**, MN-treated pig gingival tissue was imaged to demonstrate the presence of fluorophore-loaded MNs (in Red). Scale bar: 400 μm. **i**, Penetration of MN into fresh rat gingival tissue was visualized by hematoxylin and eosin (H&E) staining. **j**, *In vitro* degradation of MNs over time in PBS containing collagenase enzyme or human saliva at 37°C under gentle shaking. **k**, FITC-conjugated gelatin was used as the support layer to measure the rate of gelatin base dissolution. **l**, Cumulative *in vitro* release of tetracycline was assessed from the dissolution of gelatin base (burst release) and from GelMA MNs loaded with PLGA-tetracycline NPs (sustained release) at 37°C and pH 7.4. **m,** Antibacterial effect of designed patches against *P.g.* Full tetracycline MN includes tetracycline-loaded gelatin base and tetracycline-loaded PLGA NPs in MNs. The data in **j-m** are presented as mean ± standard deviation (SD) (n = 5).

2.3.3 Delivery of antibiotics by periodontal MN patch and antibacterial effects in vitro.

We designed periodontal MN patch to deliver antibiotics in two stages: first, a burst release during the dissolution of patch base (gelatin), and second, a sustained delivery by PLGA NPs embedded in GelMA MNs. Due to the hydrophobicity of tetracycline, tetracycline-HCl was used for the patch base formulation as it is more water-soluble. As the gelatin base melt at 37ºC in an aqueous environment, the release of tetracycline from the gelatin base was linear and the whole base disappeared after ~10 minutes, shown in **Figure 2-1k**. For PLGA NPs synthesis, tetracycline was dissolved in organic solvent and NPs were synthesized by ultrasonication. The loading efficiency was calculated to be around 70%, and the particle sizes had a relatively uniform distribution around 150 nm (**Figure 2-S6**). Inclusion of antibiotic in both gelatin base and encapsulated PLGA NPs provided sustained and prolonged release profiles (**Figure 2-1l**).

Antibacterial properties of designed patches were evaluated on a standard bacterium, *E.Coli*, as well as clinically pathogenic bacteria *P.gingivalis* (*P.g.*) by using agar-plate and liquid cultures, respectively. We performed antibacterial tests to examine the effects of MN patch-released tetracycline on bacterial growth both on the surface and in solution. Tetracycline released from MN patch had a strong antibacterial activity as assessed by estimating the inhibition zone (**Figure 2-S7**). Consistent bacteria-killing of periodontal disease-causing bacteria *P.g.* was also observed in liquid culture (**Figure 2-1m**). While NP-released tetracycline partially inhibited *P.g*. growth, the full patch was able to inhibit *P.g.* growth completely. These results demonstrated

the successful loading of tetracycline into gelatin base and encapsulation of tetracycline into PLGA NPs in MNs for effective bacterial killing.

To enable a prolonged release of cytokines, we made monodisperse mesoporous SiMPs (~15 μm diameter and ~10 nm pore size) (**Figure 2-2a**) *via* a microfluidic jet spray-drying route as reported before.[153,154] Carbodiimide chemistry was utilized to modify SiMPs with heparin to improve the loading and activity maintenance of cytokines (**Figure 2-2b-c**). *In vitro* degradation of heparin-functionalized SiMPs indicated that these particles were mostly degraded in two weeks (**Figure 2-2d**). The presence of heparin ensured the efficient loading and the prolonged release of IL-4 and TGF-β (**Figure 2-2e-f**).

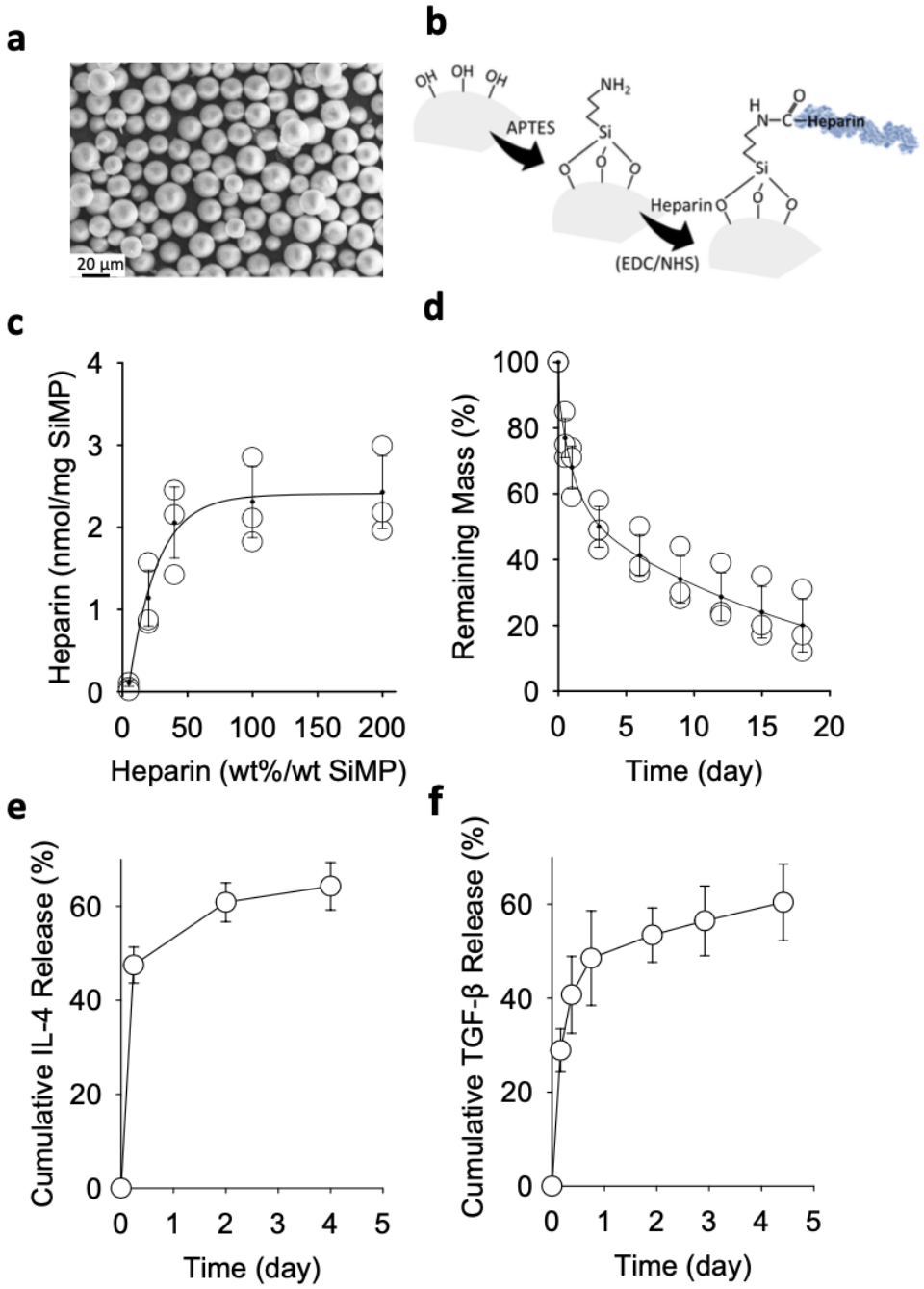

Figure 2-2. Sustained release of IL-4 and TGF-β from silica-heparin microparticles.

a, SEM image of mesoporous SiMPs. **b**, Surface chemistry to functionalize SiMP surface with heparin. **c**, The efficiency of heparin-conjugation on SiMPs with various initial amounts of heparin in the reaction mixture. **d**, *In vitro* degradation of heparin-functionalized SiMPs over time. **e-f,**

Cumulative release of IL-4 **(e)** and TGF-β **(f)** from heparin-functionalized SiMPs at 37°C. The data are presented as mean ± SD (n = 5).

2.3.4 Anti-inflammatory properties of periodontal MN patch in vitro.

To investigate whether the encapsulated cytokines were functional after SiMPs were cast into MNs, MN patches with cytokine-loaded SiMPs were placed in culture wells for a co-culture with murine bone marrow-derived macrophages (BMDMs). Macrophages are known for their plasticity to switch between proinflammatory M1 and pro-healing M2 macrophages. The macrophages can be preferentially induced to produce either inducible nitric oxide synthase (iNOS) (M1 marker) or ariginase-1 (ARG-1) (M2 marker); in addition, M1 macrophages produce inflammatory cytokines like interleukin 1b (IL-1b), and M2 macrophages upregulate mannose receptor C-type 1 (MRC-1).[139,155,156] Therefore, we examined the expression of these biological markers to characterize the status of macrophage repolarization. **Figure 2-3a** demonstrates a sustained release of IL-4 from MN patches over time. Co-culture of IL-4-releasing MN patches with BMDMs that were pre-treated with lipopolysaccharide (LPS) (**Figure 2-3b**) significantly suppressed the expression of pro-inflammatory genes such as iNOS and IL-1b while inducing anti-inflammatory genes such as MRC1 and ARG-1 (**Figure 2-3c)**. Consistently, the secretion level of inflammatory cytokines such as IL-1b into the cell culture media significantly decreased (**Figure 2-S8**). In addition, when IL-4-releasing MN patches were placed in Transwells for a no-contact co-culture with BMDMs, the same effects on pro-inflammatory and anti-inflammatory genes were observed (**Figure 2-S9**). These results demonstrated the maintenance of IL-4 activity during MN fabrication and the immunomodulatory effects of released IL-4 on macrophages.

The presence of TGF-β during T cell activation can induce the formation of Treg [157,158]. SiMPs loaded with TGF-β were encapsulated into MNs and showed a sustained release profile (**Figure 2-3d**). To determine the effects of the sustained presentation of IL-4 and TGF-β on Treg formation, we incubated primary murine $CD4^+$ (helper) T cells with activation signals (anti-CD3 and anti-CD28 antibodies) in the presence of IL-4/TGF-β-loaded MN patches. Indeed, the

sustained release of IL-4 and TGF-β significantly induced Treg formation, which was more effective than adding the soluble form of IL-4 and TGF-β in culture media (**Figure 2-3e**).

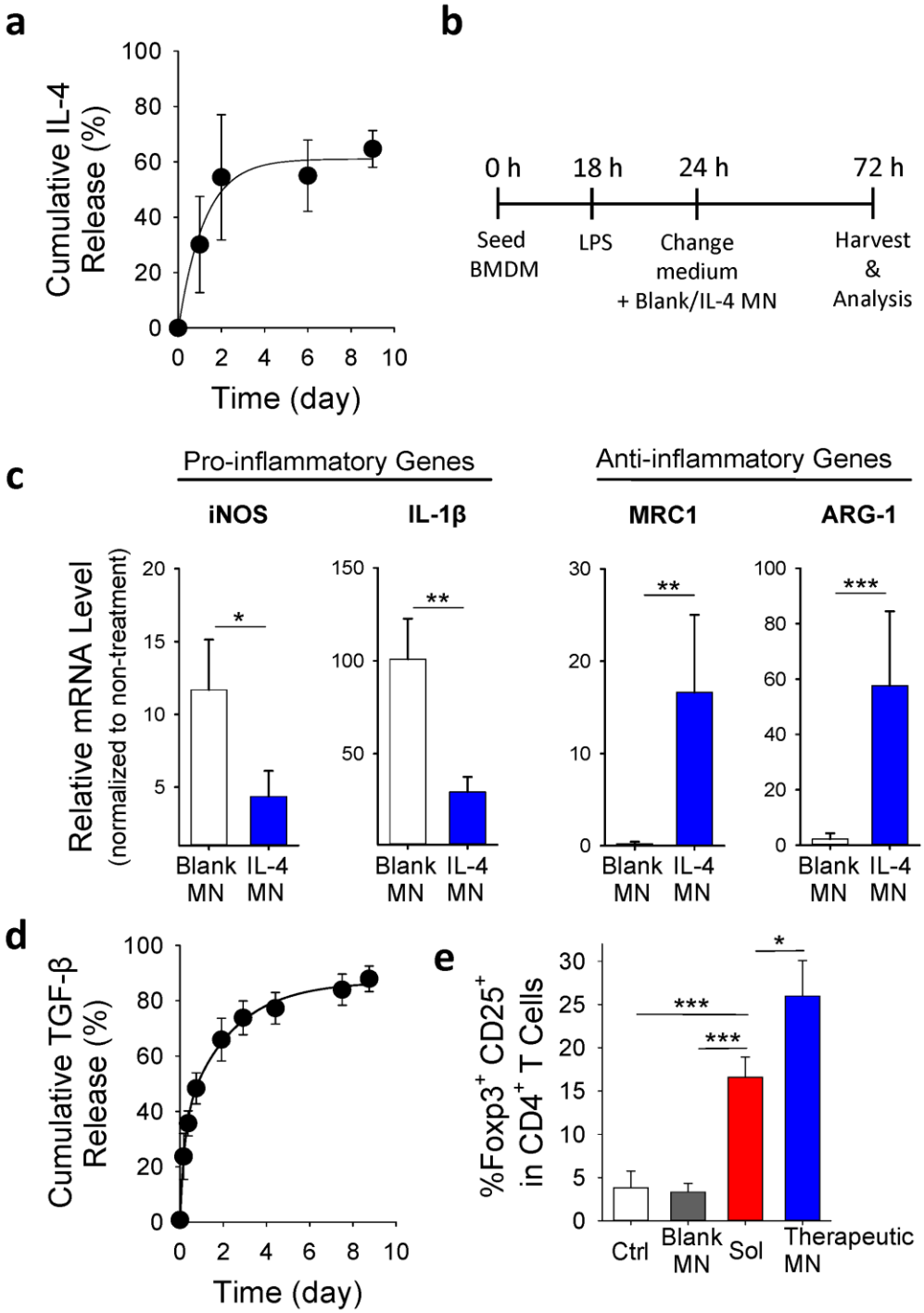

Figure 2-3. Immunomodulatory properties of MN patches *in vitro.*

a, Cumulative *in vitro* release of IL-4 from MN patches containing IL-4-loaded SiMPs at 37°C and pH 7.4. **b**, Experiment procedure of co-culturing LPS-treated BMDMs with MN patches. **c**, Effects of IL-4 released from MN patches on the gene expression of pro/anti-inflammatory markers in LPS-treated BMDMs as assessed by using qPCR. See also Figure S9 for results from no-contact setup. **d**, Cumulative *in vitro* release of TGF-β from MN patches containing TGF-β-loaded SiMPs at 37°C and pH 7.4. **e**, Effects of MN-released IL-4/TGF-β on the development of induced Treg. Naïve $CD4^+$ T-cells were treated with anti-CD3 and anti-CD28 antibodies for 4 days in the presence of IL4/TGF-β in solution (Sol), blank MN patches or MN patches with IL-4/TGF-β (Therapeutic MN), followed by flow cytometric analysis of Treg development (co-expression of Foxp3 and CD25). All data are presented as mean ± SD (n = 5). The results were analyzed using one-way ANOVA with post-hoc analysis. Statistical significance is indicated by * $p < 0.05$, ** $p < 0.01$ and *** $p < 0.001$.

2.3.5 In vivo studies of MN patches for periodontitis treatment

The functionality of the designed MN patch was tested *in vivo* by using a rat model of periodontitis. Following the periodontal disease induction, MN patches were inserted in the periodontal pocket to assess immunomodulation and tissue regeneration at cellular and tissue levels.

To better understand the mechanism of action, we extracted the periodontal tissues at the defect site to assess the population and status of local immune cells (**Figure 2-4a**). As the disease was induced by *Aggregatibacter actinomycetemcomitans* (*A.a.*) bacterial coated ligatures, we first assess the presence of bacteria by using quantitative polymerase chain reaction (qPCR). As shown in **Figure 2-4b**, therapeutic patches effectively inhibited the bacterial growth by the two-staged release of tetracycline. In addition, the level of pro-inflammatory cytokines such as tumor necrosis factor a (TNF-α; both mRNA and protein level, **Figure 2-4c-d**), IL-1β and IFN-γ (**Figure 2-S10**) was significantly reduced in the presence of therapeutic patches that delivered both immunoregulatory cytokines and antibiotics. Treatment with therapeutic patches not only decreased the inflammatory cytokines, but also increased the expression of anti-inflammatory cytokine such as IL-10 (both mRNA and protein level**, Figure 2-4e-f**), Treg marker, FOXP3 (**Figure 2-4g**) and Treg stimulating factor, TGF-β (**Figure 2-4g**). Furthermore, therapeutic MN patches induced pro-healing genes, including RUNX2, COL1A1 (type I collagen a1), BMP-2, and

OCN (osteocalcin) (**Figure 2-4h**), indicating an induction of osteogenic activity and collagen matrix synthesis in local periodontal cells.

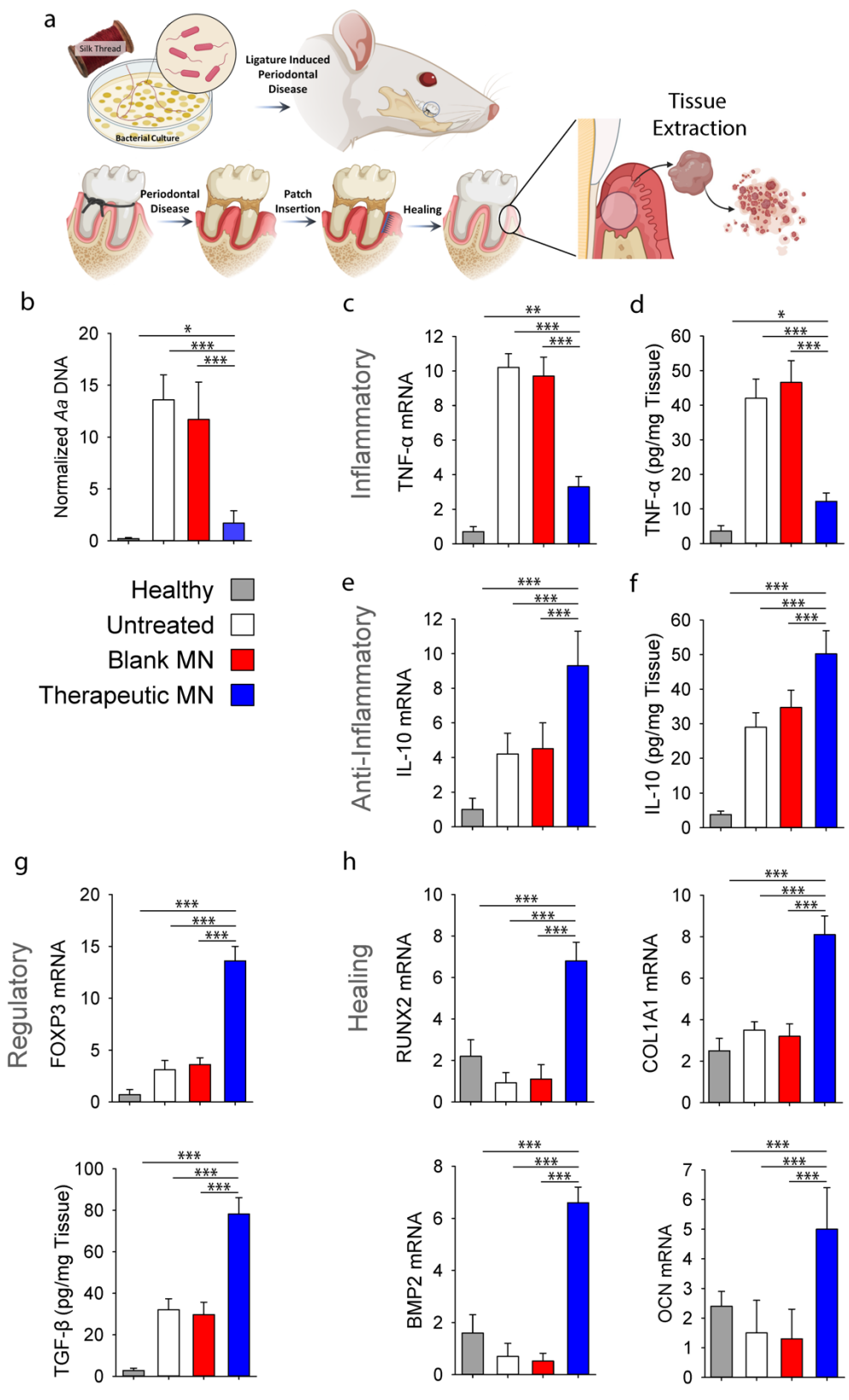
a
Silk Thread
Bacterial Culture
Ligature Induced Periodontal Disease
Tissue Extraction
Periodontal Disease
Patch Insertion
Healing
b
Normalized Aa DNA
c
Inflammatory
TNF-α mRNA
d
TNF-α (pg/mg Tissue)
Healthy
Untreated
Blank MN
Therapeutic MN
e
Anti-Inflammatory
IL-10 mRNA
f
IL-10 (pg/mg Tissue)
g
Regulatory
FOXP3 mRNA
TGF-β (pg/mg Tissue)
h
Healing
RUNX2 mRNA
COL1A1 mRNA
BMP2 mRNA
OCN mRNA

Figure 2-4. *In vivo* evaluation of the immunomodulatory effects in a rat model of periodontitis.

a, Ligature induced periodontal disease model in rats was used. **a**, Schematic representation of the proposed disease induction strategy patch placement. Mucoperiosteal flaps were elevated, uncovering the alveolar bone adjacent to the lingual aspect of the first maxillary molar to place MN at the defect site. At 8-weeks post MN insertion, buccal and palatal tissues of maxillary molars were isolated and dissociated to assess inflammatory status of tissue microenvironment. **b**, PCR analysis of *A.a.* bacterial ribosomal DNA in the periodontal tissue normalized by palatal tissue weight. **c**, Relative mRNA expression level of pro-inflammatory cytokine TNF-a. See also Figure S10. **d**, ELISA analysis of TNF-a level in the tissue. **e**, Relative mRNA expression level of anti-inflammatory cytokine IL-10. **f**, ELISA analysis of IL-10 in the tissue. **g,** Relative mRNA expression of Treg marker FOXP3 and ELISA analysis of TGF-β secretion. **h**, Relative mRNA expression level pro-healing genes RUNX2, COL1A1, BMP2 and OCN in the periodontal tissue. Healthy: healthy rats; Untreated: untreated periodontitis; Blank MN: MN patches without any therapeutic cargo; Therapeutic MN: MN patches containing both tetracycline- and IL-4/TGF-β-loaded SiMPs (Tetracycline: 0.5 mg; IL-2: 100 ng, IL-4: 40 ng, and TGF-β: 40 ng per patch). The presented data are expressed as mean ± SD (n= 5). The results were analyzed by using one-way ANOVA with post-hoc analysis. Statistical significance is indicated by * $p < 0.05$, ** $p < 0.01$ and *** $p < 0.001$.

Following the periodontal disease induction, MN patches were inserted in the periodontal defect pocket in a way for needles to face the gum tissue (**Figure 2-5a**). Four- and Eight-weeks post-treatment, saliva samples were extracted to check the level of inflammatory cytokines (**Figure 2-5b**). Consistent with the findings in periodontal tissues, the saliva from the rats treated with therapeutic patches showed a significant reduction in the secretion level of IL-1b and TNF-a, two major pro-inflammatory cytokines.

Eight weeks post-insertion, the bone regeneration at the defect site was assessed by using microcomputed tomography (μCT). Reconstructed two-dimensional (2D) and 3D images of the defect site following various treatments are exemplified in **Figure 2-5c**. These μCT images were then used to estimate the level of alveolar bone gain at each defect site. The rats treated with therapeutic patches had a significant reduction in the distance between the alveolar bone crest and cementoenamel junction (CEJ) and an increase of alveolar bone area, which was not observed in animals treated with blank patches (**Figure 2-5d**). Although the recovered bone area is not as good as healthy control but such a significant improvement only after eight weeks of treatment is among the highest reported in the literature.[159–161]

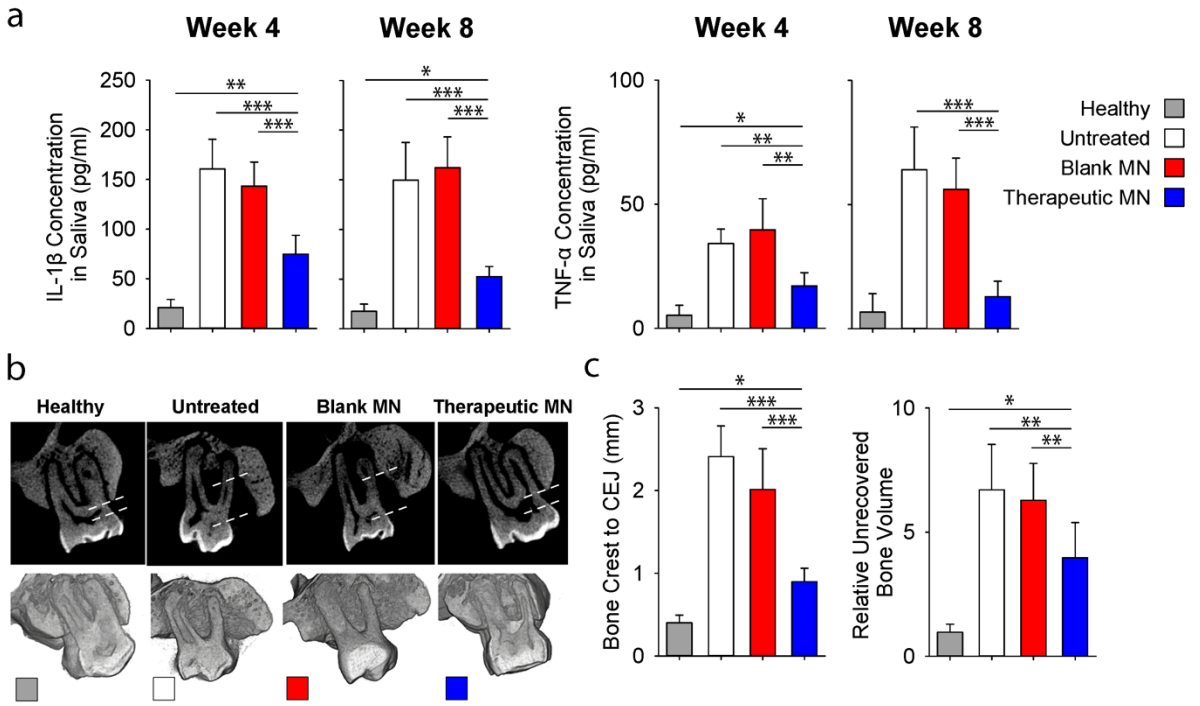

Figure 2-5. Effects of therapeutic MN patches on the regeneration of periodontal tissue *in vivo.*

Ligature induced periodontal disease model in rats was used. **a**, Quantification of inflammatory (TNF-α and IL-1β) cytokines in rat saliva at 4- and 8-weeks post MN implantation. **b**, The μCT images of the rat maxilla at 8 weeks post MN implantation. All specimens were normalized, and μCT images were calibrated to enable quantitative comparisons. Dotted line indicated the distances between bone crest and CEJ. **c**, Quantitative analysis of the vertical bone recovery as determined by measuring the distance between the bone crest and CEJ after 8-weeks of treatment. **d**, Relative volumetric bone recovery was calculated by using 3D reconstructed volume at 8 weeks post MN implantation. All data are presented as mean ± SD (n= 5). Statistical significance is indicated by * $p < 0.05$, ** $p < 0.01$ and *** $p < 0.001$ for differences between samples with different formulations.

2.4 Discussion

Periodontitis is a prevalent chronic inflammatory disease affecting tooth-supporting tissues. Although bacterial colonization of the periodontal pocket is the initial cause of the periodontitis, accumulation of destructive immune cells such as macrophages and T cells into the periodontium plays a critical role in the disease progression. Once damaged, the periodontium has a limited capacity for regeneration. Thus, the ultimate goal of periodontal therapy is the

regeneration of the periodontium. With conventional administration, insufficient local presentation of antibiotics and inadequate penetration of anti-inflammatory drugs across the transgingival layers as well as not considering the critical role of immune cells, limiting the therapeutic outcome. Therefore, the local modulation of the microbial environment and immune microenvironment with good tissue penetration is desirable.

Our patch offers four tunable modules – dissolvable base, MN arrays, NPs and SiMPs, which can be engineered to have different active pharmaceutical ingredients, and the biomaterials for each module can be further tuned to have the desirable release and degradation profile. Therefore, our patch is not only appropriate for the therapy of gingivitis and periodontitis, but also for other problems in the oral cavity, such as canker sores when loading with a different drug. During the MN fabrication process, we observed that SiMPs had intendency to settle near the tip of the MNs. Interestingly, we found that the accumulation of microparticles at the tip of the needles help increase tip strength (**Figure 2-1f**) for tissue penetration. We believe that this design will enhance the effective delivery of immunomodulatory molecules. On the other hand, if the even distribution of SiMPs is desirable, smaller particles could be used so that they would not precipitate much during centrifugation steps. In addition, surface modification of particles may increase the active interaction with the surrounding matrix to achieve a homogenous distribution of particles.

To achieve an easy-to-administer and highly effective periodontal therapy, this study tuned the modules and developed a MN patch with biodegradable MNs and dissolvable support upon application to the gingival tissue. Tetracycline is used as a model drug in our periodontal patch and it can be replaced or combined with other clinically relevant antibiotics, such as minocycline, azithromycin, metronidazole and ciprofloxacin. [162] Antibiotic-loaded PLGA NPs as well as cytokine-loaded mesoporous SiMPs control the release of active ingredients and protect the integrity of biomolecules. This design enables multi-stage release: a burst release of antibiotics from the base membrane and a sustained release of more antibiotics from MPs, as well as

immunomodulatory cytokines, IL-4 and TGF-β, from SiMPs in MNs, to suppress bacteria growth and to modulate host immune cell functions, respectively. This is the first-in-class periodontal drug delivery system with both antibacterial and immunomodulatory effects in the same patch.

Maintaining the stability and integrity of protein is crucial for delivering functional immunomodulatory cytokines and achieving effective immune modulation. Here, heparin-functionalized particles (i.e., SiMPs) can interact with the potential cytokines and stabilize them through electrostatic interaction and heparin-specific binding. An alternative approach is to directly use heparin-functionalized hydrogel to make MNs for the loading and release of cytokines and growth factors. However, the fabrication of MNs involve processes such as crosslinking and drying to achieve a sufficient mechanical strength, which may compromise the bioactivity of biomolecules. Therefore, the successful loading of a biomolecule and the preservation of its activity require biomolecule-specific test and optimization to determine the feasibility.

Finally, following the successful demonstration of immunomodulation approach, further optimization and simplification of the MN patch is required for clinical translation in dental applications. For example, instead of protein-based cytokines, small molecules capable of tuning macrophages into pro-healing phenotype may be desirable because of their better stability, easier manufacturing procedure and lower cost. Our future goal is to develop a point of care product for patients to administer easily without frequent visits to dentists and complicated surgical procedures. Over-the-counter products will further grant patients the freedom to self-educate and diagnose, thus starting treatment intervention from the early stages of periodontitis. The commercialization potential will be huge with simplified formulation and optimized materials.

2.5 Materials and Methods

Chemicals and biologicals. Unless noted otherwise, all chemicals were purchased from Sigma-Aldrich, Inc. Glassware was acid-cleaned overnight and then thoroughly rinsed with Milli-Q water.

Cell culture reagents, solutions, and dishes were obtained from Thermo Fisher Scientific Corp. unless otherwise specified.

GelMA synthesis. GelMA was prepared as previously described[150]. Briefly, 10 g of porcine skin gelatin was dissolved in 100 mL of preheated Millipore water at 60°C under constant stir. Fully dissolved gelatin solution was filtered through a membrane with 0.22 µm pore size. The filtered 10% gelatin could be used for MN patch base material as well as GelMA synthesis. Keeping the solution temperature around 50℃, 8 mL of methacrylic anhydride was added to the stirring mixture dropwise and the reaction was carried for 3 hours. To stop the reaction, a five-fold volume of warm water was added to the solution. Residual monomers and methacrylic anhydride were removed by dialysis with 12-14 kDa molecular weight cut-off dialysis tubing at 40°C for one week. GelMA polymer solution was freeze-dried and stored in 4℃ fridge.

PLGA nanoparticle synthesis. 200 mg acid terminated PLGA (50:50 lactic acid to glycolic acid ratio) was dissolved and stirred in 5 ml dichloromethane (DCM) overnight on heat. For tetracycline loaded into NPs, 15 mg tetracycline was added to 5 ml of PLGA-DCM mixture. A ten-fold volume of 1% polyvinyl alcohol (PVA) was added right before sonication at 40% power for 2 minutes with 4-second on and 2-second off cycle. The sonicated solution was poured into double volume of 0.25% PVA and stirred for 4 hours in open air to evaporate organic solvents. The samples were kept away from light if fluorescent dye was added instead of tetracycline. Low speed centrifugation (3,000 round per minute/rpm, 5 minutes) was performed to remove undesired clumps; and then ultracentrifugation at 17,000 g for 15 minutes was done twice to wash and precipitate the NPs. PLGA NPs were resuspended in 5 ml Millipore water and stored in 4℃ fridge. When 20% GelMA with NPs and SiMPs was prepared, the full formulation contained 500 µl of PLGA NPs, 10 mg of cytokine loaded SiMPs and 500 µl of 40% GelMA, which were mixed evenly.

***Mesoporous silica particle preparation*.** Monodisperse mesoporous SiMPs were formed by using a microfluidic jet spray-drying route, using cetyltrimethylammonium bromide (CTAB) and/or

Pluronic F127 as templating agents and tetraethylorthosilicate (TEOS) for silica as reported before.[153,154] Carbodiimide chemistry (NHS/EDC) was utilized to link heparin to SiMPs after treating the silica with (3-Aminopropyl)triethoxysilane (APTES) to provide primary amine groups. Briefly, 800 mg SiMPs were suspended in 50 ml dehydrated Methanol. Then, 3 ml APTES was added, and the suspension was stirred at room temperature overnight, and the final product was centrifuged at 1500 rpm for 3 minutes and washed with methanol three times, followed by drying under high vacuum overnight. For the surface functionalization of the aminated-silica particles with heparin sodium salt following activation *via* successive addition of EDC and NHS. After activation for 10 minutes, the ethanolic solution of amino-functionalized silica was added to the reaction mixture and stirred for 12 hours at room temperature. Afterwards the particles were separated by centrifugation at 1500 rpm for 3 minutes and washed several times with deionized water and ethanol to remove unreacted reagents.

The hydrolysis of heparin-coated mesoporous silica structure (without cytokines) was used to estimate the degradation rate of SiMPs. To study in vitro degradation, SiMPs were soaked in RPMI medium supplemented with 10% heat-inactivated fetal bovine serum, 1% penicillin/streptomycin, 1% sodium pyruvate, 1% HEPES buffer, and 0.1% μM beta-mercaptoethanol. The supernatant was collected from the pelleted SiMPs at designated timepoints and tested with inductively coupled plasma mass spectrometry (ICP-MS; NexION 2000, PerkinElmer) to estimate the atomic content of silicon, which was then normalized to the initial mass to estimate the remaining mass.

IL-4 and TGF-β loading into the silica particles. First, SiMPs were activated by 3-aminopropyltrimethoxysilane (APTES), and 800 mg of SiMPs was suspended in 50 mL of methanol. Then, 3 mL of APTES was added and suspension was stirred at room temperature overnight; the final product was centrifuged (1500 rpm, 3 minutes), washed with methanol five times, and dried under high vacuum. Secondly, aminated-SiMP surfaces were functionalized with heparin, and 216 mg of heparin sodium salt were dissolved in 8 mL deionized H_2O. Then, 62.1

mg EDC and 70.4 mg sulfoNHS were added successively and stirred for 5 minutes at room temperature. The amount of 1.12 mL ethanolic solution with 20 mg of the amino-functionalized SiMPs was added to the reaction mixture and stirred overnight at room temperature. Afterwards the particles were separated by centrifugation and washed several times with copious amounts of water and ethanol to remove additional free polysaccharide. They were re-dispersed in 5 mL ethanol, leading to a colloidal solution. Thirdly, heparin-modified SiMPs were incubated with 1 µg of IL-4 and 1 µg of TGF-β for cytokine loading overnight. Afterwards the microparticles were centrifuged down using tabletop centrifuge and washed three times with PBS to remove free cytokines.

MN patch fabrication. To fabricate MNs, 20% GelMA containing 0.5% photoinitiator, tetracycline-loaded NPs and IL-4/TGF-β-loaded SiMPs were casted on negative MN molds and centrifuged at 3,000 rpm for 2 minutes. The GelMA mixture was maintained at the temperature greater than 50°C throughout the procedures in order to maintain the material fluidity, but the duration of elevated temperature was minimized to protect protein integrity. Extra mixture was removed, and then 100 µl of 10% gelatin containing 5 mg/ml of tetracycline-HCl was laid evenly on the top to create a 1 cm x 1 cm patch. The MN patches were incubated under 50W/cm^2 ultraviolet light for 5 minutes. After 1 day of drying in dark at room temperature, solidified MN patches were peeled off from the molds and stored at 4°C until use.

Mechanical property of MNs. The mechanical strength of MNs was measured by compression test on a low-force mechanical testing system (5943 MicroTester, Instron, USA). The MN tips were place perpendicularly to stainless-steel plate and were pressed against another stainless-steel plate moving at constant speed of 0.5 mm/minutes. Correlations between the applied force and the deformation of the MNs were recorded. All tests were performed in triplicates.

Tetracycline release study*. In vitro* release of tetracycline was studied by incubating a single patch in 1 mL PBS (pH 7.4; supplemented with 10 mM $CaCl_2$) at 37°C under constant gentle stirring. At different time intervals, stirring was stopped and 1 µL of the supernatant was taken

from the sample. The concentration of released tetracycline was determined by measuring the absorbance at 270 nm wavelength using UV-vis spectrophotometer (Thermo Scientific NanoDrop One).

Antibacterial assay. Kirby-Bauer agar disk diffusion assay was used to test antibacterial properties of tetracycline loaded MNs against *E. Coli* and *A.a*. A free drug control was prepared by adding tetracycline solution to 8mm sterile paper disks. These paper disks were air-dried in a biosafety cabinet before use. These disks and MN patches were placed in agar plates inoculated with bacteria at 37°C. The inhibition zones were measured after 48 hours.

Animal studies. Five- to seven-week-old wild-type (C57Bl/6) mice were purchased from the Jackson Laboratory and maintained in specific pathogen-free facilities at the University of California at Los Angeles (UCLA). All experiments on mice and cells collected from mice were performed under a protocol approved by the Animal Research Committee and in accordance with UCLA's institutional policy on humane and ethical treatment of animals.

T-cell isolation and activation. Primary T cells and $CD4^+$ T cells were isolated from mouse spleen and purified using magnetic-based, negative enrichment kits (Stem Cell Technologies). Cells were counted by hemocytometer using trypan blue exclusion (Calbiochem). RPMI medium supplemented with 10% heat-inactivated fetal bovine serum, 1% penicillin/streptomycin, 1% sodium pyruvate, 1% HEPES buffer, and 0.1% μM beta-mercaptoethanol was used as T-cell culture media. For experiments to induce Treg, $CD4^+$ T cells were purified from mouse spleens by EasySep immunomagnetic negative selection (Stem Cell Technologies). Cells were then activated with anti-CD3 antibody (10 μg/mL)-coated plates supplemented with anti-CD28 antibody (2 μg/mL) in medium. At the same time, MNs loaded with cytokines (IL-4, and TGF-β) were added. After four days, cells were removed from wells and fixed, permeabilized, and stained with anti-CD25 and intracellular anti-Foxp3 antibodies for flow cytometry analysis of Tregs.

Isolation of bone-marrow derived macrophages (BMDMs). 5-to-7-week-old C57Bl/6 mice were euthanized, and hind limbs were harvest in PBS. Under sterile condition, muscles were

scraped off and the ends of bones were cut off. Bone marrow was flushed into a sterile 50-ml conical tube with 2 ml of Dulbecco's Modified Eagle Medium (DMEM)/F12 supplemented with 10% fetal bovine serum and 1% penicillin-streptomycin. Cells were pelleted and plated with mouse 50 ng/ml macrophage colony-stimulating factor (BioLegend). Following 3 days of incubation, 5 ml of fresh complete DMEM/F12 medium with 25 ng/ml macrophage colony-stimulating factor were supplied per 10-cm cell culture dish. Cells were again incubated for 3 more days. Then supernatants were discarded, and dishes were washed with PBS three times to remove non-adherent cells. BMDMs were gently scraped off the dish, pelleted, counted and seeded in new plates for further macrophage polarization and experimentation. 10 ng/ml LPS was used to induce proinflammatory macrophages, while 25 ng/ml IL-4 was used to induce pro-healing macrophages. Controls were simply adding complete DMEM/F12 medium.

RNA isolation, reverse transcription and qPCR. Total RNA was extracted by using TRIzol reagent (Life Technologies, Gaithersburg, MD, U.S.A.), and the concentration was determined from spectrophotometric optical density measurement (Thermo Scientific NanoDrop). The OD260/OD280 ratio in all samples ranged between 1.7 and 2.0 to ensure RNA purity. Reverse transcription was then carried out using Maxima SYBR Green qPCR master mix according to manufacturer's suggested protocol. The cDNA was stored at −20°C. PCR was performed by using SYBR Green kit according to manufacturer's suggested protocol on BioRad CFX96 PCR detection system. Primer sequences were as follow: GAPDH- Forward 5'CATCACTGCCACCCAGAAGACTG Reverse 5' ATGCCAGTGAGCTTCCCGTTCAG; iNOS – Forward 5' GAGACAGGGAAGTCTGAAGCAC Reverse 5'CCAGCAGTAGTTGCTCCTCTTC; IL-1 – Forward 5' TGGACCTTCCAGGATGAGGACA Reverse 5' GTTCATCTCGGAGCCTGTAGTG; MRC1 – Forward 5'GTTCACCTGGAGTGATGGTTCTC Reverse 5' AGGACATGCCAGGGTCACCTTT; ARG-1 – Forwards 5' CATTGGCTTGCGAGACGTAGAC; Reverse 5' GCTGAAGGTCTCTTCCATCACC.

Animal study. *In vivo* functionality of designed MNs was evaluated using a rat periodontal defect model, as described previously with some modifications [159,161]. Two-month-old virgin male and female Sprague Dawley rats (Harlan Laboratories, Livermore, CA) were utilized for *in vivo* testing of the proposed periodontal treatments according to approved animal protocols. The animals were divided into four groups (four rats per group): (i) healthy control, (ii) no treatment (untreated), (iii) blank MN patches, and (iv) therapeutic MN patches containing tetracycline and cytokines. Briefly, mucoperiosteal flaps were elevated in rats in groups (ii-iv), uncovering the alveolar bone adjacent to the mesiolingual aspect of the first maxillary molars. The alveolar bone covering the root surfaces on the lingual side was removed with a dental bur under constant saline irrigation, and *A.a.*-coated 5-0 silk ligature was tied around the left second molar. Silk ligature was inoculated with *A.a.* under anaerobic conditions for 24 hours before the procedure. Three weeks later, designed patches were inserted into the defect site as noted above for groups. Eight weeks post-implantation, the animals were sacrificed and the amounts of bone regeneration at defect sites were evaluated using μCT analysis. All the specimens were standardized, and μCT images were calibrated for proper comparative analysis. The vertical bone loss at each defect site was evaluated by measuring the distance between cementoenamel junction (CEJ) and alveolar bone crest as well as the relative alveolar bone area according to methods reported in the literature.[160]

Characterization of inflammatory response at defect sites. Populations of immune cells in periodontal tissue were analyzed as described previously [161]. Briefly, at 8 weeks post-implantation, buccal and palatal tissues of maxillary molars were isolated and dissociated using collagenase and DNase I (50 μg/mL) at 37°C for 15 minutes. These enzymes were then inactivated with EDTA (20 μL/mL of solution). Tissues were then disaggregated and passed through a 100-μm cell strainer to obtain a single-cell suspension. Quantitative PCR assays were used to analyze gene expression. RNA from isolated cells was isolated using Trizol reagent. RNA was reverse-transcribed and single-stranded cDNA was made using a Superscript III cDNA synthesis kit. Relative gene expression was calculated using the $2^{-\Delta\Delta Ct}$ method, with normalization to the *Ct* of

the housekeeping gene beta actin. Quantification of *A.a.* in the periodontal tissues was performed as previously reported [161]. The concentrations of inflammatory cytokines and anti-inflammatory cytokines were measured by using ELISA kits after the extraction of proteins from the gingival tissue by tissue homogenization.

Statistical analysis. The Kruskal-Wallis rank sum test, one-way ANOVA and two-tailed Student's t-test were utilized as appropriate to analyze the data at a significance of α or $p < 0.05$. Quantitative data are expressed as mean ± SD. To determine the number of specimens for the proposed experiments, power analysis was conducted based on our preliminary data.

3. DISSOLVABLE MICRONEEDLES FOR LOCALIZED DELIVERY OF BI-FUNCTIONAL MICROPARTICLES

3.1 Abstract

Periodontitis is initiated by dysbiosis of the oral microbiome. Pathogenic bacteria elicit ineffective immune responses, which damage surrounding tissues and lead to chronic inflammation. Although current treatments typically target microbial eradication, they fail to address the significance of immune cell reactions in disease progression. Here we identified a bifunctional antibiotic, azithromycin (AZM), that not only suppresses bacterial growth but also modulates the immune cells to suppress inflammation. We further engineered a fast-degrading microneedle loaded with biodegradable AZM microparticles for local and painless delivery to the gingival tissue. Inflammatory cytokines were decreased while anti-inflammatory cytokines and M2 macrophage were increased with AZM treatments *in vitro*. *In vivo* delivery of the AZM-loaded microneedle patch demonstrated significant therapeutic effects, including suppression of pro-inflammatory cytokine secretion, induction of pro-regenerative cytokines and promotion of tissue/bone regeneration markers. The bimodal action of azithromycin obviates the necessity for separate antibacterial and immunomodulatory agents, providing a practical and streamlined approach for clinical treatment. Addition of interleukin-4 microparticles to the therapeutic regimen further enhanced the immunomodulatory outcomes. Our results show that AZM-MN and AZM/IL-4-MN patches can both have great clinical potential as novel therapeutic strategies for the treatment of periodontitis.

3.2 Introduction

Periodontal disease, also known as gum disease, is a chronic inflammatory condition that affects the supporting structures of teeth, including the gums, periodontal ligament, and bone[163]. It is so common that it affects about 50% of the adults over the age of thirty globally[164]. In healthy individuals, there is a homeostasis of the oral microbiome. However, when the overall

microbiome balance gets interrupted by an outgrowth of keystone bacteria, the polymicrobial synergy and dysbiosis triggers inflammatory response and inadequately regulated immune responses evolves into chronic inflammation, leading to tissue destruction and bone loss[163,165,166]. Thus, although bacteria are the initiator, the host immune system plays a vital role in disease progression. In recent years, immunomodulation starts to gain the attention for treating periodontitis[167].

Pathogenic bacteria usually have their own tactics to counteract the normal immune responses and exacerbate the disease through virulence factors and pro-inflammatory mediators[165,168]. For instance, *Porphyromonas gingivalis* utilizes various strategies, including lipopolysaccharide, proteases, fimbriae, and other virulence factors, to enhance bacterial colonization and support the growth of the surrounding microbial community. Gingipains, a class of protease, can degrade host proteins including collagen which is involved in tissue regeneration and complement components which is an important part of innate immune response[87]. Gingipains also elicit pro-inflammatory signaling pathways to promote chronic inflammation when it is time to heal and regenerate[169]. These virulence factors play a crucial role in promoting the coaggregation of *P.g.* with other bacteria and facilitating the formation of dental biofilm[168]. Through evolution, pathogenic bacteria all evolve the ability to evade host immune response and skew appropriate immune reaction. Moreover, the accumulation of bacteria allows biofilm and plaque formation, which can be hard armors to attack, protect the bacteria from immune clearance and exacerbate the inflammatory response.

Another important factor for periodontitis progression is the immune cells, such as macrophages, and T cells[96,109,170]. They respond to the presence of bacterial pathogens and release cytokines and chemokines that trigger an inflammatory response. In the early stage of periodontitis, macrophages are the first line of defense against bacteria. They can phagocytose microbes to clear the infection and release pro-inflammatory cytokines which signal more immune cells to come. However, dysfunctional macrophages with high level of inflammatory

mediators contribute significantly to tissue damage and bone resorption. Macrophages stay as pro-inflammatory M1 phenotype and fail to transition to pro-healing M2 phenotype after the acute inflammation phase. Thus, the osteoblasts/osteoclasts balance in bone is disrupted.

T cells have many subsets with different functions. T helper 17 (Th17) has shown to be a major player in pathogenesis of periodontitis[171]. Persistent Th17 activation produces high level of pro-inflammatory cytokines, promotes the differentiation of osteoclasts and induces the production of matrix metalloproteinases (MMPs) [109,170]. Osteoclasts lead to bone resorption and MMPs degrades the extracellular matrix needed for tissue regeneration. On the other hand, T regulatory (T_{reg}) cells are immune regulators to help prevent excessive inflammation by suppressing the activity of other immune cells. But their functions are impaired, and their numbers are reduced in chronic periodontitis. Therefore, T_{reg} and related cytokine stimulation is desirable for potential therapeutic approach.

Recognizing the significance of addressing both bacterial and immune-related aspects in the treatment of periodontitis, our aim was to develop a comprehensive approach. We identified azithromycin (AZM) as an antibiotic with dual effects on both bacteria and immune cells[172–174]. It has been shown to polarize macrophages to an M2 phenotypes via inhibition of the STAT1, NF-κB and PI3K/Akt signaling pathways[173,174]. To facilitate targeted delivery, we encapsulated AZM in microparticles (MP) and incorporated these AZM MPs into dissolvable microneedle (MN) patches. Leveraging the MN patches as a delivery platform allowed for efficient tissue penetration and localized retention at the affected gingival sites. This patch-based application offers convenience to patients, enhancing compliance and enabling early intervention. Simply put, the MN patch is applied to the diseased gum, where micron-scale needles penetrate the tissue, allowing the patch matrices to dissolve and leaving the embedded MPs within the tissue for sustained release of therapeutic agents.

3.3 Results

3.3.1 Screening of bi-functional small molecules

The idea of treating periodontitis with both antibacterial and immune modulatory properties was described in our previous publication[175]. However, the safety concerns, regulatory complications, protein stability and the expenses for enclosing a protein immune modulatory drug (i.e., IL-4) are barriers for clinical use. Therefore, we searched for candidate drugs, which 1) are small molecules, 2) have immunomodulatory effects with anti-inflammatory properties and the ability to modulate macrophage phenotype from M1 to M2, and 3) may have additional benefits such as antibacterial properties or the ability to promote bone regeneration, further enhancing its efficacy in treating periodontal diseases. Through a literature search with the above selection criteria, we tested four most promising candidate drugs - *azithromycin, tofacitinib, lupeol* and *dexamethasone*. All of them have been reported to repolarize the macrophage towards M2 phenotype in various disease models[172–174,176–178]. On top of being anti-inflammatory immune modulators, azithromycin is an antibiotic; tocifatinib is a Janus Kinase (JAK) inhibitor that suppressed the expression of IL-6; lupeol is an anti-inflammatory natural product, and dexamethasone is a widely used glucocorticoid.

In bone marrow derived macrophages (BMDMs), all four immunomodulator significantly suppressed the overall immune reaction in reducing the expression of inflammatory marker inducible nitric oxide synthase (iNOS) (**Figure 3-1a**). Cytotoxicity on primary macrophages was observed at 333μM for azithromycin, at 200μM for tofacitinib, at 100μM for lupeol and at all concentrations for dexamethasone (**Figure 3-S1**). A recent study also showed that dexamethasone induced ROS generation and mitochondria-dependent apoptosis in RAW 264.7 cells via the Krüppel-like factor 9 (KLF9)[179]. While tofacitinib, lupeol and dexamethasone did not show any antibacterial effects in *A. actinomycetemcomitans (A.a.)* agar plates (**Figure 3-1b**), the efficacy of azithromycin for periodontal bacteria *A.a.* and *P.g.* was confirmed with Kirby diffusion

assay and the efficacy is comparable with a clinically-used antibiotics, minocycline (**Figure 3-S2**). Comparing AZM with conventional tetracycline (TTC) class of antibiotics[180], AZM altered macrophage polarization towards an anti-inflammatory CD163+ M2 phenotype, whereas TTC did not trigger a similar immune modulatory response (**Figure 3-1c, d**). The gating strategy for flow cytometry is shown in **Figure 3-S3**.

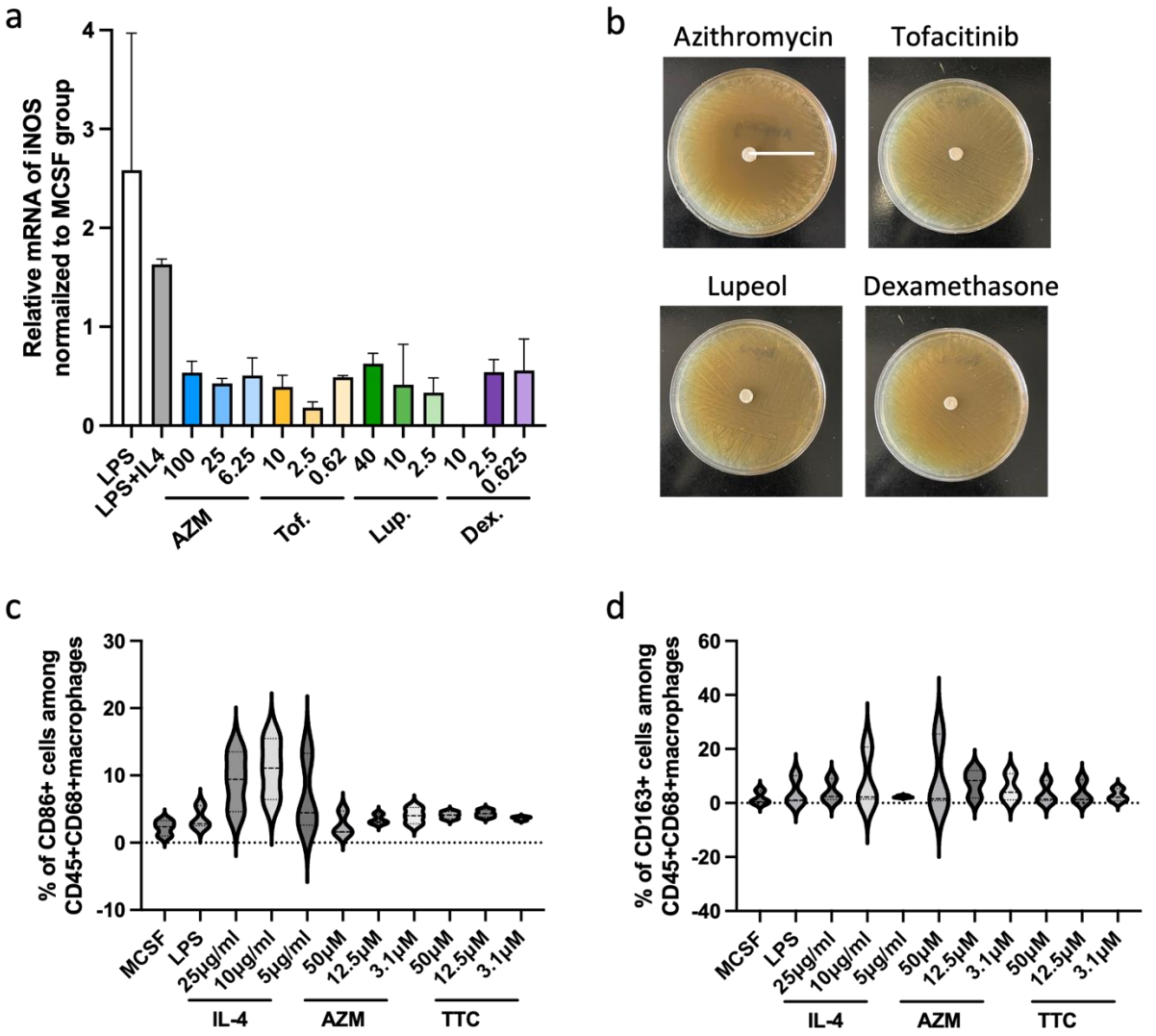

Figure 3-1. Screening of small molecules for macrophage polarization.

a, Screening of four immune modulatory small molecules (i.e. azithromycin, tofacitinib, lupeol and dexamethasone) from the literature by qPCR on mouse bone marrow-derived macrophages (mBMDM). **b,** Antibacterial properties of the compounds on dental bacteria A.a. was measured by inhibition zone on agar plates. **c,** and **d,** are the percentage of CD86+ M1 macrophages and CD163+ M2 macrophages measured by flow cytometry on primary rat bone marrow derived

macrophages (rBMDMs). MCSF group kept macrophage grow in macrophage colony-stimulating factors; LPS group was stimulated by lipopolysaccharides for 6 hours; and two antibiotics - AZM (azithromycin) and TTC (tetracycline) treatments were analyzed after stimulated by LPS for 6 hours. Data are in triplicates and responses from primary macrophages had relatively big individual variations.

3.3.2 Design and characterization of AZM-MN patch

To achieve painless and suture-free microparticle delivery to gingival tissue, we used a dissolvable microneedle (MNs) made of polyvinylpyrrolidone (PVP) (**Figure 3-2a**). AZM MPs were loaded into the dissolvable microneedle. As shown in the schematics of **Figure 3-2b**, the AZM-MN patches or strips applied to the diseased gum by dental professionals. The base would dissolve within 10 minutes leaving the embedded particles integrated into the tissue.

To have a sustained release of AZM for a prolonged effect, we loaded AZM into biodegradable polylactic-co-glycolic acid (PLGA) microparticles. Single emulsion fabrication method with homogenizing at 5000rpm for 10 min was used to generate microparticles with an average size of 5μm (**Figure 3-2c, d**) and double emulsion method was used to generate IL-4 PLGA microparticles with a similar size to AZM-MP. Moreover, various densities of PLGA 50:50 was examined and 0.6dl/g PLGA was selected since the release time of around a week was desired (**Figure 3-S4**).

MN fabrication process is illustrated in **Figure 3-S5**. Briefly, 70% ethanol were added to negative PDMS. Molds and vacuumed to prime and fill the molds. Bubbles were removed by gently scratching the mold and ethanol were removed by pipetting. 100μl mixed solution of 20% PVP, 0.75% glycerol and 1 mg of AZM MPs were casted on the molds and dried at room temperature overnight. Dried MN patches were peeled off from the mold. The resulting MNs were pyramid shape with 200μm x 200μm x 600μm, as shown in the electron microscopy images (**Figure 3-3e**). The microparticles were distribute evenly in needles while in base, more particles were present closer to the needle because of gravity (**Figure 3-3f, g**). The mechanical property

of MNs is critical for tissue penetration. Compression test of MNs indicated sufficient mechanical strength to penetrate the freshly extracted rat gingival tissues (**Figure 3-3h, i**).

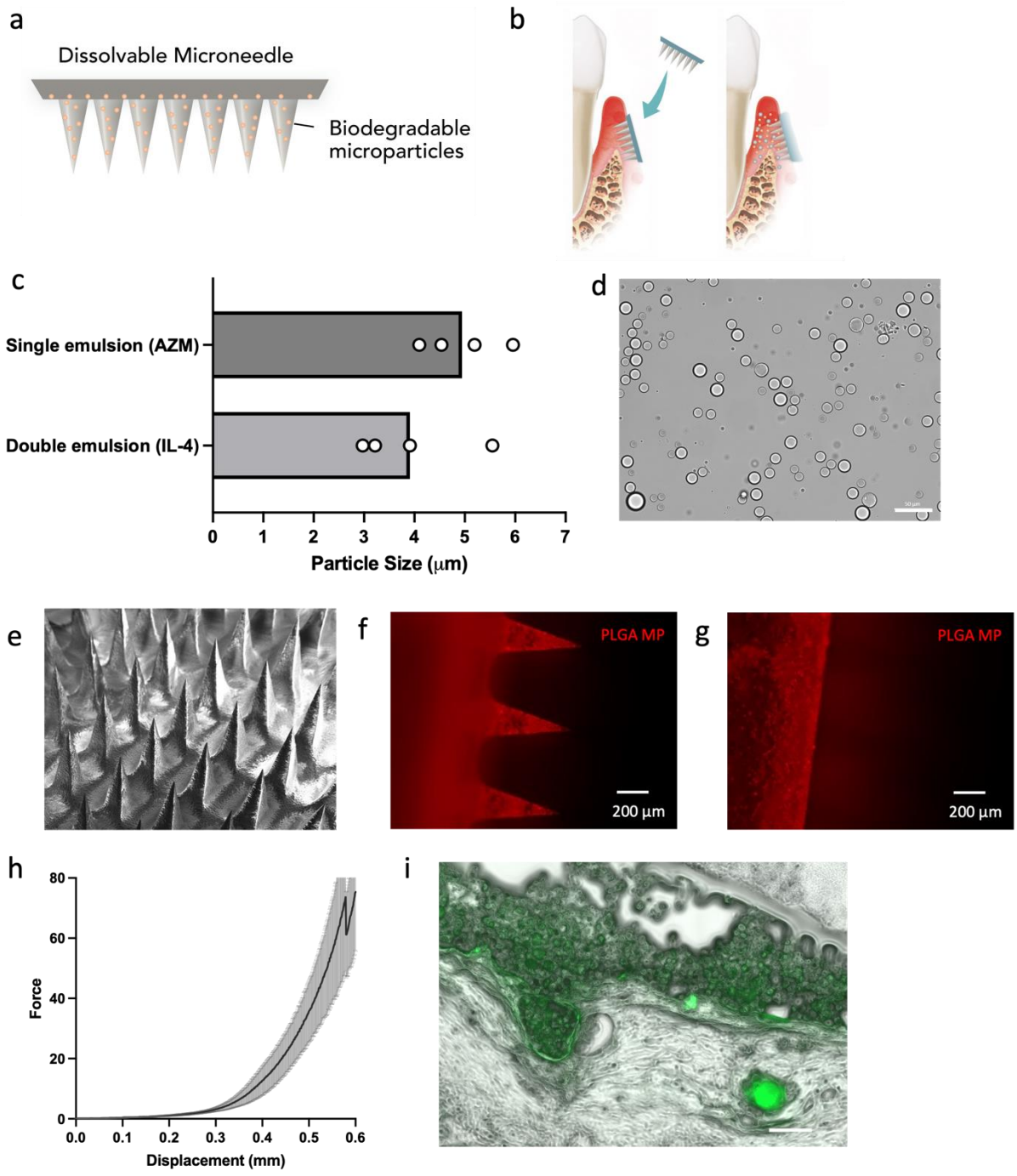

Figure 3-2. Physical Characterization of PVP microneedle.

a, Design of dissolvable PVP microneedle matrix loaded with biodegradable PLGA microparticles. **b,** Schematics of MNP application and dissolution of the administration. **c,** SEM image of

microneedles with microparticles. **d, e,** Distribution of fluorescent microparticles in needle tips and the base respectively. Scale bar of 200μm. **f,** Mechanical strength of microneedle measured by Instron machine. All data are presented as mean ± SD (n= 4). **g,** Penetration of microneedle loaded with FITC-dextran PLGA MP into fresh rat gum. Scale bar of 200μm.

3.3.3 In vitro evaluation of MN patch

Effective bacteria killing of the periodontal disease-causing bacterium *P.g*. was observed in liquid culture using released supernatant from the AZM-MN for 30 days (**Figure 3-3a, b**). It is also known the biofilm formation of dental bacteria. *A.a.* can facilitate accumulation of pathogenic microbiome and form tenaciously adherent biofilm colonies on surfaces[181]. The inhibition zone by placing AZM-MN patch on agar plates were examined to test the efficacy of antibiotics released from the path. Both *P.g*. and *A.a.* inoculation was tested, and example images shown in **Figure 3-3c, d** (full set of data in **Figure 3-S5**).

Furthermore, we investigated the immune effects of azithromycin (AZM), IL-4 and AZM+IL-4 patches on in murine primary macrophages. Inflammatory cytokines such as TNF-α, IL-1β, IL-12p70 and IL-8 were suppressed in cell culture (**Figure 3-3e**). To observe the effects to immune cells in addition to macrophages, we investigated AZM in its soluble form, as particles, and when loaded into microneedle patches (MNP) using human peripheral blood mononuclear cells (PBMCs), which consist of a mixture of lymphocytes, monocytes, and macrophages[182]. The results showed that AZM exhibited a moderate reduction in cell proliferation and significantly suppressed the expression of inflammatory cytokines TNF-α and IFN-γ (**Figure 3-S6a,b,c**).

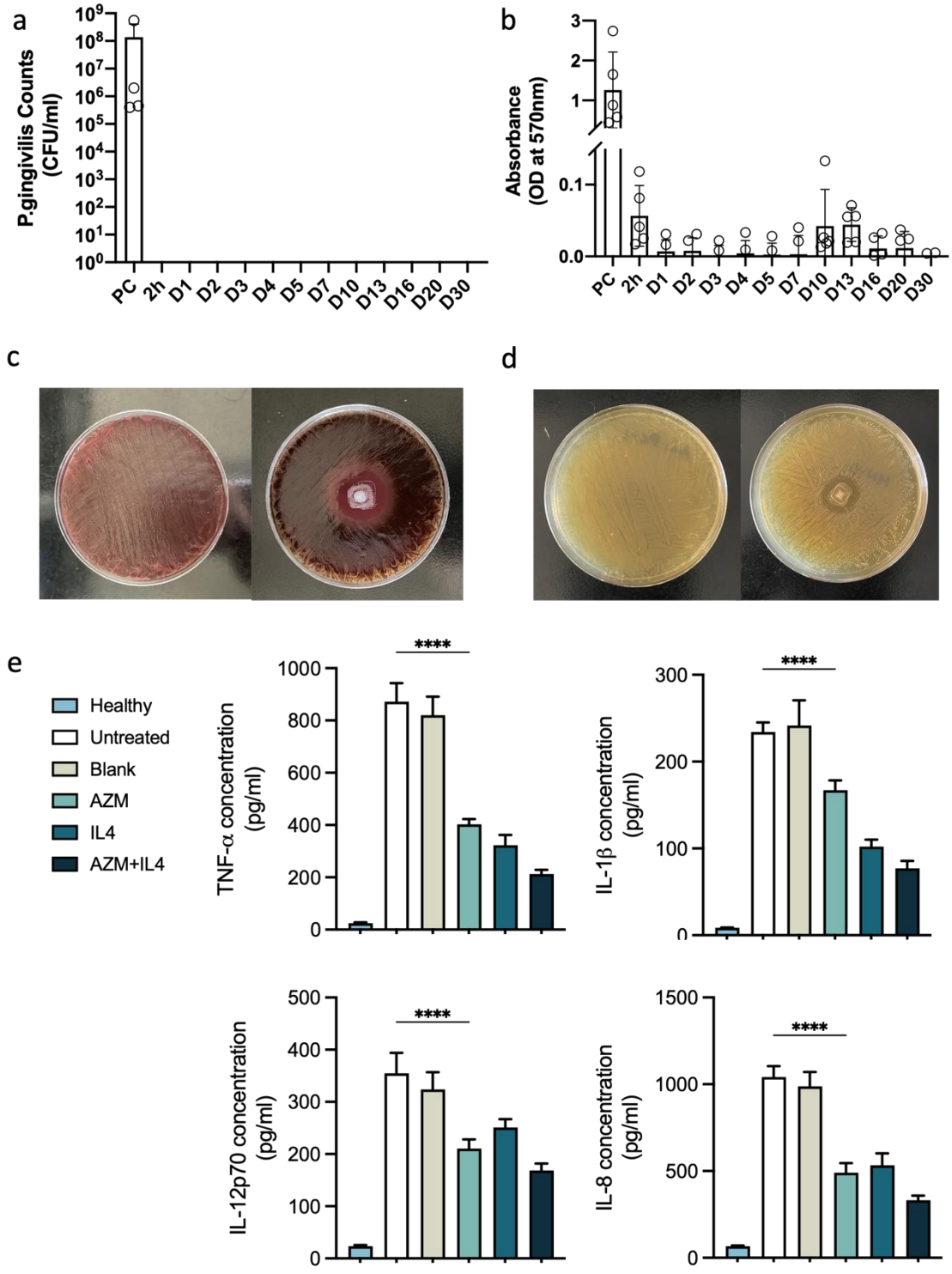

Figure 3-3. Sustained release of azithromycin from microneedles shows antibiotic effects for prolonged period and immunomodulatory effects *in vitro*

a, Size distribution of AZM and IL-4 microparticles made from single emulsion and double emulsion methods with 5000RPM homogenizing speed respectively. **b,** A bright right image of AZM microparticles. Scale bar is 50μm. **c,d,** Supernatants collected from MNP release for 30

days were tested against the P.g. growth. Bacteria growth and viability were measure by colony -forning unit (CFU) and 3-(4,5-dimethylthiazol-2-yl)-2,5-diphenyltetrazolium bromide (MTT) assay with absorbance at 570mm. All data are presented as mean ± SD (n= 4). **e,** Murine primary monocytes were activated with IFN-γ/LPS and treated with azithromycin (AZM) and IL-4-based microneedles. Cytokine production were measured by bead ELISA 24 hours post treatment, n= 4-5. Results were analyzed by using t-test. Statistical significance is indicated by asterisks: *p < 0.05, **p < 0.01, and ***p < 0.001.

3.3.4 In vivo evaluation of MN patch for periodontal treatment

We designed the MN patch for a simplified delivery of a single small molecule AZM. At the same time, MN patches with IL-4 MPs and a combination of AZM MPs and IL-4 MPs were included in the animal functionality study to investigate the impact of AZM and the additional benefits brought by IL-4. This study provided a foundation to optimize the formulation for clinical use. The efficacy of the MN patches (AZM MN, IL-4 MN, and AZM+IL-4 MN) was tested in vivo by using a ligature-induced periodontitis model in rat. After periodontal disease induction by A.a. bacterial coated ligatures, the MN patches were inserted into the periodontal pocket to assess their impact on immunomodulation and tissue regeneration at cellular and tissue levels.

To examine the efficacy of antibacterial properties, we first assess the presence of bacteria in harvest tissue at the end of eight weeks by using quantitative polymerase chain reaction (qPCR). As shown in **Figure 3-4a**, AZM and AZM+IL-4 MN patches effectively inhibited the bacterial growth whereas IL-4 alone patches suppressed bacterial growth to some extent. In addition, the level of pro-inflammatory cytokines such as interleukin-1β (IL-1β), tumor necrosis factor a (TNF-α and IFN-γ were significantly reduced in all three therapeutic groups compared to untreated or blank MN patches (**Figure 3-4b, c, d**). In addition to demonstrating a decrease in the expression of inflammatory genes at the end of treatment, the levels of inflammatory cytokines (IL-1β and TNF-α) in the gingival crevicular fluid were found to be significantly reduced over time for the therapeutic patches, as monitored every two weeks during the treatment period (**Figure 3-4e, f**).

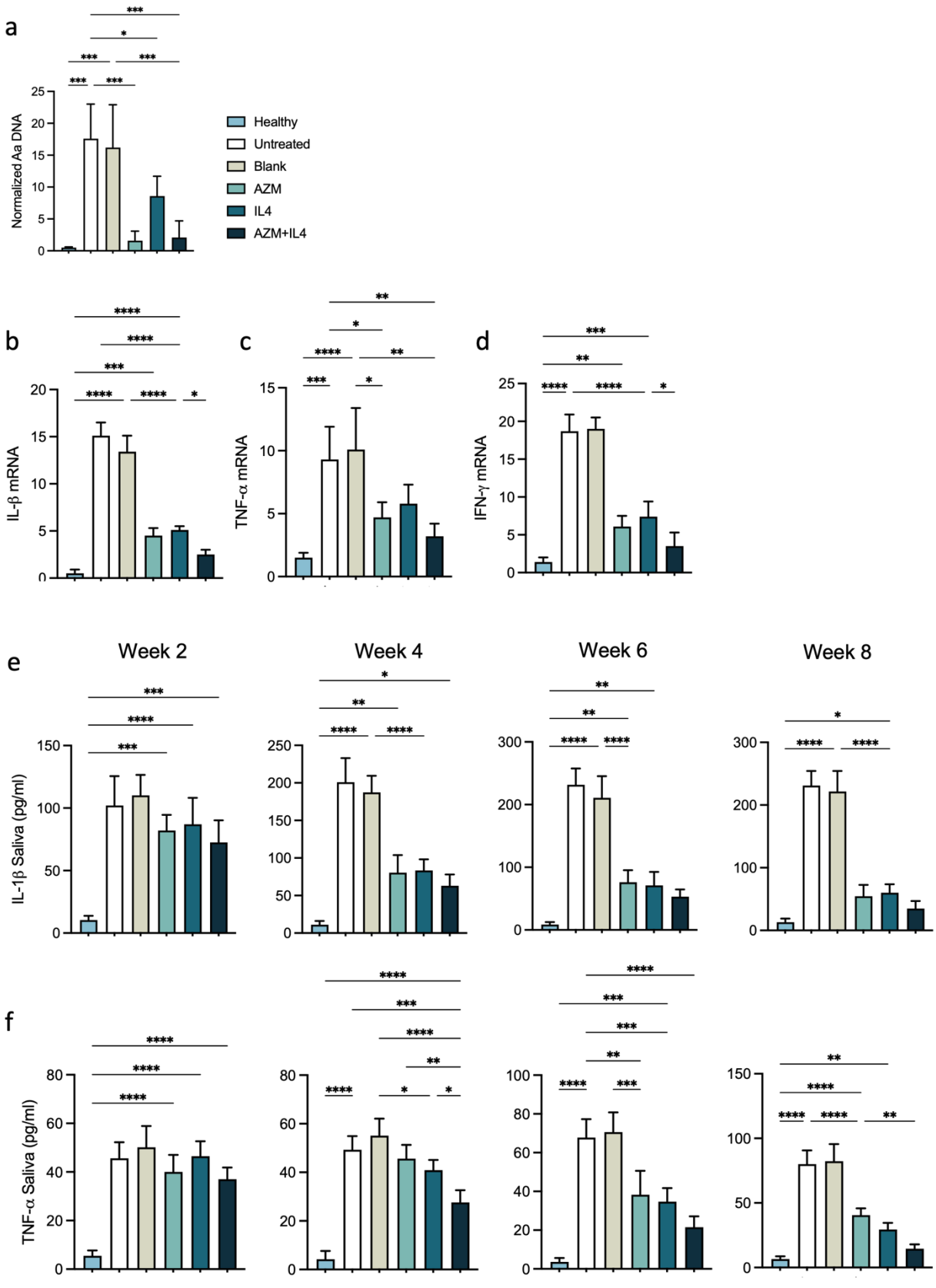
a
Normalized Aa DNA
Healthy
Untreated
Blank
AZM
IL4
AZM+IL4
b
IL-β mRNA
c
TNF-α mRNA
d
IFN-γ mRNA
e
Week 2
Week 4
Week 6
Week 8
IL-1β Saliva (pg/ml)
f
TNF-α Saliva (pg/ml)

Figure 3-4. *In vivo* evaluation of bacterial growth and inflammation in a rat model of periodontitis.

A ligature-induced periodontal disease model in rats was used. a, PCR analysis of A.a. bacterial ribosomal DNA in the periodontal tissue normalized by palatal tissue weight. **b-d,** Relative mRNA expression level of pro-inflammatory cytokine IL-1β, TNF-α and IFN-γ. **e,** ELISA analysis of IL-1b in the tissue every two weeks over eight weeks. **f,** ELISA analysis of TNF-a level in the tissue every two weeks over eight weeks. Healthy, healthy rats; untreated, untreated periodontitis; blank MN, MN patches without any therapeutic cargo; AZM+IL-4, MN patches containing both azithromycin and IL-4 PLGA MPs (azithromycin, 1 mg; IL-4, 40 ng; per patch). Data are expressed as mean ± SD (n = 5). Results were analyzed by using one-way ANOVA with post hoc analysis. Statistical significance is indicated by asterisks: *p < 0.05, **p < 0.01, and ***p < 0.001.

Treatment with therapeutic patches not only decreased the inflammatory cytokines, but also increased the expression of anti-inflammatory cytokine such as IL-10 (**Figure 3-5a**) and regulatory T cell marker, FOXP3 (**Figure 3-5b**). To further examine the local immune cell populations, the harvest gum tissues were stained and indicated a shift in the macrophage population to more M2 phenotype. The AZM group had elevated amount of CD206+ macrophages while the groups with IL-4 had a substantially greater amount of CD206+ macrophages at the diseased site (**Figure 3-5c**).

Furthermore, therapeutic MN patches induced pro-healing genes, including RUNX2 (Runt-related transcription factor 2), COL1A1 (type I collagen α1), BMP-2 (bone morphogenetic protein 2), and OCN (osteocalcin) (**Figure 3-6 a, b, c, d**), indicating an induction of osteogenic activity and collagen matrix synthesis in local periodontal tissues.

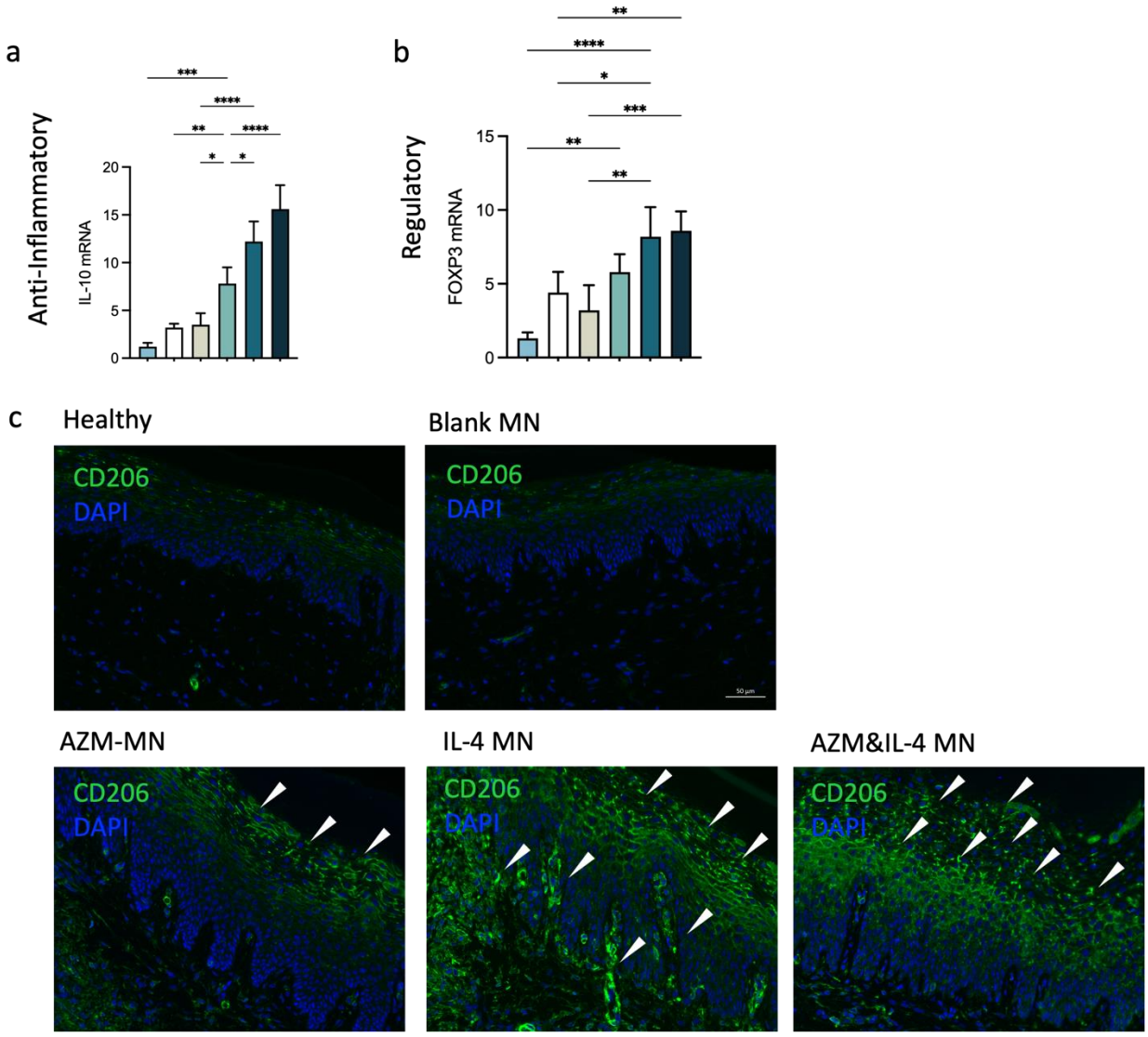

Figure 3-5. ***In vivo*** **evaluation of anti-inflammatory markers and macrophage polarization status.**

A ligature-induced periodontal disease model in rats was used. **a,** Relative mRNA expression level of anti-inflammatory cytokine IL-10. **b,** Relative mRNA expression of Treg marker FOXP3. **c,** Immunostaining of CD206+ macrophages from harvested tissue. Data are expressed as mean ± SD (n = 5). Scale bar of 50μm. Results were analyzed by using one-way ANOVA with post hoc analysis. Statistical significance is indicated by asterisks: *p < 0.05, **p < 0.01, and ***p < 0.001.

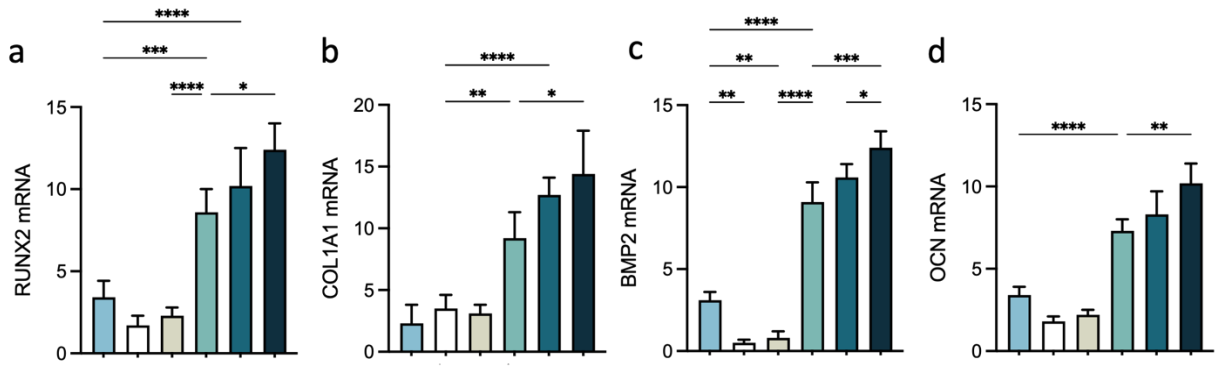

Figure 3-6. In vivo evaluation of tissue healing and bone regeneration.

In the ligature-induced periodontal disease model in rats, relative mRNA expression level pro-healing genes RUNX2, COL1A1, BMP-2, and OCN in the periodontal tissue. Data are expressed as mean ± SD (n = 5). Results were analyzed by using one-way ANOVA with post hoc analysis. Statistical significance is indicated by asterisks: *p < 0.05, **p < 0.01, and ***p < 0.001.

3.4 Discussion

Periodontitis is a chronic, destructive and inflammatory disease affecting the tooth-supporting tissues. Although pathogenic bacteria are the source of inflammation, recruitment and ineffective reaction of immune cells are the fundamental cause of irresolvable inflammation. Thus, the ultimate goal of periodontal therapy is the reverse of tissue degeneration and regenerate the periodontium. Conventional antibiotics such as the class of tetracycline do not have immune modulatory properties, but our finding shed light on the potential of azithromycin as a bifunctional therapeutic option due to its dual action of suppressing bacterial growth and modulating immune cells to suppress inflammation. We have successfully engineered a dissolvable microneedle delivery system loaded with biodegradable microparticles, which allows for painless and suture-free local placement of the therapeutics. Our results show that the azithromycin-loaded microneedle patch alone achieves satisfactory therapeutic outcomes, and the addition of interleukin-4 microparticles can further enhance its efficacy. These results highlight the potential of AZM as a comprehensive treatment option that not only targets the underlying cause of the disease but also supports the regeneration of damaged tissues. This study provides a promising

platform for the treatment of inflammatory disorders, such as periodontitis, and highlights the potential of combining drug delivery systems to improve therapeutic outcomes.

Small molecule immune modulators are also possible to be used in combination with antibiotics. Notably, even without the addition of growth factors, the small molecule immune modulators alone can still achieve regenerative effects. While azithromycin serves as an example of a dual-function agent, the inclusion of more potent small molecule immune modulators alongside antibiotics in a patch can enhance therapeutic efficacy in a combinational manner. By integrating these therapeutic components into a single treatment platform, clinicians can potentially achieve enhanced clinical outcomes, including reduced inflammation, tissue regeneration, and ultimately, improved patient outcomes.

Small molecules, unlike large biologics, are easy to fabricate and store. However, small molecules diffuse quickly and if taken orally, it affects the whole immune system throughout the body. Immune suppression of the whole immune system put patients into a high-risk state of infection. So, local immune modulation with controlled and prolonged release of immune modulators are desirable. The use of PLGA biodegradable microparticles loaded into the microneedle system ensures controlled and sustained release of the antibiotic at the target site for a localized treatment to diseased gingival tissues.

Microarray patch, as a local delivery platform, has been used in various applications including transdermal delivery, ocular delivery, and combinational delivery. Inside the oral cavity, it has been used for tongue, gingival and buccal tissues. Unlike local injection, microarray patches have multiple release points rather than a single bolus delivery. It helps with spread of therapeutic loads over a wider range of diseased area. This novel delivery method enhances the efficiency and effectiveness of treatment while minimizing discomfort for patients.

In conclusion, this study contributes to our understanding of periodontitis and proposes a novel treatment approach utilizing azithromycin as a bifunctional antibiotic. The use of a microneedle delivery system enhances the targeted and painless administration of the antibiotic

to the gingival tissue. The dual action of AZM in suppressing bacterial growth and modulating immune responses demonstrates its potential as a comprehensive therapeutic strategy for periodontitis. These findings provide a basis for further research and potentially pave the way for the development of novel and effective treatment options for this prevalent oral disease and more chronic inflammatory diseases.

3.5 Materials and Methods

Chemicals and biologicals. Unless noted otherwise, all chemicals were purchased from Sigma-Aldrich. Glassware was acid-cleaned overnight and then thoroughly rinsed with Milli-Q water. Cell culture reagents, solutions, and dishes were obtained from Thermo Fisher Scientific unless otherwise specified.

PLGA microparticle synthesis. Acid terminated PLGA (200 mg; 50:50 lactic acid-to-glycolic acid ratio) was dissolved and stirred in 5 mL dichloromethane (DCM) overnight. To fabricate AZM MPs via single emulsion method, 15 mg AZM was added to 5 mL PLGA-DCM mixture. A 10-fold volume of 1% polyvinyl alcohol (PVA) was added right before homogenization at 5000rpm for 10 min. To fabricate IL-4 MPs via double emulsion method, primary emulsion (water-in-oil) was formed by adding 10μg (200μl of 50μg/ml) IL-4 aqueous solution to 4ml of 40mg/ml PLGA organic solvents and the mixture was sonicated at 40% power for 2 min with a cycle of 4s on and 2s off. Next, secondary emulsion (oil-in-water) was formed by slowing adding 1% PVA to the primary emulsion. The secondary emulsion was homogenized at 5000rpm for 10 min.

For both AZM and IL-4 MP, the homogenized solutions were poured into 10-fold volume of 0.1% PVA and stirred for 4 h in open air to evaporate the organic solvents. Low-speed centrifugation (2,000 rpm, 5 min) was performed three times to wash and remove undesired clumps. Precipitated MPs were preserved at 4°C for short-term use and at -20°C for long-term use.

MN patch fabrication. MN molds were purchased from Micropoint Technologies (Singapore) with pyramid shape of 200μm base diameter, 750μm height and 500μm tip-to-tip spacing. To fabricate MNPs, 70% ethanol was casted on negative PDMS molds and vacuum for 5 minutes. Following the removal of bubbles and excess ethanol, 100μl suspension of MPs in 20% PVP and 0.75% glycerol were casted into the well of the mold. MNPs were air dried at room temperature overnight or at least 6 hours. Further drying could be performed by placing mirconeedle patches into vacuum for 2 hours. Solidified MN patches were peeled off from the molds and stored at 4°C until use or 20°C when IL-4 were present.

Mechanical property of MNs. The mechanical strength of MNs was measured by compression test on a low-force mechanical testing system (5943 MicroTester, Instron). The MN tips were placed perpendicularly to the stainless-steel plate and were pressed against another stainless steel plate moving at a constant speed of 0.5mm/min. Correlations between the applied force and the deformation of the MNs were recorded. All tests were performed in triplicate.

Kirby-Bauer agar disk diffusion assay was used to test the antibacterial properties of drugs against *P.g* and *A.a.* (D7SS strain). Soluble drug control discs were prepared by adding calculated amount of corresponding solution to 8 mm sterile paper disks. There were discs made from PBS, azithromycin, tofacitinib, lupeol and dexamethasone. These paper disks were air-dried in a biosafety cabinet before use. These disks and MN patches were placed in agar plates inoculated with 10^7 colonies of bacteria at 37°C. The inhibition zones were measured after several days depending on the bacteria strain.

Liquid antibacterial assay. Supernatants were collected from AZM MNP immersed in 1ml of PBS. In 48-well plates, 500μl of the supernatants was combined with 2x bacteria culture medium with a final inoculation of $5x10^7$ *P.g.* per well. After three days of growing under anerobic condition, the colony-forming units were counted per sample and MTT was used to examine the bulk

bacteria viability by adding MTT to the culture, incubating for 2 hours and measuring absorbance at 570nm.

Animal studies. Eight- to ten-week-old wild-type (C57Bl/6) mice were purchased from the Jackson Laboratory and Eight- to ten-week-old wildtype (Sprague Dawley) rats were purchased from Charles River Laboratories. Animals were maintained in specific pathogen-free facilities at the University of California, Los Angeles (UCLA). All experiments on mice/rats and cells collected from mice/rats were performed under a protocol approved by the Animal Research Committee and in accordance with UCLA's institutional policy on the humane and ethical treatment of animals.

Isolation of bone marrow-derived macrophages. Eight- to ten-week-old C57Bl/6 mice or Sprague Dawley rats were euthanized, and hindlimbs were harvested in PBS. Under sterile conditions, muscles were scraped off, and the ends of bones were cut off. Bone marrow was flushed into a sterile 50 mL conical tube with 2 mL Dulbecco's modified Eagle's medium (DMEM)/F12 supplemented with 10% fetal bovine serum and 1% penicillin-streptomycin. Cells were pelleted and plated with mouse/rat 50 ng/mL macrophage colony stimulating factor (BioLegend). Following 3 days of incubation, 5 mL fresh complete DMEM/F12 medium with 25 ng/mL macrophage colony stimulating factor was supplied per 10 cm cell culture dish. Cells were again incubated for 3 more days. Then supernatants were discarded, and dishes were washed with PBS three times to remove non-adherent cells. BMDMs were gently scraped off the dish, pelleted, counted, and seeded in new plates for further macrophage polarization and experimentation. LPS (10 ng/mL) was used to induce pro-inflammatory macrophages, while 25 ng/mL IL-4 was used to induce pro-healing macrophages. Controls were simply adding complete DMEM/F12 medium.

RNA isolation, reverse transcription and qPCR. Total RNA was extracted by using TRIzol reagent (Life Technologies, Gaithersburg, MD, U.S.A.), and the concentration was determined from spectrophotometric optical density measurement (Thermo Scientific NanoDrop). The OD260/OD280 ratio in all samples ranged between 1.7 and 2.0 to ensure RNA purity. Reverse

transcription was then carried out using Maxima SYBR Green qPCR master mix according to manufacturer's suggested protocol. The cDNA was stored at −20°C. PCR was performed by using SYBR Green kit according to manufacturer's suggested protocol on BioRad CFX96 PCR detection system. Primer sequences were as follow:

GAPDH- Forward 5'CATCACTGCCACCCAGAAGACTG Reverse 5'

ATGCCAGTGAGCTTCCCGTTCAG;

iNOS – Forward 5' GAGACAGGGAAGTCTGAAGCAC Reverse

5'CCAGCAGTAGTTGCTCCTCTTC;

Animal study. *In vivo* functionality of designed MNs was evaluated using a rat periodontal defect model, as described previously with some modifications[159,161]. Two-month-old virgin male and female Sprague Dawley rats (Harlan Laboratories, Livermore, CA) were utilized for *in vivo* testing of the proposed periodontal treatments according to approved animal protocols. The animals were divided into four groups (four rats per group): (i) healthy control, (ii) no treatment (untreated), (iii) blank MNP, (iv) AZM MNP containing azithromycin, (v) IL-4 MNP containing interleukin-4, and (vi) AZM+IL-4 MNP, containing azithromycin and IL-4. Briefly, mucoperiosteal flaps were elevated in rats in groups (ii-iv), uncovering the alveolar bone adjacent to the mesiolingual aspect of the first maxillary molars. The alveolar bone covering the root surfaces on the lingual side was removed with a dental bur under constant saline irrigation, and *A.a.*-coated 5-0 silk ligature was tied around the left second molar. Silk ligature was inoculated with *A.a.* under anaerobic conditions for 24 hours before the procedure. Three weeks later, designed patches were inserted into the defect site as noted above for groups. Eight weeks post-implantation, the animals were sacrificed and the amounts of bone regeneration at defect sites were evaluated using µCT analysis. All the specimens were standardized, and µCT images were calibrated for proper comparative analysis. The vertical bone loss at each defect site was evaluated by measuring the distance between cementoenamel junction (CEJ) and alveolar bone crest as well as the relative alveolar bone area according to methods reported in the literature.[160]

***Characterization of inflammatory response at defect sites*.** Populations of immune cells in periodontal tissue were analyzed as described previously [161]. Briefly, at 8 weeks post-implantation, buccal and palatal tissues of maxillary molars were isolated and dissociated using collagenase and DNase I (50 µg/mL) at 37°C for 15 minutes. These enzymes were then inactivated with EDTA (20 µL/mL of solution). Tissues were then disaggregated and passed through a 100-µm cell strainer to obtain a single-cell suspension. Quantitative PCR assays were used to analyze gene expression. RNA from isolated cells was isolated using Trizol reagent. RNA was reverse-transcribed and single-stranded cDNA was made using a Superscript III cDNA synthesis kit. Relative gene expression was calculated using the $2^{-\Delta\Delta Ct}$ method, with normalization to the *Ct* of the housekeeping gene beta actin. Quantification of *A.a.* in the periodontal tissues was performed as previously reported [161]. The concentrations of inflammatory cytokines and anti-inflammatory cytokines were measured by using ELISA kits after the extraction of proteins from the gingival tissue by tissue homogenization.

***Statistical analysis*.** The Kruskal-Wallis rank sum test, one-way ANOVA and two-tailed Student's t-test were utilized as appropriate to analyze the data at a significance of α or $p < 0.05$. Quantitative data are expressed as mean ± SD. To determine the number of specimens for the proposed experiments, power analysis was conducted based on our preliminary data.

4. VIRUS-LOADED MICRONEEDLES FOR IN SITU CELL REPROGRAMMING

4.1 Abstract

In situ gene delivery offers a targeted approach for transferring nucleic acid to specific cells as a desired location and has several advantages over systemic administration of genetic molecules, including convenience of administration, reduced potential side effects, and lower dosage requirements. To enhance the efficiency of gene delivery, local immune modulation has emerged as a promising strategy to modify the native immune responses at the site of delivery. To mitigate immunogenicity, we investigated the sustained local delivery of immune modulators, including suppressants such as glucocorticoids known for their anti-inflammatory and immunosuppressive effects, as well as protein immunomodulatory agents like interleukin-4 and TGF-β, which have signaling functions in immune cell pathways. In this study, we developed and optimized a novel biomaterial-based approach using a microneedle patch for co-delivery of viral vectors and immunomodulator to enhance gene delivery efficiency at the targeted site. In a subcutaneous injection model, we observed that dexamethasone, a glucocorticoid, improved the transfection efficiency of DsRed, a fluorescence marker used to assess gene delivery efficiency. Furthermore, to evaluate the therapeutic benefits of local viral delivery combined with immunomodulatory agents, we utilized GMT-retrovirus for direct cardiac reprogramming in a mouse ischemia-reperfusion model, with the microneedle patches serving as an alternative to injection. The results demonstrated that the administration of IL-4 locally in microparticles reduced inflammation in the macrophages surrounding the injection site in the pericardium, and the use of virus-loaded microneedle patches facilitated a more uniform spread of the viral vectors in the pericardium.

4.2 Introduction

In situ gene delivery refers to the delivery of genetic material directly to the target cells within their natural environment or specific anatomical site in the body[117]. Unlike ex vivo gene

transfer, which involves extracting cells from a patient, genetically modifying them in a laboratory setting, and then reintroducing them back into the patient, *in situ* gene transfer offers a more streamlined and less invasive method[117]. It eliminates the complex steps of cell isolation, culture, and re-implantation, thereby simplifying the process and reducing potential complications.

85% of *in situ* delivery uses viral vectors, but immunogenicity still limits the efficiency and time period of gene transfer[183]. Study has systematically administered immune suppressive drug to boost the transduction efficacy of Adeno-Associated Virus Serotype 9[184], but global suppression affects the whole immune system and can have many disadvantages such as increased risks of getting infections. Therefore, local immunomodulation is desirable for boosting the gene transfer efficiency at the target site without affecting the overall immunity.

In situ gene transfer holds great promise for various applications in gene therapy, regenerative medicine, and disease treatment. In recent years, the field of regenerative medicine has witnessed remarkable progress in the pursuit of novel therapies for tissue repair and organ regeneration. One groundbreaking approach that holds immense promise is *in situ* cell reprogramming, which involves the conversion of one cell type into another directly within the body, bypassing the need for laborious cell isolation, expansion, and transplantation. While traditional methods of delivering reprogramming factors, such as viruses or genetic materials, have shown efficacy *in vitro*, their translation to *in vivo* applications has remained challenging. We will use the direct cardiac reprogramming as a proof-of-concept model to show the effects of local immunomodulation to gene transfer efficacy.

Dissolvable microneedle patch (MNP) has gained considerable attention in recent years due to their ability to penetrate the skin or other tissues with minimal discomfort and tissue damage. These microneedles, with their minuscule size and high precision, enable precise and localized delivery, enhancing the efficiency and safety of in situ cell reprogramming techniques. The localized delivery offered by microneedles minimizes off-target effects and reduces the risk of systemic side effects associated with traditional systemic administration methods.

Several research groups have been utilized MNP for treating myocardial infarction. Tang, J. *et al.* delivered cardiac stromal cells for heart regeneration and MN created the channels to allow penetration of the regenerative factors secreted by stromal cells to enter the impaired myocardium[50]. Lim, S. et al. engineered adhesive MNPs by fusing biofunction peptides to mussel adhesive protein. Such double-layered adhesive microneedle bandage can overcome the dynamic and constant cardiac muscle movement and enhance therapeutics retention[51]. Shi, H. *et al.* reported the success of MNP coated with adeno-associated virus (AAV) – vascular endothelial growth factor (VEGF) for gene delivery and angiogenesis[185]. Moreover, for minimal invasive therapies, MNP that are near-infrared (NIR)-triggered self-unfolding graphene oxide (GO)-poly(vinyl alcohol) (PVA) MNP was designed and fabricated by Fan, Z. *et al*[186]. Not limited to these studies, there are ongoing innovations for minimal invasive MNP solutions for cardiac tissue regeneration from different perspectives. But no one has explored gene delivery for *in situ* cardiac cell reprogramming using MNP.

The first gene delivery using MNP was reported in early 2023. You, Y. *et al*. demonstrated the delivery of extracellular-matrix α1 type-I collagen (COL1A1) gene via MNP loaded with mRNA-encapsulating extracellular vesicles[187]. This is a non-viral approach for delivering mRNA of a therapeutic protein[188].

In this study, we delve into the cutting-edge advancements in the field of local immunomodulation for *in situ* cell reprogramming. We developed a virus-loaded microneedle with immunosuppressant and immunomodulator to modulate the local immune environment in a controlled and minimally invasive manner. We investigated how each factor contributing to virus viability and optimized the design and fabrication of these microneedles for better preservation of virus integrity. Moreover, we explore the challenges and opportunities associated with this emerging technology, including optimizing delivery efficiency, ensuring long-term stability, and ensuring the safety of the reprogramming process.

To assess the impact on gene transduction efficiency, we employed subcutaneous injection of DsRed retrovirus as a representative model for gene expression. Specifically, we investigated the effects of dexamethasone and IL-4 on this process. Dexamethasone is a synthetic glucocorticoid with known anti-inflammatory and immunosuppressive properties, while IL-4 is a protein known for its immunomodulatory functions and has potential benefits on cardiomyocytes directly. Furthermore, we utilized cardiac reprogramming from fibroblasts as a proof-of-concept model to examine the effects of dexamethasone and IL-4 on immune cells in disease contexts. This model allowed us to evaluate both the immune response and the functional outcomes of GMT (Gata4, Mef2c, and Tbx5)-transfected cells in cardiac tissues.

Through these experiments, we aimed to elucidate the influence of dexamethasone and IL-4 on gene transduction efficiency, immune cell modulation, and the subsequent cardiac functions in the context of cardiac reprogramming. By studying these effects, we aimed to gain insights into the potential therapeutic applications and mechanisms underlying immune modulation in gene therapy approaches for cardiac diseases.

4.3 Results

4.3.1 Local immune suppression enhanced gene transfer efficiency

Glucocorticoid such as dexamethasone has been administered systematically to overcome the inflammatory responses when injecting viral vectors for gene delivery[184,189,190]. For both lentivirus and adenoviruses, a transient pretreatment of dexamethasone can lower the vector-induced inflammatory immune responses and enhance the safety and efficiency of gene transfer[189,190]. In order to facilitate tissue remodeling through in situ cell reprogramming, it is desirable to transiently suppress the immune response at the local tissue to prevent vector-induced acute inflammation. Local and sustained delivery of immunomodulatory agents can be in the form of injectable hydrogels, biodegradable implants and biodegradable microneedle patches, but not limited to these local administration routes[191–194]. The objective is to achieve controlled

release of immunomodulators over time while ensuring the viability and effectiveness of viral vectors.

To investigate the feasibility and efficacy of local immunomodulation in enhancing gene transfer efficiency, we first performed subcutaneous injection of DsRed-retrovirus as a simple model to examine the gene transfer efficiency. The *in vivo* expression of DsRed was observed to be extremely weak without any additional intervention. In order to achieve immune suppression at the local tissue level, we encapsulated dexamethasone (immunosuppressant) or interleukin-4 (a cytokine) within biodegradable microparticles made of poly(lactic-co-glycolic acid) (PLGA). This allowed for sustained release of dexamethasone or IL-4 over time. To examine the individual and combinational results of these two microparticles, we tested subcutaneous injection of DsRed-retrovirus together with 1) blank MP, 2) Dex MP, 3) IL-4 MP and 4) Dex&IL-4 MP. Our data demonstrated that the administration of dexamethasone-loaded microparticles (Dex MP) significantly enhanced DsRed expression compared to the control groups receiving blank microparticles (BlankMP) without immune suppression (**Figure 4-1, Figure 4-S1**). Although IL-4 is a known immunomodulator of macrophages and T cells, it only showed a little enhancement of DsRed expression (**Figure 4-1**). However, the combination of Dex MP and IL-4 MP had a synergistic effect on boosting the DsRed gene transfer (**Figure 4-1**). The effects observed were localized due to the slow-release characteristics from the PLGA MP, resulting in a restricted diffusion zone.

These results highlight the potential of local immunomodulation using biodegradable microparticles for enhancing gene transfer efficiency. By achieving sustained release of immunosuppressive agents at the site of administration, we can effectively modulate the local immune response and improve the expression of the delivered gene. This localized approach may offer advantages in terms of targeting specific tissues and minimizing systemic side effects associated with broad immune suppression.

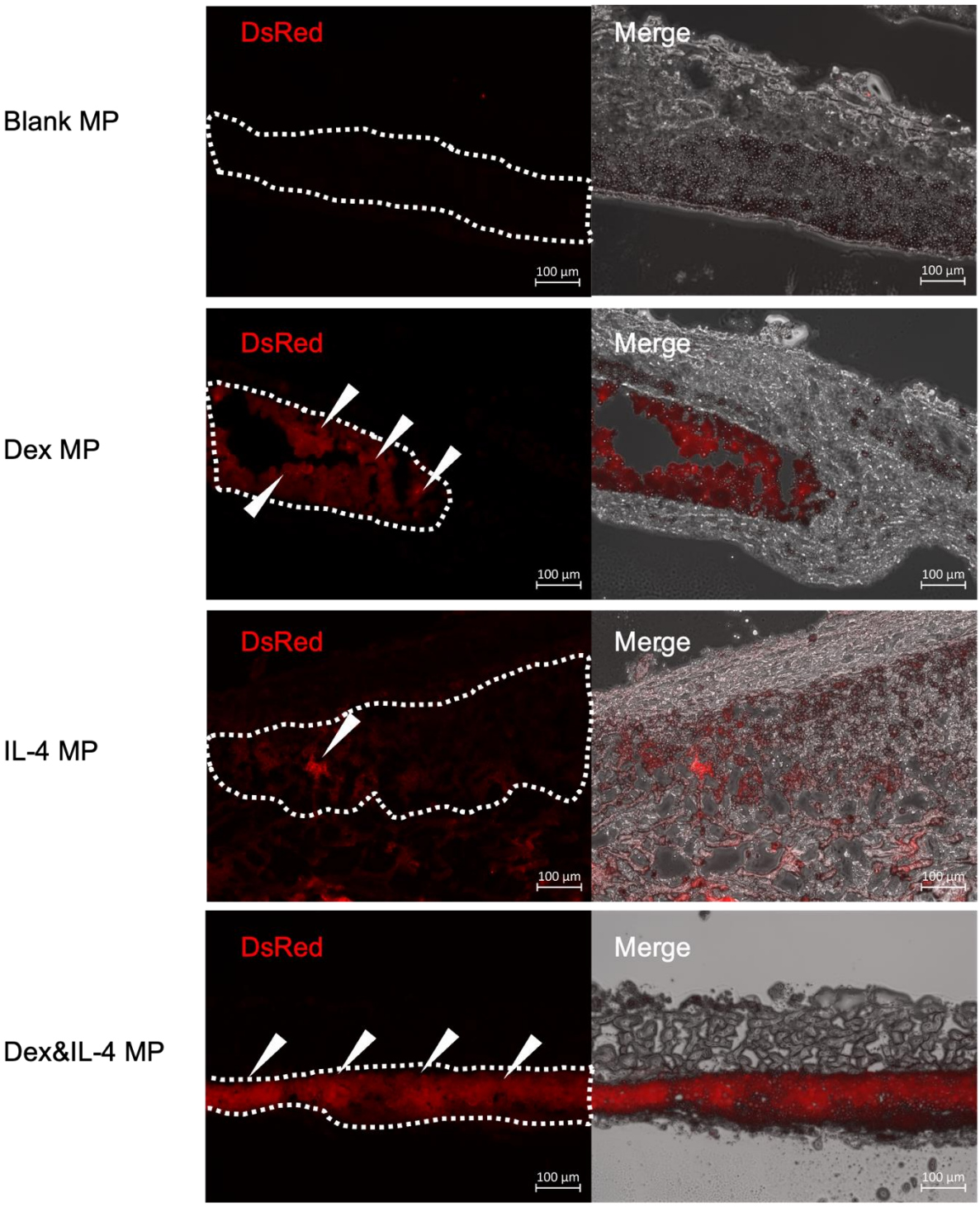

Figure 4-1. The effects of local immune suppression on *in vivo* gene transfer.

Microparticles of 5μm in size with freshly thawed DsRed-retrovirus were injected subcutaneously to the back of healthy wild-type C57/B6 mice. Shaved skins were harvest three days after injection and cryosectioned for direct imaging. Images were taken with the same exposure time of 3s. Scale bar of 100μm.

4.3.2 Design and fabrication of virus-loaded microneedle patch

We developed a microneedle platform that consists of hundreds of miniatured needles which can penetrate without causing pain. Polymeric biodegradable microneedle has the benefits of eliminating sharp disposal, easy administration, and local modulation.

The main challenge of virus-loaded microneedle fabrication is to dry polymers with virus vectors and ensure the viability of virus. Used in coated microneedles, carbohydrates especially trehalose have been used as an excipient to stabilize protein and virus structures[33,195–197]. Therefore, to ensure the virus viability after fabrication into microneedle, trehalose is used as a protectant and 15% in the final formulation was tested to be a secured amount (**Figure 4-S2**). Moreover, various factors including matrix materials, temperature, virus-trehalose ratio, drying condition, drying volume and drying speed were investigated to better understand their effects to virus viability (**Figure 4-2b-g**). With a comprehensive review of each factor, carboxymethylcellulose is selected as the matrix material for mechanically viable microneedle and won't affect virus viability. We also found that temperature is a major contributor to virus viability. The viability decreased dramatically in the first half an hour at 4°C or 20°C (room temperature) after thawing from -80°C but remained relatively stable from two to eight hours. With all the consideration, the final fabrication flow is detailed illustrated in **Figure 4-S3**.

By maximizing the loading capacity and tuning each factor that affecting the virus viability, the resulting virus-loaded MNP has comparable effectiveness to control which are freshly thawed from -80℃ (**Figure 4-2h**). It is stable at -80℃ for at least one week or -20℃ for three days (**Figure 4-2i**).

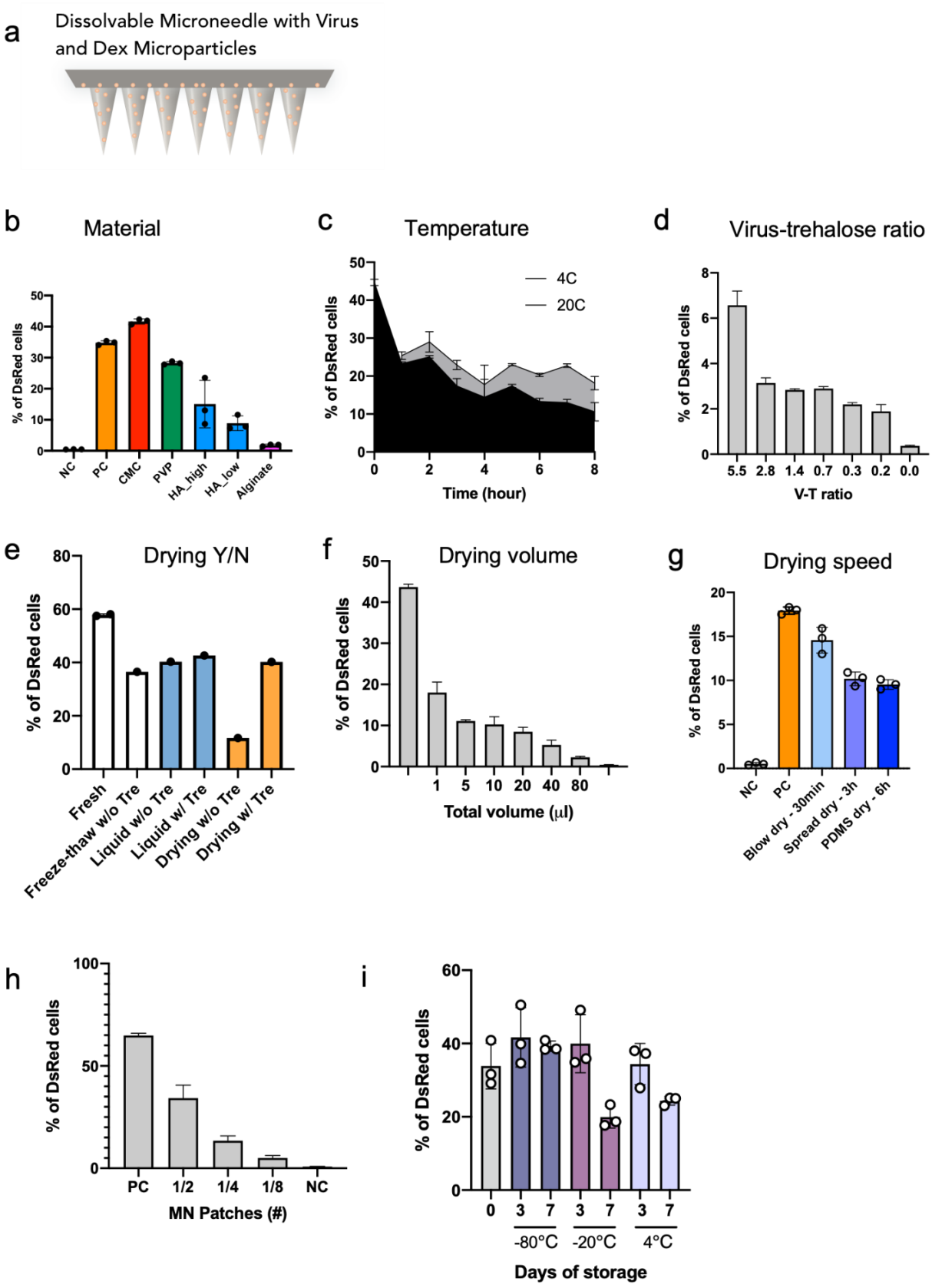
a
Dissolvable Microneedle with Virus and Dex Microparticles
b
Material
% of DsRed cells
NC
PC
CMC
PVP
HA_high
HA_low
Alginate
c
Temperature
4C
20C
% of DsRed cells
Time (hour)
d
Virus-trehalose ratio
% of DsRed cells
5.5 2.8 1.4 0.7 0.3 0.2 0.0
V-T ratio
e
Drying Y/N
% of DsRed cells
Fresh
Freeze-thaw w/o Tre
Liquid w/o Tre
Liquid w/ Tre
Drying w/o Tre
Drying w/ Tre
f
Drying volume
% of DsRed cells
1 5 10 20 40 80
Total volume (μl)
g
Drying speed
% of DsRed cells
NC
PC
Blow dry - 30min
Spread dry - 3h
PDMS dry - 6h
h
% of DsRed cells
PC 1/2 1/4 1/8 NC
MN Patches (#)
i
% of DsRed cells
0 3 7 3 7 3 7
-80°C -20°C 4°C
Days of storage

Figure 4-2. Design and optimization of DsRed-retrovirus loaded MNP.

a, Design of virus-loaded MNP. **b-g,** the effects of various factors on the transduction of DsRed into 3T3 fibroblasts. **h,** Gene transfection efficiency of MNP with various size. **i,** DsRed retrovirus viability with different storage condition for three and seven days. Data are expressed as mean ± SD (n = 3).

4.3.3 In vivo enhancement of gene transfer efficiency for cardiac reprogramming

The feasibility of gene delivery using microneedle patch for therapeutic purpose is further illustrated in cardiac reprogramming. Due to the buildup of fibroblasts after infarction, we would like to reprogram these fibroblasts directly into cardiomyocyte-like cells to improve cardiac functions. Transcription factors - Gata4, Mef2c, and Tbx5 (GMT) – are the minimum required to reprogram endogenous cardiac fibroblasts (CF) into induced cardiomyocyte-like cells (iCMs)[112]. A cardiac ischemia-reperfusion model in mice was established by ligating the left anterior descending artery (LAD), which is the largest coronary artery runs anterior to the interventricular septum in the anterior interventricular groove, extending from the base of the heart to the apex. 30 minutes of ischemia followed by removal of ligature causes reperfusion injury to the heart and creates infarction area as shown in **Figure 4-3a**. Both pericardium delivery of DsRed-retrovirus or GMT-retrovirus followed the same timeline of surgery and harvest (**Figure 4-3b**). The difference was that DsRed-retrovirus delivery did not have the injury created by ligation, but just an open-heart surgery for administration of treatments.

The *in vivo* efficacy of gene transfer and expression of MNP is evident in the detection of DsRed fluorescence after pericardium delivery in healthy B6 murine hearts (**Figure 4-3c**). Moreover, MNP showed a well distributed pattern for both DsRed expression and the wide spread of particle distribution was observed in bright field (**Figure 4-4a**). The injection depth and spread of particles was different with approximately 400μm for injection and 200μm for MNP (**Figure 4-4b,c**). This is beneficial to cover a larger area of infarction.

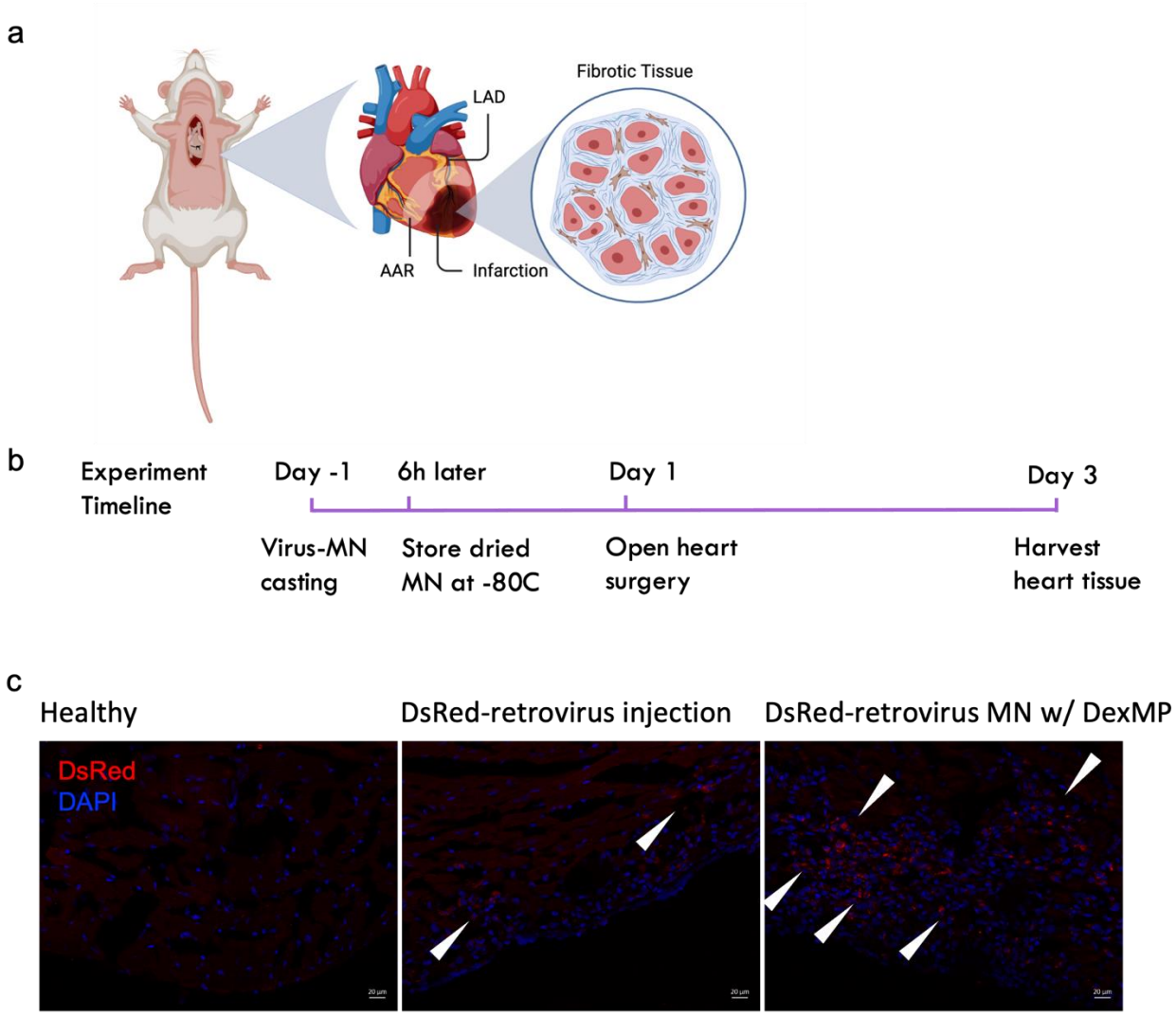

Figure 4-3. *In vivo* efficacy of gene transfer in murine heart.

a, Cardiac ischemia-reperfusion injury in mice to generate area at risk (AAR) and area of infarction. **b,** Timeline of microneedle fabrication, storage, open heart surgery and heart sample harvest. **c,** DsRed expression comparing injection and MNP to healthy groups. Scale bar of 20μm.

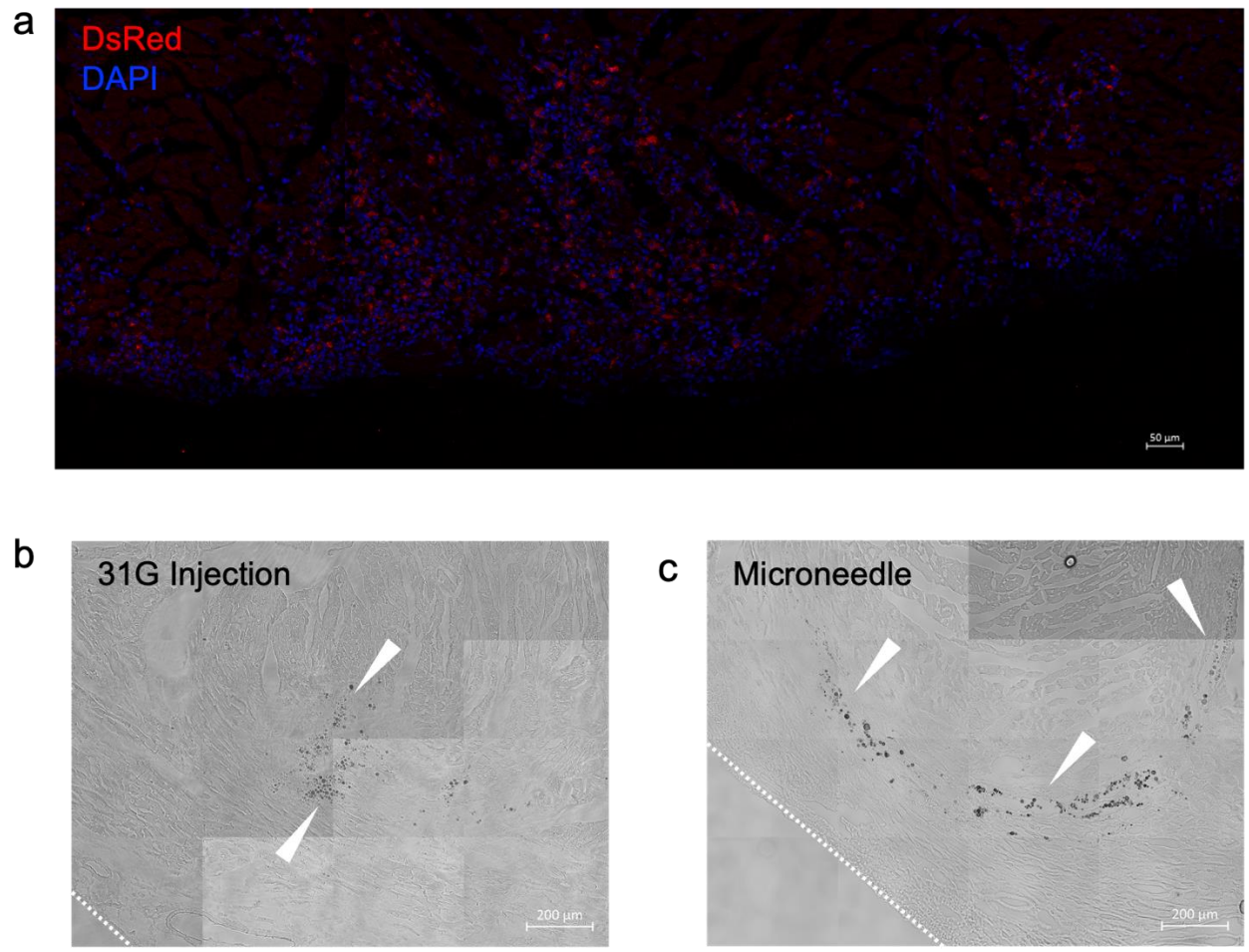

Figure 4-4. DsRed fluorescence and particle distribution.
To show a larger area under the microscope, tiles images are taken for **a,** DsRed expression in pericardium. Scale bar of 50µm. **b,c,** bright field images of injection versus MNP. Scale bar of 200µm.

Moreover, macrophage is known as a critical cell type involved in tissue repair and remodeling after cardiac infarction. So, we examined the type of macrophages recruited to the site for groups of blank MPs, dexamethasone MPs, dexamethasone and interleukin-4 MPs via injection and dexamethasone and interleukin-4 MPs via microneedle. Addition of IL-4 recruited more CD206 positive M2 macrophage and for prohealing function and regeneration (**Figure 4-5**). The number of CCR7 positive M1 macrophage was decreased (**Figure 4-6**). The data for cardiac reprogramming and cardiac function are still in progress. So far, our in vivo experiments have shown that using microneedle-based viral delivery with local immune suppression

enhanced the virus transduction efficiency in situ and delivery of IL-4 helps with recruiting prohealing macrophage for cardiac regeneration after infarction.

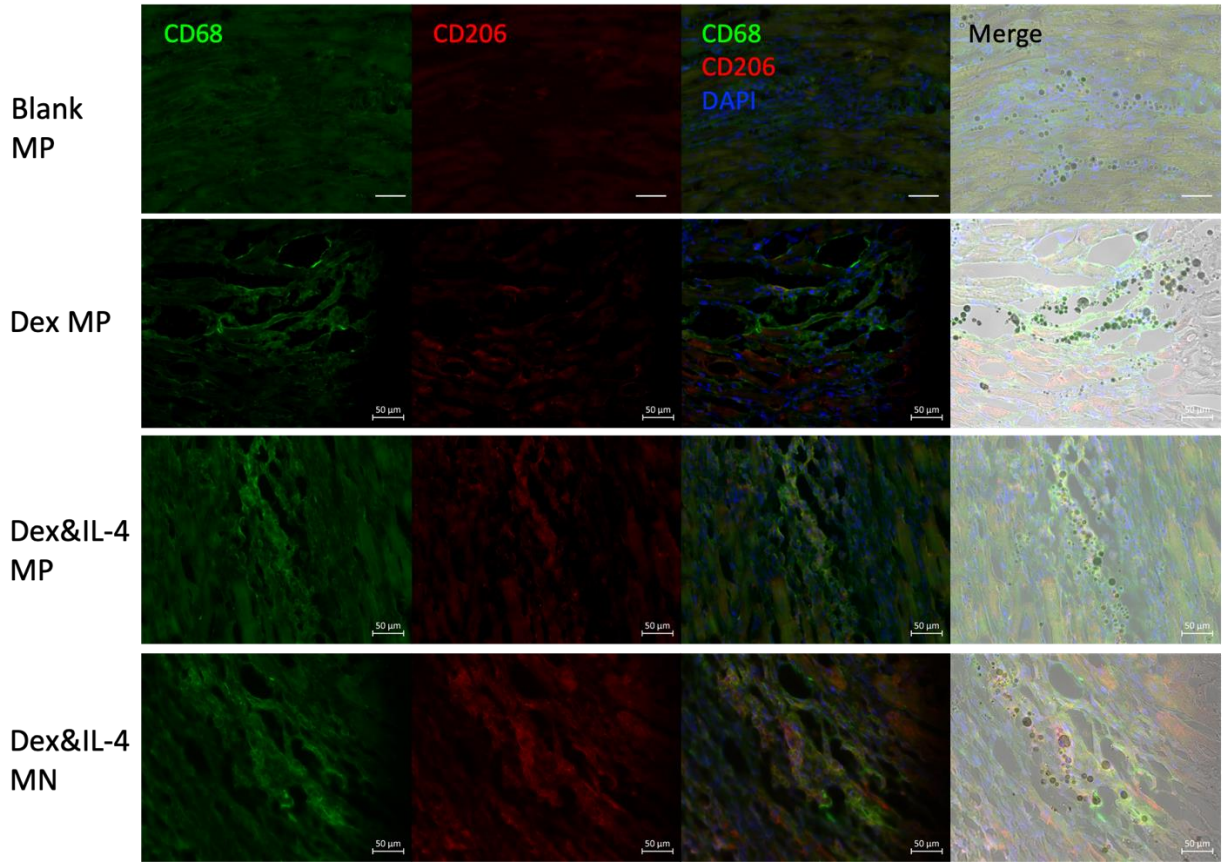

Figure 4-5. Immunostaining of macrophage marker CD68 (pan macrophage) and CD206 (M2 macrophage)

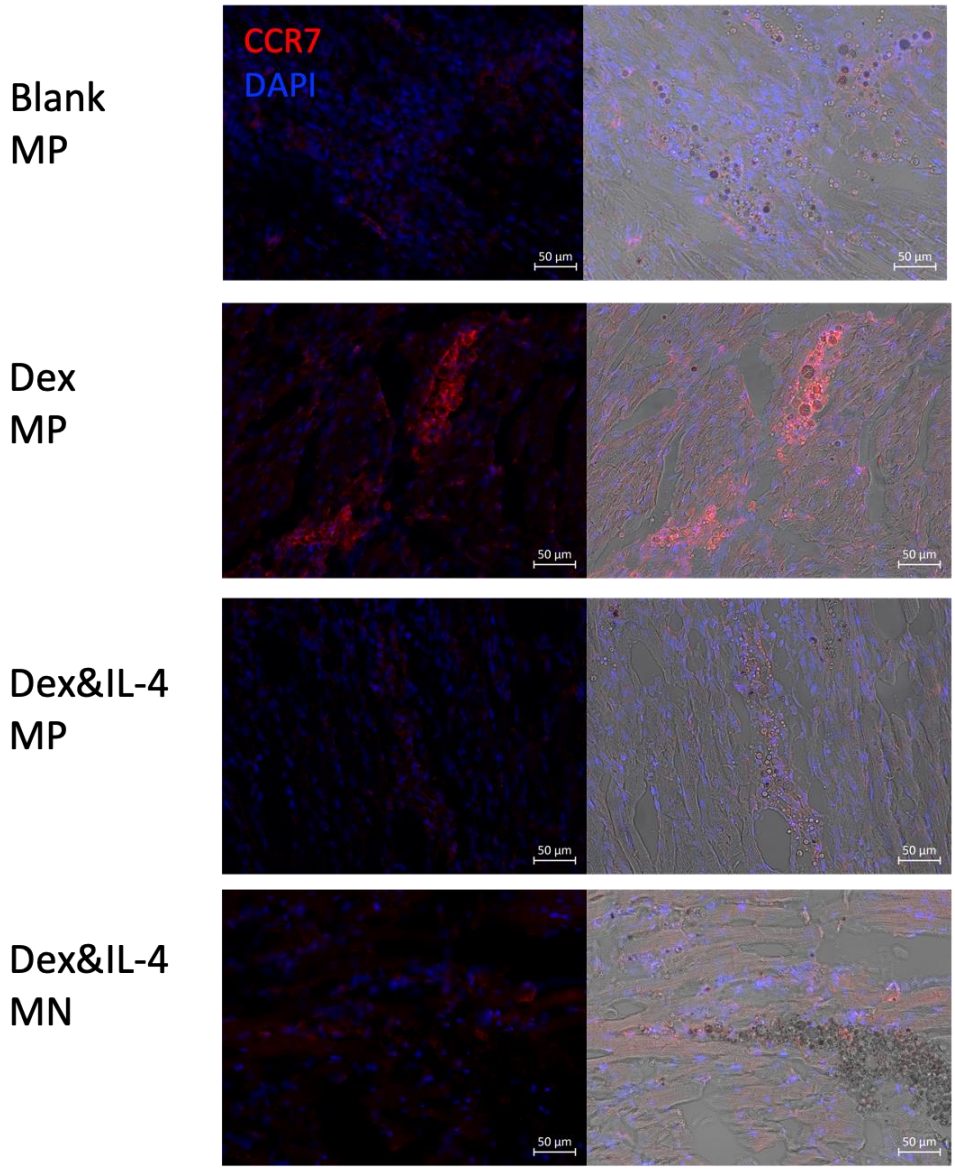

Figure 4-6. Immunostaining of macrophage marker CD206 (M2 macrophage) and CCR7 (M1 macrophage).

In summary, our study highlights the potential of local immunomodulation with dexamethasone to enhance viral transduction efficiency and the successful development of a CMC-based polymeric MN patch for efficient virus delivery. These findings contribute to the advancement of virus-based gene therapy and offer insights into the reprogramming of fibroblasts for cardiac regeneration.

4.4 Discussion

As the field of regenerative medicine continues to evolve, viral vector-based gene transfer with the help of local immunomodulation represent a game-changing tool for *in situ* cell reprogramming. Their potential to directly manipulate cells with higher efficiency within the body opens up new avenues for tissue regeneration, disease modeling, and personalized medicine. We aim to inspire further research and development, driving us closer to a future where the regeneration of damaged or diseased tissues becomes a clinical reality.

Here, we used cardiac reprogramming as a therapeutic case to illustrate the disease tissue regeneration potential. Our study demonstrates that immunomodulation with dexamethasone microparticles significantly enhances viral transduction efficiency of DsRed transgene in subcutaneous and cardiac tissue. Dexamethasone effectively suppresses immunogenicity in which the host immune cells attack on foreign viruses although they are therapeutic vectors. Lowering the immunogenicity and controlling the immune cell responses promote the survival of retroviruses thus increase their chance of entering target cells. Moreover, local delivery of dexamethasone via slow release from microparticles eliminate the side effects of suppressing overall immune system.

Furthermore, heart muscles are constantly contracting and moving to pump blood, so it adds significant difficulties for precise injection into the myocardium. To have an easier way of administration and a better spread of the therapeutic agent, we developed a carboxymethylcellulose (CMC)-based polymeric microneedle patch for efficient virus delivery, both *in vivo* and *in vitro*. Using the DsRed-retrovirus system, we evaluated the transduction efficiency by measuring DsRed expression levels. Our results demonstrated that the MN patch effectively delivered the virus to the intended target, resulting in comparable levels of DsRed expression.

Next, we explored the application of the GMT-retrovirus system to reprogram fibroblasts into cardiomyocytes within the infarct zone. As retroviruses target dividing cells, it will target the dividing fibroblasts when forming fibrosis after myocardial infarction. In this way, direct cardiac cell reprogramming from fibroblasts to functional cardiomyocyte-like cells can facilitate tissue remodeling to a prohealing state and promote tissue regeneration. Functional data of the heart are still being analyzed by collaborators from Ke Cheng's group.

Our current experimental methods still utilized open-chest surgery, but minimal invasive approaches are highly desirable to be clinically translatable. New approaches for cardiac delivery are rapidly developing to improve the surgical procedures or innovate materials with shape memories[186,198]. Endoscope can be utilized to look inside body cavity for placement of biomaterial scaffolds. Also, shape memory of biomaterials can allow delivery of a self-unfolding MNP. Our virus loaded MNP needs further optimization to accommodate clinical need for easy and minimal invasive cardiac delivery.

4.5 Materials and Methods

Chemicals and biologicals. Unless noted otherwise, all chemicals were purchased from Sigma-Aldrich. Glassware was acid-cleaned overnight and then thoroughly rinsed with Milli-Q water. Cell culture reagents, solutions, and dishes were obtained from Thermo Fisher Scientific unless otherwise specified.

PLGA microparticle synthesis. Acid terminated PLGA (200 mg; 50:50 lactic acid-to-glycolic acid ratio) was dissolved and stirred in 5 mL dichloromethane (DCM) overnight. To fabricate Dex MPs via single emulsion method, 15 mg dexamethasone was added to 5 mL PLGA-DCM mixture. A 10-fold volume of 1% polyvinyl alcohol (PVA) was added right before homogenization at 5000rpm for 10 min.

To fabricate IL-4 MPs via double emulsion method, primary emulsion (water-in-oil) was formed by adding 10μg (200μl of 50μg/ml) IL-4 aqueous solution to 4ml of 40mg/ml PLGA organic solvents and the mixture was sonicated at 40% power for 2 min with a cycle of 4s on and 2s off. Next, secondary emulsion (oil-in-water) was formed by slowing adding 1% PVA to the primary emulsion. The secondary emulsion was homogenized at 5000rpm for 10 min.

For both Dex and IL-4 MP, the homogenized solutions were poured into 10-fold volume of 0.1% PVA and stirred for 4 h in open air to evaporate the organic solvents. Low-speed centrifugation (2,000 rpm, 5 min) was performed three times to wash and remove undesired clumps. Precipitated MPs were preserved at 4°C for short-term use and at -20°C for long-term use.

MN patch fabrication. MN molds were purchased from Micropoint Technologies (Singapore) with pyramid shape of 200μm base diameter, 750μm height and 500μm tip-to-tip spacing. To fabricate MNPs, sterile distilled water was casted on negative PDMS molds and vacuum for 5 minutes. Following the removal of bubbles and excess water, 100μl suspension of MPs in 20% PVP and 0.75% glycerol were casted into the well of the mold. MNPs were air dried at room for 4 hours and placed in vacuum dry for another 2 hours. Solidified MN patches were peeled off from the molds and stored at 4°C until use or 20°C when IL-4 were present.

Mechanical property of MNs. The mechanical strength of MNs was measured by compression test on a low-force mechanical testing system (5943 MicroTester, Instron). The MN tips were placed perpendicularly to the stainless-steel plate and were pressed against another stainless-steel plate moving at a constant speed of 0.5mm/min. Correlations between the applied force and the deformation of the MNs were recorded. All tests were performed in triplicate.

Preparation and quantification of DsRed or GMT retrovirus. Platinum-E retroviral packing cell line was transfected with DsRed or GMT plasmids with FuGENE transfection reagent (Promega) according to the manufacturer's protocol. Culture medium supernatant was harvested after 48h of transfection and passed through a 0.45μm filter unit. The retroviruses in the supernatants were

concentrated by adding 1/3 volume of Retro-X concentrator and storing at 4°C overnight. Centrifugation the samples at 1500 x g for 45 minutes at 4°C collected the retrovirus into an off-white pellet. The pellet was resuspended in 1/100th of the original volume using complete DMEM. The aliquoted samples were stored at -80°C until further use.

Efficiency of transgene expression in vitro. 3T3 fibroblasts were culture in Dulbecco's modified Eagle's medium (Gibco, 11965092) supplemented with 10% fetal bovine serum and 1% penicillin-streptomycin. Subconfluent 3T3 cells were seeded in 24-well plates. Virus-containing MNPs (n=3, each MNP contained ~2x10^{11} copies of DsRed-Retrovirus) were placed into the well after 6h for cell attachment. After a 3-day incubation, the percentages of DsRed-positive cells were determined by flow cytometry. In addition, 3T3 cells in cell culture plates were imaged using fluorescence microscopy.

Animal study. Eight- to twelve-week-old wild-type (C57Bl/6) mice were purchased from the Jackson Laboratory and maintained in specific pathogen-free facilities at the University of California at Los Angeles (UCLA). All experiments on mice were performed under a protocol approved by the Animal Research Committee and in accordance with UCLA's institutional policy on humane and ethical treatment of animals. To limit the contamination and post-operative infection, the experimenter was wearing sterile surgical gloves and surgical mask. The animals were housed at temperatures of ~18-23°C, 40-60% humidity, 12-hour light/12-hour dark cycle and were allowed food and water *ad libitum*.

An established surgical method to induce myocardial infarction in mouse was used to create myocardial ischemia-reperfusion (I/R) injury through ligation of the left anterior descending artery[199]. After 30 minutes of ischemia, ligatures were removed and either injection by 31G needles or MNP were applied to the infarcted regions. Pain medicines were given for three consecutive days after the surgery at a dose of 0.1 mg/kg buprenorphine every 12h and 0.5 mg/kg

carprofen every 24h injected intraperiotoneally. At day 7, the mice will be euthanized before collecting heart samples.

Harvest of heart samples for immunostaining. Mouse hearts transfected with retrovirus were harvested at the end of the experiments by treating the samples in 4% paraformaldehyde overnight, 15% sucrose solution overnight and 30% sucrose solution overnight consequentially. Then, the treated samples were embedded and frozen in Tissue-Tek optimum cutting temperature (OCT) compound. The walls were cryosectioned horizontally at a 10-μm thickness.

Immunostaining of cryosectioned tissue samples. For immunohistochemistry, heart cryosections were rehydrated with PBS. Permeabilization was done with 0.5% Triton X-100; and protein blocking was done with 5% donkey serum in PBS. Proteins of interest in the samples were targeted with the following primary antibodies after an overnight incubation at 4°C: mouse anti-CD68/SR-D1 (1:100, Novus Biologicals), rabbit anti-CCR7 (1:100, Novus Biologies), mouse anti-CD206 (1:100, Santa Cruz Biotech), rabbit anti-CD206 (1:100, Abcam). Primary antibodies were conjugated with AF488 or AF567 secondary antibodies (1:400; Abcam). DAPI (Life Technologies, NY, USA) was used for nuclear staining. Images were taken with a Zeiss microscope.

5. CONCLUSIONS AND FUTURE WORK

5.1 Conclusions

My thesis addressed questions at the intersection of drug delivery, immuno-engineering, and regenerative medicine. The main objective was to demonstrate the potential of local immunomodulation in improving tissue regeneration by tuning the local immune environment (chapter 2 and 3) and enhancing the gene transfer efficiency for *in situ* cell reprogramming (chapter 4). Polymeric microneedle patch is explored as a local delivery method that offers minimal invasive and controlled administration of therapeutic agents directly to the specific tissues, such as gingival and cardiac tissues, which are utilized as proof-of-concept models in my study.

We have shown the development and optimization of several novel approaches for microneedle formulation of local immunomodulation to enable tissue regeneration. Our goal throughout these studies was to employ innovative biomaterial-based approaches to the design of regenerative medicine platforms. For chronic inflammation, our emphasis was on modulating the local inflammatory environment to reduce M1 macrophages and T_{17} cells, and correct the local immunity for prohealing and regenerative immune cell phenotypes. For gene transfer, our emphasis was on locally suppressing the immunity which may attack therapeutic viral vector, hence, boost the gene transfer efficiency for cell reprogramming. With different focuses, the MNP design and release profiles are different, and, in each case, certain design was proposed and optimized for the specific application.

5.1.1 Periodontal local immunomodulation

Gingival tissue is recognized for its remarkable capacity for rapid wound healing[200]. Therefore, the utilization of microneedles (MNs) can significantly enhance the delivery of therapeutic agents by facilitating their penetration into the tissue, taking advantage of the accelerated healing process that subsequently seals the therapeutic ingredients within the temporary "wound". To achieve this objective, we developed a hydrogel-based microneedle patch (MNP) incorporated with dissolvable bases, enabling sustained release of therapeutic

microparticles. Subsequently, for the purpose of clinical translation, the MNP design was simplified by incorporating fewer biomaterial components while still retaining the capability of dissolvable loading with microparticles. Local administration of immunomodulatory cytokines, such as IL-4 and TGF-β, in addition to antibiotics, represents a promising approach to mitigate the issue of exaggerated immune cell response in conjunction with bacterial overgrowth. Furthermore, the utilization of small molecule immunomodulators, such as azithromycin, has demonstrated efficacy in the treatment of periodontal diseases by effectively suppressing bacterial growth and modulating macrophage phenotypes. The promising results we observed in expression of regenerative markers such as RUNX2 (Runt-related transcription factor 2), COL1A1 (type I collagen α1), BMP-2 (bone morphogenetic protein 2), and OCN (osteocalcin), indicating an induction of osteogenic activity and collagen matrix synthesis in local periodontal tissues. MicroCT further indicated the reverse of bone degeneration and significant bone volume was observed in treatment groups comparing to untreated.

Chronic inflammation plays a critical role in numerous disease states, including asthma, heart disease, rheumatoid arthritis, fatty liver disease, inflammatory bowel disease, and obesity, among others. The success of local immune modulation in the gingival niche using MNP introduced a novel approach for regulating immune responses in local inflammation. Since tissue damage is not a result of just pathogen's activity, we gave the needed attention to immune cells while control the pathogens. Expanding the application of MNPs to target additional local sites, such as internal organs, tissues, and joints, holds significant promise and merits further investigation.

5.1.2 Gene delivery with local immunosuppression

Ensuring the preservation and functionality of viral vectors is a key challenge in gene delivery systems. To address this challenge, we investigated the optimization of fabrication conditions for microneedle patches (MNPs). Various factors including material composition,

temperature, virus-to-trehalose ratio, drying conditions, drying volume, and drying speed were systematically explored to determine their impact on virus-loaded MNP performance. Through the development of an optimized protocol, efficient gene transduction of the model gene DsRed was achieved both in vitro and in vivo. Moreover, to demonstrate the clinical potential of our approach, we conducted a proof-of-concept study focusing on cardiac reprogramming. Local delivery of the immunomodulatory cytokine IL-4 was employed to induce a shift in macrophage populations towards regenerative and less inflammatory phenotypes. The results of this study revealed the effectiveness of local IL-4 delivery in promoting a favorable macrophage phenotype conducive to tissue regeneration. These findings highlight the importance of optimized fabrication conditions for viral vector-based gene delivery and the potential of immunomodulatory strategies to enhance the regenerative capacity of target tissues. The successful translation of these techniques could significantly advance gene therapy approaches for various applications, including cardiovascular regeneration.

To conclude, by utilizing the MNP technology, we have successfully demonstrated the feasibility and efficacy of local immunomodulation to optimize the delivery of therapeutic agents to the target tissues, allowing for localized immunomodulation and enhanced gene transfer efficiency. This approach has the potential to improve tissue regeneration by creating an optimal immune environment and/or facilitating the reprogramming of cells *in situ.* With the test of

5.2 Future Work

5.2.1 Microneedle patch design

Optimization of microneedle for clinical translation. Improvement of mechanical strength, balance of strength and flexibility; safe biomaterials; microneedle shapes and spacing; chemical modification of matrix material; use therapeutic molecules as matrix materials to save space and maximize loading capacity; crystal formation for sustained release instead of microparticles.

The future optimization of microneedle patches holds great potential for clinical translation, with several key areas of focus. Firstly, enhancing the mechanical strength of the microneedles while maintaining a balance between strength and flexibility is crucial. This will ensure efficient penetration into the skin while minimizing the risk of breakage or damage. Utilizing microneedle applicator and designing appropriate applicator can be beneficial to ensure optimal penetration and increase the repeatability from people to people and batch to batch. Another important aspect is the selection of safe and biocompatible biomaterials for microneedle fabrication. Advancements in biomaterial science will enable the development of materials that are not only effective in delivering therapeutic agents but also minimize any potential adverse reactions or side effects. Chemical modifications of the matrix material can also be investigated to enhance the performance of the microneedle patch. Surface modifications or functionalization of the matrix can improve drug loading capacity, stability, and release kinetics.

Furthermore, exploring different microneedle shapes and spacing configurations can optimize drug delivery efficiency and patient comfort. The geometry of the microneedles can be tailored to specific applications, ensuring accurate and controlled delivery of therapeutic molecules. We didn't spend too much effort on optimizing the geometry ourselves but rather learn from other literatures. Future works may establish comprehensive analysis of microneedle geometry and change the shape to be the best for penetration and loading. Regarding the loading capacity, utilizing therapeutic molecules themselves as matrix materials can maximize the loading capacity and save space within the microneedle patch. This innovative approach allows for efficient co-delivery of therapeutic agents, minimizing the need for additional matrix materials. Furthermore, exploring alternative methods such as crystal formation for sustained release offers a potential alternative to traditional microparticles. Crystal formation techniques can provide controlled and prolonged release of therapeutic molecules, ensuring sustained efficacy over an extended period. For instance, we noted the formation of tetracycline crystals distributed evenly in gelatin when stored at 4°C.

Finally, adhesive MNP in wet environment holds great promise in revolutionizing mucosal delivery (i.e. oral cavity) and internal organ delivery (cardiac tissue). Retention of drugs at the local site is always a challenge for drug delivery. Currently, adhesive MNP has a layered structure consisted of polymer matrix, adhesive materials and backing materials with some has drug-loaded reservoirs. Medical-grade adhesives such as acrylic-based adhesives or silicone-based adhesives are used to assist the MNP to stay at the targeted area. The backing material of the adhesive MNP serves as a support structure and protects the microneedles during handling and storage. Common backing materials include medical-grade films, such as polyethylene terephthalate (PET) or polyurethane, which are flexible, transparent, and impermeable to moisture. In light of the advancements made in layered adhesive microneedle patches (MNPs), there is still considerable value in conducting further research to explore novel biomaterials that can offer a comprehensive one-material adhesive MNP. By focusing on developing a single biomaterial that combines the necessary adhesive, mechanical, and drug-delivery properties, a holistic approach can be achieved, simplifying the patch design and potentially improving its overall functionality and user experience.

Overall, the future optimization of microneedle patches should focus on addressing these aspects to advance their clinical translation and broaden their applicability in various therapeutic interventions.

5.2.2 Periodontal local immunomodulation

Further exploration is needed to identify and develop targeted immunomodulatory therapies specifically tailored for periodontal diseases. This involves understanding the complex immune responses and molecular pathways involved in periodontal inflammation and designing interventions that can specifically modulate these processes. In-depth understanding of the underlying mechanisms and exploration of potential druggable targets are crucial for the development of small molecule immunomodulators. In addition to chemical compounds, versatile platforms such as peptides and aptamers hold promise as therapeutic agents for local immune

modulation in periodontal diseases. By expanding our knowledge in these areas, we can advance the development of novel and effective immunomodulatory therapies for improved management of periodontal conditions.

The development of efficient and localized delivery systems for immunomodulatory agents is crucial. Researchers can focus on optimizing the design of drug delivery vehicles, such as hydrogels, nanoparticles, or microneedle patches, to enhance the targeted delivery of immunomodulatory agents to periodontal tissues. These systems should aim to achieve sustained release, improve tissue penetration, and minimize potential side effects.

5.2.3 Gene delivery with local immunosuppression

Gene delivery using viral vectors is a promising approach for efficient and targeted gene therapy. However, maintaining the integrity and activity of the virus during the fabrication of microneedle patches (MNP) presents a significant challenge. To optimize the process, new approaches are needed to ensure the virus remains viable and functional within the MNP. Through our systematic analysis of various factors, one significant barrier to be overcomed is the temperature changes during the drying process. Room temperature is still detrimental to the virus viability and freeze-thaw affect the stability of the virus, leading to a decrease in its efficacy upon delivery. Innovative methods, such as freeze drying, can be explored to improve the preservation of the virus during MNP fabrication. Freeze drying, also known as lyophilization, involves the removal of water from a frozen sample under low pressure, thus minimizing temperature change. This technique can potentially provide better protection for the virus, minimizing its degradation and maintaining its integrity throughout the drying process.To prevent virus breakdown and enhance its stability within the MNP, it is crucial to gain a deeper understanding of the nanoscale mechanisms underlying virus degradation. By studying the interactions between the virus and the surrounding materials, researchers can identify strategies to mitigate virus breakdown. This may

involve modifying the MNP matrix or incorporating protective agents that shield the virus from degradation factors.

The ability to reprogram somatic cells lay the foundation for a new branch of regenerative medicine predicated on reconnoitering these paths and directing navigation to generate cells and tissues for regenerative replacement, disease modeling, and therapeutic testing. To provide physiological environment for myocardial infarction injury repair, conductive patches and scaffolds are demonstrated to have better performance in rodent models[50]. These materials possess the ability to facilitate electrical conductivity within the cardiac tissue, thereby enhancing the regenerative process. Considering this, the development of conductive cardiac microneedle patches (MNP) represents a potential future direction for therapeutic intervention. By incorporating conductive properties into the design of cardiac MNPs, it becomes possible to not only modulate the local immune environment but also provide the desired electrophysiological characteristics. This combination of immunomodulation and electrical conductivity could offer a multifaceted approach for promoting myocardial tissue regeneration and functional recovery following myocardial infarction. Further research and exploration in this area may yield innovative strategies for improving the treatment outcomes and long-term prognosis of individuals with cardiac injuries.

Overall, we aimed to provide valuable insights into the development and application of microneedle patches as a novel local delivery method for therapeutic interventions in regenerative medicine. The results from my studies contribute to our understanding of the potential benefits of local immunomodulation and gene transfer in tissue regeneration and pave the way for further advancements in the field.

6. APPENDIX A. SUPPLEMENTARY FIGURES

6.1 Base-dissolvable Hydrogel Microneedles for Gingival Delivery of Immunomodulatory Factors

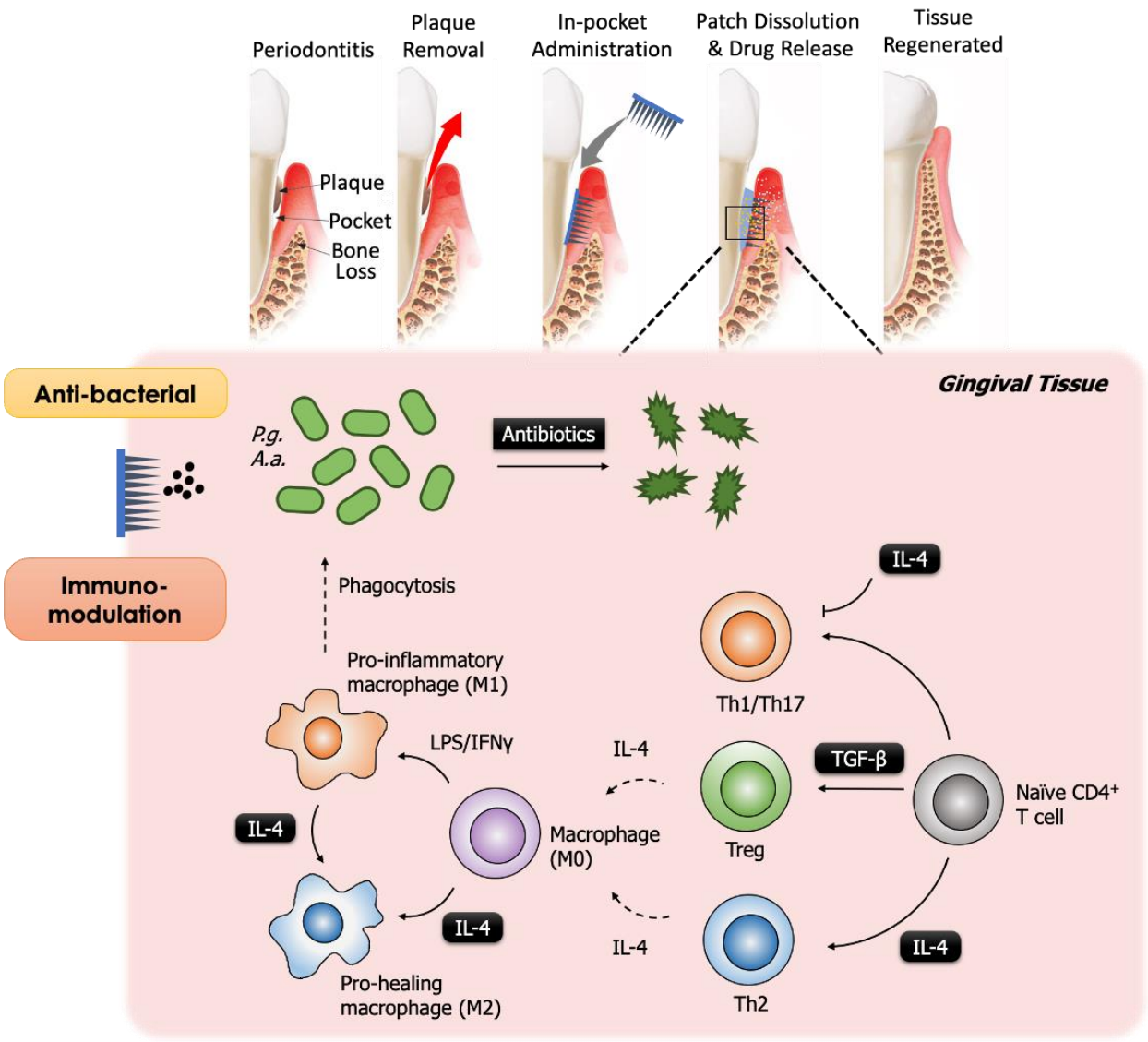

Supplementary Figure S2-1. Proposed working mechanism of designed immunotherapeutic periodontal patch.

Microneedle (MN) patch is designed to provide transgingival administration of antibiotics and anti-inflammatory cytokines. Following administration, MNs are detached from the base membrane (Gelatin) upon its dissolution, stay in gingival tissue, release their cargos, and finally degrade. The release therapeutics from MNs inside gingival tissue will alter local immune microenvironment to suppress bacterial infection, convert the pro-inflammatory macrophages and T cells into pro-healing phenotypes, and promote periodontium regeneration.

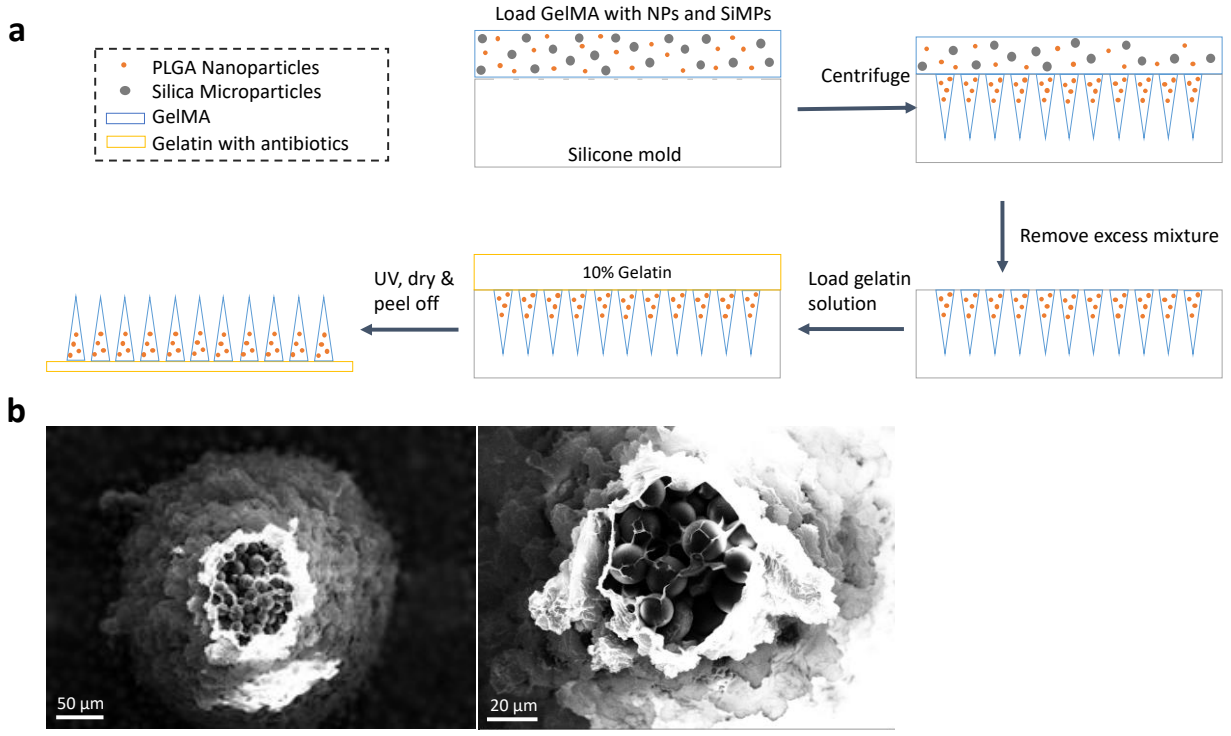

Supplementary Figure S2-2. Fabrication of particles loaded microneedle patch.

a, Schematic representation of the MN patch fabrication procedure. **b,** Encapsulated SiMPs can be seen inside the truncated MNs (from the top of the MNs) at two magnifications.

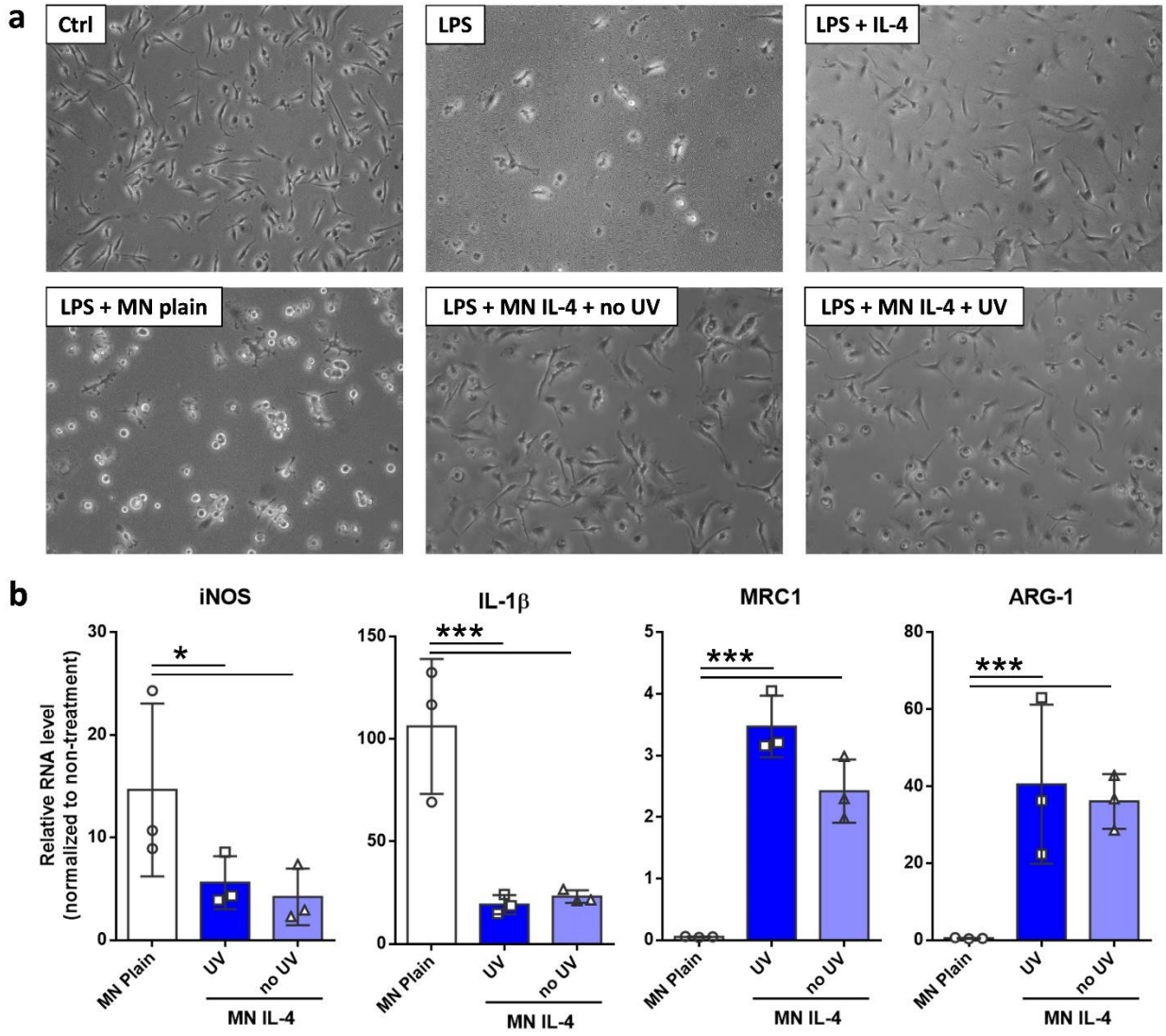

Supplementary Figure S2-3. Co-culture of primary bone marrow derived murine macrophages with IL-4-containing MNs with and without UV curing.

a, bright field microscopic images of macrophages treated with complete DMEM medium as a control (Ctrl), LPS (10ng/ml lipopolysaccharide), LPS+IL-4 (LPS for 6 hours and then 25ng/ml IL-4), LPS + blank MN (LPS for 6 hours and then placed blank MNs), LPS + IL-4 MN (LPS for 6 hours and then placed IL-4 containing MNs *without* UV crosslink), LPS + IL-4 MN + UV (LPS for 6 hours and then placed IL-4 containing MNs *with* UV crosslink). Images were taken 24 hours after LPS treatment. **b,** Quantitative polymerase chain reaction (qPCR) analysis of mRNA expression of surface markers and cytokines in macrophages in co-culture with MNs with and without UV curing. There is no significant change in the effects of IL-4 macrophage marker expression following the UV curing of the GelMA-based MNs.

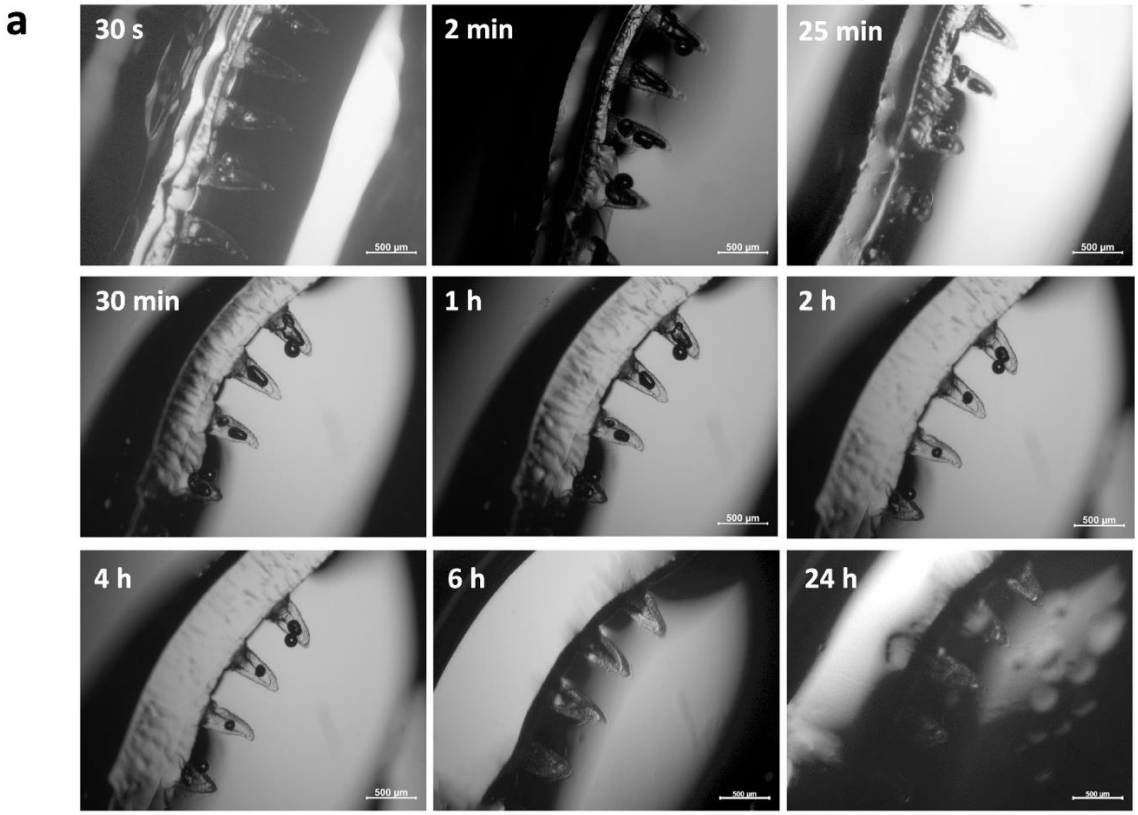

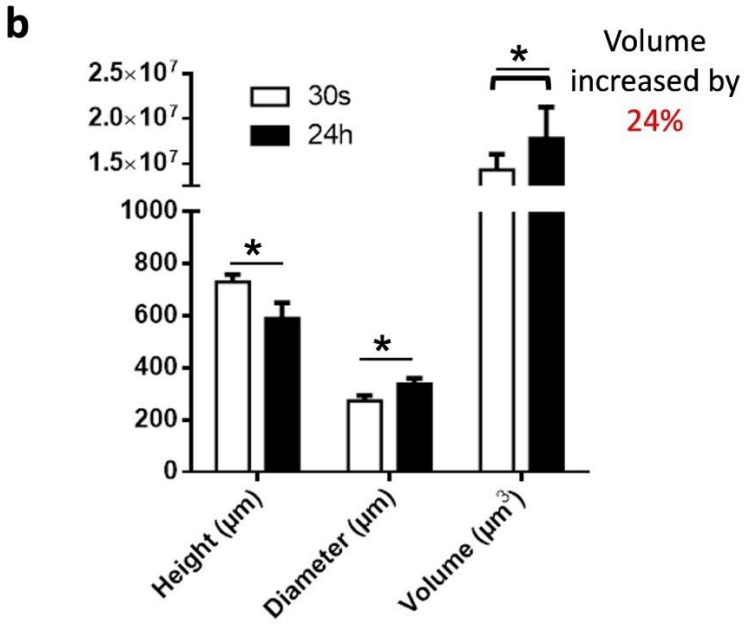

Supplementary Figure S2-4. Swelling of microneedle.

a, microscopic images showing MN swelling with time in PBS. **b,** Height, diameter and volume of swelled cones were quantified at various time points by using Image J software.

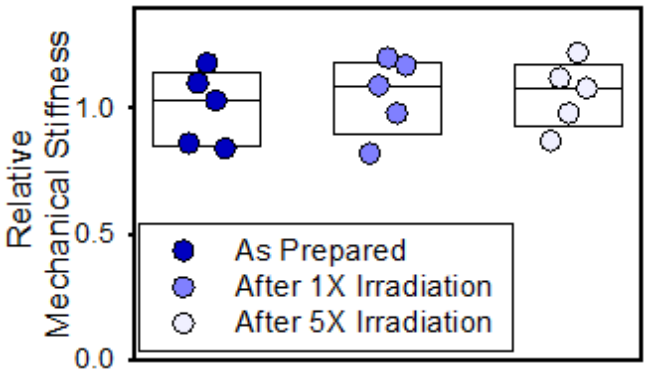

Supplementary Figure S2-5. Sterilization with x-ray irradiation.

No significant change in mechanical properties of GelMA-based MNs after 1 or 5 times of x-ray irradiation at 25 kGy dose as compared to freshly prepared samples.

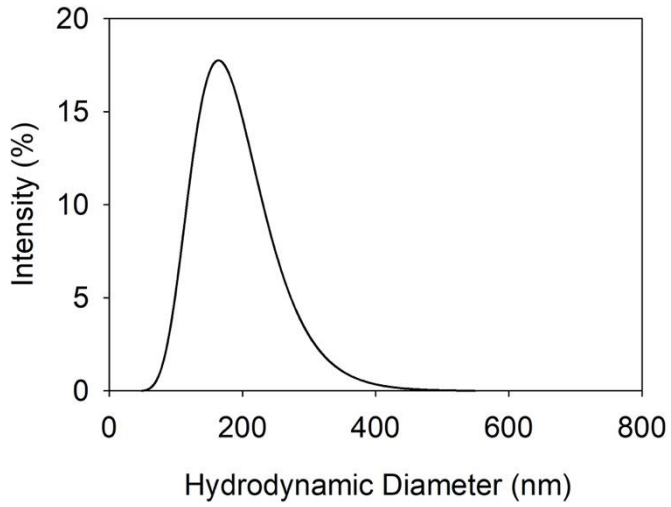

Supplementary Figure S2-6. Dynamic light scattering (DLS) was used to measure hydrodynamic diameter of PLGA-tetracycline NPs.

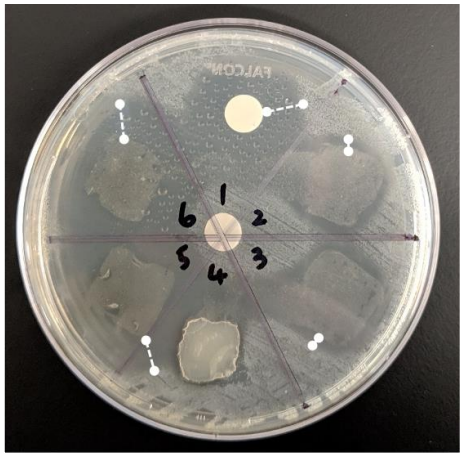

Sample #	Formulation	Inhibition Zone (mm)
1	Tet. Disk (30μg)	8.56
4	Blank MN patch (0μg)	0
2,3	Full Tet. MN patch (30μg)	2.6±0.1
5,6	Full Tet. MN patch (300μg)	13.4±0.1

Supplementary Figure S2-7.Antibacterial test.

Kirby-Bauer inhibition assay was used to assess antibacterial properties of drug-loaded patches against *E. coli*. Tetracycline disk was prepared by adding tetracycline solution to sterile paper disks and were air-dried in a biosafety cabinet. These disks and MN patches were placed in agar plates inoculated with bacteria at 37°C. The inhibition zones were measured after 48 hours.

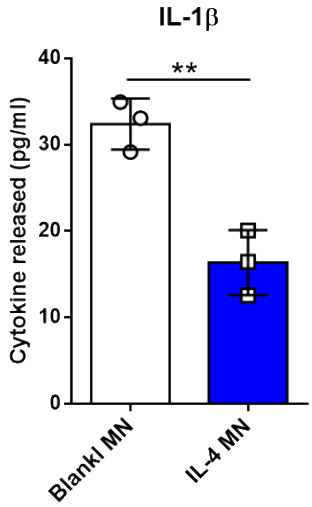

Supplementary Figure S2-8. Secreted IL-1β level after treatment of IL-4-loaded MNP.

Change in the level of secreted IL-1b by macrophages after LPS treatment in the presence of blank MN or IL-4-loaded MN patches as assessed by using ELISA (n = 3). The results were analyzed by using one-way ANOVA. Statistical significance is indicated by * $p < 0.05$, ** $p < 0.01$ and *** $p < 0.001$.

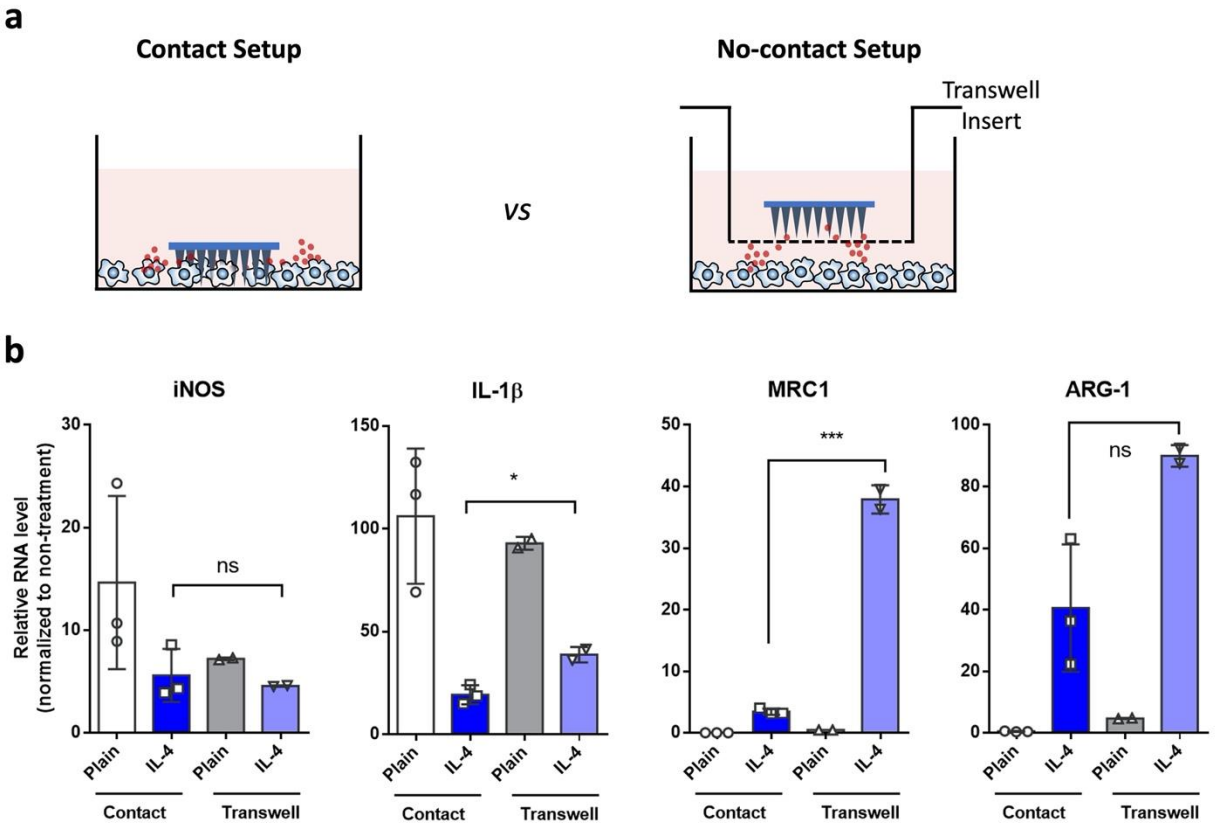

Supplementary Figure S2- 9. Effects of MN in contact with cells *in vitro*.

a, *In vitro* setup for macrophage repolarization experiments. MN patches were placed directly in plates (in contact with cells) or in Transwells (no-contact with cells) and co-cultured with BMDMs for 3 days. **b,** Changes in expression of surface markers and cytokines in macrophages after LPS treatment in the presence of blank MN or IL-4-loaded MN patches as assessed by using qPCR (n = 3). The results were analyzed using one-way ANOVA. Statistical significance is indicated by * $p < 0.05$, ** $p < 0.01$ and *** $p < 0.001$; ns= not significant.

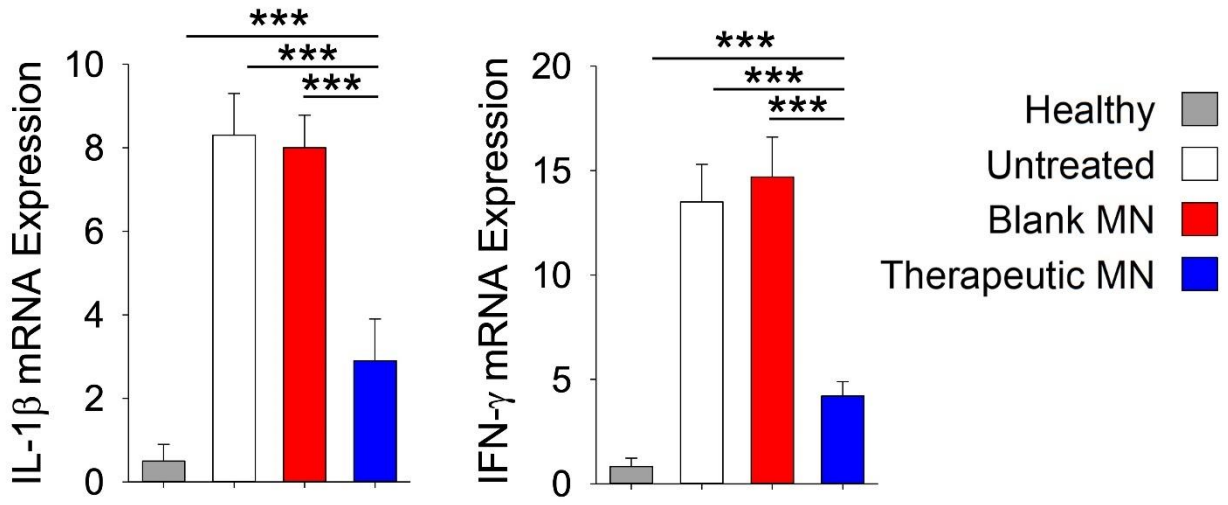

Supplementary Figure S2-10. In vivo evaluation of the immunomodulatory effects in a rat model of periodontitis.

At 8-weeks post MN insertion, buccal and palatal tissues of maxillary molars were isolated and dissociated to assess the inflammatory status of tissue microenvironment. Relative mRNA expression levels of pro-inflammatory (IL-1β and IFN-γ) genes in the periodontal tissue were quantified by qPCR. Healthy: healthy rats; Untreated: untreated periodontitis; Blank Patch: MN patches without any therapeutic cargo; Therapeutic Patch: MN patches containing both tetracycline- and cytokines-loaded particles. The presented data are expressed as mean ± SD (n= 5). The results were analyzed by using one-way ANOVA with post-hoc analysis. Statistical significance is indicated by * $p < 0.05$, ** $p < 0.01$ and *** $p < 0.001$.

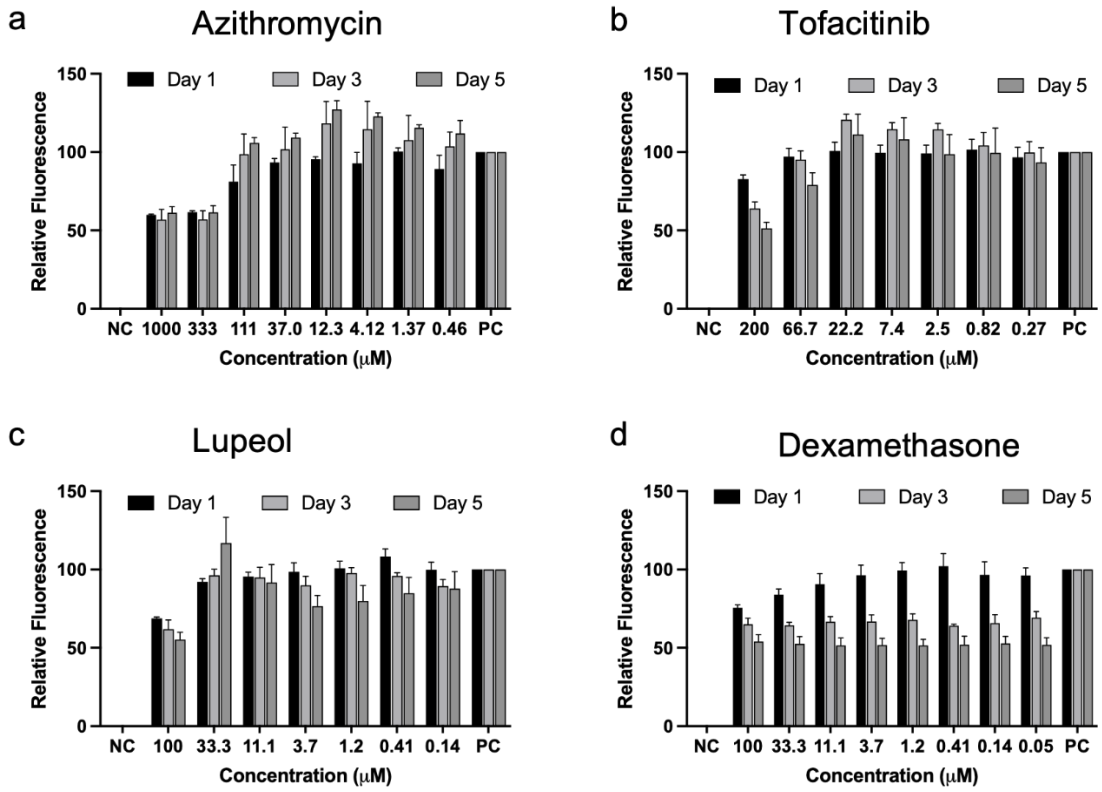

Supplementary Figure 3-1. Cytotoxicity of immunomodulators.

Cytotoxicity of **a,** azithromycin, **b,** tofacitinib, **c,** lupeol and **d,** dexamethasone was measured on primary rat BMDM. PrestoBlue cell viability reagent was used to measure cytotoxicity 1, 3, and 5 days post compound treatments. Fluorescence was read by plate reader with excitation wavelength of 560 nm and emission wavelength of 590 nm.

a

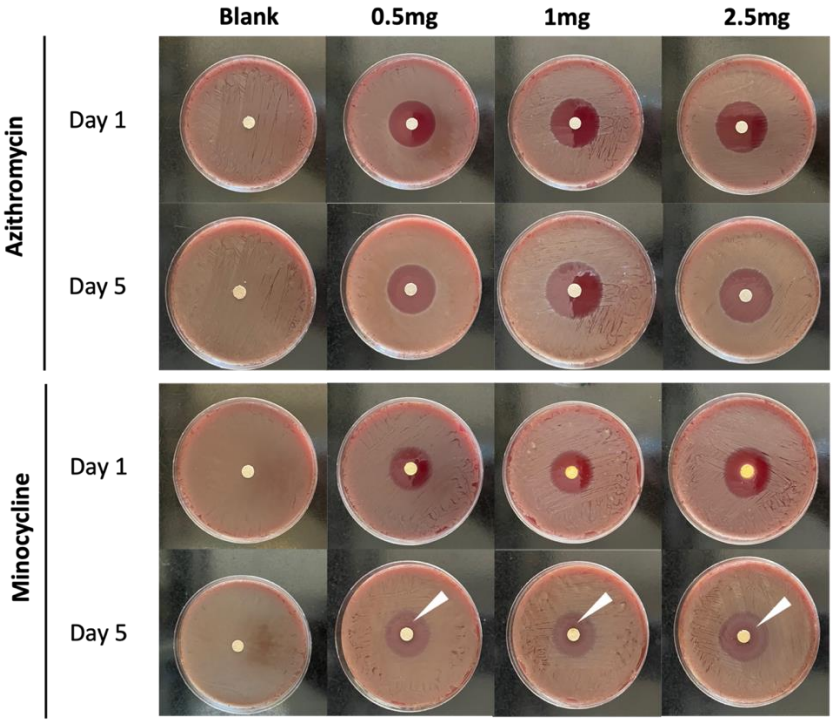

b

P.g	Dosage	0.5mg	1mg	2.5mg	Comments
Azithromycin	Day 1	14 mm	16 mm	16 mm	
	Day 5	14 mm	16 mm	16 mm	*some inward bacteria growth
Minocycline	Day 1	13 mm	14 mm	14 mm	
	Day 5	12 mm	12 mm	13 mm	*foggy zones

c

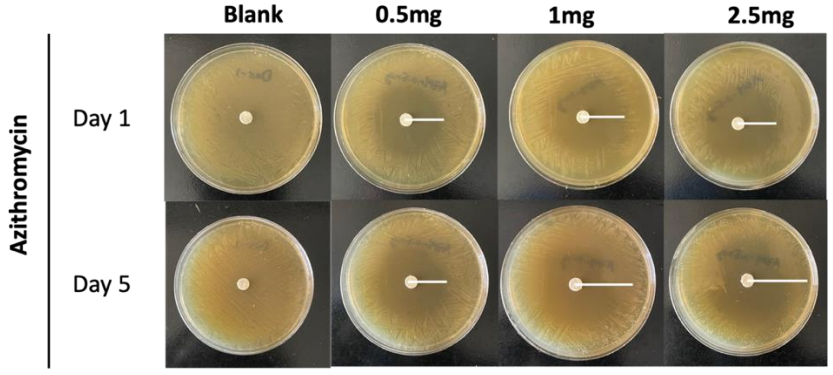

d

A.a	Dosage	0.5mg	1mg	2.5mg
Azithromycin	Day 1	1.6 mm	2.1 mm	2.1 mm
	Day 5	1.6 mm	2.5 mm	2.2 mm

Supplementary Figure 3-2. Antibacterial effects of azithromycin on *P.g.* and *A.a. plate culture*.

a,b, Image and quantification of inhibition zones on day 1 and day 5 for azithromycin and minocycline on *P.g.* and *A.a.*. **c, d,** Image and quantification of inhibition zones on day 1 and day 5 for azithromycin on *A.a.*

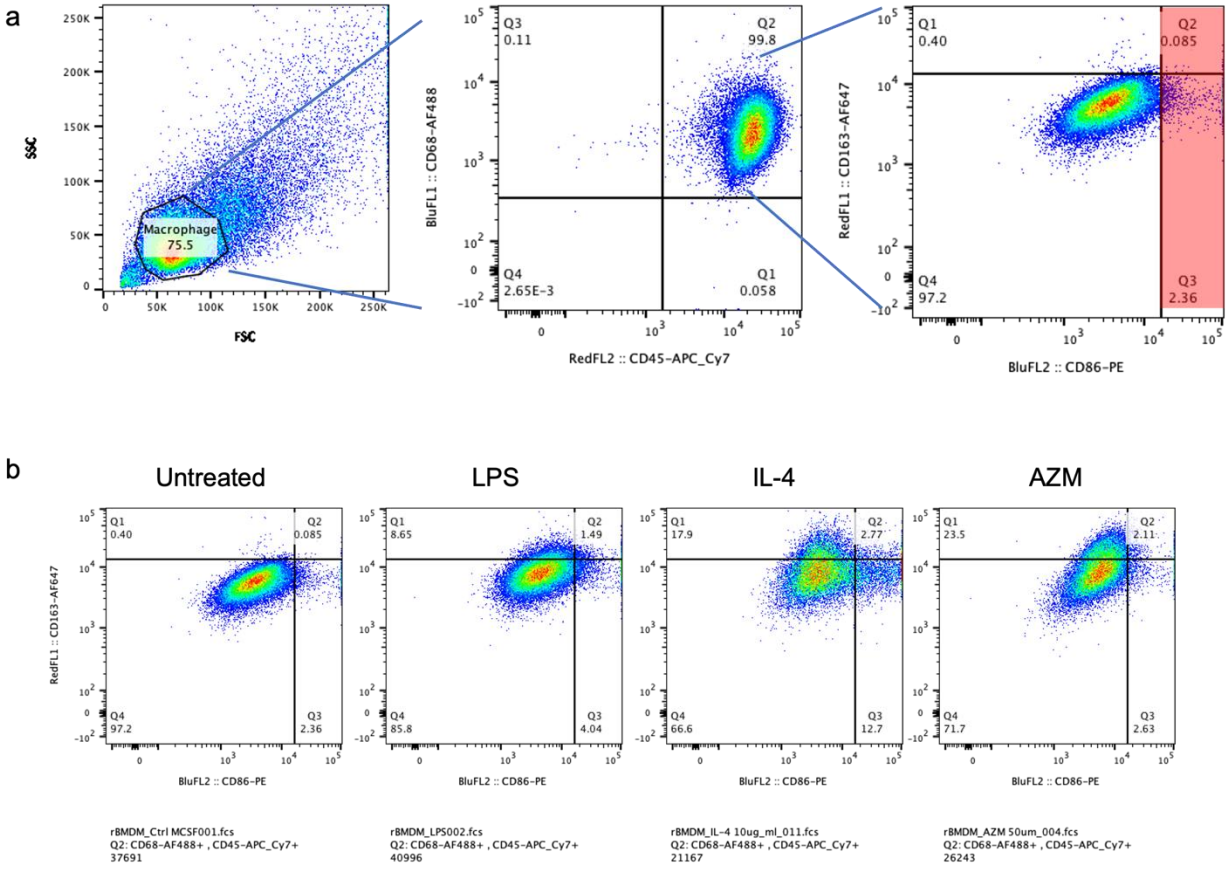

Supplementary Figure 3-3. Flow cytometry analysis gating strategy

a, Gating strategy for CD163+CD45+CD68+ macrophages. **b,** Examples of each group with CD86 and CD163 on x- and y- axis.

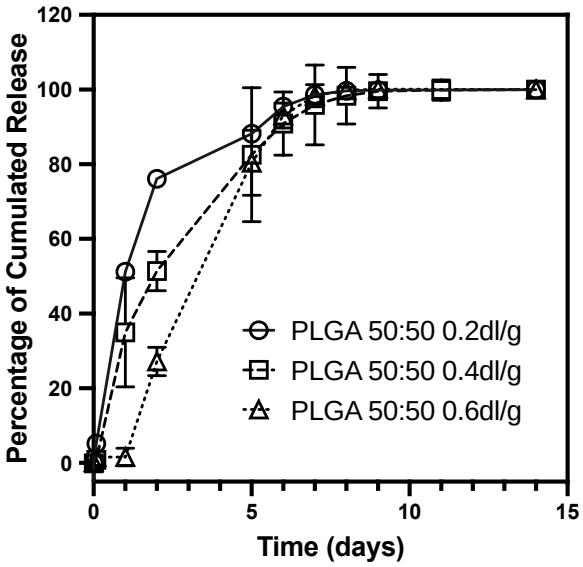

Supplementary Figure 3-4. Release profile from PLGA of various densities.

Rhodamine B was dissolved in PLGA solution and made into microparticles using single emulsion method. 1mg Rhodamine B PLGA microparticles were incubated in 1ml PBS at 37°C and supernatants were collected for 14 days.

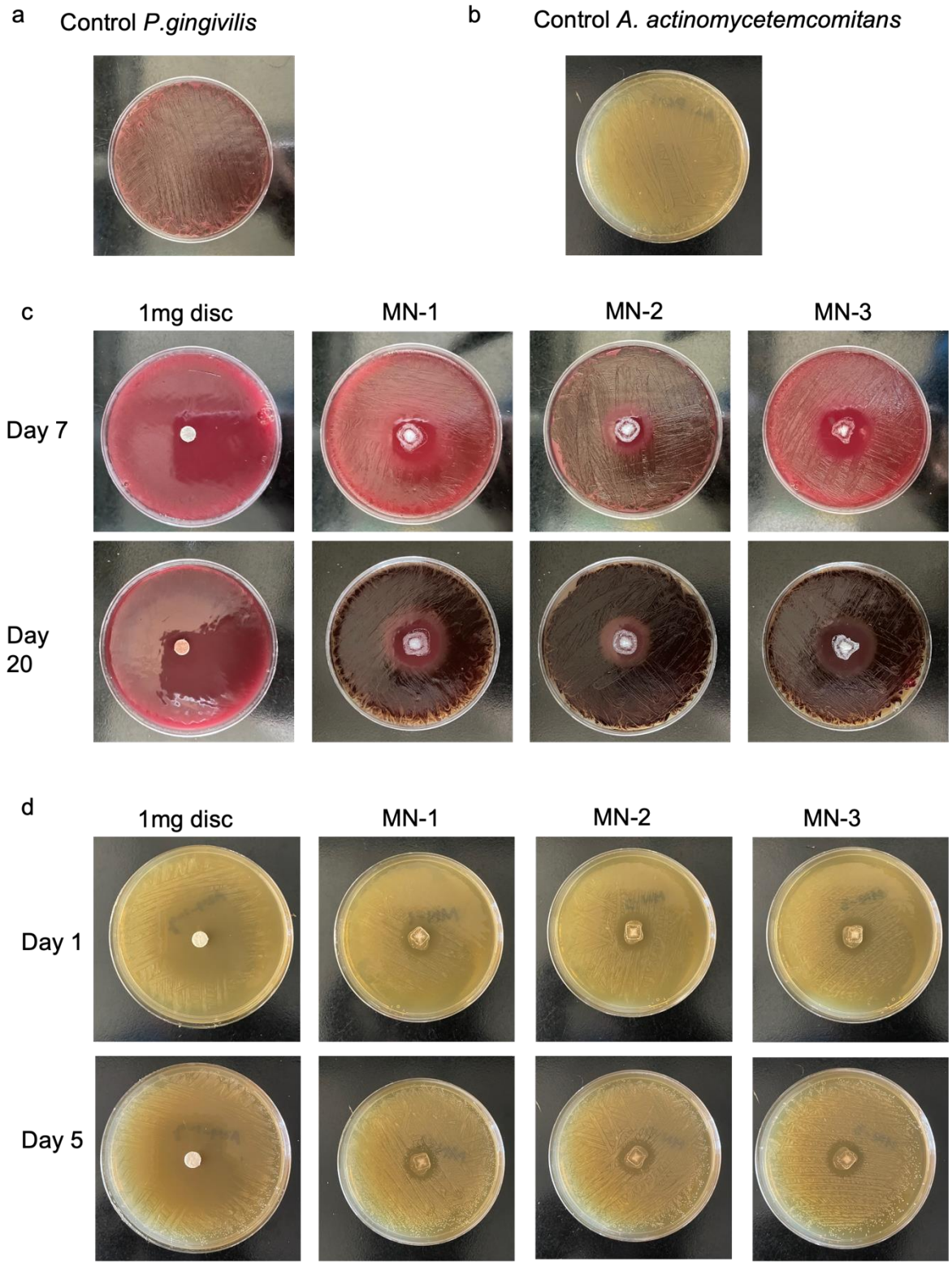

Supplementary Figure 3-5. Antibacterial effects of azithromycin on *P.g.* and *A.a.* plate culture.

a,b, Untreated control image of bacteria growth on agar plate for P.g. and A.a. **c,d,** Inhibition zone of AZM-MN on agar plates with triplicates shown.

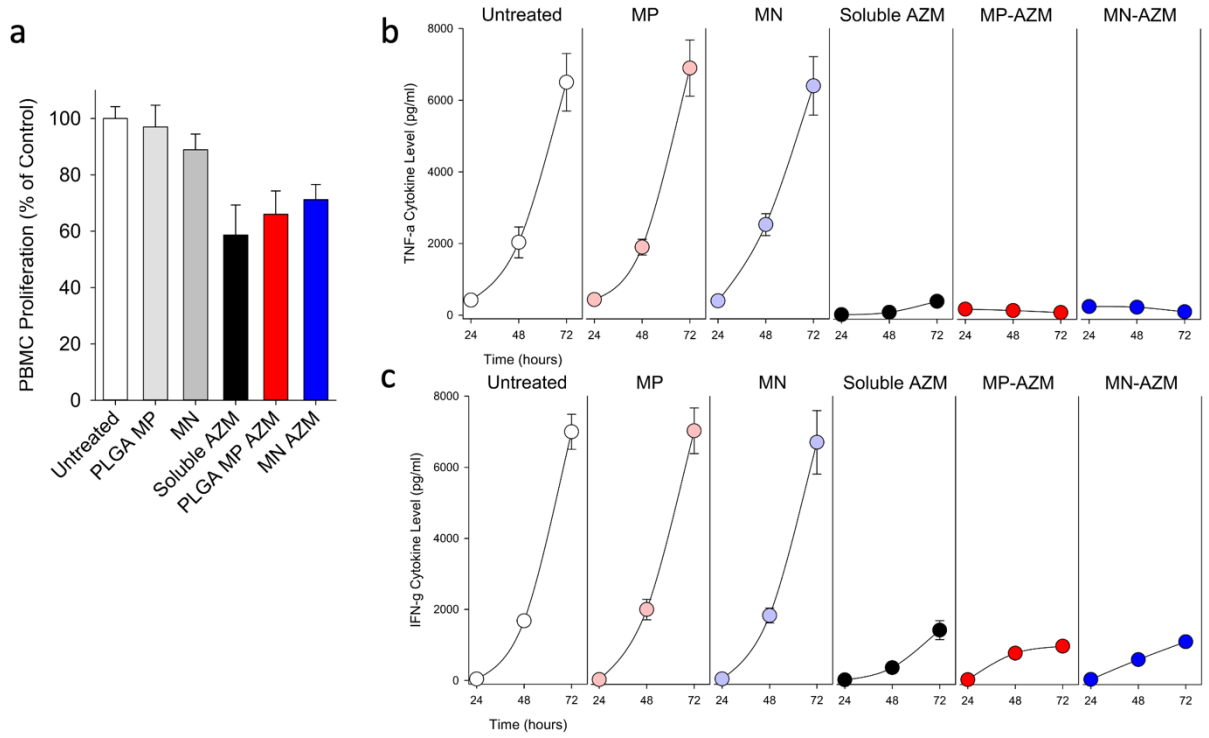

Supplementary Figure 3-6. In vitro effects of azithromycin on human PBMC.

a, Proliferation of PBMC at various treatments was measured as a percentage of untreated PBMC group. **b,** and **c,** showed the expression level of inflammatory cytokines TNF-α and IFN-γ measured by ELISA. All data are presented as mean ± SD (n= 3). Statistical significance is indicated by * $p < 0.05$, ** $p < 0.01$ and *** $p < 0.001$ for differences between samples with different formulations.

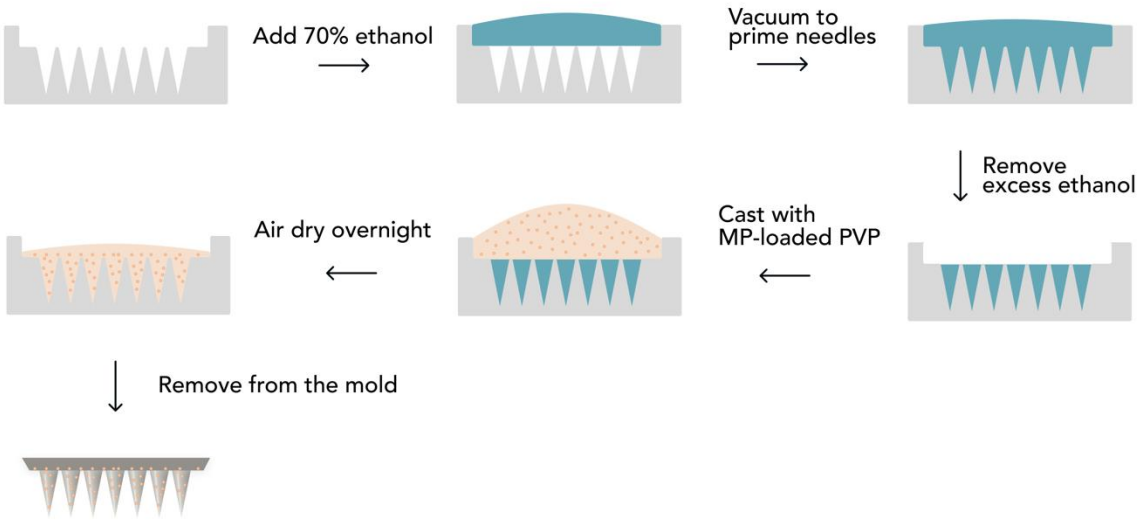

Supplementary Figure 3-7. Dissolvable microneedle fabrication strategy.

The PVP-based microneedle patches were fabricated using a vacuum method.

6.3 Virus-loaded Microneedles for In situ Cell Reprogramming

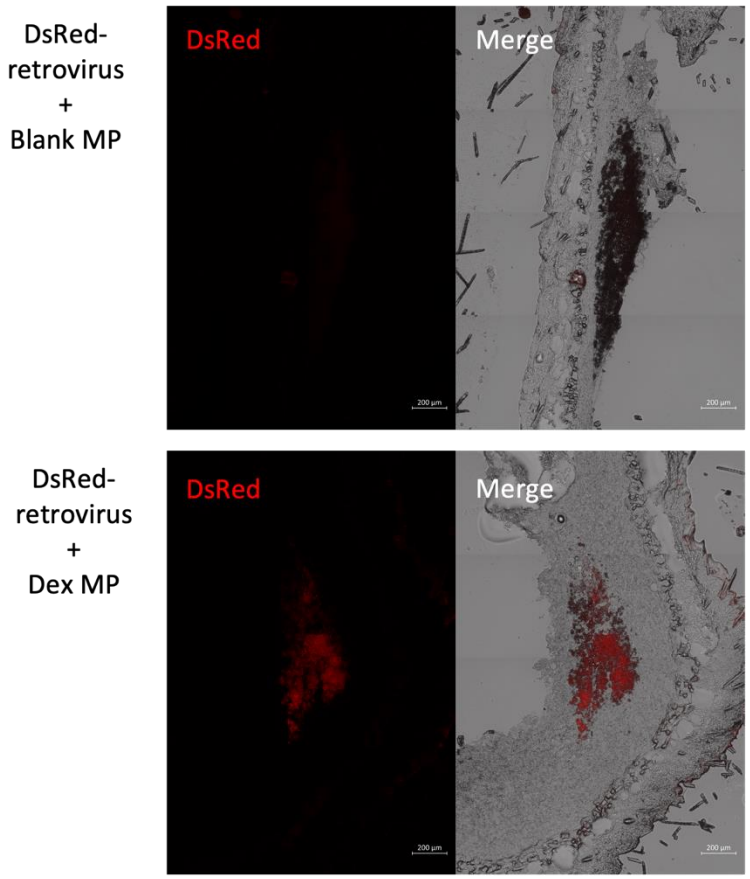

Supplementary Figure 4-1. The effects of local immune suppression on in vivo gene transfer.

Microparticles of 5μm in size with freshly thawed DsRed-retrovirus were injected subcutaneously to the back of healthy wild-type C57/B6 mice. Shaved skins were harvest three days after injection and cryosectioned for direct imaging. Tiles images were taken with the same exposure time of 3s. Scale bar of 200μm.

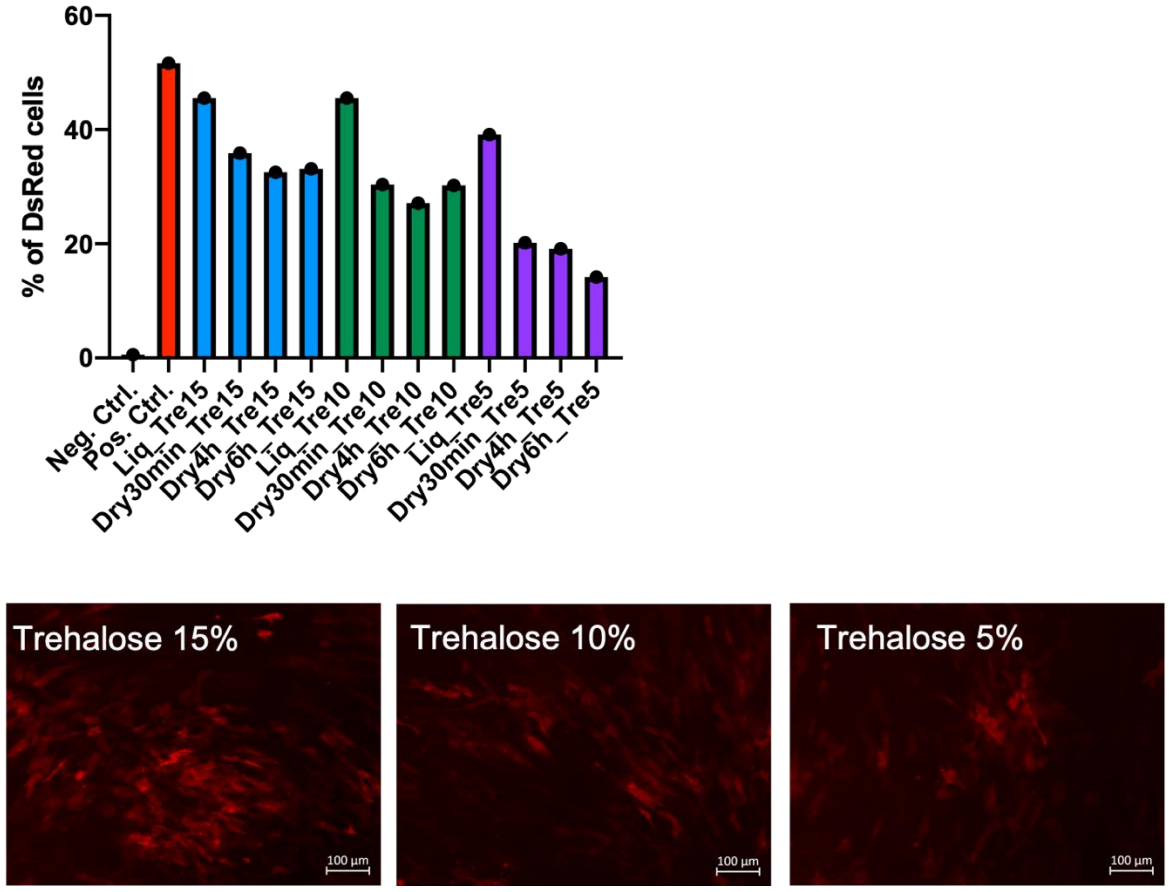

Supplementary Figure 4-2. Optimization of trehalose amount.

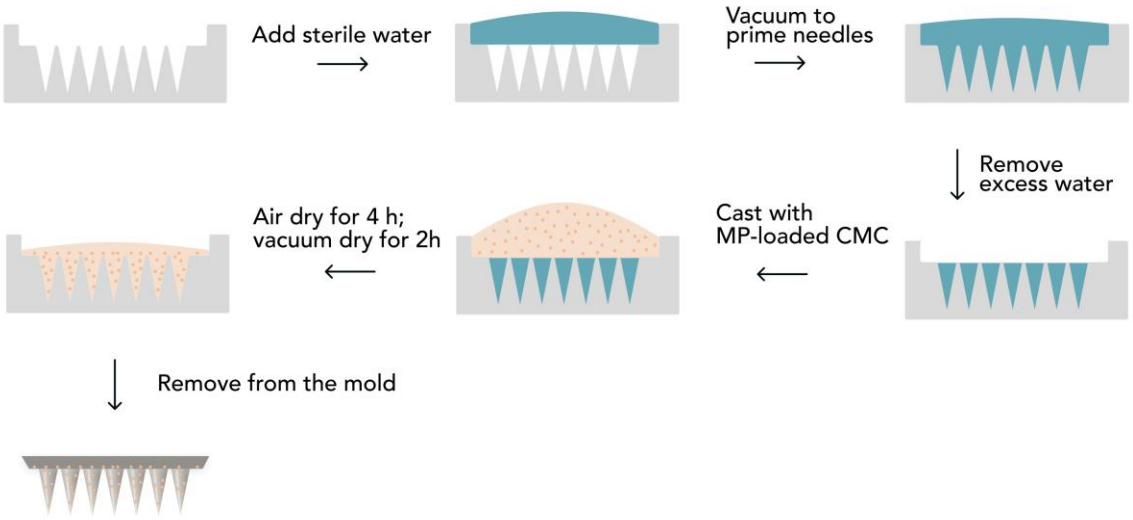

Supplementary Figure 4-3. Virus-loaded CMC-based microneedle fabrication strategy.

The microneedle patches were fabricated using a vacuum method.

7. APPENDIX B. HORMONE DELIVERY

7.1 Abstract

Testosterone is the main androgen and a critical sex hormone for the health of male. Hypogonadism or testosterone deficiency is often treated with testosterone replacement therapy to restore its normal level. While low testosterone results in impotence and decreased sexual drive, fatigue, and osteoporosis, overdose of testosterone may bring potential adverse effects including myocardial infarction, liver injury, and mood changes including depression, aggression, and hostility. Thus, a sustained and controlled release of testosterone slowly is needed. Here, we engineered a biodegradable microneedle patch (MNP) loaded with 2.5mg of testosterone. The MNP is applied to the skin to penetrate the outer most layer of dead cells and release hormone over time. Comparing to injections which peaked around 6 hours in rat transdermal application, MNP had a slower and more sustained release with peak serum concentration at 48 hours. Also, although packing the same amount of hormonal drug, MNP application led to lower serum level from time to time, thus smaller swing of testosterone level. This work is translational for developing an alternative product of hormone delivery which has better patient compliance and desirable release profile. The pre-clinical model had revealed the release profile and safety in rat.

7.2 Introduction

Testosterone is the primary sex hormone and anabolic steroid in males. It stimulates the developments of male characteristics and promotes masculine growth such as increase muscle strength and bone density. Male hypogonadism is a condition that not enough hormone is produced by testicles with symptoms like decreased sexual desire, decreased energy, decreased facial and body hair, and loss of muscle mass and bone density. Treatments usually involved testosterone replacement to restore its level to normal[201,202]. Current products on the

market have various forms such as intramuscular injections, implants, buccal system and topical applications[201].

Microneedle technology has been harnessed for the localized and controlled delivery of hormones and contraceptives[26,203–205]. The incorporation of hormones or contraceptives into the microneedle matrix enables sustained release of the active substances over an extended period. This controlled release profile ensures a steady and consistent delivery, optimizing the efficacy and duration of action. The design of MNP allows various administration schedules, ranging from single-dose to long-term release formulations[44]. The versatility of microneedle technology allows for customization of the patch design, needle length, and drug loading, enabling tailored approaches to meet the specific needs of hormone replacement therapy or contraceptive interventions.

Overall, the utilization of microneedles as a delivery platform for hormones and contraceptives presents a promising strategy for achieving localized and controlled drug release, offering potential advancements in hormone therapy and contraception. Further research and development in this field hold promise for optimizing delivery systems, improving patient outcomes, and expanding the range of applications for microneedle-based therapies.

7.3 Results

7.3.1 Optimization of MNP

First, to determine the best microneedle design for testosterone delivery, different materials were explored for MNP fabrication as summarized in **Table 7-1**. Secondly, two fabrication methods – centrifugation and vacuum were experimented for a feasible method. Vacuum method was selected because of its batch-to-batch consistency and capacity to make multiple MNP. Eventually, poly(lactic-co-glycolic acid) 50/50 was selected to make polymeric solid MNP due to its biocompatibility and frequent usage in FDA-approved applications.

Table 7-1. Microneedle material design

MNP Design	MN type	Release profile	Material selection	Advantages	Limitation
Polymeric solid needle	Biodegradable	Prolonged	PLGA, PLA, PGA	High loading capacity Simple process	Release can be too slow. (~2 weeks)
Hydrogel solid needle	Dissolving	Burst	4% Hyaluronic acid, 10% CMC, 15% PVP	Quick release	Only one material per patch. Loading capacity.
Nanoparticles	Dissolving + biodegradable NP	Moderate	PLGA nanoparticles + hydrogel needles	Relatively quicker release	Loading capacity. Mechanical strength

Additionally, various organic solvents were optimized for dissolving PLGA and compatible with the vacuum methods. To meet the criteria of a good solvent for this application, the organic solvent should not 1) evaporate too fast during the vacuum process, nor 2) cause significant deformation of the PDMS mold, like swelling of the mold. **Table 7-2** displayed the organic solvent we tried and their chemical properties. Experiments showed that 1,4-dioxane can be an excellent organic solvent as its boiling point is close to water and perform well during vacuum and won't swell PDMS mold significantly. We can choose based on different need.

Table 7-2. Properties of each organic solvent

Solvent	Boiling point	Safety level	Solubility	Swelling ratio	Decision
Dichloromethane (DCM)	40℃	C2; 6mg/day	200mg/ml PLGA	57%	✗ Swell significantly
Acetone	56℃	C3	200mg/ml PLGA	28%	✓ but its evaporation is still too fast
1,4-Dioxane	101℃	C2; 3.8mg/day	250mg/ml PLGA	21%	✓ BEST candidate
Water	100℃	Safe	45% (w/v) aq 2-hydroxypropyl-β-cyclodextrin:	0%	✗ precipitates when added polymers to

			soluble 18.2 mg/ml		cyclodextrin solution

With all these considerations, the final design is shown in **Figure 7-1**, which is composed of two layers with the first layer of PLGA containing testosterone and the second layer of pure PLGA. We used 50μl of 10% PLGA in 1,4-dioxane with 50mg/ml testosterone for the fist layer. After drying overnight, another 50μl of 10% PLGA in 1,4-dioxane was added as the second layer. Therefore, each patch contains 2.5g testosterone.

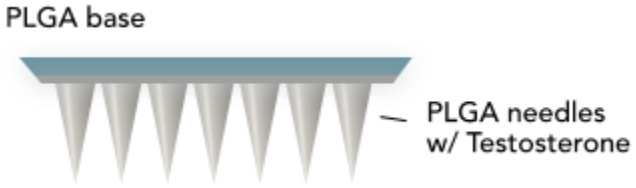

Figure 7-1. Schematics of MNP design.

7.3.2 Characterization of MNP

The mechanical strength of PLGA MNP with and without testosterone were tested by compression test using Instron moving at the speed of 0.5mm/min. PLGA MNP did not show significant change of its mechanical property after adding testosterone. Force vs displacement plots (**Figure 7-2a,b)** showed a buckling of the tips by a sudden drop of the force and bending tips were observed after compression tests. But due to the nice mechanical properties of PLGA, only the tip of the needle was affected (**Figure 7-2c**).

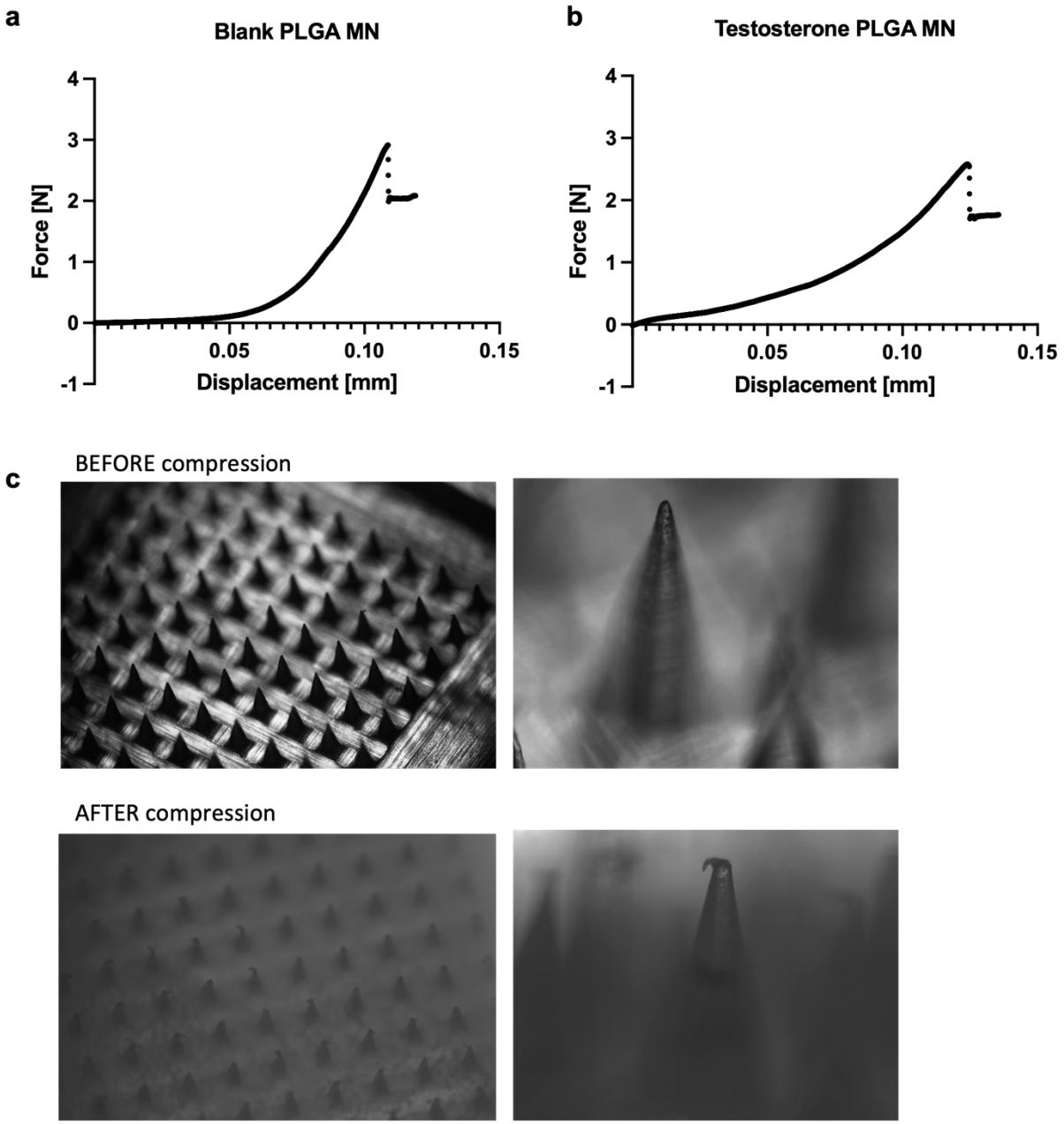

Figure 7-2. Mechanical test of MNPs.

Mechanical strength of **a,** blank PLGA MN and **b,** testosterone PLGA MN were measured by Instron compression test. **c,** Brightfield images of before and after compression tests for testosterone PLGA MN.

7.3.3 In vitro drug release profile

Testosterone MNP were 10% ethanol and water to measure the release of testosterone into the solution. It was observed that PLGA degraded faster in water, but due to the low solubility of

hormone in aqueous, there is a limit of about 20μg/ml for the concentration of testosterone in water. Thus, 10% ethanol was used as an alternative solvent. PLGA degraded slower in 10% ethanol, but ethanol facilitated the solubility of hormone and allowed a wider range of release detection. Our data for 30-day release showed an accumulated release of about 2.5mg as expected from the MNP loading amount with the majority of the drug release in the first three days (**Figure 7-3**).

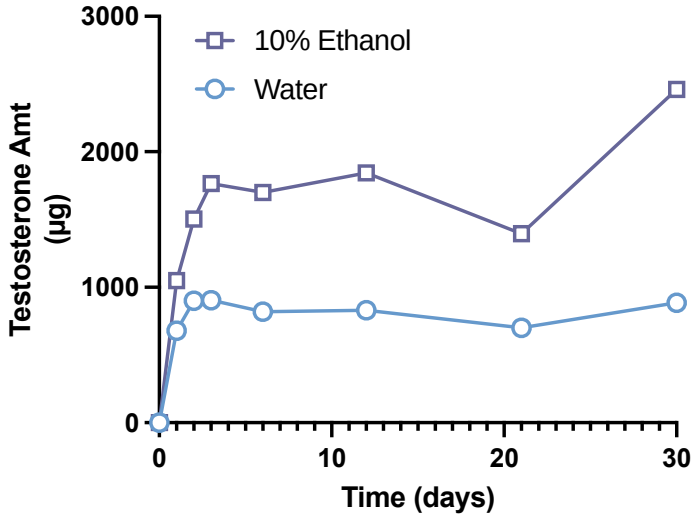

Figure 7-3. Release of testosterone from MNP *in vitro.*

Testosterone MN were placed in 50ml conical tube of 10% ethanol and water and the accumulated release amount of testosterone was plotted for 30 days.

7.3.4 In vivo drug release profile

The release profile of testosterone was monitored in jugular catheterized rats after placement of MNP and compared with testosterone by injection. Bloods were drawn according to the designed schedule for 5 days (**Figure 7-4a**). MNP showed a more sustained and slower release with peak at 48hours, whereas injection had a peak of drug in blood at 6 hours (**Figure 7-4b,c**). However, not all the amount in patch can be delivered to the body through skin absorption. Thus, the drug concentration in blood of microneedle group is lower than that of the injection group.

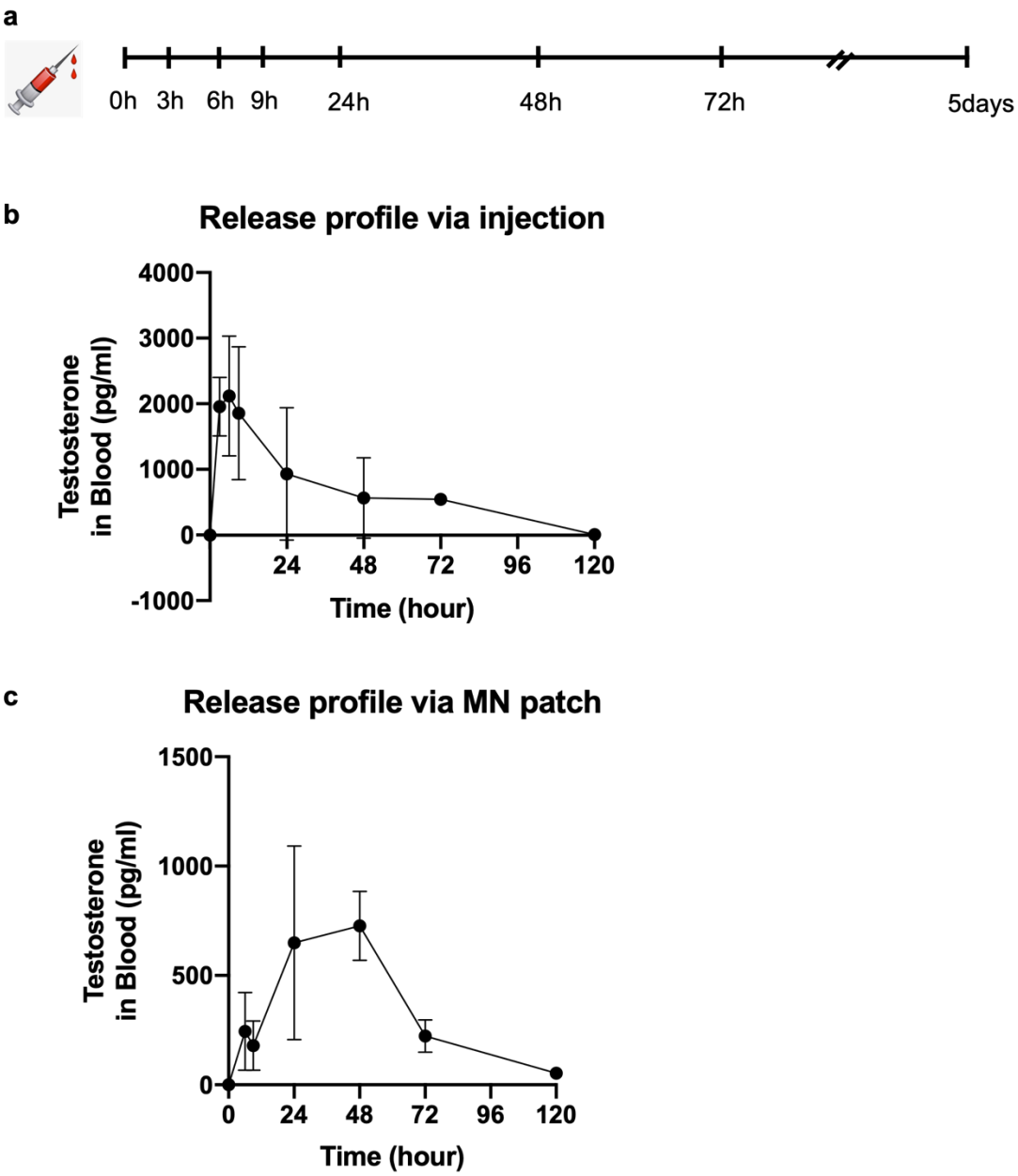

Figure 7-4. Release profiles of testosterone.

a, the blood drawing schedule for experimental animals. **b,c,** Release profile of testosterone by injection and MNP respectively.

7.4 Discussion

Sustained release testosterone MNP provides a convenient and effective way for testosterone replacement therapy. These patches deliver testosterone through the skin via

microneedles, providing controlled and sustained release. It controls the release of hormone and unlikely to cause a burst release and hormone swings to the body, according to the rat in vivo release profile. Further experiments are to be done to optimize the packaging of MNP for easiness to use and to characterize the release in larger animals before getting to clinical trials.

7.5 Materials and Methods

MNP fabrication. MN molds were purchased from Micropoint Technologies (Singapore) with pyramid shape of 200μm base diameter, 750μm height and 500μm tip-to-tip spacing. To fabricate MNPs, 100 mg acid terminated PLGA (50:50 lactic acid to glycolic acid ratio) was dissolved in 1 ml 1,4-dioxane overnight. 50mg testosterone was dissolved in 1ml of PLGA solution. The 50μl of 50mg/ml testosterone/PLGA/organic solution were casted on negative PDMS molds and vacuum for 5 minutes. Bubbles were removed and MNPs were dried at room temperature overnight or at least 6 hours. A second layer of PLGA solution without active ingredients were applied to the patch to form a stronger backing and dry overnight. Further drying were performed in 60℃ oven for 2 hours to evaporate any residual solvents. Solidified MN patches were peeled off from the molds and stored at 4°C until use.

Mechanical property of MNs. The mechanical strength of MNs was measured by compression test on a low-force mechanical testing system (5943 MicroTester, Instron, USA). The MN tips were place perpendicularly to stainless-steel plate and were pressed against another stainless-steel plate moving at constant speed of 0.5 mm/minutes. Correlations between the applied force and the deformation of the MNs were recorded. All tests were performed in triplicates.

In vitro testosterone release*. In vitro* release of testosterone was studied by incubating a single MNP in 50 mL PBST (PBS at pH 7.4 with 0.02% Tween-20) and 50 mL PBST with 10% ethanol at 37°C under constant shaking. At different time points, 500 µL of the supernatant was taken from the sample and replaced with fresh PBST/ethanol solution. The concentration of released

testosterone was determined by high-performance liquid chromatography (HPLC) at UCLA core facility.

In vivo testosterone release. Twelve jugular catheterized rats were purchased from Charles River Laboratory and the catheters were maintained as instructed from the vendor. One day before MNP placement, the hairs on the back of the animal were shaved and further removed by Nair and cleaned with water. When applying the patch, MNP was placed on the back of the rats and pressed for 30 seconds. 3M™ Tegaderm™ was placed on top to hold MNP in place. Blood was collected into heparin-coated collection tubes at designed time points for 5 days. Plasma was separated by collecting the upper layer after centrifugation at 1500g for 15min at 4°C.

Diethyl ether was used to extract the hormones from collected plasma three times and evaporated the solvents by heating to 30°C under a gentle stream of nitrogen. Testosterone amount in plasma was measured by ELISA kit following manufacturer's instruction (Cat # 582701, Cayman Chemical Company).

8. APPENDIX C. MECHANOBIOLOGY OF IMMUNE CELLS

Available online at www.sciencedirect.com

ScienceDirect

Current Opinion in Biotechnology

Unraveling the mechanobiology of immune cells

Xuexiang Zhang[1], Tae-Hyung Kim[2,4], Timothy J Thauland[3], Hongjun Li[1], Fatemeh Sadat Majedi[1], Chau Ly[1,2], Zhen Gu[1], Manish J Butte[3], Amy C Rowat[2] and Song Li[1]

Immune cells can sense and respond to biophysical cues — from dynamic forces to spatial features — during their development, activation, differentiation and expansion. These biophysical signals regulate a variety of immune cell functions such as leukocyte extravasation, macrophage polarization, T cell selection and T cell activation. Recent studies have advanced our understanding on immune responses to biophysical cues and the underlying mechanisms of mechanotransduction, which provides rational basis for the design and development of immune-modulatory therapeutics. This review discusses the recent progress in mechanosensing and mechanotransduction of immune cells, particularly monocytes/macrophages and T lymphocytes, and features new biomaterial designs and biomedical devices that translate these findings into biomedical applications.

Addresses
[1] Department of Bioengineering, University of California, Los Angeles, CA 90095, USA
[2] Department of Integrative Biology and Physiology, University of California, Los Angeles, CA 90095, USA
[3] Division of Immunology, Allergy, and Rheumatology, Department of Pediatrics, University of California, Los Angeles, CA 90095, USA
[4] Department of Pathology, University of New Mexico School of Medicine, Albuquerque, NM 87106, USA

Current Opinion in Biotechnology 2020, **66**:236–245

This review comes from a themed issue on **Tissue, cell and pathway engineering**

Edited by **Li Tang**, **Peng Xu** and **Haoran Zhang**

For a complete overview see the Issue and the Editorial

Available online 30th September 2020

https://doi.org/10.1016/j.copbio.2020.09.004

0958-1669/© 2020 Elsevier Ltd. All rights reserved.

Introduction

Immune cells employ numerous strategies to combat infections and maintain tissue homeostasis. They originate from hematopoietic stem cells and differentiate into myeloid (i.e. basophils, neutrophils, eosinophils, monocytes and mast cells) and lymphoid (i.e. T cells and B cells) lineages, which have distinct roles in the innate and adaptive immune systems respectively. Sensing and responding to mechanical cues is critical for immune cells to interact with their neighboring cells, surrounding extracellular matrix (ECM), and other cells for immunosurveillance and effector functions [for reviews, see Refs. 1–3].

Accumulative evidence suggests that biophysical cues, in addition to biochemical signals, play an important role in modulating immune cells functions. Through the process of mechanotransduction, cells can convert external biophysical stimuli into intracellular biochemical signals [2], which may lead to cytoskeletal re-organization, gene regulation and/or epigenetic modification of chromatin [3] (Figure 1). Many cell adhesion molecules (CAMs) involved in cell-cell communication can serve as mechanosensors, including integrins, selectins and cadherins [for review, see Ref. 4]. Integrins and focal adhesion complexes are also important for cell-matrix interaction. Another category of mechanosensor includes ion channels for gating soluble ions such as Ca^{2+}, Na^{+} and K^{+}. For example, a mechanosensitive ion channel, Piezo1 has been shown to sense mechanical cues in both macrophages and T cells [5••,6]. Furthermore, in lymphocytes, T cell receptors (TCRs) and B cell receptors (BCRs) are mechanically essential for recognizing antigens and activating effector functions. Lymphocyte function-associated antigen 1 (LFA-1) is an integrin that not only functions as a receptor for cell adhesion during migration but also mediates T cell activation as the secondary signal (Signal 2) where TCR and peptide-major histocompatibility complexes (pMHC) interaction provides the primary signal (Signal 1). Both integrin-ligand interaction and TCR-pMHC interaction can form catch bond that exhibits extended bond life upon tangential forces [2].

Mechanical signals on cell surface can further propagate *via* intracellular structures such as cytoskeleton and nucleoskeleton and induce the reorganization of these structures. In addition, signaling molecules (e.g. Rho GTPases) and transcription factors may serve as mechanotransducers to relay signals and regulate cytoskeleton dynamics and gene expression. For instance, yes-associated protein 1 (YAP1) emerges as an important mechanotransducer for sensing a wide range of environmental factors such as ECM rigidity, cell density, cell shape, stretching and shear stress [for review, see Ref. 7].

In this review, we summarize recent findings on mechanotransduction in innate immunity and adaptive immunity with a focus on macrophages and T lymphocytes. We then discuss how fundamental insights into the

Figure 1

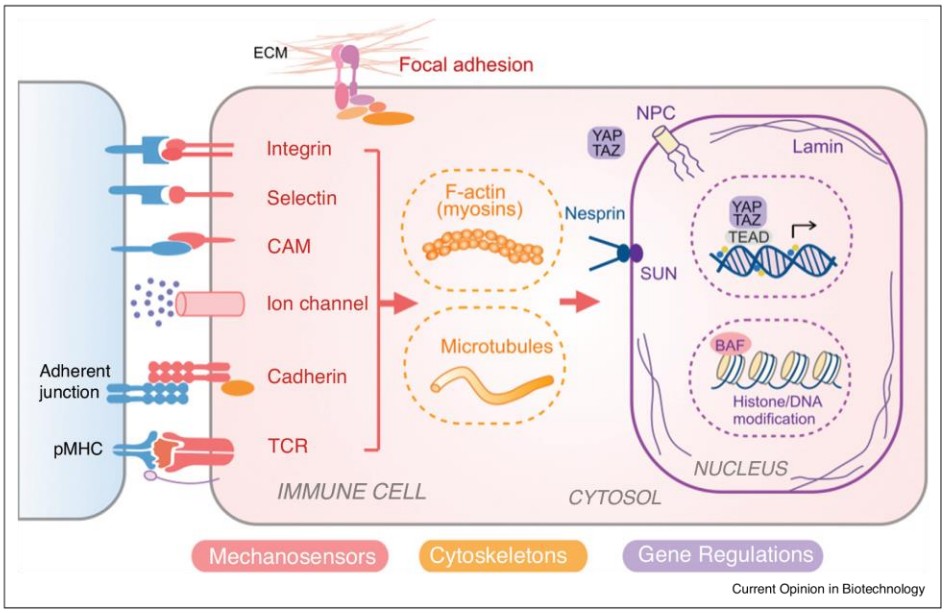

Mechanotransduction network in immune cells. Immune cells can sense the biophysical cues by receptors including integrins (i.e. LFA-1, Mac-1, VLA-4), selectins (i.e. P-selectin, L-selectin), cell adhesion molecules (CAMs) (i.e. ICAM-1, VCAM), ion channels (i.e. Piezo1), cadherins and T cell receptor (TCR). These signals can be transduced through cytoskeleton (actin, microtubule) and nucleoskeleton (e.g. lamin), and/or converted into biochemical signaling events. The mechanotransduction process not only affects the mechanical structure and property of cell and nucleus, but also regulates immune cell phenotypes and functions *via* transcriptional factors (e.g. YAP/TAZ) and epigenetic modifications.
*Abbreviation: LFA: Lymphocyte Function-associated Antigen; Mac1: Macrophage-1 Antigen; VLA-4: Integrin $\alpha 4\beta 1$ (very late antigen-4); ICAM: Intercellular Adhesion Molecule 1; VCAM: Vascular Cell Adhesion Protein 1.

mechanobiology of immune cells can inspire the design of engineering tools, biomaterials, and drug delivery platforms for tissue regeneration and cancer immunotherapy.

Mechano-regulation of innate immunity

Innate immunity consists of first-line responses against pathogens. Macrophages fill a crucial role in the host defense to clear pathogens and maintain tissue homeostasis, which are evidently regulated by both biochemical and biomechanical cues [for reviews, see Refs. 8–11]. Firstly, like other immune cells, monocytes need to migrate to inflamed sites. Mechanotransduction during cell trafficking will be briefly discussed here as it has been widely studied regardless of cell types and functions [for reviews, see Ref. 12,13]. Subsequently, biophysical cues in the extracellular environment such as interstitial flow, cyclical forces, stretching, spatial confinement as well as matrix stiffness, can influence the activation and polarization of macrophages, which will be the focus in this review.

Cell trafficking

Throughout their lifetime, immune cells exert and receive mechanical stresses as they travel through the circulation, attach to the blood vessel wall, and extravasate into local tissue niches (Figure 2a–c, see figure legends for detailed description) [2]. Immune cells express integrins, selectins and chemokine receptors to interact with the ligands on endothelial cells (ECs) or respond to a chemical gradient for adhesion and transmigration. Mechanotransduction enables the process of monocytes extravasation and lymphocytes homing. Additionally, cytoskeletal proteins such as actin and non-muscle myosin II mediate rapid changes in cytoskeletal architecture on the timescale of seconds, a response rate essential for the motility of immune cells. While macrophages mainly adapt mesenchymal migration mediated through specific cell-ECM adhesion, amoeboid migration that lacks substantial cell-ECM attachment is an alternative migration mode in three-dimensional (3D) ECM [13].

Macrophage deformability

Soluble biochemical signals such as endogenous hormones and foreign pathogens are capable of triggering mechanical changes and influencing cellular behaviors (Figure 2d). For example, stress hormones —

Figure 2

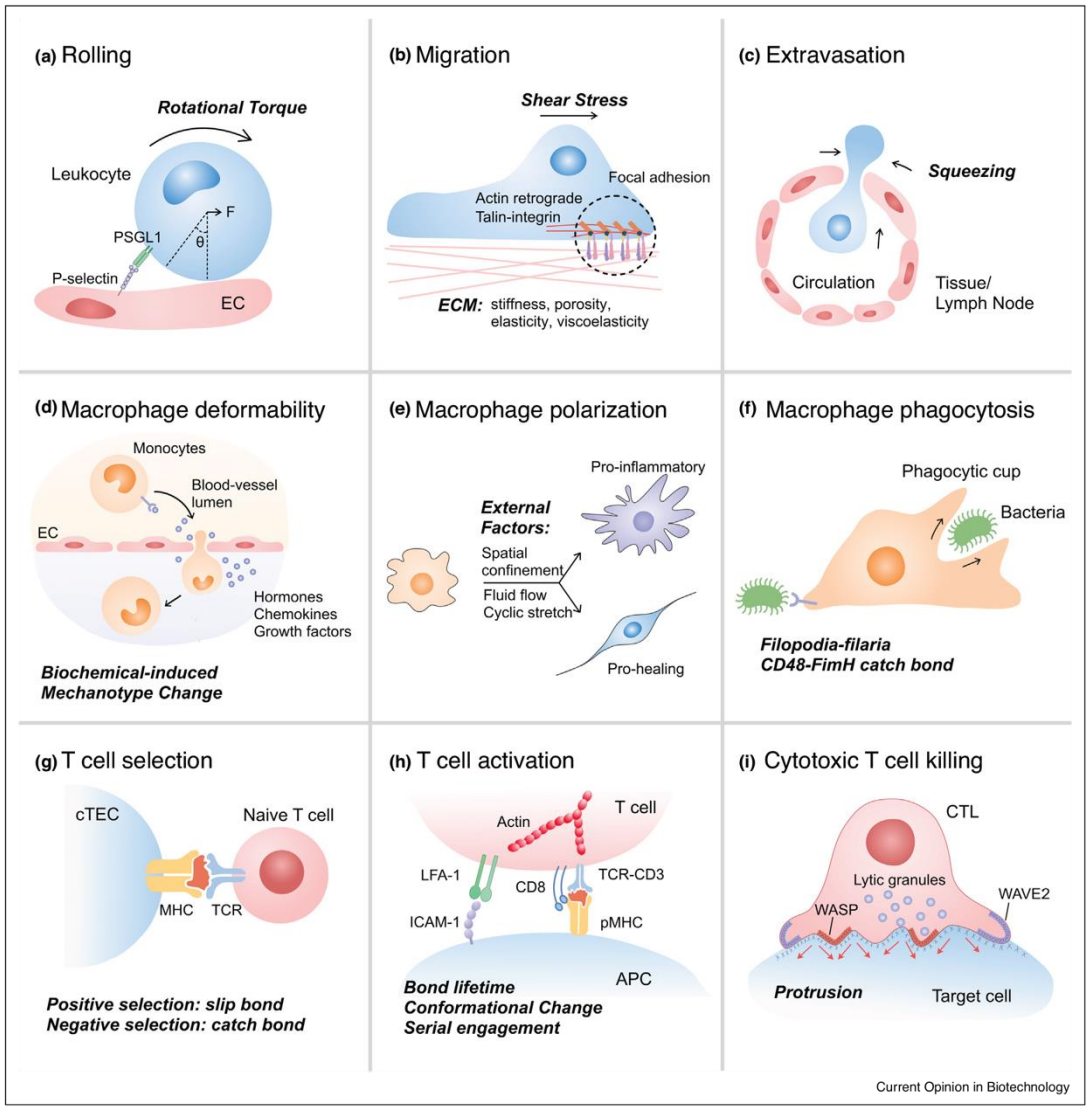

Mechanical factors regulate immune cell functions. **(a)** Because of the flow of body fluids, cell experiences rolling and steering. **(b)** Actin polymerization happens at the leading edge of the cell; constant retrograde flow of actin and myosin contraction propels the cell for migration. Interaction of integrins and formation of focal adhesion are important characteristics for adhesion-dependent mesenchymal migration. Some well-known receptor-ligand pairs involved in the adhesion on endothelial cells (ECs) include LFA-ICAM-1, Mac1-multiple ligands, VLA-4-VCAM, P-selection-PSGL-1, CCR2-CCL2, CCR5-CCL5. **(c)** Neutrophils and monocytes navigate *via* blood circulation and extravasate through the capillary epithelium to a specific inflammatory site for clearance of pathogen. T lymphocytes are also squeezed through cell-cell junctions when trafficking through the high epithelial venules. **(d–f)** Examples of mechanotransduction involved in innate immunity such as (d) macrophage deformability, (e) macrophage polarization and (f) macrophage phagocytosis. **(g–i)** Example of mechanotransduction in adaptive immunity such as (g) T cell selection in the thymus, (h) T cell activation and (i) Cytotoxic T cell killing.
*Abbreviation: PSGL-1: P-selectin glycoprotein ligand-1; CCR: C-C chemokine receptor; CCL: Chemokine (C-C motif) ligand.

epinephrine and norepinephrine — govern fight-or-flight responses by modulating muscle contraction [14]. Stress hormone activation of the β-adrenergic receptor (β-AR) signaling pathway further impacts macrophage mechanobiology, decreasing the deformability of macrophage cells through the rearrangement of branched filamentous actin in the cortical region [15]. Such a decrease in cell deformability induced by β-AR activation is also associated with an increase in macrophage phagocytosis and chemotaxis [15]. Moreover, environmental pathogens can change host cell mechanotypes. For example, the activation of nucleotide-binding oligomerization domain-like receptors (NLRs) by Salmonella infection, especially NLRC4, results in reduced cell deformability of mouse bone marrow-derived macrophages as determined using an optical stretcher [16]. The resultant cell stiffening in response to NLRC4 inflammasome activation prevents further uptake and bacterial dissemination [17]. Taken together, these studies suggest that the modulation of cell mechanotypes by soluble external cues from the host or pathogens can regulate macrophage functions during physiological and pathological conditions.

Macrophage polarization

Guided by chemokines and cytokines, macrophages can polarize into different phenotypes such as pro-inflammatory (M1) or pro-healing (M2) (Figure 2e). Physiologically relevant forces due to interstitial flow and hydrostatic pressure may regulate the polarization of macrophages. In most solid tumors, tumor-residing macrophages experience elevated levels of interstitial fluid flow compared to normal tissue [16]. Interstitial flow polarizes mouse bone marrow-derived macrophages towards a M2-like phenotype *via* integrin/Src-mediated signaling [18]. Mimicking mechanical cues that are experienced by macrophages in the lung, cyclical hydrostatic pressure initiates an inflammatory response *via* the mechanically activated ion channel Piezo1 [5••, for additional stretch effects on macrophages, see Ref. 10].

In addition to dynamic forces, spatial confinement modulates the polarization and function of macrophages. Macrophages adopt different geometries *in vivo* [19]. The confinement of macrophages using cell crowding, 3D microwells, or 2D micropatterning to limit their spreading results in the suppression of pro-inflammatory gene expression profile by reducing actin polymerization, lowering the nuclear translocation of myocardin-related transcription factor-A (MRTF-A), and modulating epigenetic modification and chromatin compaction *via* upregulation of histone deacetylase-3 (HDAC-3) [20••]. Using a similar 2D micropatterning approach to control macrophage cell shape and elongation without exogenous cytokines leads to the expression of M2 phenotype markers [21•]. Such shape-induced polarization is abrogated when actin and actomyosin contractility are inhibited by pharmacological agents, suggesting a role of the cytoskeleton and/or cell geometry in regulating macrophage polarization [22].

The mechanical environment — including the stiffness of the surrounding tissue or matrix — is another source of biophysical cues that modulate immune responses. The elastic modulus in different tissues can vary from a few kilopascals (kPa) in bone marrow and brain to several megapascals (MPa) in cartilages and bones [23]. On stiff polyacrylamide hydrogels (323 kPa), THP-1 derived macrophages are primed towards a pro-inflammatory phenotype with impaired phagocytosis, while soft (11 kPa) and medium (88 kPa) stiffness prime cells towards an anti-inflammatory, highly phagocytic phenotype [23]. Soft substrates (4 kPa) result in suppressed expression of M1-related genes while increasing selected M2-related genes in THP-1 cells compared to stiff substrate (>10 MPa) [24]. Interestingly, substrate stiffness can influence M2 polarization indirectly *via* modulating paracrine function of mesenchymal stem cells (MSCs). Human MSCs (hMSCs) cultured on soft substrates produced significantly higher levels of immunomodulatory and trophic factors compared to hMSCs cultured on rigid substrates, which result in M2 polarization of macrophages [25].

Phagocytosis

As professional phagocytes, macrophages must identify, catch and engulf pathogens. Stiffness, shape and size of the prey can all influence the formation of the phagocytic cup. Generally, increasing the size of preys is the most effective way to catch macrophages' attention [8]. Stiffer preys can more efficiently initiate phagocytosis, and such phenomenon is more significant in rod-shaped rather than spherical particles [8]. These trends may relate to how easy to establish receptor-ligand interaction between the macrophage and the invader and how well the macrophage can exert forces through the actin filaments and microtubules. Once the macrophage catches a surface-bound pathogen, they exploit single fimbrium-filopodium contacts to anchor pathogens *via* catch bonds, helping them extend the bond life and hold onto the prey (Figure 2f) [8].

Mechano-regulation of adaptive immunity

Adaptive immune responses — mediated by lymphocytes — are also modified and potentiated by mechanical cues at the molecular, cellular, and tissue level. Because of the highly mechano-sensitive interactions of TCRs with pMHC on the surface of antigen presenting cells (APCs), mechanotransduction is crucial during T cell selection, development, activation, and, effector function [for reviews, see Refs. 26–28]. Advances in single-cell experimental tools have aided greatly in expanding our understanding of TCR mechanotransduction [for reviews, Refs. 1,29]. Here, we highlight recent advances in our understanding of mechanobiology at different stages of a T cell's life cycle.

T cell selection

Unlike innate immune cells that express a fixed set of pattern recognition receptors, the T cell population has a diverse set of TCRs, allowing for recognition of foreign peptide antigens from pathogens. After rearrangement of TCRs *via* V(D)J recombination, positive and negative selection in the thymus interacting with cortical thymic epithelial cell (cTEC) ensures that T cells possess TCRs that can interact with the specific MHC molecules with appropriate force-dependent binding affinity. Interestingly, the mechanotransduction mechanisms mediating positive and negative selection are distinct, with slip bonds dominating during positive selection and catch bonds induced during negative selection (Figure 1g) [30••].

T cell activation

T cell activation requires the recognition of cognate pMHC on the surface of APCs by TCRs, generating cytoskeleton tension through nucleation of actin foci *via* Wiskott–Aldrich syndrome protein (WASP) and contraction of the resultant actin filaments by myosin II and leading to formation of immune synapses (Figure 1h) [31•].

T cells must maintain a low enough activation threshold to rapidly scan secondary lymphoid organs for scant, low-affinity foreign antigens, yet high enough to prevent autoimmune responses to self-antigens. The magnitude, duration, frequency, and timing of triggering forces on TCRs all contribute to a ligand-discrimination process that determines whether T cell activation will occur. TCR triggering is recognized as a nonequilibrium process that requires energy [32]. More details on the role of physical forces on T cell triggering have recently been revealed, as factors such as types of bond (i.e. catch, ideal versus slip [28]) and types of motion (i.e. stable synapses versus motile kinapses [33]). Stimulatory and non-stimulatory ligands can bind to TCRs with similar affinity, but only stimulatory ligands form catch bonds, which strengthen during disengagement and couple binding to signaling [34]. At the level of a single TCR-pMHC interaction, agonist, but not antagonist, ligands can sustain mechanical force to generate a conformational change of the heavy chain of MHC class I [35]. Such mechano-chemical coupling on molecular level provides a mechanism for TCR-pMHC catch bond formation [36••]. Triggered by antigen, Further, serial engagement with repeated pulling on TCRs is suggested to be required for T cell activation [36••; a review on serial engagement, see Ref. 32]. Taken together, bond lifetime, conformational changes and serial engagement all play important roles in TCR antigen recognition and T cell activation, but the detailed mechanism still needs further investigation.

Moreover, the flexibility of T cells — which reflects the stiffness of their cortical cytoskeleton — governs signaling differences in naïve versus effector T cells. Activated $CD4^+$ helper T cells exhibit increased deformability of their cortical cytoskeleton, which allows larger immune synapses to be formed with APCs compared to naïve T cells. The stiffer actin cortex in naïve cells is associated with greater basal activity in the RhoA-ROCK (Rho-activated kinase)-LIMK (LIM kinase) axis, resulting in decreased activity of the actin-severing enzyme cofilin [37]. In addition to cell rigidity, cytoskeletal dynamics alter TCR binding during activation. The velocity of retrograde actin flow during immune synapse formation was shown to be correlated with TCR binding kinetics [38].

At the cellular and tissue level, T cells can sense the mechanical properties of their environment. Stiffer (40 kPa) 3D hydrogel matrices augment $CD4^+$ T cell proliferation, activation and migration compared to softer matrices (4 kPa) [39]. Mechanistically, on stiffer substrates, YAP mediates enhanced translocation of nuclear factor of activated T cells (NFAT) into the nucleus, resulting in increased T cell activation and effector function [40]. Interestingly, simply applying mechanical forces *via* oscillation on a shaker leads to greater T cell expansion and activation, compared to static conditions [41], which may due to more effective encountering and contact between T cells and engineered APCs at the optimal oscillation frequency.

Besides mechanical force and environmental factors, the spatial distribution of ligands also affects how T cells perceive activation signals. Micropillar arrays embedded with anti-CD3 (activation signal) and anti-CD28 (co-stimulator) are useful platforms to investigate T cell mechanosensing on a single cell level. Microtubule organization at the cell-array interface shows the local contraction and expansion of $CD4^+$ T cells. Varying pillar height and shape induces changes in T cell cytoskeletal organization and interferon-γ secretion, which is associated with the effector functions [42•]. Artificial antigen presenting surfaces consisting of patterned micro-dot arrays surrounded by a fluid supported lipid bilayer are also useful tools for mimicking pMHC nanoclusters. TCR, zeta-chain-associated protein kinase (ZAP-70) and actin are colocalized with the ligand-dots in absence of intercellular adhesion molecule 1 (ICAM-1) — the ligand for LFA-1. However, in presence of ICAM-1 in the patterned array, actin shows global changes and accumulates peripherally, and the synapse area increases significantly. Such enhancing effects of TCR clustering on actin organization and cell spreading are exclusive to LFA-1 as the costimulatory molecule CD28 does not have the same impact [43].

Force enhances T cell cytotoxicity

When killing target cells, forces exerted by cytotoxic T cells on target cell membranes enhance the formation of

Table 1

Engineered biophysical factors to modulate immune cells

Biophysical factors	Cell types	Application summary	Ref.
Cell mechanotyping	All	Single-cell mechanotyping enables the characterization of diverse sets of specialized immune cells such as peripheral blood mononuclear cells (PBMCs) and stress-induced macrophages.	[15, 46, 61]
ECM stiffness	Macrophage	Human macrophages exhibit a wound healing phenotype on stiffer 3D fibrillar native matrices – collagen I, glycosaminoglycans (GAGs)	[62]
	Macrophage	Compared to unmodified fibrin gel, photoinitiated dityrosine-crosslinked fibrin gel increases cell spreading and motility and enhances inflammatory activation.	[51]
	T lymphocyte	Protein-coated beads made from a soft elastomer - polydimethylsiloxane (PDMS) enhance T cell expansion.	[49]
	T lymphocyte	0.5 kPa–100 kPa poly-acrylamide hydrogels: stiffer gel increases cytokine production, T cell metabolism and cell cycle progression.	[50]
	T lymphocyte	4 kPa–40 kPa RGD-modified alginate hydrogel: stiffer gel augments T-cell activation as compared to the softer material or 2D culture.	[39]
	T lymphocyte	An artificial T-cell stimulating matrix is engineered using hyaluronic acid-based hydrogel with optimized combination of the ECM environment and conjugated stimulatory signals for antigen-specific CD8+ T cell activation *ex vivo*.	[53]
Oscillatory forces	Macrophage	Cyclic mechanical compression achieved by biphasic ferrogels reduces fibrosis, M1 macrophage presence and inflammation in severe skeletal muscle injuries.	[55]
	T lymphocyte	Compared to static culture, an oscillatory mechanoenvironment doubles antigenic signal strength for $CD8^+$ T cell expansion.	[41]
Squeezing	T lymphocyte	Squeezing cells through a microfluidic device mechanically disrupts cell membrane for drug delivery and results in minimal aberrant transcriptional responses.	[54]
Microstructure confinement	Macrophage	Spatial confinement downsizes the inflammatory response of macrophages.	[23]
	Macrophage	Gelatin-based gels with smaller (30 μm) and softer (20 kPa) pores induce proinflammatory macrophages, while larger (80 μm) and stiffer pores (190 kPa) induce anti-inflammatory macrophages.	[51]
Ligand presentation	Macrophage	Fibrin matrices induce anti-inflammatory macrophages, but the soluble precursor fibrinogen stimulates inflammatory responses. Presence of both abrogate inflammation.	[58]
	T lymphocyte	Mesoporous silica micro-rods wrapped in lipid bilayers to present membrane-bounded T cell activation and co-stimulation signals.	[56•,57]
	T lymphocyte	Stimulatory signals conjugated to the engineered matrix can successfully activate $CD8^+$ T cell, whereas soluble signals have much less effects.	[53]
Mechanogenetics	T lymphocyte	By engineering the genetic circuits with a mechanosensor Piezo1 ion channel, T cells are modified to be remotely activated by the mechanical perturbance from ultrasound waves and transduce into transcriptional activation for CAR expression.	[59•]
	T lymphocyte	CAR responsiveness to soluble ligands can be fine-tuned by adjusting the mechanical coupling between the CAR's ligand-binding and signaling domains	[60]

perforin pores (Figure 1i) [44]. Also, perforin release occurs at the base of actin-rich protrusions and is regulated by the cytoskeletal regulator WASP and the Arp2/3 actin nucleation complex [45]. The coordination of perforin release and assembly by distinct actin cytoskeletal structure underscores the importance of mechanical events in the function of cytotoxic T lymphocytes (CTLs).

Applications: engineering immune cell functions

Unravelling the basic mechanobiology on molecular, cellular, and tissue levels inspires novel biomedical applications, especially in the fields of tissue regeneration and cancer immunotherapy. Novel approaches with bench-to-bed translational potentials such as patient cell mechanics measurements, T cell expansion *ex vivo*, immunoengineering *in vivo*, and genetic engineering are discussed and also summarized in Table 1.

Mechanotyping

Cellular deformability is an essential, physiologically relevant feature of immune cells. Mechanotype measurements can now be achieved with single-cell resolution and throughputs of up to 2000 cells/second by flowing a suspension of cells through microfluidic channels, squeezing the cells, and using automated image analysis to quantify metrics such as circularity and deformation timescale [46–49]. Importantly, cellular mechanotype data can provide valuable information on the status of a patient's immune system. For example, immune activation can be detected by measuring the size and deformability of cells from pleural effusions of patients. Cells from these inflamed patient pleural fluids are more deformable and larger in cell size compared to native population of leukocytes [47]. Cellular mechanotyping has potential to predict the degree of inflammation and progression of tumors in individual patients.

Materials stiffness

Immune cell responses could also be modulated by tuning the physical properties of matrix, specifically substrate stiffness. Scaffolds of both natural and synthetic biomaterials have been optimized for immune cell cultivation in 2D and 3D. Generally, a stiffer scaffold promotes T lymphocytes cell growth and activation *ex vivo* [49,50]. However, macrophages show less consistent responses to scaffold stiffness across studies due to different macrophage sources and different substrate materials and stiffness [23,24,51]. A potentially confounding factor is that scaffold mechanical properties are tightly linked to pore size and thus spatial confinement, which may also contribute to macrophage polarization [52]. A new approach using the cryoprotectant dimethyl sulfoxide (DMSO) allows the control of scaffold pore size independent of stiffness, enabling researchers to evaluate individual effects of stiffness and spatial confinement on immune cell phenotype and function in porous biomaterial scaffolds [52]. Understanding the effects of material stiffness and porosity on immune cells will provide a rational basis for the design of artificial matrix to stimulate immune cell expansion *ex vivo* and modulate immune cell functions *in situ* by mimicking APCs and/or constructing an artificial niche [39,50,53].

Dynamic environment

Besides changing the surrounding environment, externally exerting forces on immune cells can increase the efficiency of drug delivery, *in vitro* cell expansion, and *in vivo* cell function. Squeezing cells through a narrow microfluidic channel is one way to mechanically disrupt the cell membrane for effective gene delivery. Unlike electroporation, which disrupts the expression profile of human T cells, squeezing results in minimal aberrant transcriptional responses [54]. Moreover, an oscillatory mechanoenvironment shows better antigenic signal strength, compared to conventional, static culture for $CD8^+$ T cell expansion [41]. Thus, novel engineering tools and materials can be developed and tailored to control immune cell functions. For example, biphasic ferrogels, which have the mechanical capacity for large, fatigue-resistant deformation, are used for massage-like muscle stimulation [55]. In the model of severe skeletal muscle injuries in mice, macrophages subjected to cyclic mechanical compression show reduction in fibrosis, M1 macrophage and inflammation [55].

Ligand presentation

Engineering the spatial arrangement and 3D geometry of ligands is an alternative strategy to enhance immune cell activation. How a soluble ligand spatially binds to a T cell affects the efficacy of immune response. T cell activation has greater preference towards ligands physical bound to a surface, such as on lipid membranes or conjugated surfaces. Therefore, engineered scaffolds with bounded T cell activation signals is a potential strategy for *in vivo* local T cell recruitment and expansion [53,56•,57]. The difference in a free-floating ligand and physically bound ligand also affects macrophages. Whereas fibrin-gel induces anti-inflammatory macrophages secreting cytokines such as interleukin-10, the soluble precursor fibrinogen stimulates inflammatory responses [58]. Therefore, designing the presentation of chemical molecules on scaffolds can be a strategy for biomaterial innovation.

Genetic engineering

Mechanical modulation of immune cell responses could additionally be achieved by modulating mechanosensing gene circuits using systems and synthetic biology tools. In recent years, engineered T cells with chimeric antigen receptors (CAR), known as CAR-T cell therapy, have emerged as an effective, FDA-approved immunotherapy for various liquid cancers. For targeted and controlled delivery, mechanosensitive CAR T cells are constructed by harnessing the mechanosensing power of Piezo1 ion channel, so that the mechanical perturbance from ultrasonic waves can activate the CART T-cell at a desired location [59•]. In another study, TGF-β is rewired from an immune suppressive molecule to a CAR T-cell growth factor, thus achieving the first T cell response upon soluble ligand [60]. This actuation process can be precisely regulated by mechanical forces: 1) CAR receptor dimerization is required to bring the signaling domains of the CAR in proximity; 2) CAR itself needs to be mechanically rigid enough for mechanotransmission across the membrane. Such mechanical coupling can be used for fine tuning of T cell responses *via* extracellular spacer insertion to loosen the coupling [60].

Conclusions and future perspectives

Mechanotransduction in immune cells is dynamic, complex, and essential for the immune responses. Integrins, ion channels, TCRs, cytoskeletal proteins, and transcription factors form a network of mechanical signaling pathways that regulate cell mechanics, gene expression, and cellular behaviors relevant for immune cell functions. There are still knowledge gaps, especially regarding the identification of new mechanosensors and how mechano-signaling pathways are integrated across time and length scales. Moreover, besides the mechanosensitive interactions of integrin-ligand and TCR-pMHC, other conventional receptor-ligand binding events may also be affected by physical forces but have not been studied in the context of mechanobiology.

Single-cell technologies enable future investigations on mechanotransduction mechanisms with higher spatial and temporal resolution. For instance, single-cell force measurement techniques are developing to provide better spatiotemporal resolution and more accurate force sensing on cellular and even molecular level, such as the threshold of force required for TCR to trigger activation signaling. Also, single-cell sequencing deciphers the heterogeneous responses within a population of cells, and the gene expression profile can better define the phenotypes of immune cells. Florescence resonance energy

transfer (FRET) imaging, intravital two-photon imaging and other live cell imaging techniques are useful tools to monitor cell signaling events.

Understanding these foundational knowledge of immune cell mechanobiology would further guide the design of transformative biomaterials, drug delivery platforms, and synthetic biology strategies to modulate and control immune responses. Novel biomaterials with the appropriate biophysical properties, including elasticity, viscoelasticity and tunable stiffness and porosity, are needed for more precise regulation of macrophage polarization and T cell activation. By utilizing different delivery methods, the modulation of the immune cells can be local, systematic, or at certain targeted site. While material properties are usually measured as a bulk property, decoupling bulk mechanical cues like stiffness into single factors — such as chemical composition, scaffold pore size, the degree of crosslinking — will also be important to understand underlying mechanisms and be able to design the appropriate biomaterials faster for future applications. Future investigations will also be required to fully understand how multiple cues are simultaneously processed and integrated by immune cells to regulate immune responses.

Finally, biomaterial-based vaccines to selectively stimulate desirable immune cells and suppress undesirable immune responses have much value in this season of COVID-19 pandemic outbreak. Effective antigen presentation and micro-topology on biomaterials can further facilitate the proper activation of desirable immune responses. Moreover, implantable or injectable scaffolds with optimal porosity, matrix stiffness and antigen presentation may not only generate successful immune responses in short term, but also boost the generation of memory immune cells such as memory T cells and memory B cells and promote their longevity. All in all, biomaterial innovation based on mechanotransduction of immune cells can brighten the future for vaccine development and possibly establish material platforms that are robust for generating immunity towards various diseases.

Conflict of interest statement

Nothing declared.

Acknowledgements

This work is supported in part by grants from National Institute of Health (HL121450 and R56DE029157) and UCLA Eli and Edythe Broad Center of Regenerative Medicine and Stem Cell Research.

References and recommended reading

Papers of particular interest, published within the period of review, have been highlighted as:

- • of special interest
- •• of outstanding interest

1. Iskratsch T, Wolfenson H, Sheetz MP: **Appreciating force and shape — the rise of mechanotransduction in cell biology**. *Nat Rev Mol Cell Biol* 2014, **15**:825-833.

2. Zhu C, Chen W, Lou J, Rittase W, Li K: **Mechanosensing through immunoreceptors**. *Nat Immunol* 2019, **20**:1269-1278.

3. Huse M: **Mechanical forces in the immune system**. *Nat Rev Immunol* 2017, **17**:679-690.

4. Dustin ML: **Integrins and their role in immune cell adhesion**. *Cell* 2019, **177**:499-501.

5. •• Solis AG, Bielecki P, Steach HR, Sharma L, Harman CCD, Yun S, de Zoete MR, Warnock JN, To SDF, York AG *et al.*: **Mechanosensation of cyclical force by PIEZO1 is essential for innate immunity**. *Nature* 2019, **573**:69-74

This is a pioneering work to link mechanosensitive channels to innate immunity. This work demonstrates that rhythmic pressure is sensed by immune cells *via*the mechano-sensitive membrane channel PIEZO1 to coordinate immune defense in the lungs.

6. Liu CSC, Raychaudhuri D, Paul B, Chakrabarty Y, Ghosh AR, Rahaman O, Talukdar A, Ganguly D: **Cutting edge: Piezo1 mechanosensors optimize human T cell activation**. *J Immunol* 2018, **200**:1255-1260.

7. Panciera T, Azzolin L, Cordenonsi M, Piccolo S: **Mechanobiology of YAP and TAZ in physiology and disease**. *Nat Rev Mol Cell Biol* 2017, **18**:758-770.

8. Jain N, Moeller J, Vogel V: **Mechanobiology of macrophages: how physical factors coregulate macrophage plasticity and phagocytosis**. *Annu Rev Biomed Eng* 2019, **21**:267-297.

9. McWhorter FY, Davis CT, Liu WF: **Physical and mechanical regulation of macrophage phenotype and function**. *Cell Mol Life Sci* 2015, **72**:1303-1316.

10. Meli VS, Veerasubramanian PK, Atcha H, Reitz Z, Downing TL, Liu WF: **Biophysical regulation of macrophages in health and disease**. *J Leukoc Biol* 2019, **106**:283-299.

11. Gruber EJ, Leifer CA: **Molecular regulation of TLR signaling in health and disease: mechano-regulation of macrophages and TLR signaling**. *Innate Immun* 2020, **26**:15-25.

12. Humphrey JD, Dufresne ER, Schwartz MA: **Mechanotransduction and extracellular matrix homeostasis**. *Nat Rev Mol Cell Biol* 2014, **15**:802-812.

13. Yamada KM, Sixt M: **Mechanisms of 3D cell migration**. *Nat Rev Mol Cell Biol* 2019, **20**:738-752.

14. Emrick MA, Sadilek M, Konoki K, Catterall WA: **Beta-adrenergic-regulated phosphorylation of the skeletal muscle Ca(V)1.1 channel in the fight-or-flight response**. *Proc Natl Acad Sci U S A* 2010, **107**:18712-18717.

15. Kim T-H, Ly C, Christodoulides A, Nowell CJ, Gunning PW, Sloan EK, Rowat AC: **Stress hormone signaling through β-adrenergic receptors regulates macrophage mechanotype and function**. *FASEB J* 2018, **33**:3997-4006.

16. Man SM, Ekpenyong A, Tourlomousis P, Achouri S, Cammarota E, Hughes K, Rizzo A, Ng G, Wright JA, Cicuta P *et al.*: **Actin polymerization as a key innate immune effector mechanism to control Salmonella infection**. *Proc Natl Acad Sci U S A* 2014, **111**:17588-17593.

17. Lunt SJ, Fyles A, Hill RP, Milosevic M: **Interstitial fluid pressure in tumors: therapeutic barrier and biomarker of angiogenesis**. *Future Oncol* 2008, **4**:793-802.

18. Li R, Serrano JC, Xing H, Lee TA, Azizgolshani H, Zaman M, Kamm RD: **Interstitial flow promotes macrophage polarization toward an M2 phenotype**. *Mol Biol Cell* 2018, **29**:1927-1940.

19. Sharma VP, Beaty BT, Patsialou A, Liu H, Clarke M, Cox D, Condeelis JS, Eddy RJ: **Reconstitution of in vivo macrophage-tumor cell pairing and streaming motility on one-dimensional micro-patterned substrates**. *Intravital* 2012, **1**:77-85.

20. •• Jain N, Vogel V: **Spatial confinement downsizes the inflammatory response of macrophages**. *Nat Mater* 2018, **17**:1134-1144

This article describes the effect of confinement on macrophage inflammatory genes expression. When macrophage adherence is limited to a confined space, the inflammatory responses are suppressed, and such observations provide new insights into how physical cues regulate immune cell behavior.

21. • McWhorter FY, Wang T, Nguyen P, Chung T, Liu WF: **Modulation of macrophage phenotype by cell shape**. *Proc Natl Acad Sci U S A* 2013, **110**:17253-17258

This is the first article to show macrophage phenotype can be modulated by cell shape. Elongation of macrophages in micropatterned substrates promotes prohealing macrophages.

22. Handorf A, Zhou Y, Halanski M, Li W-J: **Tissue stiffness dictates development, homeostasis, and disease progression**. *Organogenesis* 2015, **11**:1-15.

23. Sridharan R, Cavanagh B, Cameron AR, Kelly DJ, O'Brien FJ: **Material stiffness influences the polarization state, function and migration mode of macrophages**. *Acta Biomater* 2019, **89**:47-59.

24. Okamoto T, Takagi Y, Kawamoto E, Park EJ, Usuda H, Wada K, Shimaoka M: **Reduced substrate stiffness promotes M2-like macrophage activation and enhances peroxisome proliferator-activated receptor gamma expression**. *Exp Cell Res* 2018, **367**:264-273.

25. Ji Y, Li J, Wei Y, Gao W, Fu X, Wang Y: **Substrate stiffness affects the immunosuppressive and trophic function of hMSCs *via* modulating cytoskeletal polymerization and tension**. *Biomater Sci* 2019, **7**:5292-5300.

26. Kumar BV, Connors TJ, Farber DL: **Human T cell development, localization, and function throughout life**. *Immunity* 2018, **48**:202-213.

27. Rushdi M, Li K, Yuan Z, Travaglino S, Grakoui A, Zhu C: **Mechanotransduction in T cell development, differentiation and function**. *Cells* 2020, **9**.

28. Rossy J, Laufer JM, Legler DF: **Role of mechanotransduction and tension in T cell function**. *Front Immunol* 2018, **9**:2638.

29. Liu B, Chen W, Evavold BD, Zhu C: **Accumulation of dynamic catch bonds between TCR and agonist peptide-MHC triggers T cell signaling**. *Cell* 2014, **157**:357-368.

30. •• Hong J, Ge C, Jothikumar P, Yuan Z, Liu B, Bai K, Li K, Rittase W, Shinzawa M, Zhang Y *et al.*: **A TCR mechanotransduction signaling loop induces negative selection in the thymus**. *Nat Immunol* 2018, **19**:1379-1390

This article is the first study to investigate the type of bonds during selection of T lymphocytes in thymus. It shows that negative selection exerts cooperative TCR–pMHC–CD8 trimolecular catch bonds whereas positive selection formed short-lived slip bonds.

31. • Kumari S, Mak M, Poh Y-C, Tohme M, Watson N, Melo M, Janssen E, Dustin M, Geha R, Irvine DJ: **Cytoskeletal tension actively sustains the migratory T-cell synaptic contact**. *EMBO J* 2020, **39**:e102783

This study explains the force generation mechanism through cytoskeleton tension during T cell synaptic contact. WASP acts as a central regulator of synapse symmetry by nucleation of actin foci and is degraded after activation.

32. Feng Y, Reinherz EL, Lang MJ: **alphabeta T cell receptor mechanosensing forces out serial engagement**. *Trends Immunol* 2018, **39**:596-609.

33. Mayya V, Judokusumo E, Abu Shah E, Peel CG, Neiswanger W, Depoil D, Blair DA, Wiggins CH, Kam LC, Dustin ML: **Durable interactions of T cells with T cell receptor stimuli in the absence of a stable immunological synapse**. *Cell Rep* 2018, **22**:340-349.

34. Sibener LV, Fernandes RA, Kolawole EM, Carbone CB, Liu F, McAffee D, Birnbaum ME, Yang X, Su LF, Yu W *et al.*: **Isolation of a structural mechanism for uncoupling T cell receptor signaling from peptide-MHC binding**. *Cell* 2018, **174**:672-687.e27.

35. Wu P, Zhang T, Liu B, Fei P, Cui L, Qin R, Zhu H, Yao D, Martinez RJ, Hu W *et al.*: **Mechano-regulation of peptide-MHC Class I conformations determines TCR antigen recognition**. *Mol Cell* 2019, **73**:1015-1027.e7.

36. •• Lin JJY, Low-Nam ST, Alfieri KN, McAffee DB, Fay NC, Groves JT: **Mapping the stochastic sequence of individual ligand-receptor binding events to cellular activation: T cells act on the rare events**. *Sci Signal* 2019, **12**

This study emphasizes the importance of stochastic sequence and binding kinetics during T cell activation. Dwell time of pMHC-TCR binding that triggers T cell activation is an order of magnitude longer than the average agonist pMHC-TCR dwell time.

37. Thauland TJ, Hu KH, Bruce MA, Butte MJ: **Cytoskeletal adaptivity regulates T cell receptor signaling**. *Sci Signal* 2017:10.

38. Colin-York H, Javanmardi Y, Skamrahl M, Kumari S, Chang VT, Khuon S, Taylor A, Chew T-L, Betzig E, Moeendarbary E *et al.*: **Cytoskeletal control of antigen-dependent T cell activation**. *Cell Rep* 2019, **26**:3369-3379.e5.

39. Majedi FS, Hasani-Sadrabadi MM, Thauland TJ, Li S, Bouchard L-S, Butte MJ: **T-cell activation is modulated by the 3D mechanical microenvironment**. *bioRxiv* 2019 http://dx.doi.org/10.1101/580886.

40. Meng KP, Majedi FS, Thauland TJ, Butte MJ: **Tissue mechanics controls T-cell activation and metabolism**. *bioRxiv* 2019 http://dx.doi.org/10.1101/581322.

41. Majedi FS, Hasani-Sadrabadi MM, Thauland TJ, Li S, Bouchard L-S, Butte MJ: **Augmentation of T-cell activation by oscillatory forces and engineered antigen-presenting cells**. *Nano Lett* 2019, **19**:6945-6954.

42. • Jin W, Tamzalit F, Chaudhuri PK, Black CT, Huse M, Kam LC: **T cell activation and immune synapse organization respond to the microscale mechanics of structured surfaces**. *Proc Natl Acad Sci U S A* 2019, **116**:19835-19840

This study captures the spatial complexity of mechanical stiffness. By observing the cell interaction with elastomer micropillar arrays, they show that T cells can sense their surrounding local rigidity.

43. Benard E, Nunes JA, Limozin L, Sengupta K: **T cells on engineered substrates: the impact of TCR clustering is enhanced by LFA-1 engagement**. *Front Immunol* 2018, **9**:2085.

44. Basu R, Whitlock BM, Husson J, Le Floc'h A, Jin W, Oyler-Yaniv A, Dotiwala F, Giannone G, Hivroz C, Biais N *et al.*: **Cytotoxic T cells use mechanical force to potentiate target cell killing**. *Cell* 2016, **165**:100-110.

45. Tamzalit F, Wang MS, Jin W, Tello-Lafoz M, Boyko V, Heddleston JM, Black CT, Kam LC, Huse M: **Interfacial actin protrusions mechanically enhance killing by cytotoxic T cells**. *Sci Immunol* 2019, **4**.

46. Gossett DR, Tse HTK, Lee SA, Ying Y, Lindgren AG, Yang OO, Rao J, Clark AT, Di Carlo D: **Hydrodynamic stretching of single cells for large population mechanical phenotyping**. *Proc Natl Acad Sci U S A* 2012, **109**:7630-7635.

47. Nyberg KD, Hu KH, Kleinman SH, Khismatullin DB, Butte MJ, Rowat AC: **Quantitative deformability cytometry: rapid, calibrated measurements of cell mechanical properties**. *Biophys J* 2017, **113**:1574-1584.

48. Rosendahl P, Plak K, Jacobi A, Kraeter M, Toepfner N, Otto O, Herold C, Winzi M, Herbig M, Ge Y *et al.*: **Real-time fluorescence and deformability cytometry**. *Nat Methods* 2018, **15**:355-358.

49. Hsieh JY, Keating MT, Smith TD, Meli VS, Botvinick EL, Liu WF: **Matrix crosslinking enhances macrophage adhesion, migration, and inflammatory activation**. *APL Bioeng* 2019, **3**:16103.

50. Lambert LH, Goebrecht GKE, De Leo SE, O'Connor RS, Nunez-Cruz S, Li T-D, Yuan J, Milone MC, Kam LC: **Improving T cell expansion with a soft touch**. *Nano Lett* 2017, **17**:821-826.

51. Saitakis M, Dogniaux S, Goudot C, Bufi N, Asnacios S, Maurin M, Randriamampita C, Asnacios A, Hivroz C: **Different TCR-induced T lymphocyte responses are potentiated by stiffness with variable sensitivity**. *eLife* 2017, **6**.

52. Jiang S, Lyu C, Zhao P, Li W, Kong W, Huang C, Genin GM, Du Y: **Cryoprotectant enables structural control of porous scaffolds for exploration of cellular mechano-responsiveness in 3D**. *Nat Commun* 2019, **10**:3491.

53. Hickey JW, Dong Y, Chung JW, Salathe SF, Pruitt HC, Li X, Chang C, Fraser AK, Bessell CA, Ewald AJ *et al.*: **Engineering an artificial T-cell stimulating matrix for immunotherapy**. *Adv Mater* 2019, **31** e1807359.

54. DiTommaso T, Cole JM, Cassereau L, Buggé JA, Hanson JLS, Bridgen DT, Stokes BD, Loughhead SM, Beutel BA, Gilbert JB *et al.*: **Cell engineering with microfluidic squeezing preserves functionality of primary immune cells in vivo**. *Proc Natl Acad Sci U S A* 2018, **115**:E10907-E10914.

55. Cezar CA, Roche ET, Vandenburgh HH, Duda GN, Walsh CJ, Mooney DJ: **Biologic-free mechanically induced muscle regeneration**. *Proc Natl Acad Sci U S A* 2016, **113**:1534-1539.

56. • Cheung AS, Zhang DKY, Koshy ST, Mooney DJ: **Scaffolds that mimic antigen-presenting cells enable ex vivo expansion of primary T cells**. *Nat Biotechnol* 2018, **36**:160-169
This engineering scaffold mimics antigen-presenting cells and provides *ex vivo* expansion for primary T cells better than current technology. It consists of a fluid lipid bilayer for membrane-bound presentation of anti-CD3 and anti-CD28 and a mesoporous silica micro-rod core for sustained release of interleukin-2.

57. Kim J, Li WA, Choi Y, Lewin SA, Verbeke CS, Dranoff G, Mooney DJ: **Injectable, spontaneously assembling, inorganic scaffolds modulate immune cells in vivo and increase vaccine efficacy**. *Nat Biotechnol* 2015, **33**:64-72.

58. Hsieh JY, Smith TD, Meli VS, Tran TN, Botvinick EL, Liu WF: **Differential regulation of macrophage inflammatory activation by fibrin and fibrinogen**. *Acta Biomater* 2017, **47**:14-24.

59. • Pan Y, Yoon S, Sun J, Huang Z, Lee C, Allen M, Wu Y, Chang Y-J, Sadelain M, Shung KK *et al.*: **Mechanogenetics for the remote and noninvasive control of cancer immunotherapy**. *Proc Natl Acad Sci U S A* 2018, **115**:992-997
Mechanosensitive CAR-T cells are constructed through engineering the mechanosensor Piezo-1 and genetic transducing modules. The engineered T cells are responsive to mechanical perturbation like ultrasound waves, thus non-invasive and remote control achieved.

60. Chang ZL, Lorenzini MH, Chen X, Tran U, Bangayan NJ, Chen YY: **Rewiring T-cell responses to soluble factors with chimeric antigen receptors**. *Nat Chem Biol* 2018, **14**:317-324.

61. Weaver WM, Tseng P, Kunze A, Masaeli M, Chung AJ, Dudani JS, Kittur H, Kulkarni RP, Di Carlo D: **Advances in high-throughput single-cell microtechnologies**. *Curr Opin Biotechnol* 2014, **25**:114-123.

62. Friedemann M, Kalbitzer L, Franz S, Moeller S, Schnabelrauch M, Simon J-C, Pompe T, Franke K: **Instructing human macrophage polarization by stiffness and glycosaminoglycan functionalization in 3D collagen networks**. *Adv Healthc Mater* 2017, **6**.

9. APPENDIX D. BIOMATERIAL-BASED IMMUNOENGINEERING TO FIGHT COVID-19 AND INFECTIOUS DISEASES

CellPress

Matter

Review

Biomaterial-based immunoengineering to fight COVID-19 and infectious diseases

Jana Zarubova,[1] Xuexiang Zhang,[1] Tyler Hoffman,[1] Mohammad Mahdi Hasani-Sadrabadi,[1] and Song Li[1,2,3,*]

SUMMARY

Infection by SARS-CoV-2 virus often induces the dysregulation of immune responses, tissue damage, and blood clotting. Engineered biomaterials from the nano- to the macroscale can provide targeted drug delivery, controlled drug release, local immunomodulation, enhanced immunity, and other desirable functions to coordinate appropriate immune responses and to repair tissues. Based on the understanding of COVID-19 disease progression and immune responses to SARS-CoV-2, we discuss possible immunotherapeutic strategies and highlight biomaterial approaches from the perspectives of preventive immunization, therapeutic immunomodulation, and tissue healing and regeneration. Successful development of biomaterial platforms for immunization and immunomodulation will not only benefit COVID-19 patients, but also have broad applications for a variety of infectious diseases.

INTRODUCTION

In 2020, coronavirus disease 2019 (COVID-19) rapidly evolved into a global public health emergency. Coronavirus SARS-CoV-2 was identified as the causative virus of the COVID-19 pandemic, with a much higher infection rate than SARS-CoV of 2003. With over 80 million people infected and 1.7 million deaths globally as of December 2020, there is an urgent need for preventive measures and therapeutic treatments. Currently there is no effective therapy for COVID-19, and for those who recover from the disease, the repair of damaged tissues and organs is challenging. On the preventive side, although significant progress has been made in vaccine development, it is not clear whether a long-term immunity can be achieved.

SARS-CoV-2 gets into cells via the binding of its spike protein to the angiotensin-converting enzyme 2 (ACE2) receptor, which is upregulated in lung epithelial cells with age.[1] The infection of lung tissue may cause overactive inflammatory responses, tissue damage, and the development of acute respiratory disease syndrome (ARDS). Innate immune cells, such as neutrophils and macrophages, are recruited directly to the infection site and release cytokines to stimulate the adaptive immune responses, mediated by T and/or B cells.[2] In healthy people, this process is efficient enough to resolve the infection in a timely manner. However, a dysfunctional and dysregulated immune response to SARS-CoV-2 infection, characterized by monocyte hyperactivation and extensive macrophage/neutrophil infiltration, causes severe lung damage and systemic effects across the body, such as prominent lymphopenia.[3] Compared with patients with mild symptoms, patients in severe and critical conditions exhibit symptoms of hyper-inflammatory cytokine storm. Elevated level of pro-inflammatory cytokines, namely interferon (IFN), tumor necrosis factor (TNF), interleukin-6 (IL-6),

Progress and potential

The COVID-19 pandemic has significantly affected the global population. The rapid development of preventative vaccines and patient treatment protocols is critical for saving lives. Engineered biomaterials can be used to induce specific immune system responses and improve effectiveness. In this review, we discuss the role of biomaterials in vaccine enhancement, infection treatments, and post-infection tissue regeneration. We identify biomaterial-based examples that help to create more effective and long-term immunization, extend drug release profiles, target specific organs to prevent side effects, control an overactive immune system during infection, and prevent and treat tissue damage. Overall, we recognize an important role for biomaterials in treatments for COVID-19 and the potential to address the challenges of infectious diseases in the future.

and IL-1β, impaired type I IFN responses, and a reduced production of IFN-β and IFN-α were identified in more severe patient groups.[3] Increased levels of hyper-inflammatory cytokines may also trigger septic shock-associated multiorgan failure, which has been predominantly observed in elderly populations.[4] Moreover, antibody responses in COVID-19 patients often seem to be weak and short-lived, which is probably caused by dysregulated humoral immune induction and defective formation of germinal centers, where pathogen-specific antibodies are generated and long-lasting memory B cells are derived.[5]

In addition, the SARS-CoV-2 infection and consequent systemic inflammation can cause endothelial dysregulation and coagulation disorder, leading to the disruption of vascular integrity, hypercoagulation, and both arterial and venous thrombosis. Whether the virus can directly attack endothelial cells[6] or whether it infects only pericytes, which are the predominant cell type expressing ACE2 at least in the central nervous system (CNS) and in the heart,[7] is not clear at this point. The most common thrombotic manifestations of COVID-19 are pulmonary embolism, acute limb ischemia, ischemic stroke, and myocardial infarction.[8] COVID-19-related coagulopathies are associated with elevated levels of several coagulation markers, including D-dimer (a fibrin degradation product)[9] and elevated von Willebrand factor antigen (a marker of endothelial cell dysfunction).[10]

Moreover, increased activation of complement, a part of innate immune system, has been suggested to amplify the prothrombotic state.[11] The complement system consists of more than 30 proteins that circulate in the blood as inactive precursors. It uses pattern recognition molecules to directly or indirectly recognize pathogens or injured host cells. It can generate pro-inflammatory mediators, increase the antibody-mediated immunity, or directly attack and destroy the pathogens. The crosstalk between the complement and coagulation system is mediated by mannan-binding lectin serine proteases (MASPs), which are able to convert prothrombin to thrombin (MASP-2)[12] and fibrinogen to fibrin (MASP-1).[13] Recently, it was reported that the N protein of SARS-CoV-2 can bind to MASP-2 and enhance its enzymatic activity.[14] Therefore, it is possible that the thrombotic complications of COVID-19 are mediated, at least in part, by complement hyperactivation.

This ongoing pandemic highlights the critical need and challenges associated with a prompt response to infectious diseases. In this review, we discuss applications of biomaterials on enhancing COVID-19 immunotherapeutics as (1) preventive vaccines, (2) treatments for infection, and (3) healing and regeneration of damaged tissues following the resolution of infection (Figure 1). First, the rapid development of effective, long-term vaccines is critical to control the further spread of emerging and re-emerging infectious diseases. Vaccines as a preventive treatment function by educating the immune system on potential foreign antigens and generating protective neutralizing antibodies as well as memory immune cells. While the development of vaccines has achieved significant progress, the role of biomaterials to elicit adequate immune reaction should not be neglected, especially for the maintenance of long-term immunity and the enhancement of immune responses in aging populations. Biomaterials can support and boost effective immune responses through stabilizing the antigen, organizing antigen presentation patterns, recruiting antigen-presenting cells (APCs), triggering pattern recognition receptors, and/or delivering antigens to the lymph nodes.[15]

Secondly, if individuals have already been infected, treatments can be categorized into either antiviral or immunomodulatory therapies based on targeting the viruses

[1]Department of Bioengineering, Henry Samueli School of Engineering and Applied Science, University of California, Los Angeles, CA 90095, USA

[2]Department of Medicine, David Geffen School of Medicine, University of California, Los Angeles, CA 90095, USA

[3]Twitter: @songli_UCLA

*Correspondence: songli@ucla.edu

https://doi.org/10.1016/j.matt.2021.02.025

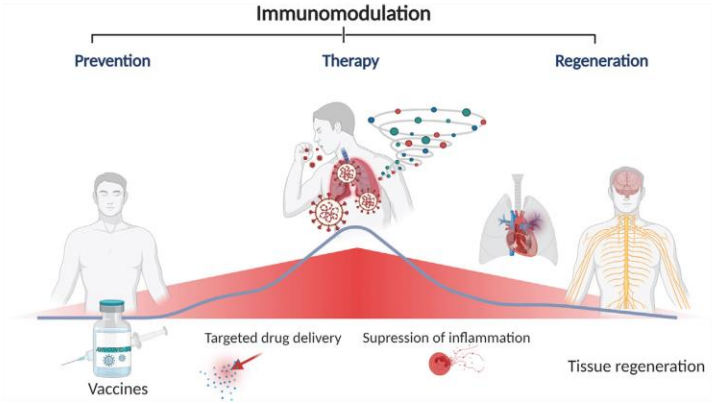

Figure 1. Immunomodulation to fight COVID-19 at different stages
Biomaterials can be engineered to enhance vaccines, delivery drugs to treat infections, modulate immune responses, and promote the recovery and/or healing of damaged tissues.

or the host immune system. According to the stage of disease progression and patient's immune response patterns, each strategy has its advantages.[16] Viruses typically induce delayed, ineffective, or dysregulated host immune system reactions. Boosting host antiviral responses with IFN treatments and/or reducing viral load by antivirals represent potential treatments for the early stage of infection.[17] As the infection progresses and host cells actively respond to the virus, the buildup of a highly inflammatory environment can subsequently trigger a cytokine storm. To mitigate an overwhelming immune response, immunomodulators can be used to minimize pathological damage and guide desirable cellular immunity to attack infected cells. Some examples of therapeutic approaches that may support proper immune responses are anti-inflammatory agents (i.e., IL-6 blocker tocilizumab), immunosuppressive drugs (i.e., glucocorticoids), checkpoint inhibitors (i.e., PD-1 inhibitor), and adaptive cell therapies.

Administration of small-molecule antivirals or macromolecule biologics is usually systemic, however, and this global modulation of the immune system may be less specific and have side effects. Therefore, biomaterials can have an impactful role in both directing drug transport and realizing targeted or local immunomodulation.

Finally, concerns related to the long-term side effects of COVID-19 infection on the large population of surviving patients have been raised. Following the clearance of a SARS-CoV-2 infection, the modulation of the immune environment in a tissue-specific manner with biomaterials can be used to support healing and regeneration of damaged tissues to prevent future complications.

In this review, we focus on biomaterial-based immunoengineering approaches to tackle a variety of pathological problems during different stages of COVID-19 and infectious diseases. Figure 1 depicts the three major stages (vaccine prevention, drug delivery for therapies, and tissue healing and regeneration) where immunomodulation can have significant impact, and outlines the overall strategies at each stage of disease progression.

Biomaterials-enhanced vaccine delivery to boost immunity

Technological platform of vaccines

Effective vaccines induce long-term antigen-specific responses by developing long-lived memory T and B cells in addition to plasma cells, which produce antibodies. Variables, such as the type of vaccine and the nature of the targeted pathogen, define the extent of contribution for each of these immune cells. Vaccine development normally takes 10 to 15 years, where the optimal antigen is selected, the vaccine composition is optimized based on the preclinical animal studies, and three phases of clinical studies are performed to evaluate the safety and efficacy of the candidate vaccine. Accelerating COVID-19 vaccine development to condense 15 years into 15 months is very challenging, not only because it is not known which immunogen and which vaccine type will be the most effective in establishing robust long-term immunoprotection, but also due to concerns about the adverse effects that the vaccine might potentially have on vulnerable individuals. One of the safety concerns about vaccines is connected to a phenomenon termed antibody-dependent enhancement (ADE).[18] Instead of inducing neutralizing antibodies that appropriately block a viral entry to the cells, a vaccine might induce the production of non-neutralizing antibodies that facilitate viral interactions with host cells to enhance inflammation and immunopathology. Previous studies on SARS-CoV or MERS-CoV showed that ADE was mainly associated with Th2-biased responses. Therefore, adjuvants promoting Th1 immune responses were preferred when designing COVID-19 vaccines. Other than safety, vaccines in clinical trials must also be effective. The levels of neutralizing antibodies as well as T cell responses, which play an important role in the immune protection against SARS-CoV-2, are evaluated to indicate vaccination efficacy.

Currently, there are more than 60 vaccines against COVID-19 in clinical trials and over 100 vaccines in preclinical phases.[19] Vaccine formulations range from weakened and replicating viruses to inactivated viruses, viral protein subunits, peptides, as well as genetic materials (i.e., DNA and RNA) (Figure 2). Weakened virus-based vaccines are still live viruses, so they can trigger the strong immune responses but require challenging development and optimization to eliminate potential risks. Some COVID-19 vaccine frontrunners are based on inactivated viruses, which are produced through established chemical or heat treatment.[20] Inactivated virus vaccines from Sinopharm and Sinovac Biotech were already approved for emergency use in China.

Protein-based vaccines can be manufactured using a variety of platforms, such as the forced expression of viral proteins in mammalian, bacterial, or yeast cells in bioreactors. These techniques are well developed in pharmaceutical industries but are limited by high costs associated with low yield and essential multistage purification of possible (human) pathogen contamination. Therefore, cost and ease of manufacturing and scale-up should be considered for the global-scale production of potential vaccines. Thus, an alternative method of cell-free production of peptides might be more appropriate; peptide-based vaccines are easier to design, optimize, manufacture, and scale-up to meet the required worldwide mandate. Last but not least, recent clinical data show a great promise on a relatively new class of vaccination by delivering genetic materials, such as DNA and RNA, that induce a host production of immunogenic proteins *in situ*. For example, the two vaccines from Pfizer-BioNTech and Moderna have been approved by the Food and Drug Administration (FDA) for emergency use, and both of them use messenger RNA (mRNA) for viral protein expression.[21] Several other leading COVID-19 vaccines (i.e., Oxford-AstraZeneca, Johnson & Johnson, CanSino) are made from segments of viral DNA, which is packaged inside the adenovirus for delivery into host cells. Recently, a similar adenovirus-based vaccine has been approved for

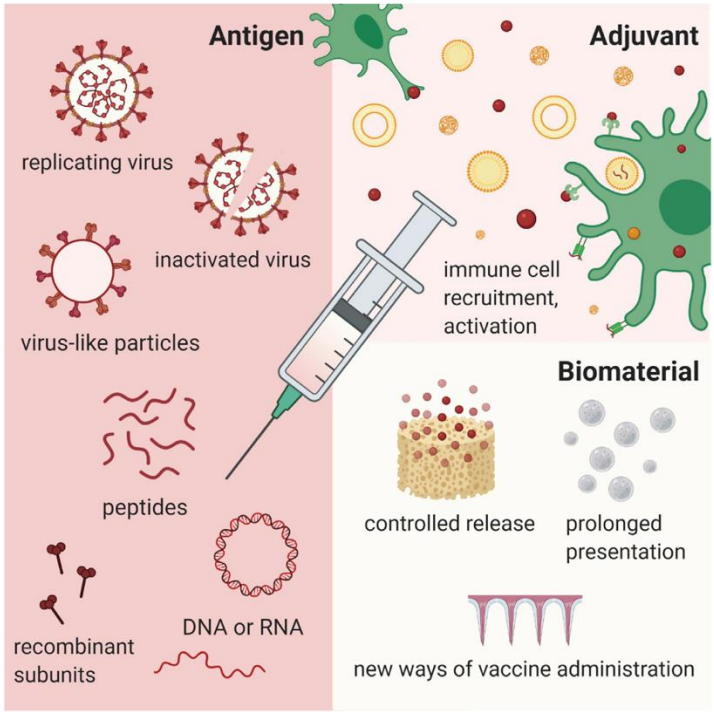

Figure 2. Approaches to develop and deliver SARS-CoV-2 vaccines
Various virus components can be used as potential vaccines, and biomaterials can be used to facilitate and enhance vaccine delivery.

Ebola. RNA- and DNA-based vaccines can tackle the common issues with scalability, flexibility, and speed of vaccine production against any new pathogens. A major advantage of mRNA vaccines is that mRNA does not need to get into a nucleus as DNA and can be directly translated into proteins within the cytoplasm, which results in higher expression efficiency.[20] Compared with RNA-based vaccines, DNA-based vaccines have the advantage of being more stable. Thus, due to the fragility of RNA, a cold chain (−80°C) is usually required for vaccine delivery and storage.

Vaccine adjuvants and delivery

Subunit vaccines containing purified antigens derived from pathogens are often weakly immunogenic. Without an adjuvant delivery system, subunit proteins or genetic materials are usually subjected to dissociation and elimination before entering host cells.[22] Adjuvant supplementation can enhance the magnitude and durability of immune responses and permit significant dose sparing. Adjuvants are mainly supposed to increase the immune cell recruitment and the production of inflammatory cytokines, enhance antigen uptake and presentation, and also facilitate antigen transport to the draining lymph node to promote the expansion and differentiation of the appropriate T and B cells (Figure 3).

The most commonly used molecular adjuvants are ligands for pattern recognition receptors, such as Toll-like receptors (TLRs), nucleotide binding oligomerization-like receptors, retinoic acid inducible gene 1-like receptors, and C-type lectin-like

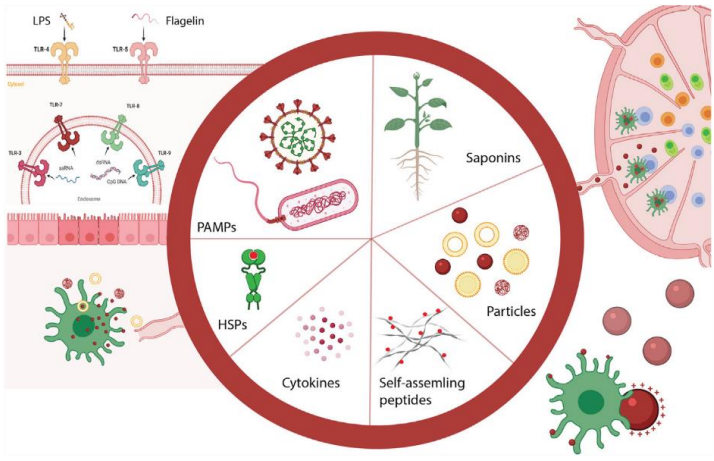

Figure 3. Boosting the vaccination via adjuvant design

Adjuvant design and their interactions with immune cells. Adjuvants work as immunostimulatory compounds to improve vaccine efficacy by boosting innate and adaptive immunity to support prolonged humoral and cellular response. The central circle is showing classes of molecular adjuvants such as pathogen-associated molecular patterns (PAMPs) and heat shock proteins with bound antigenic peptides (HSPs). Upper left part of the image is depicting Toll-like receptors (TLRs) specific for different PAMPs.

receptors, which are expressed on the cell surface or in endosomal compartments of innate immune cells. These receptors recognize conserved pathogen-associated molecular patterns (PAMPs), such as double-stranded RNA (TLR3), lipopolysaccharide (TLR4), single-stranded RNA (TLR7/8), or unmethylated CpG motifs present in bacterial DNA (TLR9).[23] PAMP recognition by innate immune cells leads to the activation of different immune pathways, including inflammasome, complement, and/or the nuclear factor κB pathway, which can stimulate the adaptive immune system but may also cause excessive inflammation and toxicity. Therefore, it is critical to carefully select the adjuvant to induce the appropriate type of immune responses to achieve effective vaccination.

Besides pathogen-derived molecules, immunostimulatory adjuvants can be derived from plants. Saponins are steroidal or triterpene glycosides, which can bind to specific carbohydrate receptors on the surface of APCs and promote their activation and production of pro-inflammatory cytokines. Saponins might also interact with cholesterol and facilitate endosomal escape and cross-presentation of antigens and thus activation of CD8 T cells.[24] Saponins containing aldehyde and ketone groups also form imines or Schiff bases with amino groups of receptors on the surface of T cells and serve as co-stimulatory signals for T cell activation.[24] The COVID-19 candidate from Novavax uses Matrix-M, which is nanoparticle adjuvant composed of saponin together with cholesterol and phospholipid, for their protein-based vaccine and achieved high level of antibody production in early clinical trials.[25,26]

Moreover, heat shock proteins with bound antigenic peptides can be utilized as adjuvants to stimulate immune responses.[27] These molecular chaperones enhance both humoral and cellular immune responses by promoting the inflammatory cytokine secretion and facilitating antigen cross-presentation by dendritic cells (DCs) leading to the increased activation of CD8+ T cells.[28]

Immunostimulatory cytokines, such as IL-2, IFN-γ, IL-12, and granulocyte-macrophage colony-stimulating factor (GM-CSF) are also studied for their adjuvant function.[29] GM-CSF,[30] for example, promotes the recruitment, maturation, and antigen presentation by DCs and elicits potent immune responses. Soluble, encapsulated, or conjugated administration of these reagents have been tested so far.

Lately, lipophilic statin drugs and small molecules called bisphosphonates have been discovered to have potent adjuvant activities. Bisphosphonates have been extensively used for the treatment of bone resorption diseases, such as osteoporosis. It is shown that they can also inhibit the mevalonate pathway in APCs,[31] which results in reduced lipidation of small GTPases, prolonged antigen presentation, increased T and B cell expansion, and antibody production.[32] In one study, the incorporation of bisphosphonates in nanoparticles was used to increase the targeting of bone metastatic breast tumors in mice[33]; however, its impact on modulating the therapeutic effects upon its interaction with immune cells has not been explored before.

However, molecular adjuvants can diffuse easily to the blood, which absorbs ten times more fluid than the lymph, to cause systemic inflammation or toxicity. Therefore, these adjuvants are often combined with other (bio)materials, namely nanoparticles or liposomes, to improve localization, safety, and efficacy. The size of the particulate adjuvant is an important factor, which can shape the extent of immune response and the protective efficacy of a vaccine. Small molecules drain to the blood, while particles of approximately 9–100 nm preferentially enter the lymphatics and can get directly to the lymph node for antigen presentation. On the other hand, larger particles (0.5–2 μm) need to be transported to the lymph node by other cells, such as macrophages.[34] These size limits, however, can be altered by the mechanical properties of the particles. It has been shown that the optimal size for the efficient lymph node uptake is around 50 nm for rigid nanoparticles, while for liposomes it is 150–200 nm.[35] Moreover, the size of immunomodulatory compounds can affect receptor crosslinking on the surface of immune cells or alter the uptake and intracellular processing of the antigen.

Besides the size, the particle charge can affect the immune cell responses. Positively charged particles are more internalized by APCs compared with neutral or negatively charged particles, and are able to induce higher innate and adaptive immune reactions.[36] Moreover, positively charged particles increase the antigen escape from endosomes and consequently cross-presentation of the antigen by APCs to CD8 T cells.[37]

For a long time, alum (aluminum hydroxide and aluminum phosphate) was the only approved adjuvant in the USA. These nanosized crystals can adsorb antigens and aggregate into larger gel clusters upon hydration.[38] The binding of the antigen to alum particles is required for optimal immune responses. This mechanism is based on the electrostatic interaction of negatively charged antigen to the positively charged aluminum hydroxide as well as ligand exchange reactions between antigen phosphate groups and alum hydroxyl groups.[39] Moreover, adsorption of antigen to alum particles slows the antigen intracellular decay and thus prolongs the presentation by APCs.[40] Alum adjuvant ability is often attributed to the establishment of an antigen depot; however, the induction of local production of pro-inflammatory factors, which recruit neutrophils, monocytes, DCs, and macrophages, seems to be the main mechanism of action.[41]

Oil-in-water nano-emulsions, such as MF59, which is composed of small squalene oil droplets (around 160 nm in diameter) stabilized by two non-ionic surfactants Span 85

and Tween 80, can elicit even stronger immune responses than alum. The MF59 immune stimulatory capacity relies on the fully formulated emulsion to recruit and activate APCs, as any of the individual components alone were not able to induce comparable immune responses.[42] Liposomes are another common type of particulate adjuvant, which can enhance immune responses even more robustly than the oil-in-water formulations. For example, the adjuvant system AS01, which can induce strong humoral and cellular immunity, is composed of liposomes of 50–100 nm in diameter from dioleoylphosphatidylcholine, cholesterol with TLR4 agonist monophosphoryl lipid A (MPLA) (a detoxified derivative of lipopolysaccharide), and a saponin QS21. Cholesterol is included in the formulation mainly to reduce the cytotoxic activity of QS21, which would otherwise make holes in cell membranes.[43]

Chitosan produced by partial deacetylation of the natural polysaccharide chitin, can also be utilized as an adjuvant, vaccine stabilizer, or delivery system.[44] This positively charged polymer has strong mucoadhesive properties and exhibits a range of immunological effects from the stimulation of inflammasome to enhanced antibody production and T cell responses. It acts through the binding to cell surface receptors, including macrophage mannose receptor and TLR-2. Internalized chitosan induces mitochondrial stress, the production of reactive oxygen species, and subsequent release of the mitochondrial DNA to the cytosol. This process activates the STING pathway, which responds to the presence of DNA in the cytosol, to induce innate and adaptive immune responses.[45]

Microparticles composed of plant-derived polysaccharide delta inulin with alginate trigger complement activation and, when co-administered with antigen, help mount a robust antigen-specific adaptive immune response consisting of both antibody- and cell-mediated immunity.[46]

Short synthetic peptides, which can self-assemble into long nanofibers, can also be used as adjuvants when coupled to antigenic peptides. The density of T and B cell epitopes displayed on the fibrils can be adjusted to raise optimal adaptive immune responses with minimal local inflammation.[47] This nanofiber vaccine can be administered intranasally to promote expansion of tissue-resident immune cells.[48]

Route of vaccine administration and targeting

The level of immune responses toward vaccination can also be significantly affected by the route of administration. While most vaccines are injected intramuscularly, subcutaneous delivery with microneedle patches and pulmonary delivery with ventilators are promising alternatives (Figure 4). Biodegradable or dissolvable microneedles provide minimally invasive transdermal delivery and can be as effective as the conventional injection for influenza.[49] Microneedle-based delivery of hepatitis B and influenza vaccines, prepared with silicon crystal or gelatin formulations, respectively, are currently under clinical evaluation.[50] There are recent reports on developing SARS-CoV-2 vaccines that utilize microneedles to deliver spike proteins in mice.[51] Microneedle platforms can be fabricated using low-cost and scalable manufacturing techniques and may be suitable for global self-administration. This would be a convenient way to distribute vaccines for pandemics, such as COVID-19, if the mass production of a formulation can be achieved. Moreover, pulmonary administration empowers respiratory mucosal immunization and can be achieved using a wide range of mucoadhesive nanoparticles. Nasal delivery of inhalable nanoparticulate powders is recently gaining research attention, particularly in vaccine applications, systemic drug delivery for the treatment of pain, and non-invasive brain targeting.[52] Interestingly, recent work has adapted this technology to deliver

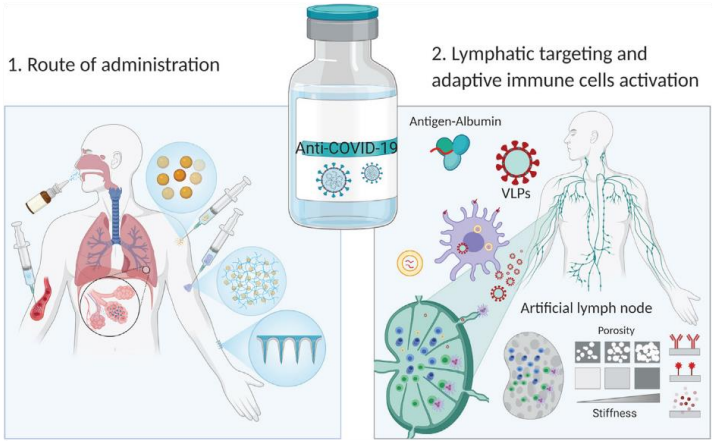

Figure 4. Biomaterials platforms to boost the immunity

A variety of vaccination techniques can be used to improve patient compliance as well as immunization efficacy. Nasal, pulmonary, intravascular, and subdermal immunizations can be performed through the use of nano- and microparticles, hydrogels, and microneedles. Biomaterials-based engineering strategies can be used to develop more effective vaccines. Particulate vaccines can be designed to drain efficiently to lymph nodes. Alternatively, the hydrogel/scaffold vaccine can act as temporary artificial lymph nodes to provide niches for immune cell programming.

therapeutic peptides, which demonstrates feasibility for the delivery for antigen peptides.[53] The ability to train the immune system at the site of viral entry may be very promising for acute or chronic respiratory infections. In this scenario, T cells can better home to both the lung interstitium and airway lumen, whereas intramuscular immunization-activated T cells are not due to entrapment within the pulmonary vasculature.[54] Some studies have also shown the benefits of having local presence of immune cells at the mucosal layer. For example, pulmonary delivery of tuberculosis vaccine increases antigen transport to draining lymph nodes and elicits antigen-specific mucosal memory.[55]

Lymphatics targeting. The lymphatics system is where immune cells are transported and memory cells are generated. Targeting the secondary lymphatic organs, such as spleen and lymph nodes, can improve the efficacy of a vaccine and provoke desirable immune responses. To achieve required spatiotemporal delivery and presentation of antigens and immunomodulatory cues, biomaterials can be designed to enhance lymphatic targeting and generate desirable populations of immune cells with minimal off-target side effects (Figure 4). Biomaterials can be engineered with physical and chemical properties, such as particle size, charge, shape, composition, and even more complicated stimuli-responsive designs.

Simple targeting to draining lymph nodes depends largely on particle size, while more sophisticated complexes are required to integrate into endogenous lymph transport processes.[56] One approach is to utilize carrier proteins, such as the endogenous and most abundant serum protein albumin for longer circulation, improved stability, and better immunogenicity. Modifying vaccine adjuvant CpG oligonucleotides with a lipophilic albumin-binding tail can spontaneously form micelles, which can hitchhike albumin. Combined with the conjugation of an antigen peptide to an albumin-binding domain, this strategy increases lymph node accumulation and

shows 30-fold increases in T cell activation.[57] Instead of albumin hitchhiking, the direct fusion of an antigen peptide to albumin reduces systemic circulation and improved proteolytic stability, as fused proteins traffic to the lymph nodes or are captured by local APCs.[58] With optimized factors, this approach improves vaccine immunogenicity by up to 90-fold and maximizes the responses to viral antigens.[58] SARS-CoV-2 proteins or peptides can be modified with an albumin-binding domain or fused to a carrier protein for lymph node targeting. Elicio Therapeutics repurposed this type of platform and showed an improvement in SARS-CoV-2-specific cellular and humoral immune responses in mice.[59]

Optimal activation of humoral immune responses also relies on appropriate antigen presentation to B cells.[60] To enhance B cell receptor engagement, lipid-based particles can be used as the base platform with the addition of MPLA as an immunostimulatory adjuvant. As simple liposomes are relatively fragile, methods have been developed to extend the lifetime and stability of synthetic vesicles. Polymeric cores of poly(lactide-co-glycolide) (PLGA) enveloped by PEGylated phospholipid bilayers provide support for the lipids and trigger strong antigen-specific immunoglobulin production.[61] Another approach was to engineer interbilayer-crosslinked multilamellar vesicles (ICMVs). These vesicles benefit from stabilized lipids due to the crosslinking of head groups of adjacent lipid bilayers. These ICMVs loaded with antigen cargos are slow to degrade in serum but are susceptible to lipase within intracellular compartments, thus inducing potent T cell and antibody responses.[62] Another category of vesicles to achieve organized antigen presentation is self-assembling nanoparticles. An early study using the glycoprotein of vesicular stomatitis virus (VSV-G) as an antigen has indicated that B cells respond promptly to highly organized VSV-G but are unresponsive to a poorly organized form of the same antigen.[63] Recently, self-assembling melittin-lipid nanoparticles were developed for lymph node targeting, which elicited activation of APCs in lymph nodes and led to a 3.6-fold increase in antigen-specific $CD8^+$ T cell responses compared with free melittin.[64] Moreover, inspired by viral self-assembling envelope and capsid proteins, virus-like particles (VLPs) arrange immunogens in organized arrays on multivalent nanoparticles. Highly organized display platforms utilize symmetric cage-forming macromolecules, such as enzyme lumazine synthase, ferritin, or self-assembling nanoparticles, to form oligomers.[65] Unlike monomeric antigen, VLPs made of HIV envelope trimer (gp140 trimer) and glycoprotein 120 (gp120) were shown to increase shuttling to follicular DCs (FDCs), concentrate at germinal centers, and enhance B cell activation.[66] The glycosylation helps antigen uptake through an innate immunity-mediated recognition pathway.[66] In addition, more sophisticated nanostructures, such as DNA origami nanoparticles, have been recently designed for nanoscale antigen presentation. Antigen copy number, spacing, affinity, dimensionality, and rigidity of the scaffold were optimized for HIV gp120 to drive functional B cell responses.[67] Furthermore, another research group has used the receptor-binding domain of Middle East respiratory syndrome coronavirus (MERS-CoV) fused with RNA interaction domain and ferritin to construct a self-assembling, protein-folding vehicle.[68] Such VLPs can also be designed with SARS-CoV-2 protein components for the optimal vaccination.

These approaches will provide tools for rapid clinical translation of potent and tissue-specific platforms for modulating pathogen-specific immunization. Recent pioneering work highlights the importance of materials design on nanoparticle-based antigen-delivery platforms to generate specific T cell responses.[69] For instance, the presentation of the same antigen (ovalbumin; [OVA] peptide) using two nanoscale delivery platforms can regulate distinct T cell fates in mice. In this case,

redox-sensitive poly(ethylene glycol)-poly(propylene sulfide) (PEG-PPS) block copolymers as components of a nanocarrier platform. Interestingly, the immobilized presentation of OVA peptide can differentiate naive T cells toward antigen-specific killer (CD8+) T cells, while the intracellular release of the same peptide via PEG-PPS nanoparticles can push T cells toward activated helper (CD4+) T cells. Helper T cells are crucial for cellular immunity as they can provide long-term memory against target antigens.[70] These results demonstrate the importance of material design and highlight the potential of using nanoscale biomaterials to engineer antigen-delivery systems for the induction of desirable T cell responses.

Last but not least, targeting lymph nodes for efficient B cell activation could be through a multistage delivery process. While there is a size preference for lymph node drainage, nanoparticles are still too big to access intra-lymph node canals. Therefore, combinations of nanoparticles and the controlled release of small-molecule cargos via programmed degradable linkers creates a two-step platform to deliver molecules inside the lymph reticular network.[71] Such advanced delivery platforms are able to consider the physiological location of certain immune responses and indicate a path to precision medicine.

Biomaterials as artificial lymph nodes. Besides developing particulate platforms to target secondary lymphoid or immunocompetent tissues, biomaterials can be used to create temporary lymph node-like depots to induce immunity against viral infections. Such a platform should be implantable via either injection or surgical placement, while being biocompatible with a controlled biodegradation rate. These macroscale therapeutic devices can be placed at target sites to precisely manage the presentation of antigens and adjuvants, lower required dose to reduce cost, improve therapeutic efficacy, and limit systemic exposure. The main function of such a construct will be the recruitment of adaptive or innate immune cells and education against target antigens. This platform can provide polyclonal activation and the expansion of immune cells to enhance immunogenicity or present specific antigens to induce a more specific immune response. With a grasp of the aspects that affect immune cell function *in vitro*, researchers have tried to focus more on designing 3D niches that offer better mimicry of the immunomodulatory signals. For example, 3D biomaterials have recently been proposed for the *in vivo* modulation of host immune cells.[72] Among various organic- or inorganic-based biomaterials, mesoporous silica-based vaccines represent a promising and versatile platform to present viral antigens, induce immune cell activation, and promote prolonged antibody production, as exemplified in the elegant work that highlights the development of mesoporous silica rod-based pore-forming platforms for *in situ* modulation of host immune cells as a vaccine against infectious diseases.[73] Soft biomaterials, including hydrogel scaffolds, can also offer a versatile platform to deliver a wide variety of therapeutics. High levels of biocompatibility, tunable physicochemical properties, controlled release, and tunable degradation profiles are among the promising characteristics of polymer-based hydrogels. In this context, injectable hydrogels and hydrogel microparticles may be more promising as they can be administered (injected) without surgical implantation. Cryogels and *in situ* pore-forming hydrogels can be used to provide interconnected micropores for the training of immune cells against target antigens. Although these materials are under development for cancer immunotherapies, a simple manipulation of formulations can repurpose these platforms for applications in infectious diseases.

Other than injectability and porous structures, several other criteria, including delivery mechanisms and release rates for each encapsulated immunological

biomolecule, should be considered when developing biomaterial-based vaccines to improve the therapeutic outcomes. Control over the temporal presentation of these molecules can be achieved by tuning the physical (e.g., charge, mesh size, and tortuosity) or chemical (e.g., degradation and bioconjugations) properties of engineered biomaterials. Considering the charge associated with most of antigens and adjuvants, charged polymers can be utilized to enhance the retention of immunological biomolecules. Similar approaches may be used to deliver small-molecule inhibitors but through hydrophobic-hydrophobic interactions. Incorporation of certain chemokines or cytokines can benefit from enhanced affinity through specific interactions with engineered peptide sequences[74] or polysaccharide like heparin.[75] Such an interaction may not only increase the retention, but also increase the biological stability of these proteins.

Mechanical properties of biomaterials are also critical as they can dictate the mobility, activation, and proliferation of recruited immune cells. Under pathological conditions, tissue stiffness increases during the viral infections, which naturally enhances T cell activation and antiviral effects. This process is mediated by changes in the structure, density, and composition of the extracellular matrix (ECM) in the infected tissues as well as in the draining lymph nodes. Experimental observations confirm the stiffening of lymph nodes in rodents from 4 to 40 kPa upon viral infection by lymphocytic choriomeningitis virus (~40 kPa).[76] This distinct stiffness can be replicated using synthetic biomaterials to provide optimal and biologically relevant activation signals for T cells.[77] Designing tissue-inspired biomaterials can help to provide an immune cell-specific microenvironment to ensure prolonged humoral and cellular immunity. The role of specific materials properties, in addition to the release profile, are being investigated when developing biomaterial-based vaccines. The creation of biomaterial-based cell homing sites that can act as a temporary lymph node with similar biological and biophysical signals can moderate the recruitment, residence, training, and fate of immune cells. This may promote immune responses to establish long-term immunity against COVID-19 or other infectious diseases.

Delivery of immunotherapy

Current treatments

The challenge of COVID-19 treatments, among other viral infections, is the balance between antiviral (preventing viral replication, expediting viral clearance, and boosting immune responses) and anti-inflammatory therapies (preventing the exacerbation of a cytokine storm that can lead to systemic complications).[78] Repurposed malaria drugs that interfere with viral entry and propagation, such as hydroxychloroquine, are under investigation for effectiveness again COVID-19. For immunomodulation, antibodies against inflammatory signals (IL-6, IL-1, and IL-2), Janus kinase pathway inhibition, intravenous immunoglobulins, and corticosteroids are under investigation.

Prophylactic anticoagulation treatment with low-molecular-weight heparin (LMWH) is currently recommended to prevent thrombotic complications.[79] However, some COVID-19 patients still developed thrombosis despite prophylaxis with LMWH.[80] Therefore, anti-complement drugs, such as narsoplimab (monoclonal antibody against MASP-2)[81] or eculizumab (monoclonal antibody that blocks complement protein C5)[82] have been tested and showed promising results in reducing endothelial damage and thrombotic risk.

The treatments that are currently under evaluation in clinical trials have been covered in recent reviews.[83] However, these platforms are typically delivered systemically, making the balance between viral clearance and prevention of overactive

immune responses difficult. Combinations of known and clinically approved therapeutics with material- and/or cell-derived components may serve to enhance treatment efficacy through localized delivery and tuned mechanisms. In this way, antiviral or immunotherapeutic regimens can be based on disease trends, such as accumulation in tissues with high ACE2 expression or tissue-specific disease states.

Targeted drug delivery to lung and cardiovascular system

The direct targeting of sites of high virus titers and immune cell accumulation should be able to enhance the antiviral effects and immunomodulation of existing therapies. Even though COVID-19 is primarily a respiratory disease, the sites of infection are not limited to the lungs. The impairment of cardiovascular function and various coagulation disorders in COVID patients are a result of the wide distribution of ACE2 receptors and expansion of viruses within the endothelium and vascular smooth muscle cells.[84] Here, we focus on the strategies to target drug delivery to the lung and cardiovascular systems that are typically inflamed as a result of a SARS-CoV-2 infection.

Firstly, biomimetic particles modified with targeting ligands or antibodies against adhesion molecules expressed on the inflamed tissue can be used for specific drug targeting. The ability to tailor the activity of the immune system, both activation and reduction, may prove efficacious in viral clearance and preventing tissue damage. These techniques are not directly related to the delivery of immunotherapies; however, the modularity of peptide or protein modifications can be easily adapted for novel therapeutic strategies. To resolve inflammatory signaling of blood vessels, one approach involves the delivery of antioxidant enzymes. The delivery of these enzymes alone lacks stability and targeting to achieve functionality at the site of inflammation. To solve this issue, an antioxidant mimetic (EUK-134) may be loaded into PEGylated liposomes conjugated to anti-PECAM-1 antibodies to improve drug stability and specifically target pulmonary ECs; this biomaterial formulation retained enzyme functionality, enhanced desired lung biodistribution, and protected against pulmonary vascular edema in a lipopolysaccharide-induced mouse injury model.[85] Lungs are highly inflamed during ARDS so the local environment is usually acidic and populated with adhesion molecules, such as intercellular adhesion molecule-1 (ICAM-1), to attract monocytes and lymphocytes. It has been reported that the use of anti-ICAM-1 antibody-coated poly(β-amino ester)/PEG nanoparticles enhances lung targeting and can release anti-inflammatory agents.[86] In this formulation, the incorporation of acid-sensitive poly(β-amino ester) domains enables pH-dependent release of drug cargo within acidic, inflamed lungs, which improves the efficacy of TPCA-1 treatment in a murine acute lung injury model, compared with free drug or untargeted drug-loaded nanoparticles. Other strategies to target inflamed vasculature include the conjugation of integrin LFA-1L domain, which binds to ICAM-1, or antibodies against E-selectin to the surface of particles or liposomes (regardless of drug cargo or material).[87] Alternatively, targeting ligands can be replaced with peptides, such as VHPKQHR[88] for VCAM-1-binding or cyclo(1,12)PenITDGEATDSGC (cLABL) peptide for high-affinity ICAM-1 binding.[89] Similar targeting strategies can be utilized to selectively deliver thrombolytic agents to treat thrombosis and embolism. For example, a modified fibrin-homing peptide (allyl-GGCR(NMe)EKA) has been used to target microenvironment-sensitive nanogels to the blood clots.[90] The acrylamide nanogels contain thrombin-sensitive cross-linkers, which enabled high intra-clot release of encapsulated thrombin inhibitor hirudin. These nanogels showed increased circulation time and bioavailability compared with hirudin alone and were able to efficiently prevent and inhibit clot formation in mouse models of pulmonary embolism and thrombosis. Another strategy

for targeted drug release is based on the increased concentration of hydrogen peroxide by activated platelets at the site of thrombus formation. H_2O_2-responsive boronate particles show site-specific release of an anti-platelet drug and potent thrombolytic and anti-inflammatory activity without adverse side effects.[91] Further approaches in biomaterial design for thrombosis can be found in a recent review.[92] The lungs possess a unique characteristic of dense capillary networks, which are quite narrow and can only pass one red blood cell (RBC) at a time. Attachment of synthetic nanoparticles onto RBC surface creates a cell hitchhiking platform where nanoparticles are sheared off when squeezing through these narrow capillaries.[93] Non-covalent attachment of nanoparticles to RBCs increases lung accumulation while reducing uptake in other organs, such as liver, spleen, and brain.[94] If combined with anti-ICAM-1 strategies, lung retention of nanoparticles is further improved.[95] Interestingly, by tuning the affinity of nanoparticles to RBCs and making them shear resistant, the target site can be shifted to the spleen where lots of APCs reside. Erythrocyte-driven immune targeting has been developed as a vaccine platform, where erythrocytes deliver antigens selectively to the lung or spleen tissues.[96] This process mimics the natural capture of pathogen by erythrocytes and may not need additional adjuvants to elicit a strong immune response.[96]

Finally, the capacity of SARS-CoV-2 to infect the heart necessitates cardiac tissue targeting for treatments. The use of a cardiac-targeting peptide (CTP)[97] and the CRPPR peptide[98] enhance the delivery and retention of an imaging agent or liposomes, respectively. In addition, a CTP fused to a membrane protein of extracellular vesicles (EVs) improves cardiomyocyte cellular uptake *in vitro* and demonstrates enhanced retention following intramyocardial injection.[99] For protein therapeutic delivery, tannic acid modifications induce aggregation and enhance cardiac tissue accumulation of peptides, viruses, and proteins following intravenous injection; an intravenous treatment of modified basic fibroblast growth factor (bFGF) promotes cardiac recovery, compared with a direct injection of unmodified bFGF, in an *in vivo* model of myocardial ischemia.[100] The presence of markers of tissue damage can also be used as a signal to influence the accumulation of nanoparticles. In one approach, polynorbornene nanoparticles with incorporated MMP-2 and MMP-9 recognition peptides, preferentially aggregate based on matrix metalloprotease (MMP) activity. This interesting approach uses particles <100 nm that can diffuse through leaky vasculature to sites of myocardial damage but do not typically persist within the tissue for long periods of time. The programmed accumulation enables localization and retention up to 28 days at the site of tissue injury.[101] Since MMPs are present during the remodeling phase following acute injury and may be involved in SARS-CoV-2 infections, they may potentially serve as a target to deliver antiviral or immunomodulatory compounds.[102]

Cell-derived drug delivery systems to modulate inflammatory response

Neutrophils, the most abundant white blood cells in the body, reside in high numbers in the lungs and are the first line of defense against invading pathogens. Upon encountering danger signals, neutrophils quickly migrate to the targeted tissue and release immunomodulatory molecules, which recruit and activate other immune cells. They also internalize pathogens and destroy them in organelles called phagosomes. Moreover, neutrophils can eliminate the invaders by releasing reactive oxygen species and granules containing enzymes and antimicrobial peptides or they can prevent the spreading of pathogens by ensnaring them in web-like structures of DNA and proteins named neutrophil extracellular traps. However, the accumulation and excessive activation of neutrophils, as in case of ARDS in COVID-19 patients, can lead to exacerbated tissue damage and increased risk of thrombosis.[103,104]

To mitigate acute inflammation, activated neutrophils can be selectively targeted with nanoparticles containing agglutinated[105] or denatured proteins,[106] which bind to Fcγ RIII receptors on activated neutrophils.[107] The feasibility of this approach is demonstrated with nanoparticles made from denatured albumin loaded with an anti-inflammatory drug, which are preferentially internalized by activated neutrophils. In contrast, nanoparticles coated by natural albumin are ignored by neutrophils. This highlights the importance of nanoparticle design on generating specific immune responses.[108] Particulate therapeutics can also be used to suppress neutrophil recruitment and accumulation in inflamed tissues. Intravenously injected microparticles can be phagocytosed by circulating neutrophils, which triggers their apoptosis and elimination by the liver. Alternatively, particles captured in the liver and internalized by resident macrophages recruit circulating neutrophils.[109] In both cases, the administration of particles during acute inflammation can decrease the numbers of circulating neutrophils and/or change their homing site, which might be a useful strategy to mitigate inflammation.

In another strategy, cells can be equipped with "cellular backpacks," polymeric particles loaded with therapeutic agents, that can be attached to the cell membrane with the use of antibodies, cell-adhesive molecules, or by covalent binding to cell surface proteins.[110] The size and shape of polymeric particles can significantly affect cellular backpack stability, because flat disk-like particles are phagocytosed less than spherical particles.[111] In this way, immune cells, such as monocytes,[112] can be utilized to deliver cargo into inflamed tissues. Furthermore, particulate drug delivery systems can be coated with cell membranes derived from different cell types, including platelets[113] or neutrophils,[114] which help reduce their immunogenicity and improve inflammation-targeting capabilities. RBCs and platelets can be fused to create hybrid membrane-cloaked nanoparticles, which show increased circulation half-life and improved homing to inflamed tissues owing to intrinsic RBC and platelet components, respectively.[115] Although adding such a feature seems interesting as it can represent the most natural biointerface, the translational and regulatory pathways appear unclear.

Besides coating nanoparticles or liposomes with cell membranes, EVs secreted by different cell types can be used to deliver drugs and vaccines, introduce targeting, or enhance regeneration. EVs are nanometer-sized phospholipid membrane-enclosed vesicles that contain bioactive components, such as nucleic acids or proteins derived from their parental cells. Based on their surface markers, EVs can be preferentially internalized by distinct cell types and tissues comparably with the membrane-coated biomimetic particles.[116] Among the most studied EVs with pro-regenerative properties are vesicles derived from mesenchymal stem cells (MSCs). These EVs have powerful immunomodulatory effects, which can be beneficial in the treatment of various inflammatory diseases, including ARDS.[117] Moreover, EV content can be further engineered to improve the therapeutic effects. This can be done by decorating EVs with antibodies/targeting ligands or loading them with various therapeutics. Passive loading by co-incubation is suitable mainly for hydrophobic drugs, which can efficiently penetrate the lipid bilayer. On the other hand, active loading techniques, such as electroporation, sonication, co-extrusion, repeated freeze–thawing, or saponin permeabilization, can be advantageous for intermediate or hydrophilic drugs.[118] EV content can also be modified through the genetic engineering of EV-secreting parental cells. For example, EV-targeting efficiency can be increased by fusing targeting peptides or proteins with the C1C2 domain of lactadherin, which binds to phosphatidylserine that is strongly enriched in EV membranes.[119] The EV circulation half-life can be prolonged by overexpressing CD47,

presenting a "don't eat me" signal, which can protect EVs from being phagocytosed.[120]

In addition to micro- and nanoparticles, artificial cells can be utilized to perform more complex regenerative or immunomodulatory tasks. For instance, artificial neutrophils have been prepared by encapsulating zeolitic imidazolate framework-8 particles with incorporated glucose oxidase and chloroperoxidase within a neutrophil membrane. Thanks to the neutrophil membrane composition, artificial neutrophils are efficiently recruited to the sites of inflammation, where they convert glucose with the use of glucose oxidase to gluconic acid and H_2O_2. Chloroperoxidase transforms these products into highly reactive HClO which can eradicate infections.[121] Another strategy engineers synthetic MSCs to mimic and apply inherent cell properties. PLGA microparticles are loaded with bioactive factors typically secreted by MSCs and coated with MSC membranes. These synthetic MSCs demonstrate regenerative potential and cryopreservation and lyophilization stability.[122] Alternative biometric designs have implemented super-soft alginate microgels to mimic the shape, mechanical properties, and surface composition of naive and activated T cells.[123] Such a platform has been developed to offer a synthetic tool to investigate the effects of inflammatory cytokines on the fate of MSCs *in vitro*.

Finally, synthetic biology tools can be used to engineer biosensor cells to execute *de novo* antiviral actions. This approach has been explored by utilizing modular chimeric synNotch receptors, which are composed of engineered extracellular receptors specific to the desired antigen, and an intracellular transcription module, which can be tailored to generate user-defined cellular responses. These cellular biosensors can be programmed to secrete IFN-β or neutralizing antibodies as an output reaction to the binding of the membrane-bound viral antigen to the extracellular region of the synNotch receptor. Through the genetic engineering process, these cells can mimic, to some extent, the immune cell responses required to suppress infections.[124]

Immunomodulation for the healing and regeneration of tissues and organs

In the previous sections, we discussed the prevention of SARS-CoV-2 viral infection with vaccine supplements and the approaches to enhance viral clearance and mediate inflammatory-related symptoms at a systemic and tissue-specific level with immunotherapies. However, the long-term pathological effects of SARS-CoV-2 infection and the potential to exacerbate or induce future complications, even in mild cases, are just beginning to be explored.[125] A high correlation of symptom severity and mortality in patients with preexisting conditions sheds light on the potential risks of organ trauma. A buildup of fibrotic scar tissues causes many of the leading cardiac and pulmonary diseases, and COVID-19-induced tissue damage may contribute to their exacerbation. The extent, location, and duration of potential tissue damage, as well as the risk of future complications, resulting from COVID-19 infection must be understood and treated accordingly to prevent future trauma in this extensive patient group.

To accomplish this, tissue damage resulting from COVID-19 infection and treatments can be retroactively understood through patient characterization and long-term follow-up; however, this information may not be available in a timely manner. Interestingly, tissue models may be adapted to predict at-risk organ systems, determine the mechanism of pathogenesis, and screen potential therapies in a high-throughput fashion. In this section, we seek to address the long-lasting damage at a tissue-specific level and identify potential post-COVID treatments, specifically

immunomodulatory biomaterial compositions that may support healing and prevent future complications. Several previously developed strategies demonstrate the key role of biomaterials for the targeted and responsive delivery of therapeutic molecules, co-localization of multiple factors, and the induction of specific immune response with relevance for COVID-19 therapeutic development.[126] We focus on the respiratory, cardiovascular, and nervous systems as they represent the primary and more severe long-term tissue damages in COVID-19 survivors. While our discussion focuses on immunomodulation for tissue healing and regeneration, many other widely explored tissue engineering approaches utilizing cell transplantation, scaffold engineering, and drug delivery can also be applied and combined with immunotherapeutic strategies.[126,127]

Respiratory system

Viral infections induce acute and chronic inflammation that significantly impact lung function, leading to pneumonia and ARDS. Following minor injury, lung epithelium possesses endogenous repair mechanisms, through activated epithelial cell proliferation, that serve to regenerate functional tissue structures. However, severe and extended inflammatory environments (in COVID-19 pneumonia and ARDS) preferentially induce apoptosis in epithelial cells. In these conditions, fibroblasts and inflammatory cells are more likely to dominate the remodeling process and replace damaged tissues with collagen-rich scars that have limited functionality.[128] Pulmonary fibrotic scarring and impacted lung function significantly reduce the quality of life and are present in up to 85% of ARDS survivors.[129,130] Previous clinical data from the SARS outbreak indicate that lung function remains abnormal for up to 3 years following infection. In a different follow-up study, a small group of patients demonstrate that SARS-induced lung scarring persists for up to 15 years after infection.[131]

The extent of prolonged lung dysfunction for COVID-19 survivors has begun to be evaluated, and is expected to pose major issues.[132] The presence of lung abnormalities scales with disease severity and persists even after the treatment and the resolution of symptoms.[133] In addition, a study in April 2020 detected the presence of lung abnormalities via computed tomography scans in asymptomatic COVID-19-positive patients.[134] This troubling discovery indicates the possibility that those unknowingly exposed to COVID-19 and asymptomatic may develop pulmonary fibrosis. An accumulation of scar tissue can lead to significant problems as it contributes to irreversible interstitial lung disease.[135] From the growing clinical insight, it is clear that strategies to address pulmonary scar tissue accumulation and support the restoration of functional tissue are required. Several tissue model systems have been developed to recapitulate key aspects of the respiratory system, such as the air–liquid interfaces and differentiated cell types, and have been characterized for COVID-19 infection.[136,137] Integration with *in vitro* models of fibroblast-mediated scarring[138] may serve to better understand COVID-19-induced fibrosis and evaluate potential therapeutic agents to properly heal scar tissues.

The design criteria of potential tissue-regenerative immunomodulation should reduce chronic fibrotic signaling, reverse scar tissue formation, and restore functional lung tissue. Components of previously reported biomaterial-mediated pulmonary fibrotic treatments may serve as ideal candidates. Anti-fibrotic and anti-inflammatory therapeutics, such as pirfenidone and nintedanib, repurposed from idiopathic pulmonary fibrosis, are already under evaluation for the prevention of COVID-19-induced scarring.[130,139] These treatments target fibroblast proliferation, collagen deposition, and TNF-α/IL-1β pro-inflammatory signaling. In addition, modulation of immune mechanisms, specifically blocking fibrotic fibroblast-immune cell

signaling motifs (CD47 or PD-L1) and cytokines (IL-6 or IL-11), have been implicated for the prevention and reversal of pulmonary scarring.[18,140] Like previously mentioned approaches, the use of biomaterials as delivery vehicles can enhance the efficacy, localization, and retention of delivered therapeutic molecules compared with a systemic delivery. Drug–material formulations can be tailored to achieve novel delivery mechanisms and desirable release rates, with a reduction of systemic side effects. In one approach, the encapsulation of pirfenidone within modular interpenetrating polymeric network microspheres is sufficient to achieve a more therapeutically desired controlled release profile following oral delivery, compared with the clinically available Pirfenex.[141] In another example, the internasal delivery of IL-10 via hyaluronan and heparin-based hydrogels further decreases inflammatory and fibrotic markers in a bleomycin-induced pulmonary fibrosis mouse model, compared with the delivery of IL-10 alone. This formulation combines the biocompatibility and biodegradability of hyaluronan with the ability of heparin to bind IL-10 to enhance stability and extend the release rate. Interestingly, positive results of the hydrogel–IL-10 treatment as both a preventive and treatment of fibrosis were demonstrated.[142] Biomaterials can also be used to deliver and retain cellular therapeutics within the lungs, with and without active targeting motifs. In a recent example, MSC-laden alginate-based microgels demonstrated enhanced circulation time following intravenous injection and, as seen in most intravenous cellular applications, accumulated within the lungs.[143] MSCs, in particular, have potent immunomodulatory potential and have already been identified for a potential role in COVID-19 therapeutics.[144,145] Alginate networks allow for the diffusion of soluble inflammatory cues into the microgels to induce intrinsic anti-inflammatory stem cell secretion while also protecting against rapid immune clearance.[143] As previously mentioned, cell-based backpacks, based on the homing of specific cell types to fibrotic markers, can also be used to deliver therapeutic payloads to reverse fibrotic scarring.[146] In this study, drug-loaded PLGA/PEG nanoparticles were conjugated to monocytes, which demonstrated MMP-2-induced release and lung injury homing, respectively. This formulation incorporates a multistage targeting and release cascade through specific cell or peptide conjugation to explicitly induce the internalization of astaxanthin/trametinib-loaded nanoparticles within injured alveolar epithelial cells to reverse fibrosis.

Cardiovascular system

As a result of viral infection, cytokine storm, or antiviral treatments, both cardiac tissue and the vascular system may suffer from lasting damage. In cases of a direct viral infection of the heart, a chronic immune response is the main contributor to the degradation of the ECM and induction of fibrosis.[147] Fundamentally, intrinsic heart healing is limited by the lack of cardiomyocyte proliferation and active remodeling processes.[148] Recent reviews have covered the specific mechanisms of COVID-19-induced cardiac damage and risks of long-term damage.[149] The prevalence and unknown duration of cardiovascular complications associated with COVID-19 represents an unmet clinical need; elevated levels of troponin, indicating the presence of acute cardiac injury, were found in 20%–30% of hospitalized COVID-19 patients.[150] Cardiac swelling, scarring, reduced ejection fraction, and high troponin T levels remain even after COVID-19 recovery.[151] Initial studies have identified that markers of cardiac damage and inflammation can last up to at least 10 weeks after initial diagnosis.[152] These symptoms are indicative of more severe complications, namely heart hypoxia, myocarditis, arrhythmias, and eventual heart failure.

Approaches to support the restoration of damaged cardiac tissue following the resolution of a COVID-19 infection are required to reduce the risks of developing chronic conditions. Myocardial infarction treatments that prevent sustained

inflammation-mediated tissue damage and support functional ECM production can potentially address the needs of COVID-19 patients. However, the timing of treatment (presence/absence of viral particles) and mechanism of damage (viral or immune mediated) may affect the immunomodulation required. The localized delivery of anti-inflammatory factors, TIMP-3, IL-10, IL-2, and IL-19, via biomaterial carriers dictates cellular recruitment and survival to improve the extent of healing and regeneration.[153] One example utilizes a poly(ethylene argininylaspartate diglyceride) and heparin coacervate to locally co-deliver FGF-2 and IL-10 with an extended release profile. Intramyocardial injection of this formulation enhances regenerative outcomes following myocardial infarction, compared with free protein or single-protein coacervate delivery.[154] Macrophage polarization toward an M2 regenerative phenotype plays a key role in limiting the extent of tissue damage. In one approach, IL-33 overexpression vectors are delivered intravenously with polyethyleneimine.[155] This delivery mechanism, which utilizes polyethyleneimine complexed with DNA vectors to induce exogenous IL-33 expression, induces specific cell-secreted cytokines as an alternative to cytokine delivery. This treatment enhances the endogenous production of IL-4 and subsequent M2 macrophage polarization to improve myocarditis outcomes in a mouse model. An interesting strategy uses an injectable alginate-based hydrogel to deliver CSF-1 and IL-4 into the heart and demonstrates the potential to promote regenerative macrophages.[156] Recently, the role of B cells in exacerbating inflammation and reducing M2 polarization has been identified;[157] treatments, such as pirfenidone, to address this mechanism may serve as a potential therapeutic.[158] In addition, the role of autoimmunity, in which cardiac proteins can activate and sustain an adaptive immune response, in the context of tissue healing and regeneration has been highlighted.[159] SARS-CoV-2, like other viruses that induce myocarditis, triggers cardiac autoimmunity that prolongs tissue damage, which should be addressed by potential therapies.[160,161] Along these aims, siRNA against CSF-1 is loaded in lipid nanoparticles and delivered intravenously in mouse models of virus- or autoimmune-mediated myocarditis. In both cases, the inhibition of CSF-1 reduces the infiltration of inflammatory monocytes into the heart and is sufficient to lessen the extent of tissue damage.[162] Interestingly, even with a reduced inflammatory response, viral clearance is not hindered.

Immune cells can also promote revascularization of affected tissues. Pro-inflammatory M1 macrophages are important at the beginning of angiogenic process, when they secrete pro-angiogenic factors, such as vascular endothelial growth factor,[163] while M2 macrophages dominate at the later time points when they stabilize blood vessels and promote anastomoses.[164] Thus, immune-instructive biomaterials, which can guide the macrophage phenotype change by sequential release of multiple immunomodulatory factors, might be helpful for vascular regeneration. This strategy was used to promote angiogenesis and regeneration by initial release of IFN-γ followed by prolonged release of IL-4 from a decellularized scaffold.

Apart from macrophages, revascularization of damaged tissues can be enhanced by biomaterials concentrating pro-healing T cell subtypes. Animals previously vaccinated with an antigen and Th2 immune response-inducing adjuvant show enhanced vascularization and regeneration of ischemic tissue after receiving the same antigen released from the biomaterial scaffold, which attracts and concentrates antigen-specific CD4+ Th2 T cells.[165]

Nervous system

Like the aforementioned organ systems, the cells and structure of the CNS is susceptible to viral infection and immunogenic collateral damage.[166] Human brain

organoids have been utilized to characterize the invasion potential of SARS-CoV-2 and identify potential treatments, such as Sofosbuvir.[167] The presence of COVID-19 infection within the CNS induces a wide range of long-term systemic symptoms and risks. Neurological complications resulting from coronavirus infections leads to symptoms, such as fatigue, depression, and musculoskeletal pain that affect quality of life. MERS and SARS follow-up studies identified sustained chronic fatigue symptoms in patients at 12–36 months following the initial infection.[168,169] The risk of direct infection is particularly troubling as viral latency and sustained inflammation is likely. Chronic neural inflammation, namely the overexpression of IL-1, IL-6, TNF-α, IL-1B, and IFN-γ, is associated with demyelination and the progression of neurodegenerative diseases, such as Parkinson and Alzheimer disease.[170,171] The persistence of viral load within the CNS, as documented with other coronaviruses, can trigger or contribute to the development of neurological disorders.[172]

Preventative therapeutics must be developed to prevent the chronic degeneration of the CNS and development of neurological diseases. One possible mechanism of treatment is through the modulation of inflammation to support remyelination. Microglia, macrophages, and T regulatory cells intrinsically support the differentiation of oligodendrocytes to regenerate myelin sheaths.[173,174] In an interesting approach that combines targeting moieties with the delivery of immunomodulatory factors, leukemia inhibitory factor is encapsulated in PLGA nanoparticles with NG2 chondroitin sulfate antibodies. These particles target and stimulate the differentiation of oligodendrocyte precursor cells to mature phenotypes *in vitro* and improve the extent of myelination in an *in vivo* mouse model of CNS degeneration.[175]

CONCLUSIONS AND FUTURE DIRECTIONS

The modulation of immune responses has great potential for the prevention and treatment of infectious diseases, such as COVID-19. However, conventional pharmaceutical interventions lack the spatiotemporal control for robust and precise immune activities. Biomaterials create applicable platforms for enhanced immune responses upon vaccination and targeted and controlled drug delivery, local immunomodulation, and minimally invasive methods for drug administration. Biomaterial-based approaches to guide the immune system to fight viral infections and regenerate damaged tissue can be developed and adopted from other fields, such as cancer immunotherapy and stem cell engineering. Because these platforms are not limited by the type of virus, new combinatorial treatments are valuable in creating more effective treatments for a variety of infectious diseases in any future epidemic or pandemic. Tables 1 and 2 highlight examples of each biomaterial-based approach we discuss in this review for the improvement of preventive immunization, therapeutic treatments, and tissue healing and regeneration. In addition, biomaterials can have broad applications in many other aspects, such as personal protection equipment, diagnosis devices, and organ-on-chip disease modeling.[15]

Regarding COVID-19, there are still more problems to be addressed using immunomodulatory interventions. As the risk for severe illness increases with age, a critical need is the modulation of the immune responses in senior populations. The homeostatic and regenerative capacity of T cells declines with age. Thymic T cell generation, T cell receptor repertoire diversity, and the self-renewing potential of T cell populations reduce throughout the adult lifetime.[176] In addition, coronaviruses often cause reinfections, and it is not clear whether current vaccines are effective in inducing long-term immunity.[177] Therefore, building T memory cell populations via vaccines and promoting effective antigen-specific T cell clonal expansion upon

Table 1. Biomaterials approaches for various issues of COVID-19

Issues	Biomaterial approaches	Biomaterial examples	Refs
Insufficient immune responses	vaccine adjuvants	• ligands for PPRs • plant-derived: saponins • heat shock proteins • immunostimulatory cytokines • bisphosphonates • nanoparticles (alum particles, oil-in-water nano-emulsions, liposomes) • self-assembling peptides	23–48
Immune cells are densely packed in the secondary lymphatic organs Antigen presentation to immune cells	lymphatics targeting artificial lymph nodes	• erythrocyte hitchhiking • albumin hitchhiking or conjugating • lipid-based nanoparticles • self-assembling nanoparticles • virus-like particles • poly(ethylene glycol-poly(propylene sulfide) (PEG-PPS) • mesoporous silica rods • hydrogel scaffolds	56–71 71–77
Primary infection site at lung with high virus titer	lung targeting	• anti-ICAM-1 antibody coated • erythrocyte hitchhiking • pulmonary ventilation	85–96
Excessive inflammation of cardiac tissue/vasculature Thrombosis	cardiovascular targeting	• PECAM-1 and VCAM-1 antibody conjugation • cardiac-targeting peptides (CTP, CRPPR) • tannic acid-induced aggregation • MMP-2/MMP-9 recognition peptides	97–102

infection are potential strategies to address weakened and insufficient immune responses. Furthermore, due to the complexity of T cell interaction with major histocompatibility complexes, immunoinformatic studies using data science and machine learning approaches can facilitate the identification of potential B and T cell epitopes for peptide vaccine development.[178,179]

Besides the special consideration for the elderly population, the replication of viruses and increase in viral burden continually stimulate positive-feedback immune responses. This process may cascade into an overactive immune response that results in fatal conditions, such as cytokine storms in some COVID-19 patients. Biomaterial composition or biomaterial-based drug delivery systems can be engineered with bioresponsive components, which can regulate biological processes and the location, timing, and release profile of drug cargo.[15] Integration of artificial intelligence (AI) at the development stage of biomaterial–drug formations can be utilized to determine optimal configurations for ideal release profiles and maximal therapeutic effects.[180] In addition, AI can be used to expedite the development of the next-generation of immunotherapeutics through better design of biomaterials and predictions of cell-specific interactions, efficacy, or risk of adverse events.[181] The appropriate biomaterial strategy will enable the generation of desired immune responses to prevent or treat cytokine storm. In particular, nanomaterials have been implicated by others for their role in COVID-19 therapy due to their modular drug-loading capabilities, delivery mechanisms, tissue targeting, and symptom relief.[108]

Moreover, the transfer of biomaterial designs from bench to bedside is a practical issue, especially for infectious diseases. The scale-up feasibility and manufacturing costs should be taken into consideration while designing biomaterial products. The complexity and simplicity of a biomaterial solutions should be well balanced to enable both reliable clinical outcomes and easy mass production. In addition, the adaptation of biomaterials and/or drug formulations that have already been used in FDA-approved applications can reduce the regulatory burden and time of

Table 2. Biomaterials approaches toward tissue and organ healing of COVID-19-related issues

Issues	Biomaterial approaches	Biomaterial examples	Refs
Damage of lung tissue (reduced lung function)	anti-fibrotic immunomodulatory therapies	• microparticles for extended release of anti-inflammatory agents • hydrogel delivery platforms (hyaluronan) • cell-laden alginate microparticles for immunomodulation and lung targeting • PLGA/PEG nanoparticles conjugated to monocytes	140–145
Damage of cardiac tissue (reduced heart function)	anti-inflammatory agents for macrophage polarization	• PEI-mediated gene delivery • injectable alginate hydrogels • lipid nanoparticle siRNA delivery	153,154,156,162,165
Damage to nervous system (increased risk of neurodegenerative diseases)	anti-inflammatory remyelination	• PLGA nanoparticles conjugated with anti-NG2 chondroitin sulfate antibodies	175

approval. Thus, building a history of using biomaterials for various applications will favor fast clinical approval upon an outbreak.

Finally, just as the use of biomaterials for infectious diseases utilizes strategies from other disciplines, biomaterial solutions that can modulate and balance inflammatory and anti-inflammatory responses to COVID-19 will also have translatable applications for cancer vaccines, chronic infections, and tissue repair.

ACKNOWLEDGMENTS

This work is supported in part by grants from NIH (R56DE029157), the California Institute for Regenerative Medicine (CIRM, grant no. DISC2COVID19-11838), UCLA David Geffen School of Medicine – Oversight COVID-19 Research Committee (OCRC) (award no.: OCRC no. 45), and the Eli and Edythe Broad Center of Regenerative Medicine and Stem Cell Research Award Program. The contents of this publication are solely the responsibility of the authors and do not necessarily represent the official views of NIH (United States), CIRM, or/and other agency of the State of California.

AUTHOR CONTRIBUTIONS

All authors made substantial contributions to the content, writing, and editing of the manuscript. Figures were designed by J.Z.

DECLARATION OF INTERESTS

The authors declare no competing interests.

REFERENCES

1. Ziegler, C.G., Allon, S.J., Nyquist, S.K., Mbano, I.M., Miao, V.N., Tzouanas, C.N., Cao, Y., Yousif, A.S., Bals, J., and Hauser, B.M. (2020). SARS-CoV-2 receptor ACE2 is an interferon-stimulated gene in human airway epithelial cells and is detected in specific cell subsets across tissues. Cell *181*, 1016–1035.e9.

2. Tay, M.Z., Poh, C.M., Rénia, L., MacAry, P.A., and Ng, L.F. (2020). The trinity of COVID-19: immunity, inflammation and intervention. Nat. Rev. Immunol. *20*, 363–374.

3. Chen, Z., and Wherry, E.J. (2020). T cell responses in patients with COVID-19. Nat. Rev. Immunol. *20*, 529–536.

4. Merad, M., and Martin, J.C. (2020). Pathological inflammation in patients with COVID-19: a key role for monocytes and macrophages. Nat. Rev. Immunol. *20*, 355–362.

5. Kaneko, N., Kuo, H.-H., Boucau, J., Farmer, J.R., Allard-Chamard, H., Mahajan, V.S., Piechocka-Trocha, A., Lefteri, K., Osborn, M., and Bals, J. (2020). Loss of Bcl-6-expressing T follicular helper cells and germinal centers in COVID-19. Cell *183*, 143–157.e13.

6. Varga, Z., Flammer, A.J., Steiger, P., Haberecker, M., Andermatt, R., Zinkernagel, A.S., Mehra, M.R., Schuepbach, R.A., Ruschitzka, F., and Moch, H. (2020). Endothelial cell infection and endotheliitis in COVID-19. The Lancet *395*, 1417–1418.

7. He, L., Mäe, M.A., Muhl, L., Sun, Y., Pietilä, R., Nahar, K., Liébanas, E.V., Fagerlund, M.J., Oldner, A., Liu, J., et al. (2020). Pericyte-specific vascular expression of SARS-CoV-2 receptor ACE2—implications for microvascular inflammation and hypercoagulopathy in COVID-19. bioRxiv, 2020.2005.2011.088500.

8. Abou-Ismail, M.Y., Diamond, A., Kapoor, S., Arafah, Y., and Nayak, L. (2020). The hypercoagulable state in COVID-19: incidence, pathophysiology, and management. Thromb. Res. *194*, 101–115.

9. Levi, M., Thachil, J., Iba, T., and Levy, J.H. (2020). Coagulation abnormalities and thrombosis in patients with COVID-19. Lancet Haematol. *7*, e438–e440.

10. Goshua, G., Pine, A.B., Meizlish, M.L., Chang, C.H., Zhang, H., Bahel, P., Baluha, A., Bar, N., Bona, R.D., Burns, A.J., et al. (2020). Endotheliopathy in COVID-19-associated coagulopathy: evidence from a single-centre, cross-sectional study. Lancet Haematol. *7*, e575–e582.

11. Polycarpou, A., Howard, M., Farrar, C.A., Greenlaw, R., Fanelli, G., Wallis, R., Klavinskis, L.S., and Sacks, S. (2020). Rationale for targeting complement in COVID-19. EMBO Mol. Med. *12*, e12642.

12. Krarup, A., Wallis, R., Presanis, J.S., Gál, P., and Sim, R.B. (2007). Simultaneous activation of complement and coagulation by MBL-associated serine protease 2. PLoS One *2*, e623.

13. Dobó, J., Schroeder, V., Jenny, L., Cervenak, L., Závodszky, P., and Gál, P. (2014). Multiple roles of complement MASP-1 at the interface of innate immune response and coagulation. Mol. Immunol. *61*, 69–78.

14. Gao, T., Hu, M., Zhang, X., Li, H., Zhu, L., Liu, H., Dong, Q., Zhang, Z., Wang, Z., Hu, Y., et al. (2020). Highly pathogenic coronavirus N protein aggravates lung injury by MASP-2-mediated complement over-activation. medRxiv, 2020.2003.2029.20041962.

15. Tang, Z., Kong, N., Zhang, X., Liu, Y., Hu, P., Mou, S., Liljeström, P., Shi, J., Tan, W., and Kim, J.S. (2020). A materials-science perspective on tackling COVID-19. Nat. Rev. Mater. *5*, 847–860.

16. Subbarao, K., and Mahanty, S. (2020). Respiratory virus infections: understanding COVID-19. Immunity *52*, 905–909.

17. Lin, F.-C., and Young, H.A. (2014). Interferons: success in anti-viral immunotherapy. Cytokine Growth Factor Rev. *25*, 369–376.

18. Cui, L., Chen, S.Y., Lerbs, T., Lee, J.W., Domizi, P., Gordon, S., Kim, Y.H., Nolan, G., Betancur, P., and Wernig, G. (2020). Activation of JUN in fibroblasts promotes pro-fibrotic programme and modulates protective immunity. Nat. Commun. *11*, 2795.

19. Le, T.T., Andreadakis, Z., Kumar, A., Roman, R.G., Tollefsen, S., Saville, M., and Mayhew, S. (2020). The COVID-19 vaccine development landscape. Nat. Rev. Drug Discov. *19*, 305–306.

20. Chung, Y.H., Beiss, V., Fiering, S.N., and Steinmetz, N.F. (2020). COVID-19 vaccine frontrunners and their nanotechnology design. ACS Nano *14*, 12522–12537.

21. Quinn, S.C., Jamison, A.M., and Freimuth, V. (2020). Communicating Effectively about Emergency Use Authorization and Vaccines in the COVID-19 Pandemic (American Public Health Association).

22. Wang, Z.-B., and Xu, J. (2020). Better adjuvants for better vaccines: progress in adjuvant delivery systems, modifications, and adjuvant–antigen codelivery. Vaccines *8*, 128.

23. Duthie, M.S., Windish, H.P., Fox, C.B., and Reed, S.G. (2011). Use of defined TLR ligands as adjuvants within human vaccines. Immunol. Rev. *239*, 178–196.

24. Marciani, D.J. (2018). Elucidating the mechanisms of action of saponin-derived adjuvants. Trends Pharmacol. Sci. *39*, 573–585.

25. Keech, C., Albert, G., Cho, I., Robertson, A., Reed, P., Neal, S., Plested, J.S., Zhu, M., Cloney-Clark, S., and Zhou, H. (2020). Phase 1–2 trial of a SARS-CoV-2 recombinant spike protein nanoparticle vaccine. N. Engl. J. Med. *383*, 2320–2332.

26. Bengtsson, K.L., Song, H., Stertman, L., Liu, Y., Flyer, D.C., Massare, M.J., Xu, R.-H., Zhou, B., Lu, H., and Kwilas, S.A. (2016). Matrix-M adjuvant enhances antibody, cellular and protective immune responses of a Zaire Ebola/Makona virus glycoprotein (GP) nanoparticle vaccine in mice. Vaccine *34*, 1927–1935.

27. Suto, R., and Srivastava, P. (1995). A mechanism for the specific immunogenicity of heat shock protein-chaperoned peptides. Science *269*, 1585–1588.

28. Osterloh, A., and Breloer, M. (2008). Heat shock proteins: linking danger and pathogen recognition. Med. Microbiol. Immunol. *197*, 1–8.

29. Vermaelen, K. (2019). Vaccine strategies to improve anti-cancer cellular immune responses. Front. Immunol. *10*, 1–17.

30. Dranoff, G. (2002). GM-CSF-based cancer vaccines. Immunol. Rev. *188*, 147–154.

31. Xia, Y., Xie, Y., Yu, Z., Xiao, H., Jiang, G., Zhou, X., Yang, Y., Li, X., Zhao, M., Li, L., et al. (2018). The mevalonate pathway is a druggable target for vaccine adjuvant discovery. Cell *175*, 1059–1073.

32. Tonti, E., de Oya, N.J., Galliverti, G., Moseman, E.A., Di Lucia, P., Amabile, A., Sammicheli, S., De Giovanni, M., Sironi, L., and Chevrier, N. (2013). Bisphosphonates target B cells to enhance humoral immune responses. Cell Rep. *5*, 323–330.

33. Hasani-Sadrabadi, M.M., Dashtimoghadam, E., Bahlakeh, G., Majedi, F.S., Keshvari, H., Van Dersarl, J.J., Bertsch, A., Panahifar, A., Renaud, P., Tayebi, L., et al. (2015). On-chip synthesis of fine-tuned bone-seeking hybrid nanoparticles. Nanomedicine *10*, 3431–3449.

34. Irvine, D.J., Hanson, M.C., Rakhra, K., and Tokatlian, T. (2015). Synthetic nanoparticles for vaccines and immunotherapy. Chem. Rev. *115*, 11109–11146.

35. Hanson, M.C., Abraham, W., Crespo, M.P., Chen, S.H., Liu, H., Szeto, G.L., Kim, M., Reinherz, E.L., and Irvine, D.J. (2015). Liposomal vaccines incorporating molecular adjuvants and intrastructural T-cell help promote the immunogenicity of HIV membrane-proximal external region peptides. Vaccine *33*, 861–868.

36. Yenkoidiok-Douti, L., and Jewell, C.M. (2020). Integrating biomaterials and immunology to improve vaccines against infectious diseases. ACS Biomater. Sci. Eng. *6*, 759–778.

37. Gu, P., Wusiman, A., Zhang, Y., Liu, Z., Bo, R., Hu, Y., Liu, J., and Wang, D. (2019). Rational design of PLGA nanoparticle vaccine delivery systems to improve immune responses. Mol. Pharm. *16*, 5000–5012.

38. HogenEsch, H., O'Hagan, D.T., and Fox, C.B. (2018). Optimizing the utilization of aluminum adjuvants in vaccines: you might just get what you want. NPJ Vaccin. *3*, 51.

39. Jiang, H., Wang, Q., Li, L., Zeng, Q., Li, H., Gong, T., Zhang, Z., and Sun, X. (2018). Turning the old adjuvant from gel to nanoparticles to amplify CD8+ T cell responses. Adv. Sci. *5*, 1700426.

40. Ghimire, T.R., Benson, R.A., Garside, P., and Brewer, J.M. (2012). Alum increases antigen uptake, reduces antigen degradation and sustains antigen presentation by DCs in vitro. Immunol. Lett. *147*, 55–62.

41. Liang, F., Lindgren, G., Sandgren, K.J., Thompson, E.A., Francica, J.R., Seubert, A., De Gregorio, E., Barnett, S., O'Hagan, D.T., Sullivan, N.J., et al. (2017). Vaccine priming is restricted to draining lymph nodes and controlled by adjuvant-mediated antigen uptake. Sci. Transl. Med. *9*, eaal2094.

42. Calabro, S., Tritto, E., Pezzotti, A., Taccone, M., Muzzi, A., Bertholet, S., De Gregorio, E., O'Hagan, D.T., Baudner, B., and Seubert, A. (2013). The adjuvant effect of MF59 is due to the oil-in-water emulsion formulation, none of the individual components induce a comparable adjuvant effect. Vaccine *31*, 3363–3369.

43. Didierlaurent, A.M., Laupèze, B., Di Pasquale, A., Hergli, N., Collignon, C., and Garçon, N. (2017). Adjuvant system AS01: helping to overcome the challenges of modern vaccines. Expert Rev. Vaccin. *16*, 55–63.

44. Petrovsky, N., and Cooper, P.D. (2011). Carbohydrate-based immune adjuvants. Expert Rev. Vaccin. *10*, 523–537.

45. Carroll, E.C., Jin, L., Mori, A., Muñoz-Wolf, N., Oleszycka, E., Moran, H.B.T., Mansouri, S., McEntee, C.P., Lambe, E., Agger, E.M., et al. (2016). The vaccine adjuvant chitosan promotes cellular immunity via DNA sensor cGAS-STING-dependent induction of type I interferons. Immunity *44*, 597–608.

46. Petrovsky, N., and Cooper, P.D. (2015). Advax™, a novel microcrystalline polysaccharide particle engineered from delta inulin, provides robust adjuvant potency together with tolerability and safety. Vaccine *33*, 5920–5926.

47. Pompano, R.R., Chen, J., Verbus, E.A., Han, H., Fridman, A., McNeely, T., Collier, J.H., and Chong, A.S. (2014). Titrating T-cell epitopes within self-assembled vaccines optimizes CD4+ helper T cell and antibody outputs. Adv. Healthc. Mater. *3*, 1898–1908.

48. Si, Y., Tian, Q., Zhao, F., Kelly, S.H., Shores, L.S., Camacho, D.F., Sperling, A.I., Andrade, M.S., Collier, J.H., and Chong, A.S. (2020). Adjuvant-free nanofiber vaccine induces in situ lung dendritic cell activation and T_H17 responses. Sci. Adv. *6*, eaba0995.

49. Prausnitz, M.R., Mikszta, J.A., Cormier, M., and Andrianov, A.K. (2009). Microneedle-based vaccines. In Vaccines for Pandemic Influenza (Springer), pp. 369–393.

50. Rouphael, N.G., Paine, M., Mosley, R., Henry, S., McAllister, D.V., Kalluri, H., Pewin, W., Frew, P.M., Yu, T., and Thornburg, N.J. (2017). The safety, immunogenicity, and acceptability

of inactivated influenza vaccine delivered by microneedle patch (TIV-MNP 2015): a randomised, partly blinded, placebo-controlled, phase 1 trial. Lancet *390*, 649–658.

51. Kim, E., Erdos, G., Huang, S., Kenniston, T.W., Balmert, S.C., Carey, C.D., Raj, V.S., Epperly, M.W., Klimstra, W.B., and Haagmans, B.L. (2020). Microneedle array delivered recombinant coronavirus vaccines: immunogenicity and rapid translational development. EBioMedicine *55*, 102743.

52. Muralidharan, P., Malapit, M., Mallory, E., Hayes, D., Jr., and Mansour, H.M. (2015). Inhalable nanoparticulate powders for respiratory delivery. Nanomedicine *11*, 1189–1199.

53. Miragoli, M., Ceriotti, P., Iafisco, M., Vacchiano, M., Salvarani, N., Alogna, A., Carullo, P., Ramirez-Rodríguez, G.B., Patrício, T., and Degli Esposti, L. (2018). Inhalation of peptide-loaded nanoparticles improves heart failure. Sci. Transl. Med. *10*, eaan6205.

54. Lai, R., Afkhami, S., Haddadi, S., Jeyanathan, M., and Xing, Z. (2015). Mucosal immunity and novel tuberculosis vaccine strategies: route of immunisation-determined T-cell homing to restricted lung mucosal compartments. Eur. Respir. Rev. *24*, 356–360.

55. Li, A.V., Moon, J.J., Abraham, W., Suh, H., Elkhader, J., Seidman, M.A., Yen, M., Im, E.-J., Foley, M.H., and Barouch, D.H. (2013). Generation of effector memory T cell-based mucosal and systemic immunity with pulmonary nanoparticle vaccination. Sci. Transl. Med. *5*, 204ra130.

56. Trevaskis, N.L., Kaminskas, L.M., and Porter, C.J. (2015). From sewer to saviour—targeting the lymphatic system to promote drug exposure and activity. Nat. Rev. Drug Discov. *14*, 781–803.

57. Liu, H., Moynihan, K.D., Zheng, Y., Szeto, G.L., Li, A.V., Huang, B., Van Egeren, D.S., Park, C., and Irvine, D.J. (2014). Structure-based programming of lymph-node targeting in molecular vaccines. Nature *507*, 519–522.

58. Mehta, N.K., Pradhan, R.V., Soleimany, A.P., Moynihan, K.D., Rothschilds, A.M., Momin, N., Rakhra, K., Mata-Fink, J., Bhatia, S.N., and Wittrup, K.D. (2020). Pharmacokinetic tuning of protein–antigen fusions enhances the immunogenicity of T-cell vaccines. Nat. Biomed. Eng. *4*, 636–648.

59. Steinbuck, M.P., Seenappa, L.M., Jakubowski, A., McNeil, L.K., Haqq, C.M., and DeMuth, P.C. (2021). A lymph node-targeted amphiphile vaccine induces potent cellular and humoral immunity to SARS-CoV-2. Sci. Adv. *7*, eabe5819.

60. Irvine, D.J., and Read, B.J. (2020). Shaping humoral immunity to vaccines through antigen-displaying nanoparticles. Curr. Opin. Immunol. *65*, 1–6.

61. Bershteyn, A., Hanson, M.C., Crespo, M.P., Moon, J.J., Li, A.V., Suh, H., and Irvine, D.J. (2012). Robust IgG responses to nanograms of antigen using a biomimetic lipid-coated particle vaccine. J. Controll. Release *157*, 354–365.

62. Moon, J.J., Suh, H., Bershteyn, A., Stephan, M.T., Liu, H., Huang, B., Sohail, M., Luo, S., Um, S.H., and Khant, H. (2011). Interbilayer-crosslinked multilamellar vesicles as synthetic vaccines for potent humoral and cellular immune responses. Nat. Mater. *10*, 243–251.

63. Bachmann, M.F., Rohrer, U.H., Kundig, T.M., Burki, K., Hengartner, H., and Zinkernagel, R.M. (1993). The influence of antigen organization on B cell responsiveness. Science *262*, 1448–1451.

64. Yu, X., Dai, Y., Zhao, Y., Qi, S., Liu, L., Lu, L., Luo, Q., and Zhang, Z. (2020). Melittin-lipid nanoparticles target to lymph nodes and elicit a systemic anti-tumor immune response. Nat. Commun. *11*, 1–14.

65. Ladenstein, R., and Morgunova, E. (2020). Second career of a biosynthetic enzyme: lumazine synthase as a virus-like nanoparticle in vaccine development. Biotechnol. Rep. *27*, e00494.

66. Tokatlian, T., Read, B.J., Jones, C.A., Kulp, D.W., Menis, S., Chang, J.Y., Steichen, J.M., Kumari, S., Allen, J.D., and Dane, E.L. (2019). Innate immune recognition of glycans targets HIV nanoparticle immunogens to germinal centers. Science *363*, 649–654.

67. Veneziano, R., Moyer, T.J., Stone, M.B., Wamhoff, E.-C., Read, B.J., Mukherjee, S., Shepherd, T.R., Das, J., Schief, W.R., and Irvine, D.J. (2020). Role of nanoscale antigen organization on B-cell activation probed using DNA origami. Nat. Nanotechnol. *15*, 716–723.

68. Kim, Y.-S., Son, A., Kim, J., Kwon, S.B., Kim, M.H., Kim, P., Kim, J., Byun, Y.H., Sung, J., and Lee, J. (2018). Chaperna-mediated assembly of ferritin-based Middle East respiratory syndrome-coronavirus nanoparticles. Front. Immunol. *9*, 1093.

69. Swartz, M.A., Hirosue, S., and Hubbell, J.A. (2012). Engineering approaches to immunotherapy. Sci. Transl. Med. *4*, 148rv149.

70. Stano, A., Scott, E.A., Dane, K.Y., Swartz, M.A., and Hubbell, J.A. (2013). Tunable T cell immunity towards a protein antigen using polymersomes vs. solid-core nanoparticles. Biomaterials *34*, 4339–4346.

71. Schudel, A., Chapman, A.P., Yau, M.-K., Higginson, C.J., Francis, D.M., Manspeaker, M.P., Avecilla, A.R.C., Rohner, N.A., Finn, M., and Thomas, S.N. (2020). Programmable multistage drug delivery to lymph nodes. Nat. Nanotechnol. *15*, 491–499.

72. Cheung, A.S., Zhang, D.K., Koshy, S.T., and Mooney, D.J. (2018). Scaffolds that mimic antigen-presenting cells enable ex vivo expansion of primary T cells. Nat. Biotechnol. *36*, 160.

73. Dellacherie, M.O., Li, A., Lu, B.Y., Verbeke, C.S., Gu, L., Stafford, A., Doherty, E.J., and Mooney, D.J. (2020). Single-shot mesoporous silica rods scaffold for induction of humoral responses against small antigens. Adv. Funct. Mater. *30*, 2002448.

74. Martino, M.M., Briquez, P.S., Güç, E., Tortelli, F., Kilarski, W.W., Metzger, S., Rice, J.J., Kuhn, G.A., Müller, R., and Swartz, M.A. (2014). Growth factors engineered for super-affinity to the extracellular matrix enhance tissue healing. Science *343*, 885–888.

75. Majedi, F.S., Hasani-Sadrabadi, M.M., Kidani, Y., Thauland, T.J., Moshaverinia, A., Butte, M.J., Bensinger, S.J., and Bouchard, L.S. (2018). Cytokine secreting microparticles engineer the fate and the effector functions of T-cells. Adv. Mater. *30*, 1703178.

76. Meng, K.P., Majedi, F.S., Thauland, T.J., and Butte, M.J. (2020). Mechanosensing through YAP controls T cell activation and metabolism. J. Exp. Med. *217*, e20200053.

77. Majedi, F.S., Hasani-Sadrabadi, M.M., Thauland, T.J., Li, S., Bouchard, L.-S., and Butte, M.J. (2020). T-cell activation is modulated by the 3D mechanical microenvironment. Biomaterials *252*, 120058.

78. Alijotas-Reig, J., Esteve-Valverde, E., Belizna, C., Selva-O'Callaghan, A., Pardos-Gea, J., Quintana, A., Mekinian, A., Anunciacion-Lunell, A., and Miró-Mur, F. (2020). Immunomodulatory therapy for the management of severe COVID-19. Beyond the anti-viral therapy: a comprehensive review. Autoimmun. Rev. *19*, 102569.

79. Spyropoulos, A.C., Levy, J.H., Ageno, W., Connors, J.M., Hunt, B.J., Iba, T., Levi, M., Samama, C.M., Thachil, J., Giannis, D., et al. (2020). Scientific and Standardization Committee communication: clinical guidance on the diagnosis, prevention, and treatment of venous thromboembolism in hospitalized patients with COVID-19. J. Thromb. Haemost. *18*, 1859–1865.

80. Klok, F.A., Kruip, M., van der Meer, N.J.M., Arbous, M.S., Gommers, D., Kant, K.M., Kaptein, F.H.J., van Paassen, J., Stals, M.A.M., Huisman, M.V., et al. (2020). Incidence of thrombotic complications in critically ill ICU patients with COVID-19. Thromb. Res. *191*, 145–147.

81. Rambaldi, A., Gritti, G., Micò, M.C., Frigeni, M., Borleri, G., Salvi, A., Landi, F., Pavoni, C., Sonzogni, A., Gianatti, A., et al. (2020). Endothelial injury and thrombotic microangiopathy in COVID-19: treatment with the lectin-pathway inhibitor narsoplimab. Immunobiology *225*, 152001.

82. Annane, D., Heming, N., Grimaldi-Bensouda, L., Frémeaux-Bacchi, V., Vigan, M., Roux, A.-L., Marchal, A., Michelon, H., Rottman, M., and Moine, P. (2020). Eculizumab as an emergency treatment for adult patients with severe COVID-19 in the intensive care unit: a proof-of-concept study. EClinicalMedicine *28*, 100590.

83. Miao, Y., Fan, L., and Li, J.-Y. (2020). Potential treatments for COVID-19 related cytokine storm—beyond corticosteroids. Front. Immunol. *11*, 1445.

84. Robba, C., Battaglini, D., Pelosi, P., and Rocco, P.R. (2020). Multiple organ dysfunction in SARS-CoV-2: MODS-CoV-2. Expert Rev. Respir. Med. *14*, 865–868.

85. Howard, M.D., Greineder, C.F., Hood, E.D., and Muzykantov, V.R. (2014). Endothelial targeting of liposomes encapsulating SOD/catalase mimetic EUK-134 alleviates acute pulmonary inflammation. J. Controll. release *177*, 34–41.

86. Zhang, C.Y., Lin, W., Gao, J., Shi, X., Davaritouchaee, M., Nielsen, A.E., Mancini,

R.J., and Wang, Z. (2019). pH-responsive nanoparticles targeted to lungs for improved therapy of acute lung inflammation/injury. ACS Appl. Mater. Interfaces *11*, 16380–16390.

87. Jin, K., Luo, Z., Zhang, B., and Pang, Z. (2018). Biomimetic nanoparticles for inflammation targeting. Acta Pharm. Sin. B *8*, 23–33.

88. Nahrendorf, M., Jaffer, F.A., Kelly, K.A., Sosnovik, D.E., Aikawa, E., Libby, P., and Weissleder, R. (2006). Noninvasive vascular cell adhesion molecule-1 imaging identifies inflammatory activation of cells in atherosclerosis. Circulation *114*, 1504–1511.

89. Zhang, N., Chittasupho, C., Duangrat, C., Siahaan, T.J., and Berkland, C. (2008). PLGA Nanoparticle–peptide conjugate effectively targets intercellular cell-adhesion molecule-1. Bioconjug. Chem. *19*, 145–152.

90. Xu, X., Huang, X., Zhang, Y., Shen, S., Feng, Z., Dong, H., Zhang, C., and Mo, R. (2020). Self-regulated hirudin delivery for anticoagulant therapy. Sci. Adv. *6*, eabc0382.

91. Kang, C., Gwon, S., Song, C., Kang, P.M., Park, S.-C., Jeon, J., Hwang, D.W., and Lee, D. (2017). Fibrin-targeted and H2O2-responsive nanoparticles as a theranostics for thrombosed vessels. ACS Nano *11*, 6194–6203.

92. Su, M., Dai, Q., Chen, C., Zeng, Y., Chu, C., and Liu, G. (2020). Nano-medicine for thrombosis: a precise diagnosis and treatment strategy. Nanomicro Lett. *12*, 96.

93. Zhao, Z., Ukidve, A., Gao, Y., Kim, J., and Mitragotri, S. (2019). Erythrocyte leveraged chemotherapy (ELeCt): nanoparticle assembly on erythrocyte surface to combat lung metastasis. Sci. Adv. *5*, eaax9250.

94. Brenner, J.S., Pan, D.C., Myerson, J.W., Marcos-Contreras, O.A., Villa, C.H., Patel, P., Hekierski, H., Chatterjee, S., Tao, J.-Q., and Parhiz, H. (2018). Red blood cell-hitchhiking boosts delivery of nanocarriers to chosen organs by orders of magnitude. Nat. Commun. *9*, 1–14.

95. Anselmo, A.C., Gupta, V., Zern, B.J., Pan, D., Zakrewsky, M., Muzykantov, V., and Mitragotri, S. (2013). Delivering nanoparticles to lungs while avoiding liver and spleen through adsorption on red blood cells. ACS Nano *7*, 11129–11137.

96. Ukidve, A., Zhao, Z., Fehnel, A., Krishnan, V., Pan, D.C., Gao, Y., Mandal, A., Muzykantov, V., and Mitragotri, S. (2020). Erythrocyte-driven immunization via biomimicry of their natural antigen-presenting function. Proc. Natl. Acad. Sci. U S A *117*, 17727–17736.

97. Zahid, M., Feldman, K.S., Garcia-Borrero, G., Feinstein, T.N., Pogodzinski, N., Xu, X., Yurko, R., Czachowski, M., Wu, Y.L., Mason, N.S., et al. (2018). Cardiac targeting peptide, a novel cardiac vector: studies in bio-distribution, imaging application, and mechanism of transduction. Biomolecules *8*, 147.

98. Zhang, H., Li, N., Sirish, P., Mahakian, L., Ingham, E., Curry, F.R., Yamada, S., Chiamvimonvat, N., and Ferrara, K.W. (2012). The cargo of CRPPR-conjugated liposomes crosses the intact murine cardiac endothelium. J. Controll. Release *163*, 10–17.

99. Mentkowski, K.I., and Lang, J.K. (2019). Exosomes engineered to express a cardiomyocyte binding peptide demonstrate improved cardiac retention in vivo. Sci. Rep. *9*, 10041.

100. Shin, M., Lee, H.A., Lee, M., Shin, Y., Song, J.J., Kang, S.W., Nam, D.H., Jeon, E.J., Cho, M., Do, M., et al. (2018). Targeting protein and peptide therapeutics to the heart via tannic acid modification. Nat. Biomed. Eng. *2*, 304–317.

101. Nguyen, M.M., Carlini, A.S., Chien, M.P., Sonnenberg, S., Luo, C., Braden, R.L., Osborn, K.G., Li, Y., Gianneschi, N.C., and Christman, K.L. (2015). Enzyme-responsive nanoparticles for targeted accumulation and prolonged retention in heart tissue after myocardial infarction. Adv. Mater. *27*, 5547–5552.

102. Ueland, T., Holter, J.C., Holten, A.R., Muller, K.E., Lind, A., Bekken, G.K., Dudman, S., Aukrust, P., Dyrhol-Riise, A.M., and Heggelund, L. (2020). Distinct and early increase in circulating MMP-9 in COVID-19 patients with respiratory failure. J. Infect. *81*, e41–e43.

103. Hemmat, N., Derakhshani, A., Bannazadeh Baghi, H., Silvestris, N., Baradaran, B., and De Summa, S. (2020). Neutrophils, crucial, or harmful immune cells involved in coronavirus infection: a bioinformatics study. Front. Genet. *11*, 641.

104. Barnes, B.J., Adrover, J.M., Baxter-Stoltzfus, A., Borczuk, A., Cools-Lartigue, J., Crawford, J.M., Daßler-Plenker, J., Guerci, P., Huynh, C., Knight, J.S., et al. (2020). Targeting potential drivers of COVID-19: neutrophil extracellular traps. J. Exp. Med. *217*, e20200652.

105. Myerson, J.W., Patel, P.N., Habibi, N., Walsh, L.R., Lee, Y.-W., Luther, D.C., Ferguson, L.T., Zaleski, M.H., Zamora, M.E., Marcos-Contreras, O.A., et al. (2020). Supramolecular organization predicts protein nanoparticle delivery to neutrophils for acute lung inflammation diagnosis and treatment. bioRxiv, 2020.2004.2015.037564.

106. Chu, D., Gao, J., and Wang, Z. (2015). Neutrophil-mediated delivery of therapeutic nanoparticles across blood vessel barrier for treatment of inflammation and infection. ACS Nano *9*, 11800–11811.

107. Wang, Z., Li, J., Cho, J., and Malik, A.B. (2014). Prevention of vascular inflammation by nanoparticle targeting of adherent neutrophils. Nat. Nanotechnol. *9*, 204–210.

108. Tang, Z., Zhang, X., Shu, Y., Guo, M., Zhang, H., and Tao, W. (2020). Insights from nanotechnology in COVID-19 treatment. Nano today *36*, 101019.

109. Fromen, C.A., Kelley, W.J., Fish, M.B., Adili, R., Noble, J., Hoenerhoff, M.J., Holinstat, M., and Eniola-Adefeso, O. (2017). Neutrophil–particle interactions in blood circulation drive particle clearance and alter neutrophil responses in acute inflammation. ACS Nano *11*, 10797–10807.

110. Huang, B., Abraham, W.D., Zheng, Y., Bustamante López, S.C., Luo, S.S., and Irvine, D.J. (2015). Active targeting of chemotherapy to disseminated tumors using nanoparticle-carrying T cells. Sci. Transl. Med. *7*, 291ra294.

111. Champion, J.A., and Mitragotri, S. (2006). Role of target geometry in phagocytosis. Proc. Natl. Acad. Sci. U S A *103*, 4930–4934.

112. Anselmo, A.C., Gilbert, J.B., Kumar, S., Gupta, V., Cohen, R.E., Rubner, M.F., and Mitragotri, S. (2015). Monocyte-mediated delivery of polymeric backpacks to inflamed tissues: a generalized strategy to deliver drugs to treat inflammation. J. Controll. Release *199*, 29–36.

113. Hu, C.-M.J., Fang, R.H., Wang, K.-C., Luk, B.T., Thamphiwatana, S., Dehaini, D., Nguyen, P., Angsantikul, P., Wen, C.H., Kroll, A.V., et al. (2015). Nanoparticle biointerfacing by platelet membrane cloaking. Nature *526*, 118–121.

114. Kang, T., Zhu, Q., Wei, D., Feng, J., Yao, J., Jiang, T., Song, Q., Wei, X., Chen, H., Gao, X., et al. (2017). Nanoparticles coated with neutrophil membranes can effectively treat cancer metastasis. ACS Nano *11*, 1397–1411.

115. Dehaini, D., Wei, X., Fang, R.H., Masson, S., Angsantikul, P., Luk, B.T., Zhang, Y., Ying, M., Jiang, Y., Kroll, A.V., et al. (2017). Erythrocyte–platelet hybrid membrane coating for enhanced nanoparticle functionalization. Adv. Mater. *29*, 1606209.

116. Gao, J., Chu, D., and Wang, Z. (2016). Cell membrane-formed nanovesicles for disease-targeted delivery. J. Controll. Release *224*, 208–216.

117. Worthington, E.N., and Hagood, J.S. (2020). Therapeutic use of extracellular vesicles for acute and chronic lung disease. Int. J. Mol. Sci. *21*, 2318.

118. Fuhrmann, G., Serio, A., Mazo, M., Nair, R., and Stevens, M.M. (2015). Active loading into extracellular vesicles significantly improves the cellular uptake and photodynamic effect of porphyrins. J. Controll. Release *205*, 35–44.

119. Delcayre, A., Estelles, A., Sperinde, J., Roulon, T., Paz, P., Aguilar, B., Villanueva, J., Khine, S., and Le Pecq, J.B. (2005). Exosome display technology: applications to the development of new diagnostics and therapeutics. Blood Cell Mol. Dis. *35*, 158–168.

120. Kamerkar, S., LeBleu, V.S., Sugimoto, H., Yang, S., Ruivo, C.F., Melo, S.A., Lee, J.J., and Kalluri, R. (2017). Exosomes facilitate therapeutic targeting of oncogenic KRAS in pancreatic cancer. Nature *546*, 498–503.

121. Zhang, C., Zhang, L., Wu, W., Gao, F., Li, R.-Q., Song, W., Zhuang, Z.-N., Liu, C.-J., and Zhang, X.-Z. (2019). Artificial super neutrophils for inflammation targeting and HClO generation against tumors and infections. Adv. Mater. *31*, 1901179.

122. Luo, L., Tang, J., Nishi, K., Yan, C., Dinh, P.-U., Cores, J., Kudo, T., Zhang, J., Li, T.-S., and Cheng, K. (2017). Fabrication of synthetic mesenchymal stem cells for the treatment of acute myocardial infarction in mice. Circ. Res. *120*, 1768–1775.

123. Hasani-Sadrabadi, M.M., Majedi, F.S., Bensinger, S.J., Wu, B.M., Bouchard, L.S., Weiss, P.S., and Moshaverinia, A. (2018). Mechanobiological mimicry of helper T lymphocytes to evaluate cell–biomaterials crosstalk. Adv. Mater. *30*, 1706780.

124. Matsunaga, S., Jeremiah, S.S., Miyakawa, K., Kurotaki, D., Shizukuishi, S., Watashi, K.,

Nishitsuji, H., Kimura, H., Tamura, T., Yamamoto, N., et al. (2020). Engineering cellular biosensors with customizable antiviral responses targeting hepatitis B virus. iScience *23*, 100867.

125. Carfi, A., Bernabei, R., Landi, F., and Gemelli Against, C.-P. (2020). Persistent symptoms in patients after acute COVID-19. JAMA *324*, 603–605.

126. Dellacherie, M.O., Seo, B.R., and Mooney, D.J. (2019). Macroscale biomaterials strategies for local immunomodulation. Nat. Rev. Mater. *4*, 379–397.

127. Hubbell, J.A., Thomas, S.N., and Swartz, M.A. (2009). Materials engineering for immunomodulation. Nature *462*, 449.

128. Beers, M.F., and Morrisey, E.E. (2011). The three R's of lung health and disease: repair, remodeling, and regeneration. J. Clin. Invest. *121*, 2065–2073.

129. Ngai, J.C., Ko, F.W., Ng, S.S., To, K.W., Tong, M., and Hui, D.S. (2010). The long-term impact of severe acute respiratory syndrome on pulmonary function, exercise capacity and health status. Respirology *15*, 543–550.

130. George, P.M., Wells, A.U., and Jenkins, R.G. (2020). Pulmonary fibrosis and COVID-19: the potential role for antifibrotic therapy. Lancet Respir. Med. *8*, 807–815.

131. Zhang, P., Li, J., Liu, H., Han, N., Ju, J., Kou, Y., Chen, L., Jiang, M., Pan, F., Zheng, Y., et al. (2020). Long-term bone and lung consequences associated with hospital-acquired severe acute respiratory syndrome: a 15-year follow-up from a prospective cohort study. Bone Res. *8*, 8.

132. Salehi, S., Reddy, S., and Gholamrezanezhad, A. (2020). Long-term pulmonary consequences of coronavirus disease 2019 (COVID-19): what we know and what to expect. J. Thorac. Imaging *35*, W87–W89.

133. Wang, Y., Dong, C., Hu, Y., Li, C., Ren, Q., Zhang, X., Shi, H., and Zhou, M. (2020). Temporal changes of CT findings in 90 patients with COVID-19 pneumonia: a longitudinal study. Radiology *296*, E55–E64.

134. Meng, H., Xiong, R., He, R., Lin, W., Hao, B., Zhang, L., Lu, Z., Shen, X., Fan, T., Jiang, W., et al. (2020). CT imaging and clinical course of asymptomatic cases with COVID-19 pneumonia at admission in Wuhan, China. J. Infect. *81*, e33–e39.

135. Spagnolo, P., Balestro, E., Aliberti, S., Cocconcelli, E., Biondini, D., Casa, G.D., Sverzellati, N., and Maher, T.M. (2020). Pulmonary fibrosis secondary to COVID-19: a call to arms? Lancet Respir. Med. *8*, 750–752.

136. Suzuki, T., Itoh, Y., Sakai, Y., Saito, A., Okuzaki, D., Motooka, D., Minami, S., Kobayashi, T., Yamamoto, T., Okamoto, T., et al. (2020). Generation of human bronchial organoids for SARS-CoV-2 research. bioRxiv, 2020.2005.2025.115600.

137. Si, L., Bai, H., Rodas, M., Cao, W., Oh, C.Y., Jiang, A., Moller, R., Hoagland, D., Oishi, K., Horiuchi, S., et al. (2020). Human organs-on-chips as tools for repurposing approved drugs as potential influenza and COVID19 therapeutics in viral pandemics. bioRxiv, 2020.2004.2013.039917.

138. Sundarakrishnan, A., Zukas, H., Coburn, J., Bertini, B.T., Liu, Z.Y., Georgakoudi, I., Baugh, L., Dasgupta, Q., Black, L.D., and Kaplan, D.L. (2019). Bioengineered in vitro tissue model of fibroblast activation for modeling pulmonary fibrosis. Acs Biomater. Sci. Eng. *5*, 2417–2429.

139. Lechowicz, K., Drozdzal, S., Machaj, F., Rosik, J., Szostak, B., Zegan-Baranska, M., Biernawska, J., Dabrowski, W., Rotter, I., and Kotfis, K. (2020). COVID-19: the potential treatment of pulmonary fibrosis associated with SARS-CoV-2 infection. J. Clin. Med. *9*, 1917.

140. Ng, B., Dong, J., D'Agostino, G., Viswanathan, S., Widjaja, A.A., Lim, W.W., Ko, N.S.J., Tan, J., Chothani, S.P., Huang, B., et al. (2019). Interleukin-11 is a therapeutic target in idiopathic pulmonary fibrosis. Sci. Transl. Med. *11*, eaaw1237.

141. Soni, S.R., Bhunia, B.K., Kumari, N., Dan, S., Mukherjee, S., Mandal, B.B., and Ghosh, A. (2018). Therapeutically effective controlled release formulation of pirfenidone from nontoxic biocompatible carboxymethyl pullulan-poly(vinyl alcohol) interpenetrating polymer networks. ACS Omega *3*, 11993–12009.

142. Shamskhou, E.A., Kratochvil, M.J., Orcholski, M.E., Nagy, N., Kaber, G., Steen, E., Balaji, S., Yuan, K., Keswani, S., Danielson, B., et al. (2019). Hydrogel-based delivery of IL-10 improves treatment of bleomycin-induced lung fibrosis in mice. Biomaterials *203*, 52–62.

143. Mao, A.S., Ozkale, B., Shah, N.J., Vining, K.H., Descombes, T., Zhang, L., Tringides, C.M., Wong, S.W., Shin, J.W., Scadden, D.T., et al. (2019). Programmable microencapsulation for enhanced mesenchymal stem cell persistence and immunomodulation. Proc. Natl. Acad. Sci. U S A *116*, 15392–15397.

144. Liu, M., Zeng, X., Wang, J., Fu, Z., Wang, J., Liu, M., Ren, D., Yu, B., Zheng, L., Hu, X., et al. (2016). Immunomodulation by mesenchymal stem cells in treating human autoimmune disease-associated lung fibrosis. Stem Cell Res. Ther. *7*, 63.

145. Golchin, A., Seyedjafari, E., and Ardeshirylajimi, A. (2020). Mesenchymal stem cell therapy for COVID-19: present or future. Stem Cell Rev. Rep. *16*, 427–433.

146. Chang, X., Xing, L., Wang, Y., Yang, C.X., He, Y.J., Zhou, T.J., Gao, X.D., Li, L., Hao, H.P., and Jiang, H.L. (2020). Monocyte-derived multipotent cell delivered programmed therapeutics to reverse idiopathic pulmonary fibrosis. Sci. Adv. *6*, eaba3167.

147. Heymans, S. (2006). Inflammation and Cardiac Remodeling during Viral Myocarditis (Ernst Schering Res Found Workshop), pp. 197–218.

148. Miyawaki, A., Obana, M., Mitsuhara, Y., Orimoto, A., Nakayasu, Y., Yamashita, T., Fukada, S.I., Maeda, M., Nakayama, H., and Fujio, Y. (2017). Adult murine cardiomyocytes exhibit regenerative activity with cell cycle reentry through STAT3 in the healing process of myocarditis. Sci. Rep. *7*, 1407.

149. Nishiga, M., Wang, D.W., Han, Y., Lewis, D.B., and Wu, J.C. (2020). COVID-19 and cardiovascular disease: from basic mechanisms to clinical perspectives. Nat. Rev. Cardiol. *17*, 543–558.

150. Mitrani, R.D., Dabas, N., and Goldberger, J.J. (2020). COVID-19 cardiac injury: implications for long-term surveillance and outcomes in survivors. Heart Rhythm *17*, 1984–1990.

151. Zaim, S., Chong, J.H., Sankaranarayanan, V., and Harky, A. (2020). COVID-19 and multiorgan response. Curr. Probl. Cardiol. *45*, 100618.

152. Puntmann, V.O., Carerj, M.L., Wieters, I., Fahim, M., Arendt, C., Hoffmann, J., Shchendrygina, A., Escher, F., Vasa-Nicotera, M., Zeiher, A.M., et al. (2020). Outcomes of cardiovascular magnetic resonance imaging in patients recently recovered from coronavirus disease 2019 (COVID-19). JAMA Cardiol. *5*, 1265–1273.

153. Ferrini, A., Stevens, M.M., Sattler, S., and Rosenthal, N. (2019). Toward regeneration of the heart: bioengineering strategies for immunomodulation. Front. Cardiovasc. Med. *6*, 26.

154. Chen, W.C., Lee, B.G., Park, D.W., Kim, K., Chu, H., Kim, K., Huard, J., and Wang, Y. (2015). Controlled dual delivery of fibroblast growth factor-2 and Interleukin-10 by heparin-based coacervate synergistically enhances ischemic heart repair. Biomaterials *72*, 138–151.

155. Wang, C., Dong, C., and Xiong, S. (2017). IL-33 enhances macrophage M2 polarization and protects mice from CVB3-induced viral myocarditis. J. Mol. Cell Cardiol. *103*, 22–30.

156. Bloise, N., Rountree, I., Polucha, C., Montagna, G., Visai, L., Coulombe, K.L.K., and Munarin, F. (2020). Engineering immunomodulatory biomaterials for regenerating the infarcted myocardium. Front. Bioeng. Biotechnol. *8*, 292.

157. Li, Y., Huang, Y., Wu, W., Wei, B., and Qin, L. (2019). B cells increase myocardial inflammation by suppressing M2 macrophage polarization in Coxsackie virus B3-induced acute myocarditis. Inflammation *42*, 953–960.

158. Adamo, L., Staloch, L.J., Rocha-Resende, C., Matkovich, S.J., Jiang, W., Bajpai, G., Weinheimer, C.J., Kovacs, A., Schilling, J.D., Barger, P.M., et al. (2018). Modulation of subsets of cardiac B lymphocytes improves cardiac function after acute injury. JCI Insight *3*, e120137.

159. Sattler, S., Fairchild, P., Watt, F.M., Rosenthal, N., and Harding, S.E. (2017). The adaptive immune response to cardiac injury-the true roadblock to effective regenerative therapies? NPJ Regen. Med. *2*, 19.

160. Bracamonte-Baran, W., and Cihakova, D. (2017). Cardiac autoimmunity: myocarditis. Adv. Exp. Med. Biol. *1003*, 187–221.

161. Siripanthong, B., Nazarian, S., Muser, D., Deo, R., Santangeli, P., Khanji, M.Y., Cooper, L.T., Jr., and Chahal, C.A.A. (2020). Recognizing COVID-19-related myocarditis: the possible pathophysiology and proposed guideline for diagnosis and management. Heart Rhythm *17*, 1463–1471.

162. Meyer, I.S., Goetzke, C.C., Kespohl, M., Sauter, M., Heuser, A., Eckstein, V., Vornlocher, H.-P., Anderson, D.G., Haas, J., Meder, B., et al. (2018). Silencing the CSF-1 axis using nanoparticle encapsulated siRNA mitigates viral and autoimmune myocarditis. Front. Immunol. *9*, 2303.

163. Gurevich, D.B., Severn, C.E., Twomey, C., Greenhough, A., Cash, J., Toye, A.M., Mellor, H., and Martin, P. (2018). Live imaging of wound angiogenesis reveals macrophage orchestrated vessel sprouting and regression. EMBO J. *37*, e97786.

164. Spiller, K.L., Anfang, R.R., Spiller, K.J., Ng, J., Nakazawa, K.R., Daulton, J.W., and Vunjak-Novakovic, G. (2014). The role of macrophage phenotype in vascularization of tissue engineering scaffolds. Biomaterials *35*, 4477–4488.

165. Kwee, B.J., Seo, B.R., Najibi, A.J., Li, A.W., Shih, T.-Y., White, D., and Mooney, D.J. (2019). Treating ischemia via recruitment of antigen-specific T cells. Sci. Adv. *5*, eaav6313.

166. Pereira, A. (2020). Long-term neurological threats of COVID-19: a call to update the thinking about the outcomes of the coronavirus pandemic. Front. Neurol. *11*, 308.

167. Mesci, P., Macia, A., Saleh, A., Martin-Sancho, L., Yin, X., Snethlage, C., Avansini, S., Chanda, S., and Muotri, A. (2020). Sofosbuvir protects human brain organoids against SARS-CoV-2. bioRxiv, 125856.

168. Lee, S.H., Shin, H.S., Park, H.Y., Kim, J.L., Lee, J.J., Lee, H., Won, S.D., and Han, W. (2019). Depression as a mediator of chronic fatigue and post-traumatic stress symptoms in Middle East respiratory syndrome survivors. Psychiatry Investig. *16*, 59–64.

169. Moldofsky, H., and Patcai, J. (2011). Chronic widespread musculoskeletal pain, fatigue, depression and disordered sleep in chronic post-SARS syndrome; a case-controlled study. BMC Neurol. *11*, 37.

170. Serrano-Castro, P.J., Estivill-Torrus, G., Cabezudo-Garcia, P., Reyes-Bueno, J.A., Ciano Petersen, N., Aguilar-Castillo, M.J., Suarez-Perez, J., Jimenez-Hernandez, M.D., Moya-Molina, M.A., Oliver-Martos, B., et al. (2020). Impact of SARS-CoV-2 infection on neurodegenerative and neuropsychiatric diseases: a delayed pandemic? Neurologia *35*, 245–251.

171. Khateb, M., Bosak, N., and Muqary, M. (2020). Coronaviruses and central nervous system manifestations. Front. Neurol. *11*, 715.

172. Zhou, L., Zhang, M., Wang, J., and Gao, J. (2020). SARS-CoV-2: underestimated damage to nervous system. Trav. Med Infect Dis *36*, 101642.

173. Miron, V.E. (2017). Beyond immunomodulation: the regenerative role for regulatory T cells in central nervous system remyelination. J. Cell Commun. Signal. *11*, 191–192.

174. Miron, V.E., Boyd, A., Zhao, J.-W., Yuen, T.J., Ruckh, J.M., Shadrach, J.L., van Wijngaarden, P., Wagers, A.J., Williams, A., Franklin, R.J.M., et al. (2013). M2 microglia and macrophages drive oligodendrocyte differentiation during CNS remyelination. Nat. Neurosci. *16*, 1211–1218.

175. Rittchen, S., Boyd, A., Burns, A., Park, J., Fahmy, T.M., Metcalfe, S., and Williams, A. (2015). Myelin repair in vivo is increased by targeting oligodendrocyte precursor cells with nanoparticles encapsulating leukaemia inhibitory factor (LIF). Biomaterials *56*, 78–85.

176. Goronzy, J.J., and Weyand, C.M. (2019). Mechanisms underlying T cell ageing. Nat. Rev. Immunol. *19*, 573–583.

177. Edridge, A.W., Kaczorowska, J., Hoste, A.C., Bakker, M., Klein, M., Loens, K., Jebbink, M.F., Matser, A., Kinsella, C.M., and Rueda, P. (2020). Seasonal coronavirus protective immunity is short-lasting. Nat. Med. 1–3.

178. Peters, B., Nielsen, M., and Sette, A. (2020). T cell epitope predictions. Annu. Rev. Immunol. *38*, 123–145.

179. Li, L., Sun, T., He, Y., Li, W., Fan, Y., and Zhang, J. (2020). Epitope-based peptide vaccines predicted against novel coronavirus disease caused by SARS-CoV-2. Virus Res. *288*, 198082.

180. Hassanzadeh, P., Atyabi, F., and Dinarvand, R. (2019). The significance of artificial intelligence in drug delivery system design. Adv. Drug Deliv. Rev. *151*, 169–190.

181. Feng, R., Yu, F., Xu, J., and Hu, X. (2020). Knowledge gaps in immune response and immunotherapy involving nanomaterials: databases and artificial intelligence for material design. Biomaterials *266*, 120469.

10. REFERENCES

1. Campa-Carranza, J. N., Paez-Mayorga, J., Chua, C. Y. X., Nichols, J. E. & Grattoni, A. Emerging local immunomodulatory strategies to circumvent systemic immunosuppression in cell transplantation. *Expert Opin. Drug Deliv.* **19**, 595–610 (2022).

2. Adu-Berchie, K. & Mooney, D. J. Biomaterials as Local Niches for Immunomodulation. *Acc. Chem. Res.* **53**, 1749–1760 (2020).

3. Backlund, C., Jalili-Firoozinezhad, S., Kim, B. & Irvine, D. J. Biomaterials-Mediated Engineering of the Immune System. *Annu. Rev. Immunol.* **41**, 153–179 (2023).

4. Majedi, F. S. *et al.* Systemic enhancement of antitumour immunity by peritumourally implanted immunomodulatory macroporous scaffolds. *Nat. Biomed. Eng.* **7**, 56–71 (2023).

5. Headen, D. M. *et al.* Local immunomodulation Fas ligand-engineered biomaterials achieves allogeneic islet graft acceptance. *Nat. Mater.* **17**, 732–739 (2018).

6. Paez-Mayorga, J. *et al.* Enhanced In Vivo Vascularization of 3D-Printed Cell Encapsulation Device Using Platelet-Rich Plasma and Mesenchymal Stem Cells. *Adv. Healthc. Mater.* **9**, e2000670 (2020).

7. Paez-Mayorga, J. *et al.* Implantable niche with local immunosuppression for islet allotransplantation achieves type 1 diabetes reversal in rats. *Nat. Commun.* **13**, 7951 (2022).

8. Saleh, B. *et al.* Local Immunomodulation Using an Adhesive Hydrogel Loaded with miRNA-Laden Nanoparticles Promotes Wound Healing. *Small* **15**, e1902232 (2019).

9. Ben-Akiva, E., Est Witte, S., Meyer, R. A., Rhodes, K. R. & Green, J. J. Polymeric micro- and nanoparticles for immune modulation. *Biomater. Sci.* **7**, 14–30 (2018).

10. Lin, C.-Y. *et al.* Biodegradable polymeric microsphere-based vaccines and their applications in infectious diseases. *Hum. Vaccin. Immunother.* **11**, 650–656 (2015).

11. Wang, F.-Y., Chen, Y., Huang, Y.-Y. & Cheng, C.-M. Transdermal drug delivery systems for fighting common viral infectious diseases. *Drug Deliv. Transl. Res.* **11**, 1498–1508 (2021).

12. Kwon, K. M. *et al.* Microneedles: quick and easy delivery methods of vaccines. *Clin Exp Vaccine Res* **6**, 156–159 (2017).

13. Kim, Y.-C., Park, J.-H. & Prausnitz, M. R. Microneedles for drug and vaccine delivery. *Adv. Drug Deliv. Rev.* **64**, 1547–1568 (2012).

14. Tucak, A. *et al.* Microneedles: Characteristics, Materials, Production Methods and Commercial Development. *Micromachines* **11**, (2020).

15. Lee, C. *et al.* Comparative Study of Two Droplet-Based Dissolving Microneedle

Fabrication Methods for Skin Vaccination. *Adv. Healthc. Mater.* **7**, e1701381 (2018).

16. Kim, J. D., Kim, M., Yang, H., Lee, K. & Jung, H. Droplet-born air blowing: novel dissolving microneedle fabrication. *J. Control. release Off. J. Control. Release Soc.* **170**, 430–436 (2013).

17. Yang, H. *et al.* Centrifugal Lithography: Self-Shaping of Polymer Microstructures Encapsulating Biopharmaceutics by Centrifuging Polymer Drops. *Adv. Healthc. Mater.* **6**, (2017).

18. Li, W., Li, S., Fan, X. & Prausnitz, M. R. Microneedle patch designs to increase dose administered to human subjects. *J. Control. Release* **339**, 350–360 (2021).

19. Jung, C.-R., Lahiji, S. F., Kim, Y., Kim, H. & Jung, H. Rapidly Separable Micropillar Integrated Dissolving Microneedles. *Pharmaceutics* **12**, (2020).

20. Bediz, B. *et al.* Dissolvable microneedle arrays for intradermal delivery of biologics: fabrication and application. *Pharm. Res.* **31**, 117–135 (2014).

21. Korkmaz, E. *et al.* Therapeutic intradermal delivery of tumor necrosis factor-alpha antibodies using tip-loaded dissolvable microneedle arrays. *Acta Biomater.* **24**, 96–105 (2015).

22. Chu, L. Y., Choi, S.-O. & Prausnitz, M. R. Fabrication of dissolving polymer microneedles for controlled drug encapsulation and delivery: Bubble and pedestal microneedle designs. *J. Pharm. Sci.* **99**, 4228–4238 (2010).

23. Li, W. *et al.* Long-acting reversible contraception by effervescent microneedle patch. *Sci. Adv.* **5**, eaaw8145 (2019).

24. Huang, D., Fu, X., Zhang, X. & Zhao, Y. Christmas Tree-Shaped Microneedles as FOLFIRINOX Spatiotemporal Delivery System for Pancreatic Cancer Treatment. *Res. (Washington, D.C.)* **2022**, 9809417 (2022).

25. Guo, M., Wang, Y., Gao, B. & He, B. Shark Tooth-Inspired Microneedle Dressing for Intelligent Wound Management. *ACS Nano* **15**, 15316–15327 (2021).

26. Chu, L. Y. & Prausnitz, M. R. Separable arrowhead microneedles. *J. Control. release Off. J. Control. Release Soc.* **149**, 242–249 (2011).

27. Davis, S. P., Landis, B. J., Adams, Z. H., Allen, M. G. & Prausnitz, M. R. Insertion of microneedles into skin: Measurement and prediction of insertion force and needle fracture force. *J. Biomech.* **37**, 1155–1163 (2004).

28. Aldawood, F. K., Andar, A. & Desai, S. A Comprehensive Review of Microneedles: Types, Materials, Processes, Characterizations and Applications. *Polymers (Basel).* **13**, (2021).

29. Bhadale, R. S. & Londhe, V. Y. A systematic review of carbohydrate-based microneedles: current status and future prospects. *J. Mater. Sci. Mater. Med.* **32**, 89 (2021).

30. Turner, J. G., White, L. R., Estrela, P. & Leese, H. S. Hydrogel-Forming Microneedles: Current Advancements and Future Trends. *Macromol. Biosci.* **21**, e2000307 (2021).

31. Lee, J. W., Park, J. H. & Prausnitz, M. R. Dissolving microneedles for transdermal drug delivery. *Biomaterials* **29**, 2113–2124 (2008).

32. Panda, A., Matadh, V. A., Suresh, S., Shivakumar, H. N. & Murthy, S. N. Non-dermal applications of microneedle drug delivery systems. *Drug Deliv. Transl. Res.* **12**, 67–78 (2022).

33. Kim, Y. C. *et al.* Influenza immunization with trehalose-stabilized virus-like particle vaccine using microneedles. *Procedia Vaccinol.* **2**, 17–21 (2010).

34. Demuth, P. C., Moon, J. J., Suh, H., Hammond, P. T. & Irvine, D. J. Releasable layer-by-layer assembly of stabilized lipid nanocapsules on microneedles for enhanced transcutaneous vaccine delivery. *ACS Nano* **6**, 8041–8051 (2012).

35. Kim, Y. C. *et al.* Fabrication of microneedle patches with lyophilized influenza vaccine suspended in organic solvent. *Drug Deliv. Transl. Res.* **11**, 692–701 (2021).

36. Ray, S., Wirth, D. M., Ortega-Rivera, O. A., Steinmetz, N. F. & Pokorski, J. K. Dissolving Microneedle Delivery of a Prophylactic HPV Vaccine. *Biomacromolecules* **23**, 903–912 (2022).

37. Choi, Y. *et al.* Hepatitis B vaccine delivered by microneedle patch: Immunogenicity in mice and rhesus macaques. *Vaccine* (2023) doi:10.1016/j.vaccine.2023.05.005.

38. DeMuth, P. C. *et al.* Vaccine delivery with microneedle skin patches in nonhuman primates. *Nat. Biotechnol.* **31**, 1082–1085 (2013).

39. Chu, L. Y. *et al.* Enhanced Stability of Inactivated Influenza Vaccine Encapsulated in Dissolving Microneedle Patches. *Pharm. Res.* **33**, 868–878 (2016).

40. Vrdoljak, A. *et al.* Induction of broad immunity by thermostabilised vaccines incorporated in dissolvable microneedles using novel fabrication methods. *J. Control. Release* **225**, 192–204 (2016).

41. Rouphael, N. G. *et al.* The safety, immunogenicity, and acceptability of inactivated influenza vaccine delivered by microneedle patch (TIV-MNP 2015): a randomised, partly blinded, placebo-controlled, phase 1 trial. *Lancet* **390**, 649–658 (2017).

42. Kim, E. *et al.* Microneedle array delivered recombinant coronavirus vaccines: Immunogenicity and rapid translational development. *EBioMedicine* **55**, 1–12 (2020).

43. Lanza, J. S. *et al.* A TLR9-adjuvanted vaccine formulated into dissolvable microneedle patches or cationic liposomes protects against leishmaniasis after skin or subcutaneous immunization. *Int. J. Pharm.* **586**, 119390 (2020).

44. Tran, K. T. M. *et al.* Transdermal microneedles for the programmable burst release of multiple vaccine payloads. *Nat. Biomed. Eng.* **5**, 998–1007 (2021).

45. Jeong, H. R. *et al.* Preclinical study of influenza bivalent vaccine delivered with a two compartmental microneedle array. *J. Control. Release* **324**, 280–288 (2020).

46. Lee, K. J. *et al.* Non-transdermal microneedles for advanced drug delivery. *Adv. Drug Deliv. Rev.* **165**–**166**, 41–59 (2020).

47. Caffarel-Salvador, E. *et al.* A microneedle platform for buccal macromolecule delivery. *Sci. Adv.* **7**, 1–12 (2021).

48. Gilardi, M. *et al.* Microneedle-mediated Intratumoral Delivery of Anti-CTLA-4 Promotes cDC1-dependent Eradication of Oral Squamous Cell Carcinoma with Limited irAEs. *Mol. Cancer Ther.* **21**, 616–624 (2022).

49. Zhu, T. *et al.* Lidocaine-Loaded Hyaluronic Acid Adhesive Microneedle Patch for Oral Mucosal Topical Anesthesia. *Pharmaceutics* **14**, 1–15 (2022).

50. Tang, J. *et al.* Cardiac cell-integrated microneedle patch for treating myocardial infarction. *Sci. Adv.* **4**, eaat9365 (2018).

51. Lim, S., Park, T. Y., Jeon, E. Y., Joo, K. Il & Cha, H. J. Double-layered adhesive microneedle bandage based on biofunctionalized mussel protein for cardiac tissue regeneration. *Biomaterials* **278**, 121171 (2021).

52. Yang, S. Y. *et al.* A bio-inspired swellable microneedle adhesive for mechanical interlocking with tissue. *Nat. Commun.* **4**, 2–11 (2013).

53. Zhang, X., Chen, G., Yu, Y., Sun, L. & Zhao, Y. Bioinspired Adhesive and Antibacterial Microneedles for Versatile Transdermal Drug Delivery. *Research* **2020**, (2020).

54. Bian, N. *et al.* Immunomodulatory Biomaterials and Emerging Analytical Techniques for Probing the Immune Micro-Environment. *Tissue Eng. Regen. Med.* **20**, 11–24 (2023).

55. Wang, J., Zhang, Y., Pi, J., Xing, D. & Wang, C. Localized delivery of immunotherapeutics: A rising trend in the field. *J. Control. release Off. J. Control. Release Soc.* **340**, 149–167 (2021).

56. Soni, S. S., Alsasa, A. & Rodell, C. B. Applications of Macrocyclic Host Molecules in Immune Modulation and Therapeutic Delivery. *Front. Chem.* **9**, 658548 (2021).

57. Singh, A. & Peppas, N. A. Hydrogels and scaffolds for immunomodulation. *Adv. Mater.* **26**, 6530–6541 (2014).

58. Shoichet, M. S. Polymer Scaffolds for Biomaterials Applications. *Macromolecules* **43**, 581–591 (2010).

59. Najibi, A. J., Shih, T.-Y. & Mooney, D. J. Cryogel vaccines effectively induce immune responses independent of proximity to the draining lymph nodes. *Biomaterials* **281**, 121329 (2022).

60. Najibi, A. J. *et al.* Scaffold Vaccines for Generating Robust and Tunable Antibody Responses. *Adv. Funct. Mater.* **32**, 2110905 (2022).

61. Koh, R. H., Jin, Y., Kim, J. & Hwang, N. S. Inflammation-Modulating Hydrogels for Osteoarthritis Cartilage Tissue Engineering. *Cells* **9**, (2020).

62. Sadtler, K. *et al.* Developing a pro-regenerative biomaterial scaffold microenvironment requires T helper 2 cells. *Science* **352**, 366–370 (2016).

63. Andorko, J. I. & Jewell, C. M. Designing biomaterials with immunomodulatory properties for tissue engineering and regenerative medicine. *Bioeng. Transl. Med.* **2**, 139–155 (2017).

64. Hotaling, N. A., Tang, L., Irvine, D. J. & Babensee, J. E. Biomaterial Strategies for Immunomodulation. *Annu. Rev. Biomed. Eng.* **17**, 317–349 (2015).

65. Yousefpour, P., Ni, K. & Irvine, D. J. Targeted modulation of immune cells and tissues using engineered biomaterials. *Nat. Rev. Bioeng.* **1**, 107–124 (2023).

66. Anselmo, A. C. & Mitragotri, S. Nanoparticles in the clinic: An update. *Bioeng. Transl. Med.* **4**, e10143 (2019).

67. Horvath, D. & Basler, M. PLGA Particles in Immunotherapy. *Pharmaceutics* **15**, (2023).

68. Garland, K. M. *et al.* Microparticle Depots for Controlled and Sustained Release of Endosomolytic Nanoparticles. *Cell. Mol. Bioeng.* **12**, 429–442 (2019).

69. Dellacherie, M. O. *et al.* Single-Shot Mesoporous Silica Rods Scaffold for Induction of Humoral Responses Against Small Antigens. *Adv. Funct. Mater.* **30**, 2002448 (2020).

70. Shields, C. W. 4th *et al.* Cellular backpacks for macrophage immunotherapy. *Sci. Adv.* **6**, eaaz6579 (2020).

71. Kapate, N. *et al.* A backpack-based myeloid cell therapy for multiple sclerosis. *Proc. Natl. Acad. Sci.* **120**, e2221535120 (2023).

72. Brenner, J. S., Mitragotri, S. & Muzykantov, V. R. Red Blood Cell Hitchhiking: A Novel Approach for Vascular Delivery of Nanocarriers. *Annu. Rev. Biomed. Eng.* **23**, 225–248 (2021).

73. Myerson, J. W. *et al.* Supramolecular arrangement of protein in nanoparticle structures predicts nanoparticle tropism for neutrophils in acute lung inflammation. *Nat. Nanotechnol.* **17**, 86–97 (2022).

74. Fadel, T. R. *et al.* Enhanced Cellular Activation with Single Walled Carbon Nanotube Bundles Presenting Antibody Stimuli. *Nano Lett.* **8**, 2070–2076 (2008).

75. Fadel, T. R. *et al.* Adsorption of multimeric T cell antigens on carbon nanotubes: effect on protein structure and antigen-specific T cell stimulation. *Small* **9**, 666–672 (2013).

76. Demento, S., Steenblock, E. R. & Fahmy, T. M. Biomimetic approaches to modulating the T cell immune response with nano- and micro- particles. in *2009 Annual International Conference of the IEEE Engineering in Medicine and Biology Society* 1161–1166 (2009). doi:10.1109/IEMBS.2009.5332625.

77. Steenblock, E. R., Fadel, T., Labowsky, M., Pober, J. S. & Fahmy, T. M. An Artificial Antigen-presenting Cell with Paracrine Delivery of IL-2 Impacts the Magnitude and Direction of the T Cell Response *. *J. Biol. Chem.* **286**, 34883–34892 (2011).

78. Wynn, T. A., Chawla, A. & Pollard, J. W. Macrophage biology in development, homeostasis and disease. *Nature* **496**, 445–455 (2013).

79. Forbes, S. J. & Rosenthal, N. Preparing the ground for tissue regeneration: from mechanism to therapy. *Nat. Med.* **20**, 857–869 (2014).

80. Zhong, J. X., Raghavan, P. & Desai, T. A. Harnessing Biomaterials for Immunomodulatory-Driven Tissue Engineering. *Regen. Eng. Transl. Med.* (2022) doi:10.1007/s40883-022-00279-6.

81. Russell, D. G., Huang, L. & VanderVen, B. C. Immunometabolism at the interface between macrophages and pathogens. *Nat. Rev. Immunol.* **19**, 291–304 (2019).

82. Mosser, D. M. & Edwards, J. P. Exploring the full spectrum of macrophage activation. *Nat. Rev. Immunol.* **8**, 958–969 (2008).

83. Davies, L. C., Jenkins, S. J., Allen, J. E. & Taylor, P. R. Tissue-resident macrophages. *Nat. Immunol.* **14**, 986–995 (2013).

84. Nath, S. G. & Raveendran, R. Microbial dysbiosis in periodontitis. *J. Indian Soc. Periodontol.* **17**, 543–545 (2013).

85. Shaikh, H. F. M., Patil, S. H., Pangam, T. S. & Rathod, K. V. Polymicrobial synergy and dysbiosis: An overview. *J. Indian Soc. Periodontol.* **22**, 101–106 (2018).

86. *No Title*. (1996).

87. Li, N. & Collyer, C. A. Gingipains from Porphyromonas gingivalis - Complex domain structures confer diverse functions. *Eur. J. Microbiol. Immunol. (Bp).* **1**, 41–58 (2011).

88. Kachlany, S. C. Aggregatibacter actinomycetemcomitans leukotoxin: from threat to therapy. *J. Dent. Res.* **89**, 561–570 (2010).

89. Lasserre, J. F., Brecx, M. C. & Toma, S. Oral Microbes, Biofilms and Their Role in Periodontal and Peri-Implant Diseases. *Mater. (Basel, Switzerland)* **11**, (2018).

90. Yang, J. & Yan, H. Mucosal epithelial cells: the initial sentinels and responders controlling and regulating immune responses to viral infections. *Cell. Mol. Immunol.* **18**, 1628–1630 (2021).

91. Ley, K., Laudanna, C., Cybulsky, M. I. & Nourshargh, S. Getting to the site of inflammation: the leukocyte adhesion cascade updated. *Nat. Rev. Immunol.* **7**, 678–689 (2007).

92. Moore, K. L. *et al.* P-selectin glycoprotein ligand-1 mediates rolling of human neutrophils on P-selectin. *J. Cell Biol.* **128**, 661–671 (1995).

93. Jiang, Q. *et al.* Interactions Between Neutrophils and Periodontal Pathogens in Late-

Onset Periodontitis. *Front. Cell. Infect. Microbiol.* **11**, 627328 (2021).

94. Rath, M., Müller, I., Kropf, P., Closs, E. I. & Munder, M. Metabolism via Arginase or Nitric Oxide Synthase: Two Competing Arginine Pathways in Macrophages. *Front. Immunol.* **5**, 532 (2014).

95. Mills, C. D. Anatomy of a discovery: m1 and m2 macrophages. *Front. Immunol.* **6**, 212 (2015).

96. Sun, X. *et al.* Polarized Macrophages in Periodontitis: Characteristics, Function, and Molecular Signaling. *Front. Immunol.* **12**, 763334 (2021).

97. Zhou, L.-N. *et al.* Macrophage polarization in human gingival tissue in response to periodontal disease. *Oral Dis.* **25**, 265–273 (2019).

98. Zhuang, Z. *et al.* Induction of M2 Macrophages Prevents Bone Loss in Murine Periodontitis Models. *J. Dent. Res.* **98**, 200–208 (2019).

99. Yao, Y. *et al.* The Macrophage-Osteoclast Axis in Osteoimmunity and Osteo-Related Diseases. *Front. Immunol.* **12**, 664871 (2021).

100. Boyce, B. F., Yao, Z. & Xing, L. Osteoclasts have multiple roles in bone in addition to bone resorption. *Crit. Rev. Eukaryot. Gene Expr.* **19**, 171–180 (2009).

101. Sima, C., Viniegra, A. & Glogauer, M. Macrophage immunomodulation in chronic osteolytic diseases-the case of periodontitis. *J. Leukoc. Biol.* **105**, 473–487 (2019).

102. Usui, M. *et al.* Mechanism of alveolar bone destruction in periodontitis - Periodontal bacteria and inflammation. *Jpn. Dent. Sci. Rev.* **57**, 201–208 (2021).

103. Dunkelberger, J. R. & Song, W.-C. Complement and its role in innate and adaptive immune responses. *Cell Res.* **20**, 34–50 (2010).

104. Hajishengallis, G. *et al.* Complement-Dependent Mechanisms and Interventions in Periodontal Disease. *Front. Immunol.* **10**, 406 (2019).

105. Hajishengallis, G., Maekawa, T., Abe, T., Hajishengallis, E. & Lambris, J. D. Complement Involvement in Periodontitis: Molecular Mechanisms and Rational Therapeutic Approaches. *Adv. Exp. Med. Biol.* **865**, 57–74 (2015).

106. El-Awady, A. R., Elashiry, M., Morandini, A. C., Meghil, M. M. & Cutler, C. W. Dendritic cells a critical link to alveolar bone loss and systemic disease risk in periodontitis: Immunotherapeutic implications. *Periodontol. 2000* **89**, 41–50 (2022).

107. Elsayed, R. *et al.* Porphyromonas gingivalis Provokes Exosome Secretion and Paracrine Immune Senescence in Bystander Dendritic Cells. *Front. Cell. Infect. Microbiol.* **11**, 669989 (2021).

108. Martinez, G. J., Nurieva, R. I., Yang, X. O. & Dong, C. Regulation and function of proinflammatory TH17 cells. *Ann. N. Y. Acad. Sci.* **1143**, 188–211 (2008).

109. González-Osuna, L. *et al.* Senescent CD4(+)CD28(-) T Lymphocytes as a Potential

Driver of Th17/Treg Imbalance and Alveolar Bone Resorption during Periodontitis. *Int. J. Mol. Sci.* **23**, (2022).

110. Takahashi, K. & Yamanaka, S. Induction of Pluripotent Stem Cells from Mouse Embryonic and Adult Fibroblast Cultures by Defined Factors. *Cell* **126**, 663–676 (2006).

111. Grath, A. & Dai, G. Direct cell reprogramming for tissue engineering and regenerative medicine. *J. Biol. Eng.* **13**, 14 (2019).

112. Sadahiro, T., Yamanaka, S. & Ieda, M. Direct Cardiac Reprogramming. *Circ. Res.* **116**, 1378–1391 (2015).

113. Jayawardena, T. M. *et al.* MicroRNA Induced Cardiac Reprogramming In Vivo. *Circ. Res.* **116**, 418–424 (2015).

114. Wang, H. *et al.* Small molecules enable cardiac reprogramming of mouse fibroblasts with a single factor, Oct4. *Cell Rep.* **6**, 951–960 (2014).

115. Cao, N. *et al.* Conversion of human fibroblasts into functional cardiomyocytes by small molecules. *Science* **352**, 1216–1220 (2016).

116. Wang, J. *et al.* Reprogramming of fibroblasts into expandable cardiovascular progenitor cells via small molecules in xeno-free conditions. *Nat. Biomed. Eng.* **6**, 403–420 (2022).

117. Bulaklak, K. & Gersbach, C. A. The once and future gene therapy. *Nat. Commun.* **11**, 5820 (2020).

118. Santos, H. S. *et al.* In Situ Gene Therapy. *Curr. Gene Ther.* **21**, 406–430 (2021).

119. Shahryari, A. *et al.* Development and Clinical Translation of Approved Gene Therapy Products for Genetic Disorders. *Front. Genet.* **10**, 868 (2019).

120. Putnam, D. Polymers for gene delivery across length scales. *Nat. Mater.* **5**, 439–451 (2006).

121. Nayerossadat, N., Maedeh, T. & Ali, P. A. Viral and nonviral delivery systems for gene delivery. *Adv. Biomed. Res.* **1**, 27 (2012).

122. Dilliard, S. A. & Siegwart, D. J. Passive, active and endogenous organ-targeted lipid and polymer nanoparticles for delivery of genetic drugs. *Nat. Rev. Mater.* **8**, 282–300 (2023).

123. Wang, D., Tai, P. W. L. & Gao, G. Adeno-associated virus vector as a platform for gene therapy delivery. *Nat. Rev. Drug Discov.* **18**, 358–378 (2019).

124. Davidson, B. L. & Breakefield, X. O. Viral vectors for gene delivery to the nervous system. *Nat. Rev. Neurosci.* **4**, 353–364 (2003).

125. Cucchiarini, M. & Madry, H. Biomaterial-guided delivery of gene vectors for targeted articular cartilage repair. *Nat. Rev. Rheumatol.* **15**, 18–29 (2019).

126. Labanieh, L., Majzner, R. G. & Mackall, C. L. Programming CAR-T cells to kill cancer. *Nat. Biomed. Eng.* **2**, 377–391 (2018).

127. Gaharwar, A. K., Singh, I. & Khademhosseini, A. Engineered biomaterials for in situ tissue regeneration. *Nat. Rev. Mater.* **5**, 686–705 (2020).

128. Pihlstrom, B. L., Michalowicz, B. S. & Johnson, N. W. Periodontal diseases. *Lancet* **366**, 1809–1820 (2005).

129. Dye, B., Thornton-Evans, G., Li, X. & Iafolla, T. Dental caries and tooth loss in adults in the United States, 2011-2012. *NCHS Data Brief* 197 (2015).

130. Chen, F.-M. *et al.* A review on endogenous regenerative technology in periodontal regenerative medicine. *Biomaterials* **31**, 7892–7927 (2010).

131. Patel, S. K. *et al.* Biorelevant and screening dissolution methods for minocycline hydrochloride microspheres intended for periodontal administration. *Int. J. Pharm.* **596**, 120261 (2021).

132. Khaliq, N. U., Chobisa, D., Richard, C. A., Swinney, M. R. & Yeo, Y. Engineering microenvironment of biodegradable polyester systems for drug stability and release control. *Ther. Deliv.* **12**, 37–54 (2021).

133. Graves, D. Cytokines that promote periodontal tissue destruction. *J. Periodontol.* **79**, 1585–1591 (2008).

134. Kayal, R. A. The role of osteoimmunology in periodontal disease. *Biomed Res. Int.* **2013**, 639368 (2013).

135. Mantovani, A., Biswas, S. K., Galdiero, M. R., Sica, A. & Locati, M. Macrophage plasticity and polarization in tissue repair and remodelling. *J. Pathol.* **229**, 176–185 (2013).

136. Benoit, M., Desnues, B. & Mege, J.-L. Macrophage polarization in bacterial infections. *J. Immunol.* **181**, 3733–3739 (2008).

137. Alvarez, C. *et al.* Regulatory T cell phenotype and anti-osteoclastogenic function in experimental periodontitis. *Sci. Rep.* **10**, 19018 (2020).

138. Wang, N., Liang, H. & Zen, K. Molecular mechanisms that influence the macrophage m1-m2 polarization balance. *Front. Immunol.* **5**, 614 (2014).

139. Murray, P. J. *et al.* Macrophage activation and polarization: nomenclature and experimental guidelines. *Immunity* **41**, 14–20 (2014).

140. Raimondo, T. M. & Mooney, D. J. Functional muscle recovery with nanoparticle-directed M2 macrophage polarization in mice. *Proc. Natl. Acad. Sci. U. S. A.* **115**, 10648–10653 (2018).

141. Yang, W.-C. *et al.* Interleukin-4 Supports the Suppressive Immune Responses Elicited by Regulatory T Cells . *Frontiers in Immunology* vol. 8 1508 (2017).

142. Mokarram, N. *et al.* Immunoengineering nerve repair. *Proc. Natl. Acad. Sci. U. S. A.* **114**, E5077–E5084 (2017).

143. Stadler, A. F. *et al.* Gingival crevicular fluid levels of cytokines/chemokines in chronic

periodontitis: a meta-analysis. *J. Clin. Periodontol.* **43**, 727–745 (2016).

144. Cekici, A., Kantarci, A., Hasturk, H. & Van Dyke, T. E. Inflammatory and immune pathways in the pathogenesis of periodontal disease. *Periodontol. 2000* **64**, 57–80 (2014).

145. Hajishengallis, G. & Korostoff, J. M. Revisiting the Page & Schroeder model: the good, the bad and the unknowns in the periodontal host response 40 years later. *Periodontol. 2000* **75**, 116–151 (2017).

146. Pan, W., Wang, Q. & Chen, Q. The cytokine network involved in the host immune response to periodontitis. *Int. J. Oral Sci.* **11**, 30 (2019).

147. Prausnitz, M. R. Engineering Microneedle Patches for Vaccination and Drug Delivery to Skin. *Annu. Rev. Chem. Biomol. Eng.* **8**, 177–200 (2017).

148. Lee, K. *et al.* Non-transdermal microneedles for advanced drug delivery. *Adv. Drug Deliv. Rev.* **165**–**166**, 41–59 (2020).

149. Xu, C., Lei, C. & Yu, C. Mesoporous Silica Nanoparticles for Protein Protection and Delivery. *Front. Chem.* **7**, 290 (2019).

150. Luo, Z. *et al.* Biodegradable Gelatin Methacryloyl Microneedles for Transdermal Drug Delivery. *Adv. Healthc. Mater.* **8**, e1801054 (2019).

151. Schirmer, L., Atallah, P., Werner, C. & Freudenberg, U. StarPEG-Heparin Hydrogels to Protect and Sustainably Deliver IL-4. *Adv. Healthc. Mater.* **5**, (2016).

152. Majedi, F. S. *et al.* Cytokine Secreting Microparticles Engineer the Fate and the Effector Functions of T-Cells. *Adv. Mater.* **30**, 1703178 (2018).

153. Waldron, K. *et al.* Formation of monodisperse mesoporous silica microparticles via spray-drying. *J. Colloid Interface Sci.* (2014) doi:10.1016/j.jcis.2013.12.027.

154. Liu, W., Chen, X. D. & Selomulya, C. On the spray drying of uniform functional microparticles. *Particuology* (2015) doi:10.1016/j.partic.2015.04.001.

155. Orecchioni, M., Ghosheh, Y., Pramod, A. B. & Ley, K. Macrophage Polarization: Different Gene Signatures in M1(LPS+) vs. Classically and M2(LPS–) vs. Alternatively Activated Macrophages . *Frontiers in Immunology* vol. 10 1084 (2019).

156. Stein, M., Keshav, S., Harris, N. & Gordon, S. Interleukin 4 potently enhances murine macrophage mannose receptor activity: a marker of alternative immunologic macrophage activation. *J. Exp. Med.* **176**, 287–292 (1992).

157. Josefowicz, S. Z., Lu, L.-F. & Rudensky, A. Y. Regulatory T cells: mechanisms of differentiation and function. *Annu. Rev. Immunol.* **30**, 531–564 (2012).

158. Chen, W. *et al.* Conversion of peripheral CD4+CD25- naive T cells to CD4+CD25+ regulatory T cells by TGF-beta induction of transcription factor Foxp3. *J. Exp. Med.* **198**, 1875–1886 (2003).

159. Hasani-Sadrabadi, M. M. *et al.* Hierarchically Patterned Polydopamine-Containing Membranes for Periodontal Tissue Engineering. *ACS Nano* **13**, 3830–3838 (2019).

160. Hasani-Sadrabadi, M. M. *et al.* An engineered cell-laden adhesive hydrogel promotes craniofacial bone tissue regeneration in rats. *Sci. Transl. Med.* **12**, (2020).

161. Glowacki, A. J. *et al.* Prevention of inflammation-mediated bone loss in murine and canine periodontal disease via recruitment of regulatory lymphocytes. *Proc. Natl. Acad. Sci.* **110**, 18525–18530 (2013).

162. Prakasam, A., Elavarasu, S. S. & Natarajan, R. K. Antibiotics in the management of aggressive periodontitis. *J. Pharm. Bioallied Sci.* **4**, S252-5 (2012).

163. Kinane, D. F., Stathopoulou, P. G. & Papapanou, P. N. Periodontal diseases. *Nat. Rev. Dis. Prim.* **3**, 17038 (2017).

164. Eke, P. I., Dye, B. A., Wei, L., Thornton-Evans, G. O. & Genco, R. J. Prevalence of periodontitis in adults in the United States: 2009 and 2010. *J. Dent. Res.* **91**, 914–920 (2012).

165. Hajishengallis, G., Darveau, R. P. & Curtis, M. A. The keystone-pathogen hypothesis. *Nat. Rev. Microbiol.* **10**, 717–725 (2012).

166. Hajishengallis, G. & Lamont, R. J. Beyond the red complex and into more complexity: the polymicrobial synergy and dysbiosis (PSD) model of periodontal disease etiology. *Mol. Oral Microbiol.* **27**, 409–419 (2012).

167. Yang, B., Pang, X., Li, Z., Chen, Z. & Wang, Y. Immunomodulation in the Treatment of Periodontitis: Progress and Perspectives. *Front. Immunol.* **12**, 781378 (2021).

168. Xu, W., Zhou, W., Wang, H. & Liang, S. Roles of Porphyromonas gingivalis and its virulence factors in periodontitis. *Adv. Protein Chem. Struct. Biol.* **120**, 45–84 (2020).

169. Marschall, J. S. Porphyromonas gingivalis gingipains induce a pro-inflammatory extracellular microenvironment : the role of PAR-2 and fibronectin. in (2016).

170. Feng, Y. *et al.* Role of Interleukin-17A in the Pathomechanisms of Periodontitis and Related Systemic Chronic Inflammatory Diseases. *Front. Immunol.* **13**, 862415 (2022).

171. Cheng, W.-C. *et al.* Periodontitis-associated pathogens P. gingivalis and A. actinomycetemcomitans activate human CD14(+) monocytes leading to enhanced Th17/IL-17 responses. *Eur. J. Immunol.* **46**, 2211–2221 (2016).

172. Murphy, B. S. *et al.* Azithromycin alters macrophage phenotype. *J. Antimicrob. Chemother.* **61**, 554–560 (2008).

173. Haydar, D. *et al.* Azithromycin Polarizes Macrophages to an M2 Phenotype via Inhibition of the STAT1 and NF-κB Signaling Pathways. *J. Immunol.* **203**, 1021–1030 (2019).

174. Wang, J. *et al.* Azithromycin promotes alternatively activated macrophage phenotype in systematic lupus erythematosus via PI3K/Akt signaling pathway. *Cell Death Dis.* **9**, 1080

(2018).

175. Zhang, X. *et al.* Immunomodulatory microneedle patch for periodontal tissue regeneration. *Matter* **5**, 666–682 (2022).

176. Zhu, Y. *et al.* The pentacyclic triterpene Lupeol switches M1 macrophages to M2 and ameliorates experimental inflammatory bowel disease. *Int. Immunopharmacol.* **30**, 74–84 (2016).

177. Shiratori, H. *et al.* An in vitro test system for compounds that modulate human inflammatory macrophage polarization. *Eur. J. Pharmacol.* **833**, 328–338 (2018).

178. Jiang, K. *et al.* Local release of dexamethasone from macroporous scaffolds accelerates islet transplant engraftment by promotion of anti-inflammatory M2 macrophages. *Biomaterials* **114**, 71–81 (2017).

179. Ai, F., Zhao, G., Lv, W., Liu, B. & Lin, J. Dexamethasone induces aberrant macrophage immune function and apoptosis. *Oncol. Rep.* **43**, 427–436 (2020).

180. Sinha, S., Kumar, S., Dagli, N. & Dagli, R. J. Effect of tetracycline HCl in the treatment of chronic periodontitis - A clinical study. *J. Int. Soc. Prev. Community Dent.* **4**, 149–153 (2014).

181. Kaplan, J. B., Ragunath, C., Ramasubbu, N. & Fine, D. H. Detachment of Actinobacillus actinomycetemcomitans biofilm cells by an endogenous beta-hexosaminidase activity. *J. Bacteriol.* **185**, 4693–4698 (2003).

182. Pourahmad, J. & Salimi, A. Isolated Human Peripheral Blood Mononuclear Cell (PBMC), a Cost Effective Tool for Predicting Immunosuppressive Effects of Drugs and Xenobiotics. *Iran. J. Pharm. Res. IJPR* **14**, 979 (2015).

183. Balazs, D. A. & Godbey, W. Liposomes for use in gene delivery. *J. Drug Deliv.* **2011**, 326497 (2011).

184. Chai, Z. *et al.* Optimization of Dexamethasone Administration for Maintaining Global Transduction Efficacy of Adeno-Associated Virus Serotype 9. *Hum. Gene Ther.* **30**, 829–840 (2019).

185. Shi, H. *et al.* Microneedle-mediated gene delivery for the treatment of ischemic myocardial disease. *Sci. Adv.* **6**, eaaz3621 (2020).

186. Fan, Z. *et al.* Near-Infrared Light-Triggered Unfolding Microneedle Patch for Minimally Invasive Treatment of Myocardial Ischemia. *ACS Appl. Mater. Interfaces* **13**, 40278–40289 (2021).

187. You, Y. *et al.* Intradermally delivered mRNA-encapsulating extracellular vesicles for collagen-replacement therapy. *Nat. Biomed. Eng.* (2023) doi:10.1038/s41551-022-00989-w.

188. Yin, H. *et al.* Non-viral vectors for gene-based therapy. *Nat. Rev. Genet.* **15**, 541–555 (2014).

189. Seregin, S. S. *et al.* Transient pretreatment with glucocorticoid ablates innate toxicity of systemically delivered adenoviral vectors without reducing efficacy. *Mol. Ther.* **17**, 685–696 (2009).

190. Agudo, J. *et al.* A TLR and non-TLR mediated innate response to lentiviruses restricts hepatocyte entry and can be ameliorated by pharmacological blockade. *Mol. Ther.* **20**, 2257–2267 (2012).

191. Xie, Z., Shen, J., Sun, H., Li, J. & Wang, X. Polymer-based hydrogels with local drug release for cancer immunotherapy. *Biomed. Pharmacother.* **137**, 111333 (2021).

192. Zhong, R. *et al.* Hydrogels for RNA delivery. *Nat. Mater.* (2023) doi:10.1038/s41563-023-01472-w.

193. Yang, Y. *et al.* A novel gene delivery composite system based on biodegradable folate-poly (ester amine) polymer and thermosensitive hydrogel for sustained gene release. *Sci. Rep.* **6**, 21402 (2016).

194. Amsden, B. Novel biodegradable polymers for local growth factor delivery. *Eur. J. Pharm. Biopharm. Off. J. Arbeitsgemeinschaft fur Pharm. Verfahrenstechnik e.V* **97**, 318–328 (2015).

195. Bieganski, R. M., Fowler, A., Morgan, J. R. & Toner, M. Stabilization of active recombinant retroviruses in an amorphous dry state with trehalose. *Biotechnol. Prog.* **14**, 615–620 (1998).

196. Tian, Y. *et al.* Intradermal Administration of Influenza Vaccine with Trehalose and Pullulan-Based Dissolving Microneedle Arrays. *J. Pharm. Sci.* **111**, 1070–1080 (2022).

197. Kim, Y. C., Quan, F. S., Compans, R. W., Kang, S. M. & Prausnitz, M. R. Formulation and coating of microneedles with inactivated influenza virus to improve vaccine stability and immunogenicity. *J. Control. Release* **142**, 187–195 (2010).

198. Wang, L. *et al.* Injectable and conductive cardiac patches repair infarcted myocardium in rats and minipigs. *Nat. Biomed. Eng.* **5**, 1157–1173 (2021).

199. Xu, Z., Alloush, J., Beck, E. & Weisleder, N. A murine model of myocardial ischemia-reperfusion injury through ligation of the left anterior descending artery. *J. Vis. Exp.* (2014) doi:10.3791/51329.

200. Kou, X. *et al.* The Fas/Fap-1/Cav-1 complex regulates IL-1RA secretion in mesenchymal stem cells to accelerate wound healing. *Sci. Transl. Med.* **10**, eaai8524 (2018).

201. Barbonetti, A., D'Andrea, S. & Francavilla, S. Testosterone replacement therapy. *Andrology* **8**, 1551–1566 (2020).

202. Tsametis, C. P. & Isidori, A. M. Testosterone replacement therapy: For whom, when and how? *Metabolism.* **86**, 69–78 (2018).

203. Li, W. *et al.* Rapidly separable microneedle patch for the sustained release of a contraceptive. *Nat. Biomed. Eng.* **3**, 220–229 (2019).

204. Naito, C. *et al.* Self-dissolving microneedle arrays for transdermal absorption enhancement of human parathyroid hormone (1-34). *Pharmaceutics* **10**, 1–12 (2018).

205. Tsioris, K. *et al.* Fabrication of silk microneedles for controlled-release drug delivery. *Adv. Funct. Mater.* **22**, 330–335 (2012).